TABLE OF CONTENTS

CHAPTER 4 REACTOR

TABLE OF CONTENTS

TABLE OF CONTENTS

TABLE OF CONTENTS

LIST OF FIGURES

LIST OF FIGURES

LIST OF FIGURES

4.0 REACTOR

This chapter provides a description of the reactor design used at GGNS. The first GGNS core was supplied by General Electric, now General Electric-Hitachi (GEH). The information in the General Electric Design Topical Report NEDE-20944, October 1976 was utilized in describing this first core. The subsequent reloads have been supplied by either AREVA NP (formerly Siemens Power Corporation (SPC) and Framatome-ANP (FANP)) or General Electric-Hitachi(GEH). The information contained in various topical reports (referenced as noted in Sections 4.2, 4.3, and 4.4) was utilized in describing the reloads.

4.1   SUMMARY DESCRIPTION

The reactor assembly consists of the reactor vessel, its internal components of the core, shroud, steam separator, and dryer assemblies, and jet pumps. Also included in the reactor assembly are the control rods, control rod drive housings, and the control rod drives. Figure 3.9-8, Reactor Vessel Internals, shows the arrangement of reactor assembly components. A summary of the important design and performance characteristics is given in Section 1.3, Comparison of Principal Design Characteristics. Loading conditions for reactor assembly components are specified in Section 3.9.

4.1.1   Reactor Vessel

The reactor vessel design and description are covered in Section 5.3.

4.1.2   Reactor Internal Components

The major reactor internal components are the core (fuel, channels, control blades, and instrumentation), the core support structure (including the shroud, top guide and core plate), the shroud head and steam separator assembly, the steam dryer assembly, the feedwater spargers, the core spray spargers, and the jet pumps. Except for the Zircaloy in the reactor core, these reactor internals are stainless steel or other corrosion-resistant alloys. All major internal components of the vessel can be removed except the jet pump diffusers, the jet pump risers, the shroud, the core spray lines, spargers, and the feedwater sparger. The removal of the steam dryers, shroud head and steam

separators, fuel assemblies, in-core assemblies, control rods, orificed fuel supports, and sparger and control rod guide tubes, can be accomplished on a routine basis.

4.1.2.1   Reactor Core

4.1.2.1.1   General

The design of the boiling water reactor core, including fuel, is based on the proper combination of many design variables and operating experience. These factors contribute to the achievement of high reliability.

A number of important features of the boiling water reactor core design are summarized in the following paragraphs:

a. The BWR core mechanical design is based on conservative application of stress limits, operating experience, and experimental test results. The moderate pressure levels characteristic of a direct cycle reactor (approximately 1000 psia) result in moderate cladding temperatures and stress levels.

b. The low coolant saturation temperature, high heat transfer coefficients, and neutral water chemistry of the BWR are significant, advantageous factors in minimizing Zircaloy temperature and associated temperature-dependent corrosion and hydride buildup.

    The relatively uniform fuel cladding temperatures throughout the core minimize migration of the hydrides to cold cladding zones and reduce thermal stresses.

c. The basic thermal and mechanical criteria applied in the design have been proven by irradiation of statistically significant quantities of fuel. The design heat transfer rates and linear heat generation rates are similar to values proven in fuel assembly irradiation.

d. The design power distribution used in sizing the core represents a worst expected state of operation.

e. For Cycle - 1, the General Electric thermal analysis basis, GETAB, was applied to assure that more than 99.9 percent of the fuel rods in the core are expected to avoid boiling transition for the most severe abnormal

operational transient described in Chapter 15. Cycles 2 through 8 used the Siemens Power Corporation (SPC) THERMEX methodology with either the XN-3 or ANFB correlations. Cycles 9 through 11 used the GETAB Thermal analysis basis again. Cycles 12-16 used the AREVA NP (formerly SPC and FANP) THERMEX methodology with the ANFB-10 and SPCB correlations. Starting with Cycle 17, the GETAB thermal analysis basis is again applied. The possibility of boiling transition occurring during normal reactor operation is insignificant.

f.   Because of the large negative moderator density coefficient of reactivity, the BWR has a number of inherent advantages. These are the uses of coolant flow for load following, the inherent self-flattening of the radial power distribution, the ease of control, the spatial xenon stability, and the ability to override xenon, in order to follow load.

Boiling water reactors do not have instability problems due to xenon. This has been demonstrated by special tests which have been conducted on operating BWRs in an attempt to force the reactor into xenon instability, and by calculations. No xenon instabilities have ever been observed in the test results. All of these indicators have proven that xenon transients are highly damped in a BWR due to the large negative power coefficient of reactivity (Ref. 1).

Important features of the reactor core arrangement are as follows:

a.   The bottom-entry cruciform control rod blades (CRBs) are a mix of the General Electric Nuclear Energy (GENE) Original Equipment Manufacturer (OEM) CRBs and functional equivalents.

The OEM control rods consist of boron carbide (B_4C) in longitudinal stainless steel tubes surrounded by a stainless steel sheath. Prior to commercial operation at GGNS, rods of this design have been irradiated for more than eight years in the Dresden-I reactor and have accumulated thousands of hours of service without significant failure in operating BWR's.

b.   The fixed in-core ion chambers provide continuous power range neutron flux monitoring. A probe tube in each in-

core assembly provides for a traversing ion chamber for calibration and axial detail. Source and intermediate range monitors are located in-core and are axially retractable. The in-core location of the startup and source range instruments provides coverage of the large reactor core and provides an acceptable signal-to-noise ratio and neutron-to-gamma ratio. All in-core instrument leads enter from the bottom and the instruments are in service during refueling. In-core instrumentation is further discussed in subsection 7.6.1.5.

c.   As shown by experience obtained at Dresden 1 and other plants, the operator, utilizing the in-core flux monitor system, can maintain the desired power distribution within a large core by proper control rod scheduling.

d.   The Zircaloy-4 or Zircaloy-2 channels provide a fixed flow path for the boiling coolant, serve as a guiding surface for the control rods, and protect the fuel during handling operations.

e.   The mechanical reactivity control permits criticality checks during refueling and provides maximum plant safety. The core is designed to be subcritical at any time in its operating history with any one control rod fully withdrawn.

f.   The selected control rod pitch represents a practical value of individual control rod reactivity worth, and allows ample clearance below the pressure vessel between control rod drive mechanisms for ease of maintenance and removal.

4.1.2.1.2   Core Configuration

The reactor core is arranged as an upright circular cylinder containing a large number of fuel cells and is located within the reactor vessel. The coolant flows upward through the core. The core arrangement (plan view) and the lattice configuration are shown in Figure 4.3-1.

4.1.2.1.3   Fuel Assembly Description

As can be seen from the referenced figures, the boiling water reactor core is composed of essentially two components-fuel assemblies and control rods. The fuel assembly and control rod mechanical configurations for the initial core (see Figures 4.2-

1, through 4.2-5) were basically the standard General Electric design at that time. Reloads use similar fuel designs which are described further in this Chapter.

4.1.2.1.3.1   Fuel Rod

A fuel rod consists of UO_2 pellets and a Zircaloy-2 cladding tube. A fuel rod is made by stacking pellets into a Zircaloy-2 cladding tube which is evacuated and back filled and pressurized with helium and sealed by welding Zircaloy end plugs in each end of the tube.

The BWR fuel rod is designed as a pressure vessel. The ASME Boiler and Pressure Vessel Code, Section III, is used as a guide in the mechanical design and stress analysis of the fuel rod.

The rod is designed to withstand the applied loads, both external and internal. The fuel pellet is sized to provide sufficient volume within the fuel tube to accommodate differential expansion between fuel and clad. Overall fuel rod design is conservative in its accommodation of the mechanisms affecting fuel in a BWR environment. Fuel rod design bases are discussed in more detail in subsection 4.2.1.1.1.2.

4.1.2.1.3.2   Fuel Bundle

The current cycle fuel design contains fuel and water rods spaced and supported in a square (10x10) array by a lower and upper tie plate. This design has two important features:

a.   The bundle design places minimum external forces on a fuel rod; each fuel rod is free to expand in the axial direction.

b.   The unique structural design permits the removal and replacement, if required, of individual fuel rods.

The fuel assemblies of which the core is comprised are designed to meet all the criteria for core performance and to provide ease of handling. Selected fuel rods in each assembly differ from the others in uranium enrichment. This arrangement produces more uniform power production across the fuel assembly, and thus allows a significant reduction in the amount of heat transfer surface required to satisfy the design thermal limitations.

4.1.2.1.4   Assembly Support and Control Rod Location

All peripheral fuel assemblies are supported by the core plate. Otherwise, individual fuel assemblies in the core rest on fuel support pieces mounted on top of the control rod guide tubes. Each guide tube, with its fuel support piece, bears the weight of four assemblies and is supported by a control rod drive penetration nozzle in the bottom head of the reactor vessel. The core plate provides lateral support and guidance at the top of each control rod guide tube.

The top guide, mounted on top of the shroud, provides lateral support and guidance for the top of each fuel assembly. The reactivity of the core is controlled by cruciform control rods containing boron carbide, hafnium metal, or both and their associated mechanical hydraulic drive system. The control rods occupy alternate spaces between fuel assemblies. Each independent drive enters the core from the bottom, and can accurately position its associated control rod during normal operation and yet exert approximately ten times the force of gravity to insert the control rod during the scram mode of operation. Bottom entry allows optimum power shaping in the core, ease of refueling, and convenient drive maintenance.

4.1.2.2   Shroud

The shroud is a cylindrical, stainless steel structure which surrounds the core and provides a barrier to separate the upward flow through the core from the downward flow in the annulus, and also provides a floodable volume in the unlikely event of an accident which tends to drain the reactor pressure vessel. A flange at the top of the shroud mates with a flange on the top guide. The cylindrical wall of the top guide and the shroud head form the core discharge plenum. The jet pump discharge diffusers penetrate the shroud support below the core elevation to introduce the coolant to the inlet plenum. To prevent direct flow from the inlet to the outlet nozzles of the recirculation loops, the shroud support is welded to the vessel wall. The shroud support is designed to support and locate the jet pumps, core support structure, and the peripheral fuel assemblies.

LPCI flow is discharged into the reactor core through the LPCI couplings penetrating the shroud through three 10-inch-diameter openings below the top guide. A flow deflector welded to the inside of the shroud at each LPCI opening disperses the entering flow to reduce the flow forces on in-core instruments.

Mounted inside the top guide cylinder in the space between the top of the core and the shroud head flange are the core spray spargers with spray nozzles for injection of cooling water. The core spray spargers and nozzles do not interfere with the installation or removal of fuel from the core.

4.1.2.3   Shroud Head and Steam Separators

The shroud head consists of a flange and dome onto which is welded an array of standpipes, with a steam separator located at the top of each standpipe. The shroud head mounts on the flange at the top of the top guide and forms the cover of the core discharge plenum region. The joint between the shroud head and top guide flange does not require a gasket or other replacement sealing technique. The fixed axial flow-type steam separators have no moving parts and are made of stainless steel.

In each separator, the steam-water mixture rising from the standpipe impinges on vanes which give the mixture a spin to establish a vortex wherein the centrifugal forces separate the steam from the water. Steam leaves the separator at the top and passes into the wet steam plenum below the dryer. The separated water exits downward from the separator and enters the pool that surrounds the standpipes to enter the downcomer annulus. An internal steam separator schematic is shown in Figure 4.1-1.

The shroud head is bolted to the top guide flange by shroud head studs that have a short extension for easy access during refueling. The shroud head is guided into position on the top guide shroud via guide rods on the inside of the vessel. One objective of the shroud head stud design is to provide direct access to the studs during reactor refueling operations with minimum underwater tool manipulation during the removal and installation of the assemblies.

4.1.2.4   Steam Dryer Assembly

The steam dryer assembly is mounted in the reactor vessel above the shroud head and forms the top and sides of the wet steam plenum. Vertical guide rods on the inside of the vessel provide

alignment for the dryer assembly during installation. The dryer assembly is supported by pads extending from the vessel wall and is locked into position during operation by the reactor vessel top head. Steam from the separators flows upward into the dryer assembly. The steam leaving the top of the dryer assembly flows into vessel steam outlet nozzles which are located alongside the steam dryer assembly. Moisture is removed by the dryer vanes and flows first through a system of troughs and pipes to the pool surrounding the separators and then into the downcomer annulus between the core shroud and reactor vessel wall. The schematics of a typical steam dryer panel are shown in Figures 4.1-2 and 4.1-3.

4.1.3   Reactivity Control Systems

4.1.3.1   Operation

The control rods perform dual functions of power distribution shaping and reactivity control. Power distribution in the core is controlled during operation of the reactor by manipulation of selected patterns of rods. The rods, which enter from the bottom of the near-cylindrical reactor core, are positioned in such a manner to counterbalance steam voids in the top of the core and effect significant power flattening.

These groups of control elements, used for power flattening, experience a somewhat higher duty cycle and neutron exposure than the other rods in the control system.

The reactivity control function requires that all rods be available for either reactor scram (prompt shutdown) or reactivity regulation. Because of this, the control elements are mechanically designed to withstand the dynamic forces resulting from a scram. They are connected to bottom-mounted, hydraulically actuated drive mechanisms which allow either axial positioning for reactivity regulation or rapid scram insertion. The design of the rod-to-drive connection permits each blade to be attached or detached from its drive without disturbing the remainder of the control system. The bottom-mounted drives permit the entire control system to be left intact and operable for tests with the reactor vessel open.

4.1.3.2   Description of Rods

The General Electric Nuclear Energy (GENE) Original Equipment Manufacturer (OEM) cruciform shaped control rods contain 72 stainless steel tubes (18 tubes in each wing of the cruciform)

filled with vibration compacted boron-carbide powder. The tubes
are seal welded with end plugs on either end. Stainless steel
balls are used to separate the tubes into individual
compartments. The stainless steel balls are held in position by a
slight crimp in the tube. The individual tubes act as pressure
vessels to contain the helium gas released by the boron-neutron
capture reaction.

The tubes are held in a cruciform array by a stainless steel
sheath extending the full length of the tubes. A top handle, shown
in Figure 4.2-5, aligns the tubes and provides structural
rigidity at the top of the control rod. Rollers, housed in the
handle, provide guidance for control rod insertion and
withdrawal. A bottom casting is also used to provide structural
rigidity and contains positioning rollers and a parachute-shaped
velocity limiter. The handle and lower casting are welded into a
single structure by means of a small cruciform post located in the
center of the control rod. A steel stiffener is located
approximately at the midspan of each cruciform wing. The control
rods can be positioned at 6-in. steps and have a nominal
withdrawal and insertion speed of 3 in./sec.

The velocity limiter is a device which is an integral part of the
control rod and protects against the low probability of a rod drop
accident. It is designed to limit the free fall velocity and
reactivity insertion rate of a control rod so that minimum fuel
damage would occur. It is a one-way device, in that control rod
scram time is not significantly affected.

Control rods are cooled by the core leakage (bypass) flow. The
core leakage flow is made up of recirculation flow that leaks
through the several leakage flow paths, which are:

   a.   The area between fuel channel and fuel assembly nosepiece

   b.   The area between fuel assembly nosepiece and fuel support
        piece

   c.   The area between fuel support piece and core plate

   d.   The area between core plate and shroud

The GENE Marathon and Marathon Ultra HD control rods were
designed to be a direct replacement for any BWR/6 control rod.
A detailed description of the GE Marathon and Marathon Ultra HD
control rods can be found in Section 4.2.1.2.2. Figures 4.2-6c
shows the Marathon Control rod. The Marathon Ultra HD control
rod is similar to the Marathon.

4.1.3.3   Supplementary Reactivity Control

[HISTORICAL INFORMATION] [The control requirements of the initial core are designed to be considerably in excess of the equilibrium core requirements because of the long initial operating cycle.] The core control requirements are met by use of the combined effects of the movable control rods and a supplemental burnable poison. The supplementary burnable poison is gadolinia (Gd_2O_3) mixed with UO_2 in several fuel rods in each fuel bundle.

4.1.4   Analysis Techniques

4.1.4.1   Reactor Internal Components

[HISTORICAL INFORMATION] [Computer codes that were used for the analysis of the internal components are listed as follows:

    a.   MASS

    b.   SNAP (MULTISHELL)

    c.   GASP

    d.   NOHEAT

    e.   FINITE

    f.   DYSEA

    g.   SHELL 5

    h.   HEATER

    i.   FAP-71

    j.   CREEP-PLAST

Detailed descriptions of these programs are given in the following subsections:]

4.1.4.1.1   MASS (Mechanical Analysis of Space Structure)

4.1.4.1.1.1   Program Description

[HISTORICAL INFORMATION] [The program, proprietary of the General Electric Company, is an outgrowth of the PAPA (Plate and Panel Analysis) program originally developed by L. Beitch in the early

1960s. The program is based on the principle of the finite element method. Governing matrix equations are formed in terms of joint displacements using a "stiffness-influence-coefficient" concept originally proposed by Beitch (Ref. 2). The program offers curved beam, plate, and shell elements. It can handle mechanical and thermal loads in a static analysis and predict natural frequencies and mode shapes in a dynamic analysis.]

4.1.4.1.1.2   Program Version and Computer

[HISTORICAL INFORMATION] [The Nuclear Energy Division is using a past revision of MASS. This revision is identified as revision "0" in the computer production library. The program operates on the Honeywell 6000 computer.]

4.1.4.1.1.3   History of Use

[HISTORICAL INFORMATION] [Since its development in the early 1960s, the program has been successfully applied to a wide variety of jet-engine structural problems, many of which involve extremely complex geometries. The use of the program in the Nuclear Energy Division also started shortly after its development.]

4.1.4.1.1.4   Extent of Application

[HISTORICAL INFORMATION] [Besides the Jet Engine and Nuclear Energy Divisions, the Missile and Space Division, the Appliance Division, and the Turbine Division of General Electric have also applied the program to a wide range of engineering problems. The Nuclear Energy Division (NED) uses it mainly for piping and reactor internals analyses.]

4.1.4.1.2   SNAP (MULTISHELL)

4.1.4.1.2.1   Program Description

[HISTORICAL INFORMATION] [The SNAP Program, which is also called MULTISHELL, is the General Electric Code which determines the loads, deformations, and stresses of axisymmetric shells of revolution (cylinders, cones, discs, toroids, and rings) for axisymmetric thermal boundary and surface load conditions. Thin shell theory is inherent in the solution of E. Peissner's differential equations for each shell's influence coefficients. Surface loading capability includes pressure, average temperature, and linear through wall gradients; the latter two

may be linearly varied over the shell meridian. The theoretical
limitations of this program are the same as those of classical
theory.]

4.1.4.1.2.2   Program Version and Computer

[HISTORICAL INFORMATION] [The current version maintained by the
General Electric Jet Engine Division at Evandale, Ohio, is being
used on the Honeywell 6000 computer in GE/NED.]

4.1.4.1.2.3   History of Use

[HISTORICAL INFORMATION] [The initial version of the Shell
Analysis Program was completed by the Jet Engine Division in 1961.
Since then, a considerable amount of modification and addition
has been made to accommodate its broadening area of application.
Its application in the Nuclear Energy Division has a history
longer than 10 years.]

4.1.4.1.2.4   Extent of Application

[HISTORICAL INFORMATION] [The program has been used to analyze
jet engine, space vehicle, and nuclear reactor components.
Because of its efficiency and economy, in addition to
reliability, it has been one of the main shell analysis programs
in the Nuclear Energy Division of General Electric.]

4.1.4.1.3   GASP

4.1.4.1.3.1   Program Description

[HISTORICAL INFORMATION] [GASP is a finite element program for
the stress analysis of axisymmetric or plane two-dimensional
geometries. The element representations can be either
quadrilateral or triangular. Axisymmetric or plane structural
loads can be input at nodal points. Displacements, temperatures,
pressure loads, and axial inertia can be accommodated. Effective
plastic stress and strain distributions can be calculated using a
bilinear stress-strain relationship by means of an iterative
convergence procedure.]

4.1.4.1.3.2   Program Version and Computer

[HISTORICAL INFORMATION] [The GE version, originally obtained
from the developer, Professor E. L. Wilson, operates on the
Honeywell 6000 computer.]

4.1.4.1.3.3   History of Use

[HISTORICAL INFORMATION] [The program was developed by E. L. Wilson in 1965 (Ref. 3). The present version in GE/NED has been in operation since 1967.]

4.1.4.1.3.4   Extent of Application

[HISTORICAL INFORMATION] [The application of GASP in GE/NED is mainly for elastic analysis of axisymmetric and plane structures under thermal and pressure loads. The GE version has been extensively tested and used by engineers in the company.]

4.1.4.1.4   NOHEAT

4.1.4.1.4.1   Program Description

[HISTORICAL INFORMATION] [The NOHEAT program is a two-dimensional and axisymmetric transient nonlinear temperature analysis program. An unconditionally stable numerical integration scheme is combined with iteration procedure to compute temperature distribution within the body subjected to arbitrary time and temperature-dependent boundary conditions.

This program utilizes the finite element method. Included in the analysis are the three basic forms of heat transfer, conduction, radiation, and convection, as well as internal heat generation. In addition, cooling pipe boundary conditions are also treated. The output includes temperature of all the nodal points for the time instants by the user. The program can handle multitransient temperature input.]

4.1.4.1.4.2   Program Version and Computer

[HISTORICAL INFORMATION] [The current version of the program is an improvement of the program originally developed by I. Farhoomand and Professor E. L. Wilson of University of California at Berkeley (Ref. 4). The program operates on the Honeywell 6000 computer.]

4.1.4.1.4.3   History of Use

[HISTORICAL INFORMATION] [The program was developed in 1971 and installed in the General Electric Honeywell computer by one of its original developers, I. Farhoomand, in 1972. A number of heat transfer problems related to the reactor pedestal have been satisfactorily solved using the program.]

4.1.4.1.4.4   Extent of Application

[HISTORICAL INFORMATION] [The program using finite element formulation is compatible with the finite element stress-analysis computer program GASP. Such compatibility simplified the connection of the two analyses and minimizes human error.]

4.1.4.1.5   FINITE

4.1.4.1.5.1   Program Description

[HISTORICAL INFORMATION] [FINITE is a general-purpose, finite element computer program for elastic stress analysis of two-dimensional structural problems including: (1) plane stress, (2) plane strain, and (3) axisymmetric structures. It has provision for thermal, mechanical, and body force loads. The materials of the structure may be homogeneous or inhomogeneous and isotropic or orthotropic. The development of the FINITE program is based on the GASP program. (See subsection 4.1.4.1.3.)]

4.1.4.1.5.2   Program Version and Computer

[HISTORICAL INFORMATION] [The present version of the program at GE/NED was obtained from the developer J. E. McConnelee of GE/Gas Turbine Department in 1969 (Ref. 5). The NED version is used on the Honeywell 6000 computer.]

4.1.4.1.5.3   History of Use

[HISTORICAL INFORMATION] [Since its completion in 1969, the program has been widely used in the Gas Turbine and the Jet Engine Departments of the General Electric Company for the analysis of turbine components.]

4.1.4.1.5.4   Extent of Usage

[HISTORICAL INFORMATION] [The program is used at GE/NED in the analysis of axisymmetric or nearly axisymmetric BWR internals.]

4.1.4.1.6   DYSEA

4.1.4.1.6.1   Program Description

[HISTORICAL INFORMATION] [The DYSEA (Dynamic and Seismic Analysis) program is a GE proprietary program developed specifically for seismic and dynamic analysis of RPV and internals/building system. It calculates the dynamic response of linear structural system by either temporal modal superposition or response spectrum method. Fluid-structure interaction effect in the RPV is taken into account by way of hydrodynamic mass.

Program DYSEA was based on program SAPIV with added capability to handle the hydrodynamic mass effect. Structural stiffness and mass matrices are formulated similar to SAPIV. Solution is obtained in time domain by calculating the dynamic response mode by mode. Time integration is performed by using Newmark's ß-method. Response spectrum solution is also available as an option.]

4.1.4.1.6.2   Program Version and Computer

[HISTORICAL INFORMATION] [The DYSEA version now operating on the Honeywell 6000 computer of GE, Nuclear Energy Systems Division, was developed at GE by modifying the SAPIV program. Capability was added to handle the hydrodynamic mass effect due to fluid-structure interaction in the reactor. It can handle 3-dimensional dynamic problems with beam, trusses, and springs. Both acceleration time histories and response spectra may be used as input.]

4.1.4.1.6.3   History of Use

[HISTORICAL INFORMATION] [The DYSEA program was developed in the summer of 1976. It has been adopted as a standard production program since 1977 and it has been used extensively in all dynamic and seismic analyses of the RPV and internals/building system.]

4.1.4.1.6.4   Extent of Application

[HISTORICAL INFORMATION] [The current version of DYSEA has been used in all dynamic and seismic analysis since its development. Results from test problems were found to be in close agreement with those obtained from either verified programs or analytic solutions.]

4.1.4.1.7   SHELL 5

4.1.4.1.7.1   Program Description

[HISTORICAL INFORMATION] [SHELL 5 is a finite shell element
program used to analyze smoothly curved thin shell structures
with any distribution of elastic material properties, boundary
constraints, and mechanical thermal and displacement loading
conditions. The basic element is triangular whose membrane
displacement fields are linear polynomial functions, and whose
bending displacement field is a cubic polynomial function (Ref.
6). Five degrees of freedom (three displacements and two bending
rotations) are obtained at each nodal point. Output displacements
and stresses are in a local (tangent) surface coordinate system.

Due to the approximation of element membrane displacements by
linear functions, the in-plane rotation about the surface normal
is neglected. Therefore, the only rotations considered are due to
bending of the shell cross section and application of the method
is not recommended for shell intersection (or discontinuous
surface) problems where in-plane rotation can be significant.]

4.1.4.1.7.2   Program Version and Computer

[HISTORICAL INFORMATION] [A copy of the source deck of SHELL 5 is
maintained in GE/NED by Y. R. Rashid, one of the originators of
the program. SHELL 5 operates on the UNIVAC 1108 computer.]

4.1.4.1.7.3   History of Use

[HISTORICAL INFORMATION] [SHELL 5 is a program developed by Gulf
General Atomic Incorporated (Ref. 7) in 1969. The program has been
in production status at Gulf General Atomic, General Electric,
and other major computer operating systems since 1970.]

4.1.4.1.7.4   Extent of Application

[HISTORICAL INFORMATION] [SHELL 5 has been used at General
Electric to analyze reactor shroud support and torus.
Satisfactory results were obtained.]

4.1.4.1.8   HEATER

4.1.4.1.8.1   Program Description

[HISTORICAL INFORMATION] [HEATER is a computer program used in the hydraulic design of feedwater spargers and their associated delivery header and piping. The program utilizes test data obtained by GE using full scale mockups of feedwater spargers combined with a series of models which represent the complex mixing processes obtained in the upper plenum, downcomer, and lower plenum. Mass and energy balances throughout the nuclear steam supply system are modeled in detail (Ref. 8).]

4.1.4.1.8.2   Program Version and Computer

[HISTORICAL INFORMATION] [This program was developed at GE/NED in FORTRAN IV for the Honeywell 6000 computer.]

4.1.4.1.8.3   History of Use

[HISTORICAL INFORMATION] [The program was developed by various individuals in GE/NED beginning in 1970. The present version of the program has been in operation since January 1972.]

4.1.4.1.8.4   Extent of Application

[HISTORICAL INFORMATION] [The program is used in the hydraulic design of the feedwater spargers for each BWR plant, in the evaluation of design modifications, and the evaluation of unusual operational conditions.]

4.1.4.1.9   FAP-71 (Fatigue Analysis Program)

4.1.4.1.9.1   Program Description

[HISTORICAL INFORMATION] [The FAP-71 computer code, or Fatigue Analysis Program, is a stress analysis tool used to aid in performing ASME Code, Section III, structural design calculations. Specifically, FAP-71 is used in determining the primary plus secondary stress range and number of allowable fatigue cycles at points of interest. For structural locations at which the $3S_m$ (P+Q) ASME Code limit is exceeded, the program can perform either (or both) of two elastic-plastic fatigue life evaluations: (1) the method reported in ASME Paper 68-PVP-3 and (2) the present method documented in Paragraph NB-3228.3 of the

1971 edition of the ASME Code, Section III. The program can accommodate up to 25 transient stress states of as many as 20 structural locations.]

4.1.4.1.9.2   Program Version and Computer

[HISTORICAL INFORMATION] [The present version of FAP-71 was completed by L. Young of GE/NED in 1971 (Ref. 9). The program currently is on the NED Honeywell 6000 computer.]

4.1.4.1.9.3   History of Use

[HISTORICAL INFORMATION] [Since its completion in 1971, the program has been applied to several design analyses of GE BWR vessels.]

4.1.4.1.9.4   Extent of Use

[HISTORICAL INFORMATION] [The program is used in conjunction with several shell analysis programs in determining the fatigue life of BWR mechanical components subject to thermal transients.]

4.1.4.1.10   CREEP/PLAST

4.1.4.1.10.1 Program Description

[HISTORICAL INFORMATION] [A finite element program is used for the analysis of 2-dimensional (plane and axisymmetric) problems under conditions of creep and plasticity. The creep formulation is based on the memory theory of creep in which the constitutive relations are cast in the form of hereditary integrals. The material creep properties are built into the program and they represent annealed 304 stainless steel. Any other creep properties can be included if required.

The plasticity treatment is based on kinematic hardening and von Mises' yield criterion. The hardening modulus can be constant or a function of strain.]

4.1.4.1.10.2 Program Version and Computer

[HISTORICAL INFORMATION] [The program can be used for elastic-plastic analysis with or without the presence of creep. It can also be used for creep analysis without the presence of instantaneous plasticity. A detailed description of theory is given in Reference 11. The program is operative on Univac-1108.]

4.1.4.1.10.3 History of Use

[HISTORICAL INFORMATION] [This program was developed by Y. R. Rashid (Ref. 11) in 1971. It underwent extensive program testing before it was put on production status.]

4.1.4.1.10.4 Extent of Application

[HISTORICAL INFORMATION] [The program is used at GE/NED in the channel cross section mechanical analysis.]

4.1.4.2 Fuel Rod Thermal Analysis

Fuel thermal design analyses are performed utilizing the classical relationships for heat transfer in cylindrical coordinate geometry with internal heat generation. Conditions of 100 percent and at least 116 percent of rated power are analyzed corresponding to steadystate and short-term transient operation. Abnormal operation transients are also evaluated to assure that the damage limit of 1.0 percent cladding plastic strain is not violated. The strength theory, terminology, and strain-stress categories presented in the ASME Boiler and Pressure Vessel Code, Section III, are used as a guide in the mechanical design and stress analysis of the fuel rods.

4.1.4.3 Reactor Systems Dynamics

Subsection 4.4.4.6 provides a complete stability analysis for the reactor coolant system.

4.1.4.4 Nuclear Engineering Analysis

The analysis techniques are described and referenced in subsection 4.3.3. The codes used in the analysis are:

Computer Code	Function Lattice Physics
Model	Calculates average few-group cross sections, bundle reactivities, and relative fuel rod powers within the fuel bundle

Computer Code	Function Lattice Physics
BWR Reactor Simulator	Calculates 3-dimensional nodal power distributions, exposures and thermal hydraulic characteristics as burnup progresses.

4.1.4.5 Neutron Fluence Calculations

Calculations of the best estimate neutron fluence, and its uncertainty, to the Grand Gulf Nuclear Station (GGNS) reactor pressure vessel (RPV), core shroud and top guide horizontal and vertical welds, as well as to several beltline vessel nozzles have been performed. The fluence calculations were carried out using a three dimensional (3D) neutron transport model for each fuel cycle starting from cycle 1 through cycle 21. The 3D neutron transport calculations were benchmarked on a plant-specific basis by comparing calculated results against previously performed core region two dimensional (2D) synthesis data as well as by calculation of the measured-to-calculated (M/C) ratios for GGNS dosimetry. In addition, a comprehensive benchmarking report, Reference 16, of MP Machinery and Testing methods has been prepared.

The neutron transport calculational procedures and dosimetry analysis methods meet standards specified by the NRC and ASTM as appropriate. In particular, the transport analysis meets the requirements of Regulatory Guide 1.190 (RG 1.190). Since RG 1.190 is focused on 2D synthesis methods, it is strictly applicable to analyses in the active fuel region. Nevertheless, the guidance provided in RG 1.190 was followed to the extent practical for modeling work in the regions above and below the active fuel region. The 3D neutron transport calculations were used to determine detailed fluence profiles at the end of cycle 21 (28.088 EFPY), and projected to exposures of 35 EFPY and 54 EFPY, Reference 17.

Additional vessel fluence calculations, which comply with the requirements of Regulatory Guide 1.190, are described in Section 4.3.2.8.

4.1.4.6   Thermal-Hydraulic Calculations

The digital computer program is a parallel flow path used to perform the steady-state BWR reactor core thermal-hydraulic analysis. Program input includes the core geometry, operating power, pressure, coolant flow rate and inlet enthalpy, and power distribution within the core. Output from the program includes core pressure drop, coolant flow distribution, critical power ratio, and axial variations of quality, density, and enthalpy for each channel type.

4.1.5   Deleted

4.1.6   References

1. Crowther, R. L., "Xenon Considerations in Design of Boiling Water Reactors," APED-5640, June 1968

2. Beitch, L., "Shell Structures Solved Numerically by Using a Network of Partial Panels," AIAA Journal, Volume 5, No. 3, March 1967

3. Wilson E. L., "A Digital Computer Program For the Finite Element Analysis of Solids With Non Linear Material Properties," Aerojet General Technical Memo No. 23, Aerojet General, July 1965

4. Farhoomand, I., and Wilson E. L., "Non-Linear Heat Transfer Analysis of Axisymmetric Solids," SESM Report SESM71-6, University of California at Berkeley, Berkeley, California, 1971

5. McConnelee J. E., "Finite-Users Manual," General Electric TIS Report DF 69SL206, March 1969

6. Clough R. W. and Johnson C. P., "A Finite Element Approximation For the Analysis of Thin Shells," International Journal Solid Structures, Vol. 4, 1968

7. "A Computer Program For the Structural Analysis of Arbitrary Three-Dimensional Thin Shells," Report No. GA-9952, Gulf General Atomic

8. Burgess, A. B., "User Guide and Engineering Description of HEATER Computer Program," March 1974

9. Young, L. J., "FAP-71 (Fatigue Analysis Program) Computer Code," GE/NED Design Analysis Unit R. A. Report No. 49, January 1972

10. Deleted

11. Rashid Y. R., "Theory Report for CREEP-PLAST Computer Program," GEAP-10546, AEC Research and Development Report, January 1972

12. Deleted

13. Deleted

14. Deleted

15. Deleted

16. MPM-614993, Rev. 5, Benchmarking of MPM Methods for Nuclear Plant Neutron Transport Calculations

17. MPM-814779, Rev. 5 Neutron Transport Analysis for Grand Gulf Nuclear Station

WET STEAM

RETURNING WATER

STEAM WATER MIXTURE

WATER LEVEL

RETURNING WATER

TURNING VANES
(INLET NOZZLE)

STANDPIPE

CORE DISCHARGE PLENUM
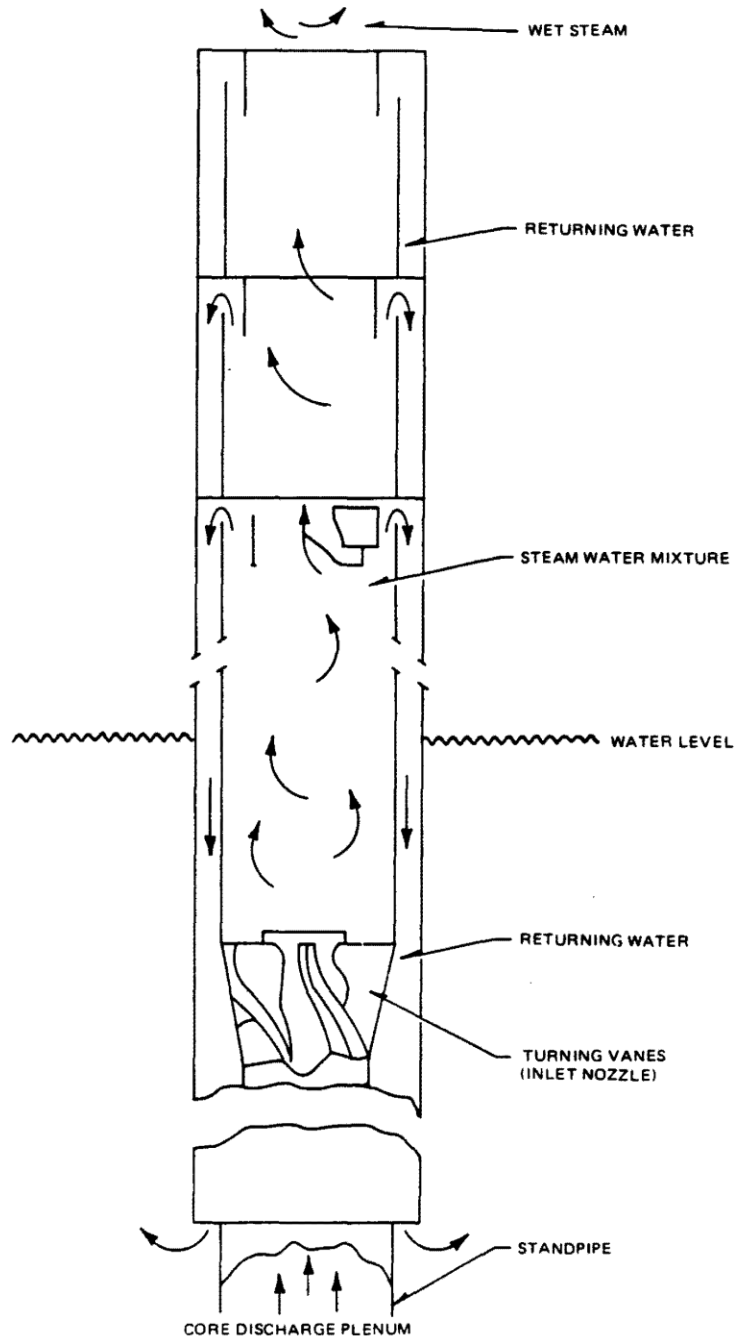
GRAND GULF NUCLEAR STATION UNIT 1 UPDATED FINAL SAFETY ANALYSIS REPORT	STEAM SEPARATOR FIGURE 4.1-1

STEAM FLOW
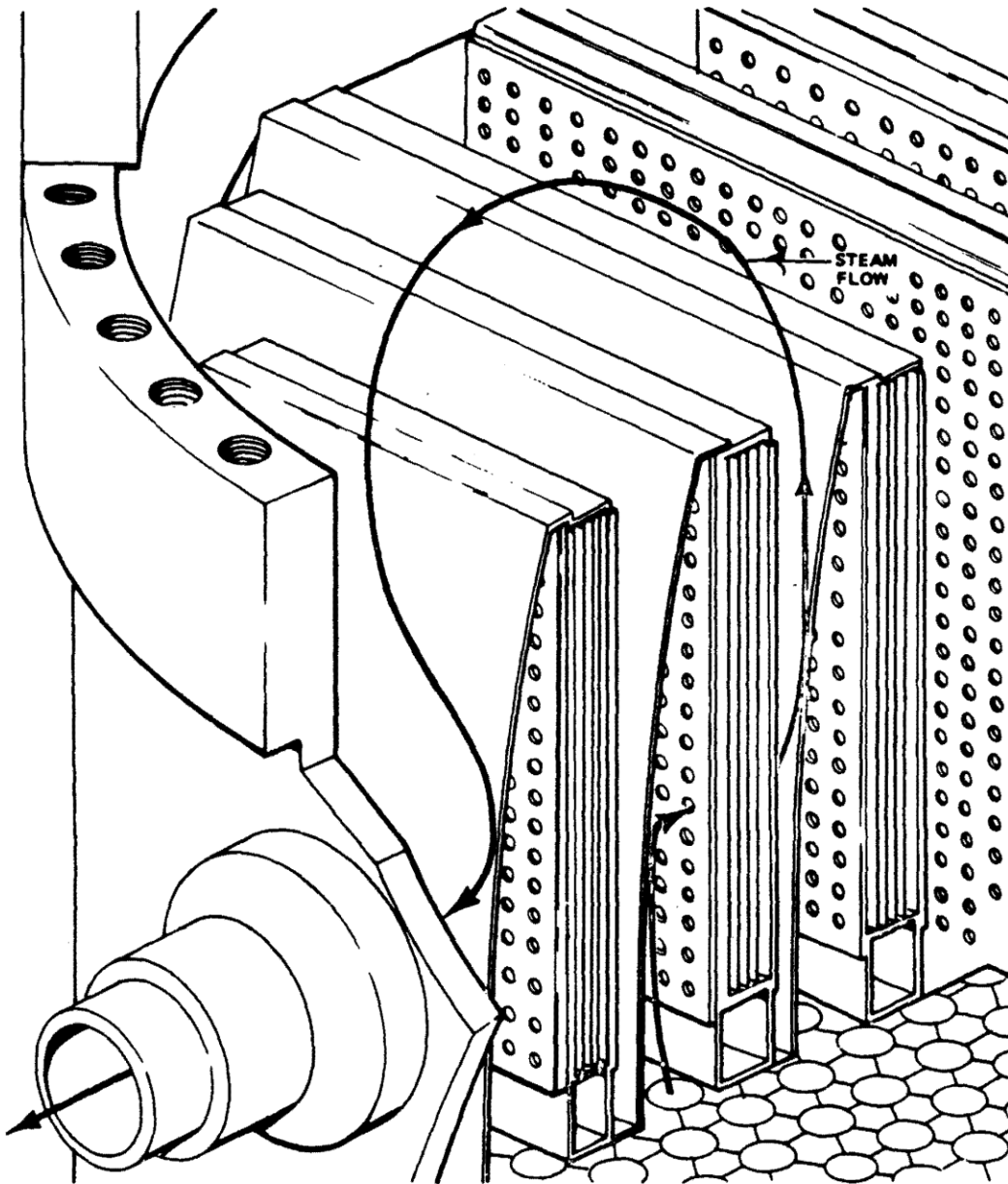
GRAND GULF NUCLEAR STATION UNIT 1 UPDATED FINAL SAFETY ANALYSIS REPORT	STEAM DRYER PANEL FIGURE 4.1-2

CROSS-SECTION VIEW

VANES

COLLECTING TROUGH
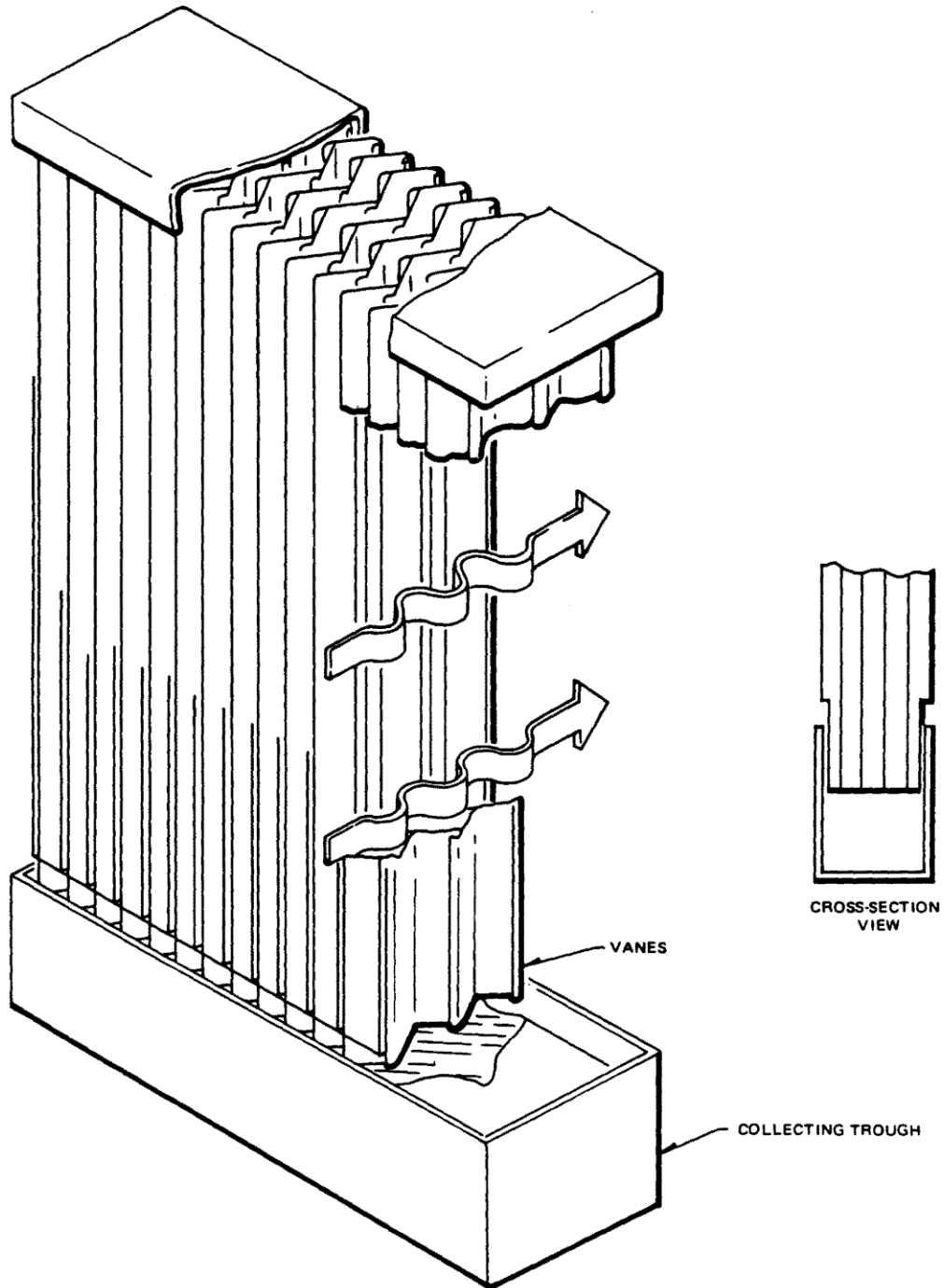
GRAND GULF NUCLEAR STATION UNIT 1 UPDATED FINAL SAFETY ANALYSIS REPORT	STEAM DRYER FIGURE 4.1-3

4.2   FUEL SYSTEM DESIGN

4.2.1   General and Detailed Design Bases

4.2.1.1   General Design Bases

The following paragraphs define the general mechanical design bases that are considered in defining the design of the fuel assembly and its components and the control assembly and its components. In addition the fuel design shall meet the limits on linear heat generation rate (LHGR) which shall not be exceeded during steady state operation. The design basis for each of the fuel system damage, failure, and coolability criteria identified by Section II.A of Standard Review Plan 4.2, except control rod reactivity, are provided in Subsection 2.2 of Reference 51. The generic information provided in Reference 51 is supplemented by plant specific, cycle specific information and analysis that is contained in a Supplemental Reload Licensing Report.

4.2.1.1.1   Fuel Assembly and Its Components

4.2.1.1.1.1   Safety Design Bases

The fuel assembly is designed to ensure, in conjunction with the core nuclear characteristics (see Section 4.3), the core thermal and hydraulic characteristics (see Section 4.4), the plant equipment characteristics, and the instrumentation and protection system, that fuel damage will not result in the release of radioactive materials in excess of the guideline values of 10 CFR 20, 50, and 100.

The mechanical design process emphasizes that:

a.   The fuel assembly shall provide substantial fission product retention capability during all potential operational modes.

b.   The fuel assembly shall provide sufficient structural integrity to prevent operational impairment of any reactor safety equipment.

Assurance of the design basis considerations is provided by the following fuel assembly capabilities:

Pressure and Temperature Capabilities

The fuel assembly and its components are capable of withstanding the predicted thermal, pressure, and mechanical interaction loadings occurring during startup testing, normal operation, and abnormal operation without impairment of operational capability.

Handling Capability

The fuel assembly and each component thereof is capable of withstanding loading predicted to occur during handling without impairment of operational capability

Earthquake Loading Capability (1/2 SSE)

The fuel assembly and each component thereof is capable of sustaining in-core loading predicted to occur from an operating basis earthquake (OBE), when occurring during normal operating conditions without impairment of operational capability.

Earthquake Loading Capability (SSE)

The fuel assembly and each component thereof is capable of sustaining in-core loading predicted to occur from a safe shutdown earthquake (SSE) when occurring during normal operation without:

a.   Exceeding deflection limits which allow control rod insertion

b.   Fragmentation or severance of any bundle component

Accident Capability

The capability of the fuel assembly to withstand the control rod drop accident, the pipe breaks inside containment accidents, the fuel handling accident, the recirculation pump seizure accident, and the pipe breaks outside the containment accidents is determined by analysis of the specific event.

The ability of the fuel assembly and its components to provide the preceding capabilities is evaluated by one or more of the following:

a.   Analyses developed and design ratios formulated to measure results against acceptance criteria. (See subsection 4.2.1.1.1.3.)

b.   Analytical procedures based upon classical methods which do not change, and are patterned after the ASME Boiler and Pressure Vessel Code Section III. This procedure allows analytical comparisons of new and old designs and maintains consistency of design characteristics. (See subsection 4.2.1.1.1.4.)

c.   Experience and testing. (See subsections 4.2.1.2, 4.2.4, and 4.2.5.)

4.2.1.1.1.2   Basis for Fuel Rod Safety Evaluation

Fuel damage is defined as a perforation of the fuel rod cladding which would permit the release of fission products to the reactor coolant.

The mechanisms which could cause fuel damage in reactor operational transients and which are considered in fuel evaluations are: (1) rupture of the fuel rod cladding due to strain caused by relative expansion of the UO_2 pellet and (2) severe overheating of the fuel rod cladding caused by inadequate cooling. (See subsection 4.2.1.2.1.5.)

4.2.1.1.1.3   Design Ratios

Design ratios are used by various supporting analyses and are defined by the following relationship: D.R. = A/L where D.R. is the design ratio, L is the limiting parameter value, and A is the actual parameter value. Design ratios of less than one shall be demonstrated for component parameters influenced by loading conditions which may affect the structural or dimensional integrity of the fuel assembly or any component thereof.

[HISTORICAL INFORMATION] [A description of the structural considerations for the initial core is provided below.

a.   Limiting Parameter Values

1.   Normal and Upset Design Conditions

Limiting parameter values for each component shall be determined in the following manner as defined by Table 4.2-1.

For stress resulting from mean value or steadystate loading, the limiting value shall be determined by

consideration of the material 0.2 percent offset
yield strength or the equivalent strain, as
established at operating temperature.

For stress resulting from load cycling, limiting
parameter values shall be determined from fatigue
limits.

For stress resulting from loading of significant
duration, the limiting parameter shall be determined
from considerations of stress rupture as defined by
the Larson-Miller parameter. If metal temperatures
are below the level of applicability of stress
rupture for the material or if the yield strength is
more limiting, then the limiting value of stress
shall be determined from consideration of the
material 0.2 percent offset yield strength or the
equivalent strain, as established at operating
temperatures.

Where stress rupture and fatigue cycling are both
significant, the following limiting condition shall
be applied:

$$\left(\frac{\text{actual time at stress}}{\text{allowable time at stress}}_{I=1 \text{ to } n} + \frac{\text{actual number of cycles}}{\text{allowable cycles at stress}}_{I=1 \text{ to } m} \right) \leq 1$$

Critical instability loads shall be derived from test
data when available or from analytical methods when
applicable test data are not available.

Deflection limits shall be those values of component
deformation which could cause an undesirable event
such as impairment of control rod movement or an
excessive bypass flow rate.

2. Emergency and Faulted Design Conditions

Limiting parameter values shall be determined in the
following manner as defined by Table 4.2-1.

    (a)   Stress limits shall be determined from consideration of the ultimate tensile strength or equivalent strain of the material, as established at operating temperatures.

    (b)   Critical instability loads shall be determined from test data when available or from analytical methods when applicable test data are not available.

    (c)   Deflection limits shall be those values of deformation that, if occurring, could lead to a more serious consequence such as prevention of control rod insertion.

b.   Actual Parameter Values

Actual parameter values shall be determined from the following considerations:

1.   Effective stresses shall be determined at each point of interest using the theory of constant elastic strain energy of distortion:

$$2\sigma_e^{\,2} = (\sigma_x - \sigma_y)^2 + (\sigma_y - \sigma_z)^2 + (\sigma_z - \sigma_x)^2 + 6(\sigma_{xy}^{\,2} + \sigma_{yz}^{\,2} + \sigma_{zx}^{\,2})$$

2.   Stress concentration may be applied only to the alternating stress component.

3.   Design values of instability loads shall be scaled up to allow for uncertainty in manner of load application, variation in modulus of elasticity, and difference between the actual case and theoretical one.

4.   Calculated values of deflection for comparison with deflection limits may be based on the resulting permanent set after load removal if load removal occurs before damage may result.]

4.2.1.1.1.4   Maximum Allowable Stresses, Cycling and Fatigue Limits

[HISTORICAL INFORMATION] [The strength theory, terminology, and stress categories presented in the ASME Boiler and Pressure Vessel Code, Section III, are used as a guide in the mechanical

design and stress analysis of the reactor fuel rods. The mechanical design is based on the maximum shear stress theory for combined stresses. The equivalent stress intensities used are defined as the difference between the most positive and least positive principal stresses in a triaxial field. Thus, stress intensities are directly comparable to strength values found from tensile tests. Table 4.2-2 presents a summary of the typical basic stress intensity limits that are applied for Zircaloy-2 cladding.

The fatigue analysis for the initial core utilized the linear cumulative damage rule (Miner's hypothesis, Ref. 1) and the Zircaloy fatigue design basis of Reference 2. This correlation includes a safety factor of 2 on stress or 20 on cycles (whichever is more conservative). The fatigue analysis was based on the cycles shown in Table 4.2-3. The expected time duration for each of the subject cyclic loadings is not specified and for the startup and reduced power cycles can vary according to the reactor status and power demand. The cyclic condition relating to overpower transients would result from an operator error or equipment malfunction, and would, therefore, be expected to be of short duration (less than 8 hours). Additional information regarding the basis for the fatigue analysis is presented in Section 6 of Reference 4.]

For the current reload fuel, information on the fatigue analysis is provided in Reference 51 (GEH).

4.2.1.1.2   Control Assembly and Its Components

Safety Design Basis

The reactivity control mechanical design shall include control rods and gadolinia burnable poison in selected fuel rods within fuel assemblies and shall meet the following safety design bases.

   a.   The control rods shall have sufficient mechanical strength to prevent displacement of their reactivity control material.

   b.   The control rods shall have sufficient strength and be so designed as to prevent deformation that could inhibit their motion.

   c.   Each control rod shall have a device to limit its free fall velocity sufficiently to avoid damage to the nuclear system process barrier by the rapid reactivity increase

resulting from a free fall of one control rod from its fully inserted position to the position where the drive was withdrawn.

4.2.1.2   Detailed Design Bases

4.2.1.2.1   Fuel Assembly and Its Components

The following paragraphs present the detailed bases which are considered in defining the design of the fuel assembly and its components.

4.2.1.2.1.1 Material Selection and Properties

The materials will be compatible with BWR conditions and retain their design capability during reactor operation. The mechanical, chemical, thermal, and radiation properties utilized as design bases are presented in Section 3 of Reference 3 for the initial core and Reference 67 for the current GNF2 fuel. The basic materials used in fuel assemblies are Zircaloy-2 and Zircaloy-4, Type-304 stainless steel, Inconel X and ceramic uranium dioxide and gadolinia.

4.2.1.2.1.2 Effects of Irradiation

a.   Cladding Properties, Fuel Swelling

Irradiation affects both fuel and cladding material properties. The effects include increased cladding strength and reduced cladding ductility. In addition, irradiation in a thermal reactor environment results in the buildup of both gaseous and solid fission products within the UO fuel pellet which tend to increase the pellet diameter, i.e., fuel irradiation swelling. [HISTORICAL INFORMATION] [The irradiation swelling model for the initial core was based on data reported in References 5 and 6 as well as an evaluation of all applicable high exposure data (Ref. 7). Pellet internal porosity and pellet-to-cladding gap are specified such that the thermal expansion and irradiation swelling are accommodated for the worst case dimensional tolerances throughout life.] Fuel irradiation swelling due to the volumetric expansion of the current GNF2 fuel material and fuel rod fission gas release and internal pressure are analyzed by the NRC approved PRIME model and computer program as described in Reference 67.

b.   Fuel Pellet-to-Cladding Gap and Gap Conductance

The primary purpose of the gap between the UO fuel pellet and Zircaloy cladding is to accommodate differential diametral expansion of fuel pellet and cladding and, thus, preclude the occurrence of excessive gross diametral cladding strain. A short time after reactor startup, the fuel cracks radially and redistributes out to the cladding. Experience has shown, however, that the gap volume remains available in the form of radial cracks to accommodate gross diametral fuel expansion.

[HISTORICAL INFORMATION] [For the initial core, the value of pellet-to-cladding thermal conductance used was 1000 Btu/h-ft²-F. This design value was empirically derived from post-irradiation data on exposed fuel with an initial pellet-to-cladding gap which is significantly larger than that employed in the General Electric fuel design.] For the current GNF2 fuel, the pellet-cladding interaction and gap conductance were determined by the NRC approved PRIME model and computer program as described in Reference 67.

[HISTORICAL INFORMATION] [The use in the initial core of the constant value of 1000 Btu/h-ft²-F for the pellet-cladding thermal conductance was found to be a conservative assumption when applied in conjunction with the integral fuel design models. Specifically, the design fission gas release model employed in the determination of fuel rod plenum size and cladding wall thickness was shown to over-predict available data on fission gas release when applied with a pellet-cladding thermal conductance value of 1000 Btu/h-ft²-F. Similarly, the design model for relative fuel cladding expansion (pellet-to-cladding interaction) also was shown to be very conservative relative to available data when a value of 1000 Btu/h-ft²-F is used for pellet-cladding thermal conductance (Ref. 7). Additional discussion and evaluation of the pellet-to-clad gap conductance of G.E. BWR fuel pre-pressurized to three atmospheres is contained in References 33 through 36.]

c.   Axial Ratcheting

[HISTORICAL INFORMATION] [Axial ratcheting of fuel
cladding is not considered in BWR fuel rod design.
Prototypical fuel rods have been operated in the Halden
test reactor with axial elongation transducers. No
significant axial ratcheting has been observed (Ref. 8).]

d.   Fuel Melting Temperature

[HISTORICAL INFORMATION] [Fission product buildup tends to
cause a slight reduction in fuel melting temperature. The
melting point of UO is considered to decrease with
irradiation at the rate of 32°C/ 10,000 (MWd/MT) based on
data from Reference 9.]

e.   Fuel Thermal Conductivity

[HISTORICAL INFORMATION] [For the initial core, in the
temperature range of interest (500°C), the fuel thermal
conductivity was not considered to be significantly
affected by irradiation as reported in Reference 10.] The
current reload accounted for the effects of irradiation as
reported in Reference 67.

f.   Fission Gas Release

A small fraction of the gaseous fission products is
released from the fuel pellets to produce an increase in
fuel rod internal gas pressure. [HISTORICAL INFORMATION]
[In general, such irradiation effects on fuel performance
have been characterized by available data and are
considered in determining design features and performance.
Thus, the irradiation effects on fuel performance are
inherently considered when determining whether or not the
stress intensity limits and temperature limits are
satisfied.] The effects of fuel swelling due to fuel rod
fission gas release and internal pressure are analyzed by
the NRC approved PRIME model and computer program as
described in Reference 67.

4.2.1.2.1.3   Flow-Induced Vibration

Flow-induced fuel rod vibrations depend on such parameters as
flow velocity, fuel rod geometry, fuel spacer pitch, fundamental
rod frequency and the excitation forces due to fluctuating
pressures. The stresses resulting from flow-induced vibrations
are considered in the mechanical design and evaluations of the

fuel rods. These stresses are compared to stress intensity limits as noted in subsection 4.2.1.1.1.4. Additional information may be found in Reference 65.

The flow-induced vibration effecting other fuel assembly components, are based upon testing and/or operational experience which, to date, has shown no significant adverse effects.

4.2.1.2.1.4   Fuel Densification

The fuel densification design bases include the effects of (1) power spikes due to axial gap formation; (2) increase in linear heat generation rate (LHGR) due to pellet length shortening; (3) creep collapse of the cladding due to axial gap formation; and (4) changes in stored energy due to decreased pellet-cladding thermal conductance resulting from increased radial gap size. [HISTORICAL INFORMATION] [For the initial core, the fuel densification models described in References 11, 12, and 13 were used.] The current GNF2 fuel densification model is described in Reference 67. Analyses of the effects of fuel densification on the design are contained in subsection 4.2.3.2.8.

4.2.1.2.1.5   Fuel Rod Damage Mechanisms

As noted in subsection 4.2.1.1.1.2, the mechanisms which could cause fuel damage are rupture of the fuel rod cladding due to strain caused by relative expansion of the UO pellet and severe overheating of the fuel rod cladding due to inadequate cooling.

A value of 1 percent plastic strain of the Zircaloy cladding has been defined as the limit below which fuel damage due to overstraining of the fuel cladding is not expected to occur. The 1 percent plastic strain value is based on data on the strain capability of irradiated Zircaloy cladding segments from fuel rod operated in several BWRs (Ref. 7). None of the data obtained falls below the 1 percent plastic strain value; however, a statistical distribution fit to the available data indicates the 1 percent plastic strain value to be approximately the 95 percent point in the total population. This distribution implies, therefore, a small (less than 5 percent) probability that some cladding segments may have plastic elongation less than 1 percent at failure.

The fuel cladding integrity safety limit ensures that fuel damage due to severe overheating of the fuel rod cladding, caused by inadequate cooling, is avoided.

4.2.1.2.1.6   Dimensional Stability

The fuel assembly and fuel components are designed to assure dimensional stability in service. The fuel cladding and channel specifications include provisions to preclude dimensional changes due to residual stresses. In addition, the fuel assembly is designed to accommodate dimensional changes that occur in service due to thermal differential expansion and irradiation effects. For example, the fuel rods are free to expand axially independently of one another.

4.2.1.2.1.7   Fuel Shipping and Handling

The two major handling loads considered are (1) the loads due to maximum upward acceleration of the fuel assembly while grappled and (2) the loads due to impact of the fuel assembly into the fuel support while grappled.

During shipment, the fuel bundle is in a horizontal position with flexible packing material installed to minimize shipping loads.

Fuel bundle shipping procedures are qualified by a test performed on each new design, and each individual bundle is inspected relative to important dimensional characteristics following shipment to verify that no dimensional deviations have occurred.

4.2.1.2.1.8   Capacity for Fission Gas Inventory

A plenum is provided at the top of each fuel rod to accommodate the fission gas released from the fuel during operation. [HISTORICAL INFORMATION] [For the initial core, the design basis was to provide sufficient volume to limit the fuel rod internal pressure so that cladding stresses do not exceed the limits given in Table 4.2-2 during normal operation and for short-term transients of 16 percent or less above the peak normal operating conditions.] For the current GNF2 fuel the design basis is that the rod internal pressure should not exceed the system pressure (1055 psia nominal) by a specified amount as discussed in Reference 65.

a.   Fuel Rod Internal Pressure

Fuel rod internal pressure is due to the helium which is backfilled during rod fabrication, the volatile content of the UO_2, and the fraction of gaseous fission products

which are released from the UO_2. The available fission gas retention volume is conservatively determined and the fuel rod internal pressure is calculated.

b.   Fission Gas Generation and Release

[HISTORICAL INFORMATION] [A quantity of 1.35 x 10^{-3} gram moles of fission gas is produced per MWd of power production. In fuel rod pressure and stress calculations for the initial core, 4.0 percent of the fission gas produced was assumed to be released from any UO_2 volume at a temperature less than 3000°F and 100 percent released from any UO_2 above 3000°F. The above basis was demonstrated by experiment to be conservative over complete range of design temperature and exposure conditions (Ref. 7).

Fission gas release effects for the initial core were analyzed for burnups greater than 20,000 MWd/MT. This analysis was addressed generically in Reference 38. Positions stated therein are applicable to the Grand Gulf design. Plant specific numbers relative to this analysis for Grand Gulf are tabulated in Table 4.2-14.]

Fission gas release effects for the current GNF2 fuel rod fission gas release and internal pressure is analyzed by the NRC approved PRIME model and computer program as described in Reference 67.

c.   Plenum Creepdown and Creep Collapse

Creepdown and creep collapse of the plenum are not considered because significant creep in the plenum region is not expected. The fuel rod is designed to be free-standing throughout its lifetime. The temperature and neutron flux in the plenum region are considerably lower than in the fueled region, thus the margin to creep collapse is substantially greater in the plenum. Direct measurements of irradiated fuel rods have given no indication of significant creepdown of the plenum.

4.2.1.2.1.9   Deflection

The operational fuel rod deflections considered are the deflections due to:

a. Manufacturing tolerances

b. Flow-induced vibration

c. Thermal effects

d. Axial load

There are two criteria that limit the magnitude of these deflections. One criterion is that the cladding stress limits must be satisfied; the other is that the fuel rod-to-rod and rod-to-channel clearances must be sufficient to allow free passage of coolant water to all heat transfer surfaces.

4.2.1.2.1.10 Fretting Wear and Corrosion

Fretting wear and corrosion have been considered in establishing the fuel mechanical design basis. Individual rods in the fuel assembly are held in position by spacers located at intervals along the length of the fuel rod. Springs are provided in each spacer cell so that the fuel rod is restrained to avoid excessive vibration.

4.2.1.2.1.11 Potential for Water-Logging Rupture

The potential and consequences of operating with waterlogged failed fuel rods have been considered. A survey of available information, including test results and observations of fuel failures in commercial reactors, indicates that rupture of the fuel rod should not result in failure propagation or significant fuel assembly damage that would affect coolability of the fuel bundle.

4.2.1.2.1.12 Potential for Hydriding

The fuel design bases relative to the clad hydriding mechanism are to assure, through a combination of engineering specifications and strict manufacturing controls, that production fuel will not contain excessive quantities of moisture or hydrogenous impurities. An engineering specification limit on the amount of hydrogen permitted in a manufactured fuel rod is defined which is less than or equal to the limit stated in Section II.A.1.d of Section 4.2 of the Standard Review Plan in NUREG-0800. Procedural controls are utilized in manufacturing to prevent introduction of hydrogenous impurities such as oils, plastics, etc., into the fuel rod.

4.2.1.2.1.13 Stress-Accelerated Corrosion

Stress corrosion cracking, the phenomenon whereby ductile material, such as Zircaloy-2, experiences non-ductile fracture, has been identified as a factor in pellet-cladding interaction fuel failure. The simultaneous action of certain corrosive agents and local stresses for an extended period of time has been observed to embrittle Zircaloy-2 at temperatures typical of those achieved in light water reactors. Samples of Zircaloy-2 fractured in the presence of cadmium or iodine in out-of-pile tests, for example, show very little reduction in area and the fracture surface appears non-ductile. Pellet-cladding interaction type failures also exhibit very little reduction area and a non-ductile fracture surface appearance.

For Cycle 17 through the present cycle, barrier cladding was reloaded at GGNS. This barrier design has been extensively tested and found to significantly improve the cladding resistance to pellet-cladding interaction failures. A large barrier cladding experience base exists; even with no power ramp restrictions, few pellet-cladding interaction failures have occurred.

4.2.1.2.1.14 Fuel Reliability

The fuel component characteristics which can influence fuel reliability include (1) the fuel pellet thermal and mechanical properties, dimensions, density, and U-235 enrichment; (2) the Zircaloy cladding thermal and mechanical properties, dimensions, and defects; (3) the fuel rod internal void volume and impurities; (4) the fuel rod-to-rod and rod-to-channel spacing; and (5) the spring constants of the fuel rod spacer springs which maintain contact between the spacer and the fuel rods. Important fuel pellet, cladding, and associated hardware characteristics, and dimensions are provided in Table 4.2-4 and Figure 4.2-1 (initial core).

The large volume of irradiation experience to date with BWR fuel indicates only a few mechanisms which have actually had a direct impact on fuel reliability; namely, cladding defects, excessive deposition of system corrosion products, cladding hydriding resulting from hydrogen impurity, and pellet-cladding interaction.

The cladding defects have been virtually eliminated through implementation of improved quality inspection equipment and more stringent quality control requirements during fuel fabrication.

Excessive deposition of corrosion products has also been virtually eliminated through improved control of corrosion product impurities in the reactor feedwater.

Cladding hydriding is the result of excessive amounts of hydrogenous impurities (moisture and/or hydrogenous material) inadvertently introduced into the rod during the fuel fabrication process. The fuel fabrication process currently includes strict control of hydrogenous materials during fabrication to minimize possible failures due to hydriding.

4.2.1.2.1.15 Design Basis for Fuel Assembly Surveillance

The fuel vendors maintain an active fuel assembly surveillance program specifically intended to monitor performance in operating reactors to identify and characterize unexpected phenomena which can influence fuel integrity and performance. Outage-oriented examinations are performed contingent on fuel availability as influenced by plant operation. Typically, peak duty fuel assemblies (with respect to exposure, linear heat generation rate, and the combination of both) are designated as lead assemblies for a particular design and are selectively inspected. Numerous other assemblies are routinely inspected employing the nondestructive techniques discussed in subsection 4.2.4.3. Additional information regarding fuel surveillance is contained in subsection 4.2.4.3.

Grand Gulf has two independent methods for on-line fuel rod failure detection: 1) off-gas radiation monitors and 2) the main steam line radiation monitor. These are described in Section 11.5.

4.2.1.2.2   Control Assembly and Its Components

The following paragraphs present the detailed bases which are considered in defining the design of the control assembly and its components.

4.2.1.2.2.1 Design Acceptability

The acceptability of the control rod and control rod drive under scram loading condition is demonstrated by functional testing instead of analysis or adherence to formally defined stress limits.

4.2.1.2.2.2   Control Rod Clearances

The basis of the mechanical design of the control rod blade clearances is that there shall be no interference which will restrict the passage of the control rod blade.

4.2.1.2.2.3   Mechanical Insertion Requirements

Mechanical insertion requirements during normal operation are selected to provide adequate operability and load following capability, and to be able to control the reactivity addition resulting from burnout of peak shutdown xenon at 100 percent power.

Scram insertion requirements are chosen to provide sufficient negative reactivity to meet all safety criteria for plant operational transients.

4.2.1.2.2.4   Material Selection

The selection of materials for use in the control rod design is based upon their in-reactor properties. The irradiated properties of Type-304 austenitic stainless steel which comprises the major portion of the assembly, B_4C powder, Inconel-X, and Stellite are well known and are taken into account in establishing the mechanical design of the control rod components. The Marathon design uses a high purity stabilized enhanced type 304 stainless steel, referred to as RAD RESIST 304S, to provide high resistance to irradiation assisted corrosion cracking. Niobium and Tantalum are added to the high purity 304 stainless steel to provide greater protection against irradiation assisted corrosion cracking. HP348 stainless steel of similar property has been demonstrated successfully in both control rod absorber tube and fuel cladding applications. HP348 stainless steel absorber tube material has achieved approximately 3% cladding strain at 100% burnup without failure. The basic cruciform control rod design and materials have been operating successfully in all General Electric reactors.

4.2.1.2.2.5   Radiation Effects

The radiation effects on B_4C powder include the release of gaseous products and the B_4C cladding is designed to sustain the resulting internal pressure buildup. The corrosion rate and the physical properties, e.g., density, modulus of elasticity, dimensional

aspects, etc., of austenitic stainless steel and Inconel-X are essentially unaffected by the irradiation experienced in the BWR reactor core. The effects upon the mechanical properties, i.e., yield strength, ultimate tensile strength, percent elongation, and ductility on the 304 stainless steel cladding, also are well known and are considered in mechanical design.

The nuclear lifetime of a control rod is defined as that integrated neutron absorption that results in a 10 percent reduction in the relative worth ($\Delta K/K$) of any significant axial section of the rod. Control rod lifetime, in terms of residence time, is dependent on capacity factor and mode of actual core operation.

The mechanical lifetime of the control blade is limited by the stress intensity in the most limiting tube reaching the design limit. A design stress intensity limit of 16,600 psi (about 1/2 of the material's unirradiated yield strength) is used for control blade/absorber rod design life calculations. An internal pressure of 4,200 psi corresponds to this stress intensity limit for the most limiting conditions of tube dimensional tolerances, B_4C density, etc.

4.2.1.2.2.6 Positioning Requirements

Rod positioning increments (not lengths) are selected to provide adequate power shaping capability. The combination of rod speed and notch length must also meet the limiting reactivity addition rate criteria.

4.2.1.2.2.7 Burnable Poison Rods

The design basis of the initial core supplementary fuel/ reactivity control rods (UGdO) is the same as UO fuel rods. Additional information on urania-gadolinia physical and irradiation characteristics and material properties is provided in Reference 67.

4.2.2   General Design Description

4.2.2.1   Core Cell

A core cell consists of a control rod and the four fuel assemblies which immediately surround it. Figure 4.2-1 (initial core) provides core cell dimensions. Each core cell is associated with a four-lobed fuel support piece. Around the outer edge of the core, certain fuel assemblies are not immediately adjacent to a control rod and are supported by individual peripheral fuel support pieces.

The top guide is an "egg-crate" structure of stainless steel bars which form a 4-bundle cell. The four fuel assemblies are lowered into this cell and, when seated, springs mounted at the tops of the channels force the channels into the corners of the cell such that the sides of the channel contact the grid beams (see Figure 4.2-2).

4.2.2.2   Fuel Assembly

A fuel assembly consists of a fuel bundle and the channel which surrounds it (see Figure 4.2-3). The fuel assemblies are arranged in the reactor core to approximate a right circular cylinder inside the core shroud. Each fuel assembly is supported by a fuel support piece and the top guide.

The general configuration of the fuel assembly and the detailed configurations of the assembly components are the results of the evolutionary change in customer, performance, manufacturing, and serviceability requirements and the experience obtained since the initial design conception. A summary of fuel assembly mechanical data for the various designs used at GGNS is presented in Table 4.2-4.

4.2.2.2.1   Fuel Assembly Orientation

Proper orientation of fuel assemblies in the reactor core is readily verified by visual observation and is assured by verification procedures following core loading. Five separate visual indications of proper fuel assembly orientation exist:

   a.   The channel fastener assemblies, including the spring and guard used to maintain clearances between channels, are located at one corner of each fuel assembly adjacent to the center of the control rod.

b.   The identification boss on the fuel assembly handle points
       toward the adjacent control rod.

c.   The channel spacing buttons are adjacent to the control
       rod passage area.

d.   The assembly identification numbers which are located on
       the fuel assembly handles are all readable from the
       direction of the center of the cell.

e.   There is cell-to-cell replication.

Experience has demonstrated that these design features are
clearly visible so that any misoriented fuel assembly would be
readily distinguished during core loading verification.

4.2.2.3   Fuel Bundle

Seven different fuel designs have been used at GGNS as summarized
in Table 4.2-4. [HISTORICAL INFORMATION] [For the initial core,
the fuel bundle contained 62 General Electric fuel rods and two
water rods which were arranged in a square 8x8 array. For Cycles 2
through 4, the reload fuel was similar but was supplied by Siemens
Power Corporation (SPC). Also for Cycle 4, four SPC lead bundles
were loaded. These bundles contained 76 fuel rods (of two
different sizes) and five water rods which are arranged in a
square 9x9 array. This similar design was used for the Cycle 5
thru 8 reloads. For Cycles 9 through 11, GE11 bundles have been
reloaded. The GE11 contained 66 full length fuel rods, 8 part
length fuel rods, and two large center water rods arranged in a
9x9 array. For Cycles 12 through 16, AREVA NP Atrium-10 bundles
were reloaded. The Atrium-10 contains 83 full length fuel rods, 8
part length fuel rods, and a large water channel arranged in a
10x10 array. For Cycle 17, GE14 bundles were loaded. The GE14
contains 78 full length fuel rods, 14 part length fuel rods, and 2
water rods arranged in a 10x10 array.] Starting with Cycle 18,
GNF2 bundles were loaded. The GNF2 fuel contains 78 full length
fuel rods, 14 part length fuel rods and 2 water rods arranged in a
10x10 array.

The fuel rods and water rods (or water channel for the Atrium-10)
are spaced and supported by the lower and upper tie plates. The
lower tie plate has a nosepiece which has the function of
supporting the fuel assembly in the reactor. The upper tie plate
has a handle for transferring the fuel bundle from one location to
another. The identifying assembly number is engraved on the top of

the handle and a boss projects from one side of the handle to aid in assuring proper fuel assembly orientation. Both upper and lower tie plates are fabricated from Type-304 stainless steel castings. Finger springs are also employed and located between the lower tie plate and the channel for the purpose of controlling the bypass flow through that flowpath (see subsection 4.2.2.3.6). Zircaloy fuel rod spacers equipped with Inconel-X springs maintain rod-to-rod spacing. For GNF2 fuel, finger springs are not used. The bypass flow is controlled by a thick bottom end on the channel. Additionally, the GNF2 spacers are made entirely from Alloy x750 material.

4.2.2.3.1   Fuel Rods

Each fuel rod consists of high density (typically equal or greater than 94.5 percent theoretical density) UO_2 fuel pellets stacked in a Zircaloy-2 cladding tube which is evacuated, backfilled with helium at 3 atmospheres pressure or greater, and sealed by Zircaloy end plugs welded in each end. The active fuel column may include a zone of naturally enriched (0.711 wt percent U-235) or depleted (0.40 wt percent U-235) pellets at the top and bottom. The fuel rod cladding thickness is adequate to be essentially free-standing under the 1000 psia BWR environment. Adequate free volume is provided within each fuel rod in the form of pellet-to-cladding gap and plenum region at the top of the fuel rod to accommodate thermal and irradiation expansion of the UO_2 and the internal pressures resulting from the helium fill gas, impurities, and gaseous fission products liberated over the design life of the fuel. A plenum spring, or retainer, is provided in the plenum space to prevent movement of the fuel column inside the fuel rod during fuel shipping and handling (see Figure 4.2-4).

For fuel reloaded into the core prior to Cycle 12 and after Cycle 16, two types of fuel rods are utilized in a fuel bundle: tie rods and standard rods (Figure 4.2-4) (For the GE11,GE14 and GNF2 fuel, part length fuel rods are also used). The eight tie rods in each bundle have lower end plugs which thread into the lower tie plate casting and threaded upper end plugs which extend through the upper tie plate casting. A stainless steel nut is installed on the upper end plug to hold the fuel bundle together. These tie rods support the weight of the assembly only during fuel handling operations when the assembly hangs by the handle; during operation, the fuel rods are supported by the lower tie plate. For

the GNF2 fuel introduced in Cycle 18, 78 rods are standard rods and 14 rods are part-length rods. The part length rods extend only 1/3 and 2/3 as high as the standard fuel rods.

For GEH fuel, starting with Cycle-9, barrier cladding was introduced. This cladding is similar to the Zircaloy-2 used in the past except the inner approximate 10% of the cladding is Zirconium. Extensive testing and operational experience has demonstrated this cladding is much more resistant to pellet-cladding failures.

The GNF2 fuel has an Inconel-X expansion spring which is located over the upper end plug shank of each rod in the assembly to keep the rods seated in the lower tie plate while allowing independent axial expansion by sliding within the holes of the upper tie plate. Additional information concerning the fuel rod expansion spring is provided in Reference 65.

The fuel bundles incorporate the use of small amounts of gadolinium as a burnable poison in selected standard fuel rods.The irradiation products of this process are other gadolinium isotopes having low cross sections. The control augmentation effect disappears on a predetermined schedule without changes in the chemical composition of the fuel or the physical makeup of the core. Some assemblies contain more gadolinia than others to improve transverse power flattening. Also, some assemblies contain axially distributed gadolinia to improve axial power flattening. Gd_2O_3 is uniformly distributed in the UO_2 pellet and forms a solid solution. The gadolinia-urania fuel rods have either characteristic extended upper end plugs, marked upper end plugs, and/or unique man-readable serial numbers.

4.2.2.3.1.1   Fuel Pellets

The fuel pellets consist of high density ceramic uranium dioxide manufactured by compacting and sintering uranium dioxide powder into right cylindrical pellets with chamfered edges. Some of the pellets contain small amounts of gadolinia as a burnable poison. The average pellet immersion density is typically equal to or greater than 94.5 percent of the theoretical density of UO_2. Ceramic uranium dioxide is chemically inert to the cladding at operating temperatures and is resistant to attack by water. Several U-235 enrichments are used in the fuel assemblies to reduce the local power peaking factor. The upper and lower ends of

the active fuel length in each rod may contain naturally enriched or depleted uranium pellets. Fuel element design and manufacturing procedures have been developed to prevent errors in enrichment locations within a fuel assembly.

4.2.2.3.2   Water Rods

Each fuel bundle has either one, two, or five hollow water tubes, one of which (the spacer-positioning water rod) positions the Zircaloy fuel rod spacers axially in the fuel bundle. The water rods are made from Zircaloy-2 tubing or Zircaloy-4 square channels. The spacer-positioning water rod is equipped with tabs or rings which are welded to its exterior. Several holes are drilled around the circumference of each of the water rods near each end to allow coolant water to flow through the rod.

Differential thermal expansion between the fuel rods and the water rods can introduce axial loadings into the water rod through the frictional forces between the fuel rods and the spacers. [HISTORICAL INFORMATION] [For the initial core the testing which was performed to address this condition and to verify the water rod/spacer conceptual design is discussed in Section 2 of Reference 4 and in Reference 14. This testing is applicable to the reload fuel given the similarities in the designs.]

4.2.2.3.3   Fuel Spacer

The primary function of the fuel spacer is to provide lateral support and spacing of the fuel rods, with consideration of thermal-hydraulic performance, fretting wear, strength, neutron economy, and producibility. The spacer represents an optimization of these considerations.

The mechanical loadings on the spacer structure during normal operation and transients result from the rod positioning spacer spring forces and from local loadings at the water rod-spacer positioning device. During a seismic event, the spacer must transmit the lateral acceleration loadings from the fuel rods into the channel, while maintaining the spatial relationship between the rods.

As noted, the spacer represents an optimization of a number of considerations. Thermal-hydraulic development effort has gone into designing the particular configuration of the spacer parts. The resultant configurations give enhanced hydraulic performance.

Extensive flow testing has been performed employing prototypical spacers to define single-phase and two-phase flow characteristics.

During the blowdown portion of the postulated loss-of-coolant accident (LOCA), the hydraulic (pressure differential) forces on the spacer are of about the same magnitude as those present during normal or transient operation of the fuel. There are no significant lateral hydraulic forces on the spacer, because the fuel channel maintains the normal flow path during the blowdown.

4.2.2.3.4   Fuel Channel

The fuel channel enclosing the fuel bundle is fabricated from a zirconium alloy and performs three functions: (1) the channel provides a barrier to separate two parallel flow paths-one for flow inside the fuel bundle and the other for flow in the bypass region between channels; (2) the channel guides the control rod and provides a bearing surface for it; and (3) the channel provides rigidity for the fuel bundle. The channel is open at the bottom and makes a sliding seal fit on the lower tie plate surface. At the top of the channel, two diagonally opposite corners have welded tabs, one of which supports the weight of the channel from a raised post on the upper tie plate. One of these raised posts has a threaded hole, and the channel is attached using the threaded channel fastener assembly, which also includes the fuel assembly positioning spring. Channel-to-channel spacing is provided for by means of spacer buttons located on the upper portion of channel adjacent to the control rod passage area. Axial differential thermal expansion between any bundle and the channel is accommodated at the lower tie plate. The current GNF2 fuel channels have 120 mil thick channel corners, however, the side walls are thinner.

In addition to meeting design limits, assurance that the channels maintain their dimensional integrity, strength, and spatial position throughout their lifetime is provided for through specifications on the channel materials and manufacturing processes and by quality measurements and process qualifications to ensure compliance with these specifications.

Under situations of adverse tolerance stackup, differential thermal expansion between the stainless steel tie plates and the channel can result in an interference fit; however, the resultant stress and strain levels in the channel do not exceed design

limits. The loads and resultant stress imposed on the fuel channel in the event of control rod interference are also within design limits.

4.2.2.3.5   Tie Plates

The upper and lower tie plates serve the functions of supporting the weight of the fuel and positioning the rod ends during all phases of operation and handling. The loading on the lower tie plate during operation and transients is comprised of the fuel weight, the weight of the channel, and the forces from the expansion springs at the top of the fuel rods. The loading on the upper tie plate during operation is due to the expansion spring force. The expansion springs permit differential expansion between the fuel rods without introducing high axial forces into the rods.

Most of the loading on the lower tie plate is due to the weight of the fuel rods and the channel, which are not cyclic loadings. During accidents, the tie plates are subjected to the normal operational loads plus the blowdown and seismic loadings. During handling, the tie plates are subjected to acceleration and impact loadings.

For the GEH fuel starting with the Cycle 9 reload, smaller flow holes have been used in the lower tie plate. These smaller holes minimize the possibility that debris could pass into the fueled region of the bundle. The GNF2 fuel, first loaded in Cycle 18, uses the Defender lower tie plate assembly to provide protection from debris in the coolant.

4.2.2.3.6   Finger Springs

Finger springs were originally employed to control the bypass through the channel-to-lower tie plate flow path. Increases in channel wall permanent deflection at the lower tie plate resulting from creep deformation at operating conditions result in increased bypass flow through the channel to lower tie plate flow path. Changes in the flow through this path affect the total core bypass flow, which, in turn, affects the active coolant flow, void coefficient, and operational transients. Control of the bypass flow for GNF2 fuel is accomplished by a thicker channel side wall at the bottom of the channel. This increased side thickness provides additional resistance to channel bulge so that the bypass flow is adequately controlled without finger springs.

4.2.2.4   Reactivity Control Assembly

4.2.2.4.1   GENE OEM Control Rods

The control rods perform the dual function of power shaping and
reactivity control. A design drawing of the control blade is seen
in Figure 4.2-5. Power distribution in the core is controlled
during operation of the reactor by manipulating selected patterns
of control rods. Control rod displacement tends to counterbalance
steam void effects at the top of the core and results in
significant power flattening.

The control rod consists of a sheathed cruciform array of
stainless steel tubes filled with boron-carbide powder. The
control rods are 9.804 inches in total span and are separated
uniformly throughout the core on a 12-inch pitch maximum. Each
control rod is surrounded by four fuel assemblies.

The main structural member of a control rod is made of Type-304
stainless steel and consists of a top handle, a bottom casting
with a velocity limiter and control rod drive coupling, a vertical
cruciform center post, and four U-shaped absorber tube sheaths.
The top handle, bottom casting, and center post are welded into a
single skeletal structure. The U-shaped sheaths are resistance
welded to the center post, handle, and castings to form a rigid
housing to contain the boron-carbide-filled absorber rods.
Rollers at the top and bottom of the control rod guide the control
rod as it is inserted and withdrawn from the core. The control
rods are cooled by the core bypass flow. The U-shaped sheaths are
perforated to allow the coolant to circulate freely about the
absorber tubes. Operating experience has shown that control rods
constructed as described above are not susceptible to dimensional
distortions.

The boron-carbide (BC) powder in the absorber tubes is compacted
to about 70 percent of its theoretical density. The boron-carbide
contains a minimum of 76.5 percent by weight natural boron. The
boron-10 (B-10) minimum content of the boron is 18 percent by
weight. Absorber tubes are made of Type-304 stainless steel. Each
absorber tube is 0.220 in. in outside diameter and has a 0.027-in.
wall thickness. Absorber tubes are sealed by a plug welded into
each end. The boron-carbide is longitudinally separated into
individual compartments by stainless steel balls at approximately
16-in. intervals. The steel balls are held in place by a slight

crimp of the tube. Should boron-carbide tend to compact further in service, the steel balls will distribute the resulting voids over the length of the absorber tube.

4.2.2.4.2 GENE Marathon and Marathon Ultra HD Control Rods

The GE Marathon and Marathon Ultra HD control rods are designed to be compatible with and a direct replacement for, any of the current control rod assemblies in the BWR/6 S lattice core configurations. The envelope dimensions within the core for the Marathon and Marathon Ultra control rods are the same as the original equipment control rods and the initial reactivity worth is approximately equal to the original equipment control rods. The structural material used in the Marathon and Marathon Ultra control rod is HP304S stainless steel. This material is less susceptible to Irradiation Assisted Corrosion Cracking. The absorbing material contained in the GE Marathon rods may consist of both B_4C and Hafnium and provide a higher Boron-10 capture level than the GE original equipment design.

4.2.2.4.3 Velocity Limiter

The control rod velocity limiter (see Figure 4.2-6a) is an integral part of the bottom assembly of each control rod. This engineered safeguard protects against high reactivity insertion rate by limiting the control rod velocity in the event of a control rod drop accident. It is a one-way device in that the control rod scram velocity is not significantly affected but the control rod dropout velocity is reduced to permissible limit.

The velocity limiter is in the form of two nearly mated conical elements that act as a large clearance piston inside the control rod guide tube. The lower conical element is separated from the upper conical element by four radial spacers 90 degrees apart and is at a 15 degree angle relative to the upper conical element, with the peripheral separation less than the central separation.

The hydraulic drag forces on a control rod are proportional to approximately the square of the rod velocity and are negligible at normal rod withdrawal or rod insertion speeds. However, during the scram stroke the rod reaches high velocity, and the drag forces must be overcome by the drive mechanism.

To limit control rod velocity during dropout but not during scram, the velocity limiter is provided with a streamlined profile in the scram (upward) direction.

Thus, when the control rod is scrammed, water flows over the smooth surface of the upper conical element into the annulus between the guide tube and the limiter. In the dropout direction, however, water is trapped by the lower conical element and discharged through the annulus between the two conical sections. Because this water is jetted in a partially reversed direction into water flowing upward in the annulus, a severe turbulence is created, thereby slowing the descent of the control rod assembly to less than 5 ft/sec.

4.2.3   Design Evaluations

4.2.3.1   Results of Fuel Rod Thermal-Mechanical Evaluations

4.2.3.1.1   Evaluation Methods

Methods for predicting fuel/cladding interaction in fuel design analyses have been discussed and compared to data in Reference 7 for the initial core. Important material properties used for analysis are provided in Table 4.2-5. The mechanical evaluations reported here were performed at a power level equal to the license limit plus a power spike allowance, wherever applicable. Additional details regarding methods used for the initial core are presented in Section 11 of Reference 4 and Appendix B of Reference 15. Additional discussion of the analyses for GEH fuel prepressurization to three atmospheres is contained in References 33 and 36. The thermal and mechanical performance of the current GNF2 fuel is predicted and analyzed through the PRIME model and computer program which has been approved by the NRC (Ref. 68). The PRIME code addresses the effects of fuel/cladding thermal expansion, fuel phase change volume change, fuel irradiation swelling, densification, relocation, and fission gas release, fuel-cladding axial slip, cladding creepdown, irradiation hardening and thermal annealing of irradiation hardening, pellet and cladding plasticity and creep, pellet hot pressing and plastic collapse, and development of a porous pellet rim at high exposure.

[HISTORICAL INFORMATION] [For the initial core; continuous functional variations of mechanical properties with exposure were not employed since the irradiation effects became saturated at very low exposure. At beginning of life, the cladding mechanical properties employed were the unirradiated values. At subsequent times in life, the cladding mechanical properties employed were the saturated irradiated values. The only exception to this was

that unirradiated mechanical properties were employed above the temperatures for which irradiation effects on cladding mechanical properties are assumed to be annealed out.] For the GEH reloads, the affects of irradiation on cladding strength were explicitly accounted for (Reference 67).

In the GEH design analysis, the calculated stress and the yield strength or ultimate strength are combined into a dimensionless quantity called the design ratio. This quantity is the ratio of calculated stress intensity to the design stress limit for a particular stress category. The design stress limit for a particular stress category is defined as a fraction of either the yield strength or ultimate strength, whichever is lower. Thus, the design ratio is a measure of the fraction of the allowable stress represented by the calculated stress.

Analyses are performed to show that the stress/strain limits are not exceeded during continuous operation with LGHRs up to the design operating limit, or during transient operation above the design operating limit. Stresses due to external coolant pressure, internal gas pressure, thermal effects, spacer contact, flow-induced vibration, and manufacturing tolerances are considered.

4.2.3.1.2   Fuel Damage Analysis

As noted in subsection 4.2.1.1.1.2, fuel damage is defined as a perforation of the fuel rod cladding which would permit the release of fission products to the reactor coolant.

For fresh UO_2 fuel, the calculated LHGR corresponding to 1 percent diametral plastic strain of the cladding, is approximately 19 kW/ft. Later in life, the calculated LHGR corresponding to 1 percent diametral plastic strain decreases as the gap between the pellet and cladding decreases due to pellet swelling and cladding creepdown. To ensure that one percent plastic strain will not be exceeded, during both steady-state operation and anticipation operational occurrences, LHGR limits are established for each fuel design.

The addition of small amounts of gadolinia to UO_2 results in a reduction in the fuel thermal conductivity and melting temperature. The result is a reduction in the LHGRs calculated to cause 1 percent plastic diametral strain for gadolinia-urania

fuel rods. However, to compensate for this the gadolinia-urania fuel rods are designed to provide margins similar to standard UO_2 rods.

4.2.3.1.3   Steady State Thermal-Mechanical Performance

The fuel has been designed to operate at core rated power with sufficient design margin to accommodate reactor operations and satisfy the mechanical design bases discussed in detail in subsection 4.2.1. In order to accomplish this objective, the fuel was designed to operate at a maximum steady state linear heat generation rate, plus an allowance, wherever applicable, for densification power spiking.

Thermal and mechanical analyses have been performed which demonstrate that the mechanical design bases are met for the maximum operating power and exposure combination throughout fuel life. Design analyses have been performed for the fuel which show that the stress/strain limits are not exceeded during continuous operation with LHGRs up to the operating limit, nor for short term transient operation up to at least 16 percent above the peak operating limit. Stresses due to external coolant pressure, internal gas pressure, thermal gradients, spacer contact, flow-induced vibration, and manufacturing tolerances were considered. Additional information regarding this type of analysis is provided in References 4 (Section 11), 33, and 35 for the initial core and Reference 67 for the GNF2 fuel.

4.2.3.2   Results from Fuel Design Evaluations

The design evaluations for each of the fuel system damage, failure, and coolability criteria identified in Section II.C of the Standard Review plan 4.2, except control rod reactivity, are provided in Subsection 2.2 of Reference 51(GESTAR II). As stated in GESTAR II, "Fuel design compliance with the fuel licensing acceptance criteria constitutes USNRC acceptance and approval of the fuel without specific USNRC review." The fuel provider for GGNS provides a Compliance Report (Ref 65) to show that all of the criteria in GESTAR II have been met. The generic information provided in Reference 51 is supplemented by plant specific, cycle specific information and analysis that is contained in a Supplemental Reload Licensing Report. The PRIME thermal-mechanical computer code described in Section 4.2.3.1.1 is also part of the evaluation methods used at GGNS for demonstrating the GNF2 fuel meets all design requirements.

4.2.3.2.1 Flow-Induced Fuel Rod Vibrations

Flow induced fuel rod vibration is not considered to be a viable
life-limiting or failure mechanism based on extensive fuel
operating experience. Fuel inspections, both visual inspections
during normal refueling outages, and more detailed non-
destructive examinations have not indicated any anomolous
performance associated with fuel rod vibration. Additional
information on flow induced vibration may be found in Reference 15
for the initial core and Reference 65 for the current GEH reload.

4.2.3.2.2 Potential Damaging Temperature Effects During Transients

There are no predicted significant temperature effects during a
power transient resulting from a single operator error or single
equipment malfunction. For purposes of maintaining adequate
thermal margin during normal steady state operation, the minimum
critical power ratio must not be less than the required MCPR
operating limit, and the maximum LHGR is maintained below the
design LHGR for the plant. The core and fuel design basis for
steady state operation, i.e., MCPR and LHGR limits, have been
defined to provide margin between the steady state operating
condition and any fuel damage condition to accommodate
uncertainties and to assure that no fuel damage results even
during the worst anticipated transient condition at any time in
life. Specifically the MCPR operating limit is specified such
that at least 99.9 percent of the fuel rods in the core are
expected not to experience boiling transition during the most
severe abnormal operational transient. The calculated fuel rod
cladding strain for this class of transient is significantly
below the calculated damage limit.

4.2.3.2.3 Fretting Wear and Corrosion

[HISTORICAL INFORMATION] [Tests of this design have been
conducted both out-of-reactor as well as in-reactor prior to
application in a complete reactor core basis. All tests and post-
irradiation examinations have indicated that fretting corrosion
does not occur. Post-irradiation examination of many fuel rods
has indicated only minor fretting wear. Excessive wear at spacer
contact points has never been observed with the current spacer
configuration. Additional information regarding these tests and
inspection of operating fuel is presented in Section 10 of

Reference 4 and Sections 4.7 and 4.8 of Reference 14 for the initial core] Fretting related to the current GNF2 fuel is addressed in Reference 65.

4.2.3.2.4   Fuel Rod Cycling and Fatigue Analysis

[HISTORICAL INFORMATION] [For the initial core, less than 5 percent of the allowable fatigue life was consumed. Additional information regarding this analysis is provided in Section 12 of Reference 4.] The fatigue analysis for the current core loading is completed by the PRIME model and computer program as described in Reference 67. The usage factors were well below the failure limit.

4.2.3.2.5   Fuel Rod Bowing

[HISTORICAL INFORMATION] [Fuel inspections, both visual inspections during normal refueling outages and more detailed non-destructive examinations as a part of the vendor's fuel surveillance program, have provided no indication of rod bowing as a viable failure or life-limiting mechanism. This successful operating experience has been supported by fuel mechanical analyses which predict an insignificant amount of fuel rod bowing (typically <~20 mils). These analyses consider the influence of initial bow, tubing eccentricity, fast neutron flux, and thermal gradients on the potential for in-reactor creep bowing. In addition, full scale thermal hydraulic tests have been conducted to assess the effects of gross fuel rod bowing. Based on results of these tests, it has been concluded that even for severe rod bowing in the most limiting rods in the assembly there is a negligible effect on critical power performance.] Bowing for the current GNF2 fuel is discussed in Reference 67.

4.2.3.2.6   Fuel Assembly Dimensional Stability

[HISTORICAL INFORMATION] [For the initial core, mechanical analyses were performed to assess the effects of the differential thermal expansion between the tie plates and spacer grids. The differential thermal expansion introduces a bending stress of less than 400 psi at the end of the fuel tube. Additional information regarding the model employed in this calculation is presented in Section 4 of Reference 3. These analyses are applicable to the reloads given the similarities in the designs.]

4.2.3.2.7   Temperature Transients with Waterlogged Fuel Element

As indicated in subsection 4.2.1.2.1.11, the potential for waterlogging has been considered in the fuel design.

In the unlikely event that a waterlogged fuel element does exist in a BWR core, it should not have significant potential for cladding burst.

4.2.3.2.7.1   Energy Release for Rupture of Waterlogged Fuel Elements

[HISTORICAL INFORMATION] [Experiments have been performed to show that waterlogged fuel elements can fail at a lower damage threshold than nonwaterlogged fuel during rapid reactivity excursions from the cold condition (Refs. 16 and 17), i.e., ~60 cal/gm as compared to >300 cal/gm. However, it has been shown (Ref. 30) that the resultant mechanical energy release for waterlogged rods, even for significant energy depositions (~400 cal/gm), is of little consequence and is well below the energy released for nonwaterlogged rods subjected to comparable energy depositions.]

4.2.3.2.8   Fuel Densification Analyses

The amount of densification employed in the following models was determined through the use of models defined in References 11, 12, and 13 for the initial core and Reference 67 for the current GEH reload.

4.2.3.2.8.1   Power Spiking Analysis

For the initial core power spiking due to the formation of axial gaps in the fuel column was addressed as discussed below. For the current GEH reload, power peaking is addressed in Reference 65.

[HISTORICAL INFORMATION] [The equation employed to calculate maximum gap size for the initial core is as described in Reference 12:

$$\frac{\Delta L}{L} = \frac{\Delta \rho}{2} + 0.0025$$

where

ΔL =   maximum axial gap length

L	=	fuel column length
$\Delta\rho$	=	the average change in density as measured by thermal simulation for 24 hours at 1700°C
2	=	anisotropic factor applied to densification
0.0025	=	allowance for irradiation induced cladding growth and axial strain caused by fuel cladding mechanical interaction

The resulting power spiking penalty at the top of the core is 2.2 percent. The power spiking penalty as a function of elevation from the bottom of the core can be conservatively expressed by:

$$\frac{\Delta P}{P_x} = \frac{\Delta P}{P_L} \bullet \frac{X}{L}$$

where

$\frac{\Delta P}{P_x}$	=	power spiking penalty at elevation x from bottom of core
$\frac{\Delta P}{P_L}$	=	power spiking penalty at top of core
X	=	elevation from bottom of core
L	=	fuel column length

The power increase described by the above equation as a function of axial position added to the license limit LHGR (13.4 kW/ft for the initial core) has been considered in design and safety analysis, wherever applicable. This ensures, with better than 95 percent confidence, that no more than one rod will exceed the power evaluated due to random occurrence of power spikes resulting from axial fuel column gaps.

The results of the power spiking analysis for normal operation was utilized in the analysis of transients and accidents wherever applicable for the initial core. The control rod drop accident is unique in the respect that it begins at the cold condition and is not affected by normal operating power level. Further, the existence of fuel column gaps can result in power spiking in the cold condition during a control rod drop which should thus be considered in the evaluation of this accident. For this purpose, a separate power spiking analysis was performed using the same

assumptions as indicated above, but employing a power spike versus gap size calculated to occur in the cold condition with zero voids. This analysis was performed with the maximum gap size predicted at the top of the core in order to maximize the power spiking effect. This analysis yielded a 99 percent probability that any given fuel rod would have a power spike <5 percent.]

4.2.3.2.8.2   Cladding Creep Collapse

For the initial core and GEH reloads, a cladding collapse analysis was performed employing the standard General Electric finite element model (Ref. 13, 51, and 66). [HISTORICAL INFORMATION] [Figure 4.2-7 presents the cladding mid-wall temperature versus time employed in the initial core analysis. No credit was taken for internal gas pressure due to released fission gas or volatiles. The internal pressure due to helium backfill during fabrication was considered. Based on the analysis results, cladding collapse was not calculated to occur.]

4.2.3.2.8.3   Increased Linear Heat Generation Rate

[HISTORICAL INFORMATION] [A fuel pellet expands 1.2 percent in going from the cold to hot condition at 13.4 kW/ft. While this increase in length from the cold to hot condition is not taken credit for in either design calculations or in the process of core performance analysis during reactor operation, the expansion more than offsets the decrease in pellet length due to densification.

The following expression is employed to calculate the decrease in fuel column length due to densification in calculation of an increase in linear heat generation rate:

$$\frac{\Delta L}{L} = \frac{\Delta \rho}{2}$$

where

$\Delta \rho$ =   the average change in density as measured by thermal simulation for 24 hours at 1700°C

2   =   anisotropic factor applied to densification.

Using the equation above, the pellet decrease in length due to densification is less than the increase in length due to thermal expansion of the pellet in going from cold to hot condition. Therefore, no power increase is calculated due to densification.]

4.2.3.2.8.4   Stored Energy Determination

The effects on stored energy due to densification are accounted for in the LOCA evaluation.

4.2.3.2.9   Fuel Cladding Temperatures

[HISTORICAL INFORMATION] [Fuel cladding temperatures as a function of heat flux for the initial core are shown in Figure 4.2-8 for beginning of life conditions and in Figure 4.2-9 for late in life conditions. The temperatures employed in mechanical design evaluations are calculated using a conservative design allowance for the increase in resistance to surface heat transfer due to the accumulation of system corrosion products on the surface of the rod (crud) and cladding corrosion (zirconium oxide formation).]

4.2.3.2.10   Incipient Fuel Center Melting

Incipient center melting is expected to occur in fresh UO_2 fuel rods at a linear heat generation rate of approximately 20.5 kW/ft. This condition corresponds to the integral:

$$\int_{32°F}^{T_{melt}} kdt = 93 \text{ W/cm}$$

The value of the above integral decreases slightly with burnup, as a result of the decrease in fuel melting temperature with increasing exposure.

4.2.3.2.11   Energy Release During Fuel Element Burnout

Boiling transition does not necessarily correspond to a fuel damage threshold. [HISTORICAL INFORMATION] [In-reactor experiments to assess the effect of operation of zircaloy clad UO_2 fuel rods after the onset of transition boiling have been conducted by a number of different experimenters (Refs. 25-29). Postirradiation examinations conducted on the fuel tested verified that no cladding failure, and no appreciable cladding degradation occurred for fuel that experienced peak cladding temperatures less than ~2000°F.]

The metal-water chemical reaction between zirconium and water is given by:

$$Zr + 2H_2O \rightarrow ZrO_2 + 2H_2 - \Delta H$$
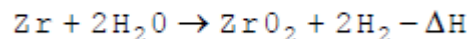
where $-H = 140$ cal/g-mole. The reaction rate is conservatively given by the familiar Baker-Just rate equation,

$$W^2 = 33.3 \times 10^6 \ \tau \ exp \left(\frac{-45500}{RT} \right)$$

where W is milligrams of zirconium reacted per cm² of surface area, τ is time (seconds), R is the gas constant, (cal/mole- K), and T is the temperature of zirconium (K). This rate equation has been shown to be conservatively high by a factor of 2 (Ref. 18). The above equation can be differentiated to give the rate at which the thickness of the cladding is oxidized. This yields

$$th = \frac{A_1}{\Delta X} \ exp \left(-\frac{A_2}{T} \right)$$

where

th	=	rate at which the cladding thickness is oxidizing
X	=	oxidized cladding thickness
A_1, A_2	=	appropriate constants
T	=	reaction temperature

The reaction rate is inversely proportional to the oxide buildup; therefore, at a given cladding temperature the reaction rate is self-limiting as the oxide builds up. The total energy release from this chemical reaction over a time period is given by,

$$Q_\tau = \int_{\tau_1}^{\tau_2} N_{rods} \ (-\Delta H) \ C \ L \ \rho \Delta X \ dt$$

where

N_{rods}	=	number of rods experiencing boiling transition (at temperature T)
$-\Delta H$	=	heat of reaction
C	=	cladding circumferences
L	=	axial length of rod experiencing boiling transition
ρ	=	density of, zirconium

This equation can be integrated and compared to the normal bundle energy release if the following conservative assumptions are made:

a.   At an axial plane all the rods experience boiling transition and are at the same temperature. This is highly conservative since if boiling transition occurs it will normally occur on the high power rods(s).

b.   Boiling transition is assumed to occur uniformly around the circumference of a rod. This generally occurs only at one spot.

c.   The rods are assumed to reach some temperature T instantaneously and stay at this temperature for an indefinite amount of time.

[HISTORICAL INFORMATION] [This integration has been performed for the initial core per axial foot of bundle and the total energy release as a function of time has been compared to the total energy release of a high power bundle (~6 MW) over an equal amount of time. The results are shown in Figure 4.2-10. For example, if the temperature of all the rods along a 1-ft section of the bundle were instantly increased to 1500°F, the total amount of energy that has been released at 0.1 second is 0.4 percent of the total energy that has been released by the bundle (6 MW x 0.1 second).] Note that the fractional energy release decreases rapidly with time even though a constant temperature is maintained. This is because the reaction is self-limiting as previously discussed.

The amount of energy released is dependent on the temperature transient and the surface area that has experienced heatup. This, of course, is dependent on the initiating transient. For example, if boiling transition was to occur during steady state operating conditions, the cladding surface temperature would range from 1000 to 1500°F depending on the heat fluxes and heat transfer coefficient. Even assuming all rods experience boiling transition instantaneously, the magnitude of the energy release is seen to be insignificant. Significant boiling transition is not possible at normal operating conditions or under conditions of abnormal operational transients because of the thermal margins at which the fuel is operated. It can, therefore, be concluded that the energy release and potential for a chemical reaction is not an important consideration during normal operation or abnormal transients.

4.2.3.2.12   Fuel Rod Behavior Effects from Coolant Flow Blockage

The behavior of fuel rods in the event of coolant flow blockage is covered in Reference 19 for the initial core.

4.2.3.2.13   Channel Evaluation

Channel analytical models and evaluation results are contained in Reference 20 for the standard GEH-supplied channels. For the GEH interactive channel (such as used for the current GNF2 bundle design), finite element analyses were performed as discussed in Reference 65.

4.2.3.2.14   Fuel Shipping and Handling

Analyses of the major handling loads have been performed and the resulting fuel assembly component stresses are within design limits. Additional information on fuel handling and shipping loads is presented in Section 5 of Reference 3 (for the initial core) and References 51 and 65 for the GNF2 reloads.

4.2.3.2.15   Fuel Assembly - SSE and LOCA Loadings

[HISTORICAL INFORMATION] [For the initial core, the evaluation of combined safe shutdown earthquake (SSE) and loss-of-coolant accident (LOCA) loadings was generically addressed in Reference 32. Conservative load combinations were evaluated for the plant specific analyses, and the bounding values are presented in Table 3.9-2(b). Fuel assembly design is determined to be structurally adequate to withstand these load combinations. The upward lift of the fuel assembly predicted during these analyses is negligible.]

For the current GNF2 fuel, the combined SSE and LOCA loadings on the fuel assembly were evaluated relative to assembly deformation and liftoff. The results are provided in Reference 65.

4.2.3.3   Reactivity Control Assembly Evaluation (Control Rods)

4.2.3.3.1   Materials Adequacy Throughout Design Lifetime

The adequacy of the materials throughout the design life was evaluated in the mechanical design of the control rods. The primary materials; B_4C powder, Hafnium, Rad Resist 304S, and 304 austenitic stainless steel, have been found suitable in meeting the demands of the BWR environment.

4.2.3.3.2   Dimensional and Tolerance Analysis

Layout studies are done to assure that, given the worst combination of extreme tolerance ranges of the assembly, no interference exists which will restrict the passage of control rods. In addition, preoperational verification is made on each control blade system to show that the acceptable levels of operational performance are met.

4.2.3.3.3   Thermal Analysis of the Tendency to Warp

The various parts of the control rod assembly remain at approximately the same temperature during reactor operation, negating the problem of distortion or warpage. Mechanical design allows for what little differential thermal growth can exist. A minimum axial gap is maintained between absorber rod tubes and the control rod frame assembly for that purpose. In addition, dissimilar metals are avoided to further this end.

4.2.3.3.4   Forces for Expulsion

An analysis has been performed which evaluates the maximum pressure forces which could tend to eject a control rod from the core.

If the collet remains open, which is unlikely, calculations indicate that the steady state control rod withdrawal velocity would be 2 ft/sec for a pressure-under line break, the limiting case for rod withdrawal.

4.2.3.3.5   Effect of Fuel Rod Failure on Control Rod Channel Clearances

The control rod drive mechanical design ensures a sufficiently rapid insertion of control rods to preclude the occurrence of fuel rod failures which could hinder reactor shutdown by causing significant distortions in channel clearances.

4.2.3.3.6   Effect of Blowdown Loads on Control Rod Channel Clearances

The fuel channel load resulting from an internally applied pressure is evaluated, utilizing a fixed beam analytical model under a uniform load. Tests to verify the applicability of the analytical model indicate that the model is conservative. For the OEM control blade, a roller at the top of the control rod guides the blade as it is inserted. If the gap between channels

is less than the diameter of the roller, the roller deflects the channel walls as it makes its way into the core. The friction force is a small percentage of the total force available to the control rod drives for overcoming such friction, and it is concluded that the main steam line break accident does not impede the insertability of the control rod. The Marathon and Marathon Ultra HD control blades do not incorporate rollers at the top of the blade and therefore are bounded by the OEM control blade analysis.

4.2.3.3.7   Mechanical Damage

Analysis has been performed for all areas of the control system showing that system mechanical damage does not affect the capability to continuously provide reactivity control.

The following discussion summarizes the analysis performed on the control rod guide tube.

The guide tube can be subjected to any or all of the following loads:

   a.   Inward load due to pressure differential

   b.   Lateral loads due to flow across the guide tube

   c.   Deadweight

   d.   Seismic

In all cases analysis was performed considering both a recirculation line break and a steam line break, events which result in the largest hydraulic loadings on a control rod guide tube.

Two primary modes of failure were considered in the guide tube analysis: exceeding allowable stress and excessive elastic deformation. It was found that the allowable stress limit will not be exceeded and that the elastic deformations of the guide tube never are great enough to cause the free movement of the control rod to be jeopardized.

4.2.3.3.7.1 First Mode of Failure

The first mode of failure is evaluated by the addition of all the stresses resulting from the maximum loads for the faulted condition. This results in the maximum theoretical stress value for that condition. Making a linear supposition of all calculated stresses and comparing this value to the allowable limit defined

by the ASME Boiler and Pressure Vessel Code yields a factor of safety of approximately 3. For faulted conditions, the factor of safety is approximately 4.2.

4.2.3.3.7.2   Second Mode of Failure

Evaluation of the second mode of failure is based on clearance reduction between the guide tube and the control rod. The minimum allowable clearance is about 0.1 in. This assumes maximum ovality and minimum diameter of the guide tube and the maximum control rod dimension. The analysis showed that if the approximate 6000 psi for the faulted condition were entirely the results of differential pressure, the clearance between the control rod and the guide tube would reduce by a value of approximately 0.01 in. This gives a design margin of 10 between the theoretically calculated maximum displacement and the minimum allowable clearance.

4.2.3.3.8   Analysis of Guide Tube Design

Two types of instability were considered in the analysis of guide tube design. The first was the classic instability associated with vertically loaded columns. The second was the diametral collapse when a circular tube experiences external to internal differential pressure.

The limiting axially applied load is approximately 77,500 lbs resulting in a material compressive stress of 17,450 psi (Code allowable stress). Comparing the actual load to the yield stress level gives a design margin greater than 20 to 1. From these values it can be concluded that the guide tube is not an unstable column.

When a circular tube experiences external to internal differential pressure, two modes of failure are possible depending on whether the tube is "long" or "short." In the analysis here, the guide tube is taken to be an infinitely long tube with the maximum allowable ovality and minimum wall thickness. The conditions will result in the lowest critical pressure calculation for the guide tube (i.e., if the tube was "short," the critical pressure calculation would give a higher number). The critical pressure is approximately 140 psi. However, if the maximum allowable stress is reached at a pressure lower than the critical pressure, then that pressure is limiting. This is the case for a BWR guide tube. The allowable stress of 17,450 psi will be reached at approximately 93 psi. Comparing the maximum

possible pressure differential for a steam line break to the limiting pressure of 93 psi gives a design margin greater than 3 to 1. Therefore, the guide tube is not unstable with respect to differential pressure.

4.2.3.3.9   Evaluation of Control Rod Velocity Limiter

The control rod velocity limiter limits the free fall velocity of the control rod to a value that cannot result in nuclear system process barrier damage.

4.2.3.3.10   Channel Bowing

The fuel and core design safety analysis addresses the potential effects of channel bow based on the applicable fuel vendor(s) channel management guidelines. Channel bow impacts are also appropriately included in the development of core operating limits. Core design will preclude or minimize excessive channel bow induced control blade interference issues as much as practical within overall core design and operating requirements. If the core configuration contains control rods which are identified as susceptible to control blade interference from channel bow, the most vulnerable locations will be periodically tested to confirm the interference criteria are met.

4.2.4   Testing and Inspection

4.2.4.1   Fuel, Hardware, and Assembly

Rigid quality control requirements are enforced at every stage of fuel manufacturing to ensure that the design specifications are met. Written manufacturing procedures and quality control plans defined the steps in the manufacturing process. Fuel cladding is subjected to 100 percent dimensional inspection and ultrasonic inspection to reveal defects in the cladding wall. Destructive tests are performed on representative samples from each lot of tubing, including chemical analysis, tensile, and burst tests. Integrity of end plug welds is assured by standardization of weld processes based on radiographic and metallographic inspection of welds. Fuel rod inspection includes metallographic and radiographic examination of fuel rods on a sample basis. Completed fuel rods are helium leak tested to detect the escape of helium through the tubes and end plugs or welded regions. Sample tests are performed for qualification. Production samples are tested as a check on the process and process controls. UO_2 powder

characteristics and pellet densities, composition, and surface finish are controlled by regular sampling inspections. UO_2 weights are recorded at every stage in manufacturing.

Fuel rods are individually numbered prior to fuel loading to (1) identify which pellet group is to be loaded in each fuel rod; (2) identify which position in the fuel assembly each fuel rod is to be loaded; and (3) facilitate total fuel material accountability for a given project. Each finished fuel rod is scanned to screen out any possible but unlikely enrichment deviations.

Further identification of individual fuel rod gadolinia concentrations and uranium enrichments may also be accomplished by markings or geometric differences in the upper end plug shank for each differing rod.

Fuel assembly inspections consist of complete dimensional checks of channels and fuel bundles prior to shipment. Fuel bundles are given another dimensional inspection of significant dimensions at the reactor site prior to use. The method of the postshipment fuel inspection is outlined in Table 4.2-6.

4.2.4.2 Testing and Inspection (Enrichment and Burnable Poison Concentrations)

The shutdown reactivity requirement is verified during initial fuel loading and at any time that core loading is changed. Nuclear limitations for control rod drives are verified by periodically testing the individual system. Test capabilities are described in the appropriate subsections.

The following serves to identify the various tests and inspections employed in verifying the nuclear characteristics of the fuel and reactivity control systems.

4.2.4.2.1 Enrichment Control Program

The incoming UF and the resultant UO_2 powder are verified by emission spectroscopy for impurities.

The sintered pellet is also sampled for impurities. Chemical verification of impurities is also performed for O/U determination.

Each rod is scanned to screen out any possible but unlikely enrichment deviations.

All assemblies and rods of a given project are inspected to assure overall accountability of fuel quantity and placement for the project.

4.2.4.2.2   Gadolinia Inspections

The same rigid quality control requirements observed for standard UO_2 fuel are employed in manufacturing gadolinia-urania fuel. Gadolinia bearing UO_2 fuel pellets of a given enrichment and gadolinia concentration are maintained in separate groups throughout the manufacturing process.

The following quality control inspections are made:

  a.   Gadolinia concentration in the gadolinia-urania powder blend is verified.

  b.   Sintered pellet UO_2-Gd_2O_3 solid solution homogeneity across a fuel pellet is verified by examination of metallographic specimens.

  c.   Gadolinia-urania pellet identification is verified.

  d.   Gadolinia-urania fuel rod identification is checked.

4.2.4.2.3   Reactor Control Rods

Inspections and tests are conducted at various points during the manufacture of control rod assemblies to assure that design requirements are being met. All boron carbide lots are analyzed and certified by the supplier. Among the items tested are:

  a.   Chemical composition

  b.   Boron weight percent

  c.   Boron isotopic content

  d.   Particle size distribution

Following receipt of the boron carbide and review of material certificates, additional samples from each lot are tested including those previously listed. Control is maintained on the BC powder through the remaining steps prior to loading into the absorber rod tubes.

Certified test results are obtained on other control rod components. The absorber rod tubing is subjected to extensive testing by the tubing supplier including 100 percent ultrasonic examination. Metallographic examinations are conducted on several tubes randomly selected from each lot to verify cleanliness and absence of conditions resulting from improper fabrication, cleaning, or heat treatment. Other checks are made on the subassemblies and final control rod assembly, including weld joints inspected and B_4C loading.

4.2.4.3　　Surveillance Inspection and Testing of Irradiated Fuel Rods

Fuel vendors have active programs of surveillance of production BWR fuel. The schedule of inspection is, of course, contingent on the availability of the fuel as influenced by plant operation.

Inspection techniques used include:

a.　Leak detection tests, such as "sipping"

b.　Visual inspection with various aids such as binoculars, borescope, periscope, and/or underwater TV with a photographic record of observations as appropriate

c.　Nondestructive testing of selected fuel rods by ultrasonic test techniques

d.　Dimensional measurements of selected fuel rods

Unexpected conditions or abnormalities which may arise, such as distortions, cladding perforation, or surface disturbances, are analyzed. Resolution of specific technical questions indicated by site examinations may require examination of selected fuel rods in radioactive material laboratory facilities.

The results of the program are used to evaluate the fuel design methods and criteria and are generally reviewed with the Division of Reactor Licensing and documented in generic fuel experience licensing topical reports.

[HISTORICAL INFORMATION] [In addition to the above surveillance programs, four 9x9-5 lead fuel assemblies were introduced at GGNS during the refueling for cycle-4. These assemblies were intended to provide one cycle of operating experience prior to a full

reload of a similar design the following cycle. Detailed inspection of the lead fuel assemblies was performed at the end of Cycle 6 with no unexpected conditions noted (Reference 56).]

4.2.5   Operating and Developmental Experience

4.2.5.1   Fuel Operating Experience

[HISTORICAL INFORMATION] [The initial GGNS core was supplied by General Electric. Prior to GGNS operation, General Electric had designed, fabricated, and put into operation over 55,000 fuel bundles containing approximately 3.2 million fuel rods. The design used at GGNS was introduced by General Electric in 1973 and achieved an annual fuel rod reliability of 99.993%.

Reload Cycles 2 through 8 used fuel designs from Siemens Power Corporation. As of 1993, Siemens Power Corporation has manufactured over 14,500 BWR fuel bundles with approximately 1,000,000 fuel rods either being irradiated or discharged. Of these rods, 401,000 are of the 8x8 design introduced at GGNS starting in Cycle 2 and 440,000 are of the 9x9 design introduced starting in Cycle 5. Siemens Power Corporation has demonstrated excellent fuel reliability. Reload Cycles 9 through 11 used the GE11 fuel design. GEH achieved excellent fuel reliability with this design. Reload Cycles 12 through 16 used the ATRIUM-10 fuel design from AREVA NP. This design demonstrated excellent fuel reliability. GEH fuel was reintroduced starting in Cycle 17. GE14 reload fuel design has also demonstrated excellent fuel reliability.] The GNF2 design introduced in cycle 18 is expected to have the same excellent fuel reliability as the GE14 based on the similarity of key design features.

4.2.5.2   Fuel Development Experience

[HISTORICAL INFORMATION] [The production of Zircaloy clad UO_2 pellet fuel experience described in subsection 4.2.5.1 is supplemented by a large amount of in-pile and out-of-pile developmental work. The developmental work to date has been employed to test a wide range of design characteristics, to investigate various mechanisms affecting the performance of the fuel rod, and to extend irradiation experience to higher local combinations of fuel rod power and exposure than covered by production fuel. In addition, participation in the DOE's Fuel Improvement Program has resulted in improved PCI-resistant fuel designs.]

Page intentionally deleted

4.2.5.3   Fuel Rod Perforation Experience

[HISTORICAL INFORMATION] [The early BWR fuel experience has been
extensively described in previous reports. In general, the
Zircaloy-2 cladding performance in the very early plants was
good; however, some fuel failure mechanisms were exposed and
corrected and are not significantly affecting current fuel
performance. Details of this experience are provided in
References 7, 21, and 22. The current fuel design incorporates
improvements in design and manufacturing which provide confidence
that a high degree of reliability can be expected.

Operation with failed fuel rods has shown that the fission product
release rate from defective fuel rods can be controlled by
regulating power level. The rate of increase in released activity
apparently associated with progressive deterioration of failed
rods has been deduced from chronological plots of the offgas
activity measurements in operating plants. These data indicate
that the activity release level can be lowered by lowering the
local power density in the vicinity of the fuel rod failure. These
measured data also indicate that sudden or catastrophic failure
of the fuel assembly does not occur with continued operation and
that the presence of a failed rod in a fuel assembly does not
result in propagation of failure to neighboring rods. Shutdown
can be scheduled, as required, for repairing or replacing fuel
assemblies that have large defects.

Evaluation of the fission product release rate for failed fuel
rods shows a wide variation in the activity release levels.
Designers have attempted to relate the release rates to detect
type, size, and specific power level. These data support the
qualitative observations that fission product release rates are
functions of power density and that progressive deterioration is
a function of time.]

4.2.5.4   Channel Operating Experience

[HISTORICAL INFORMATION] [General Electric Company has more than
144,000 Zircaloy channels in operating reactors and surveillance
of their performance is ongoing. Carpenter Technology is another
supplier of GGNS channels. Carpenter Technology has produced over
30,000 Zircaloy channels since 1958. The Carpenter Technology
channels for use at GGNS are the equivalent of the GEH channels
and will have similar performance.

The performance of the channels currently in operation has shown
no tendency for gross in-service deformations that might
challenge control rod drive (CRD) performance. However distortion
has caused limited indications of channel/control-blade
interference and has been identified as a potential life-limiting
phenomenon. Separate reports/communications on this subject have
been provided (Ref. 20, 23, 24, 51, 60 and 63).]

4.2.6   Deleted

4.2.7   References

1.   Miner M. A., "Cumulative Damage in Fatigue," Applied
     Mech., 12, Transactions of the ASME, 67 (1945)

2.   O'Donnell, W. F., and Langer B. F., "Fatigue Design Basis
     for Zircaloy Components," Nuclear Science and Engineering,
     Vol. 20, 1964, pp 1-12

3.   "BWR 6 Fuel Design," June 1976 (NEDO-20948-P)

4.   "General Electric Boiling Water Reactor Generic Reload
     Application for 8x8 Fuel," March 25, 1976 (NEDO-20360-1P),
     Revision 4

5.   "Effect of High Burnup on Zircaloy Clad, Bulk UO Plate
     Fuel Element Samples," September 1962 (WAPD-TM-283)

6.   "Irradiation Behavior of Zircaloy Clad Fuel Rods
     Containing Dished End UO Pellets," July 1967 (WAPD-TM-629)

7.   Williamson, H. E., and Ditmore D. C., "Experience with BWR
     Fuel Through September 1971," May 1972 (NEDO-10505)

8.   Ditmore, D. C. and Elkins R. B., "Densification
     Considerations in BWR Fuel Design and Performance,"
     December 1972 (NEDM-10735)

9.   Christenson J. A., "Melting Point of Irradiated Uranium
     Dioxide," February 1965 (WACP-6065)

10. "Thermal Conductivity of Uranium Dioxide," Technical
     Report Series No. 59, IAEA, Vienna, 1966

11. Supplement 1 to the Technical Report on Densification of
     General Electric Reactor Fuels, December 1973

12. Moore, V. A., letter to Mitchell, I. S. "Modified GE Model for Fuel Densification," Docket 50-321, March 22, 1974

13. "Creep Collapse Analysis of BWR Fuel Using Safe Collapse Model," August 1974 (NEDE-20606) (Proprietary), (NEDO-20605) (Nonproprietary)

14. "8x8 Fuel Bundle Development Support," February 1975 (NEDO-20377)

15. "General Electric Boiling Water Reactor Generic Reload Application for 8x8 Fuel," May 1975 (NEDO-20360) (Supplement 4)

16. Stephan, L. A., "The Response of Waterlogged UO2 Fuel Rods to Power Bursts," April 1969 (IDO-ITR-105)

17. Stephan, L. A., "The Effects of Cladding Material and Heat Treatment on the Response of Waterlogged UO2 Fuel Rods to Power Bursts," January 1970 (IN-ITR-111).

18. "Thermal Response and Cladding Performance of an Internally Pressurized, Zircalogy Clad, Simulated BWR Fuel Bundle Cooled by Spray Under Loss-of-Coolant Conditions," April 1971 (GEAP-13112)

19. "Consequences of a Postulated Flow Blockage Incident in a BWR," October 1977 (NEDO-10174, Rev 1)

20. "BWR Fuel Channel Mechanical Design and Deflection," September 1976 (NEDE-21354-P), GE Proprietary

21. Elkins, R. B., "Experience with BWR Fuel Through September 1974," June 1975 (NEDO-20922)

22. Williamson, H. E., and Ditmore, D. C., "Current State of Knowledge High Performance BWR Zircaloy Clad UO2 Fuel," May 1970 (NEDO-10173)

23. "Fuel Channel Deflections," May 1974 (NEDE-20386)

24. Hinds, J. A., letter to Skovholt, D. J. dated November 28, 1973, "Interim Report - BWR Fuel Channel Deflections"

25. Olson, H. P., "In-Pile Burnout Protection Demonstrated at HBWR," Euro Nuclear, December 1964

26. Boyden, J. E., Levy, S., Lyons, M. F., Sorlie, T., "Experience with Operating BWR Fuel Rods Above the Critical Heat Flux," Nucleonics, April 1965, Volume 23, No. 4

27. Kjaerheim, G., Rolstad, E., "BWR Burnout Experiments," Nuclear Engineering International, December 1968

28. Sorlie, T., "Consequences of Operating Zircaloy-2 Clad Fuel Rods Above the Critical Heat Flux," October 1965, APED-4986

29. Redpath, W., "Winfrith SGHWR In-Reactor Dryout Tests," Journal of the British Nuclear Energy Society, 1974, 13(1) pp. 87-97

30. Thompson, L. N., et al., "Light Water Reactor Fuel Behavior Program Description: RIA Fuel Behavior Experiment Requirements," USAEC Report RE-S-76-170, September 1976

31. Potts, G. A., "Urania-Gadolinia Nuclear Fuel Physical and Irradiation Characteristics and Material Properties," January 1977 (NEDE-20943) Proprietary, (NEDO-20943) Nonproprietary

32. "BWR Fuel Assembly Evaluation of Combined SSE and LOCA Loadings (Amendment No. 3)," NEDE-21175-3P, July 1982

33. Elkins, R. B., "Fuel Rod Prepressurization Amendment 1," May 1978 (NEDO-23786-1)

34. Letter, E. D. Fuller to O. D. Parr, "NRC Request for Additional Information on Fuel Rod Prepressurization," June 8, 1978

35. Letter, E. D. Fuller to O. D. Parr, "NRC Request for Additional Information on Fuel Rod Prepressurization," August 14, 1978

36. Elkins, R. B., "Fuel Rod Prepressurization," March 1978 (NEDE-23786-1-P)

37. Deleted

38. Letter, R. E. Engel, GE, to T. A. Ippolito, NRC, "Extension of ECCS Performance Limits," dated May 6, 1981.

39. Deleted

40. Chandler, J. C., "Grand Gulf Unit 1 Cycle 2 Reload Analysis", Advanced Nuclear Fuels Corporation Report XN-NF-86-35, Appendix F, Revision 3, August 1986

41. Macduff, R. B., et al, "Grand Gulf Unit 1 Cycle 5 Reload Analysis", Advanced Nuclear Fuels Corporation Report ANF-90-022, Appendix A, Revision 2, August 1990

42. Merckx, K. R., "Cladding Collapse Calculational Procedure", Advanced Nuclear Fuels Corporation Report JN-72-23, November 1972

43. Merckx, K. R., and Hoppe, N. E., "RAMPEX Pellet-Clad Interaction Evaluation Code for Power Ramps", Advanced Nuclear Fuels Corporation Report XN-NF-573(P), May 1982

44. Deleted

45. Zimmermann, H., "Untersuchungun zum Schwellen and Spaltgasverhalten in Osidischem Kernbrennstoff unter Nuetronenbestranhlung", KFK-2467, June 1977

46. Deleted

47. Deleted

48. Deleted

49. Deleted

50. Potts, G.A., "Fuel Rod Thermal-Mechanical Analysis Methodology (GESTR-MECHANICAL)," August 1992 (NEDC-32079P)

51. GE Nuclear Energy, "General Electric Standard Application for Reactor Fuel (GESTAR II)," NEDE-24011-P-A and NEDE-24011-P-A-US, (Proprietary); and NEDO-24011-P-A and NEDO-24011-P-A-US, (Non-Proprietary), (latest approved revision)

52. Deleted

53. Deleted

54. Deleted

55. Deleted

56. "Inspection of SPC 8x8 and 9x9 Fuel Assemblies at Grand Gulf, September 1994," Siemens EMF-94-195(P)

57. Deleted

58. Deleted

59. Deleted

60. EMF-93-177(P)(A) Revision 1, "Mechanical Design for BWR Fuel Channels," dated August 2005.

61. "Maneuvering and Conditioning Criteria for Atrium-10 Fuel with Non-Liner Cladding (REMACCX-10) to Use with POWERPLEX-III," Framatome-ANP, EMF-2480(P) Rev. 1, December 2003.

62. Deleted

63. Safety Communication (SC) 08-05, "Updated Surveillance Program for Channel-Control Blade Interference Monitoring," Revision 1, December 2008.

64. Deleted

65. Global Nuclear Fuel, "GNF2 Advantage Generic Compliance with NEDE-24011-P-A (GESTAR II)," NEDC-33270P, Revision 9, Dec.2017.

66. "Cladding Creep Collapse Licensing Topical Report," NEDC 33139P-A, July 2005.

67. GE-Hitachi Nuclear Energy,"The PRIME Model for Analysis of Fuel Rod Thermal-Mechanical Performance," Technical Bases - NEDC-33256P-A, Qualification - NEDC-33257P-A, and Application Methodology - NEDC-33258P-A, September 2010.

68. USNRC Letter to GNF-Americas, "Letter Transmitting Final Safety Evaluation for GNF Topical Reports NEDC-33256P, NEDC-33257P, and NEDC-33258P, The PRIME Model for Analysis of Fuel Rod Thermal-Mechanical Performance," January 22, 2010.

TABLE 4.2-1: [HISTORICAL INFORMATION] CONDITIONS OF DESIGN RESULTING FROM IN-REACTOR PROCESS CONDITIONS COMBINED WITH EARTHQUAKE LOADING

CONDITIONS OF DESIGN

Reactor Initial	Percent of Safe Shutdown Earthquake Imposed		
Conditions	**0%**	**50%**	**100%**
Start-up Testing	Upset	--	--
Normal	Normal	Upset	Faulted
Abnormal	Upset	--	--

TABLE 4.2-2: [HISTORICAL INFORMATION] STRESS INTENSITY LIMITS

	Yield Strength (S_y)	Ultimate Tensile Strength (S_u)
Primary Membrane Stress	≤ 2/3	≤ 1/3 to 1/2
Primary Membrane Plus Bending Stress Intensity	≤ 1	≤ 1/2 to 3/4
Primary Plus Secondary Stress Intensity	≤ 2	≤ 1.0 to 1.5

TABLE 4.2-3: [HISTORICAL INFORMATION] ESTIMATED NUMBER OF CYCLES FOR EACH CYCLIC CONDITION USED FOR FATIGUE ANALYSIS

Cyclic Condition	Estimated Cycles
Room temperature to 100% power	~4/yr
Hot standby to 100% power	~12/yr
50% power to 100% power	~60/yr
75% power to 100% power	~250/yr
100% power to 116% power	~1/2 yr

The above is applicable for the initial core. For the current GNF2 fuel see Reference 51.

TABLE 4.2-4: FUEL DATA

Core	GE 8x8	ANF 8x8	ANF 9x9-5	GE11	Atrium-10	GE14[j]	GNF2[j]
Reloads	Initial Core	Cycles 2-4	Cycle 5[c]-8	Cycle 9-11	Cycle 12-16	Cycle 17	Cycle $\geq$ 18
Number of Fuel Assemblies	800	800	800	800	800	800	800
Fuel Cell Spacing (Control Rod Pitch), in.	12	12	12	12	12	12	12
Total Number of Fueled Rods	49600[a]	49600[a,d]	60800[a,d]	59,200[a,d]	72,800[a,d]	73,600[a,d]	73,600[a,d]
Core Power Density (Rated Power) kW/ℓ	54.14	54.14	54.14	54.14	55.06	55.06	55.06
Total Core Heat Transfer Area, ft^2	78398	78560	86240	79520	90642	90160	90522
Control Rod Thickness, in.	0.328	0.328	0.328	0.328	0.328	0.328	0.328

Fuel Assembly Data

	GE 8x8	ANF 8x8	ANF 9x9-5	GE11	Atrium-10	GE14[j]	GNF2[j]
Nominal Active Fuel Length, in.	150[b]	150[b]	150[b]	146[e]	149[g]	150.0[i]	150.0[i]
Fuel Rod Pitch, in.	0.636	0.636	0.563	0.566	0.510		
Fuel Rod Spacing, in.	0.153	0.152	0.120-0.146	0.126	0.114		
Fuel Bundle Heat Transfer Area, ft^2	98	98.2	107.8	99.4	113.3		
Fuel Channel Wall Thickness, in.	0.120	0.120	0.120	0.120/0.075	0.114/0.067		

TABLE 4.2-4: FUEL DATA (Continued)

Core	GE 8x8	ANF 8x8	ANF 9x9-5	GE11	Atrium-10	GE14[j]	GNF2[j]
Channel Width (Inside), in.	5.215	5.215	5.215	5.278	5.278		
Fuel Assembly Pitch, in.	6.0	6.0	6.0	6.0	6.0	6.0	6.0
Fuel Assembly Cross Section, in.²	5.455x 5.455	5.455x 5.455	5.455x 5.455	5.518x 5.518	5.258x 5.258		
Spacer Pitch, in	20.15	20.15	20.15	20.15	20.15		
Fuel Rod Data							
Outside Diameter, in.	0.483	0.484	0.417/0.443	0.440	0.396		
Cladding Inside Diameter, in.	0.419	0.414	0.360/0.382	0.384	0.348		
Cladding Thickness, in.	0.032	0.035	0.0285/0.0305	0.028	0.024		
Fission Gas Plenum Length, in.	9.48	10.02	9.62	14.14[f]	11.07[g]		
Pellet Immersion Density, %TD	95	94.5	94.5	96.5	95.85		
Pellet Outside Diameter, in.	0.410	0.405	0.353/0.3745	0.376	0.341		
Pellet Length, in.	0.410	Variable	Variable	0.380	0.413[h]		
Water Rod Data							
Outside Diameter, in.	0.591	0.484	0.417/0.546	0.980	–		
Inside Diameter, in.	0.531	0.414	0.360/0.522	0.920	–		
Number of Water Rods	2	2	5	2	–		

TABLE 4.2-4: FUEL DATA (Continued)

Water Channel Data

Outside envelope, in.	1.378
Wall Thickness	0.0285

All values are typical

[a] Does not include water rods.

[b] Includes the Natural U at the top and bottom of the fuel column.

[c] Not including the four SPC 9x9-5 LTAs loaded in Cycle-4.

[d] Assumes full core of this fuel design.

[e] This is the active length of the uranium oxide fuel rods. The godalina bearing rods are 138 inches and the part length rods are 90 inches.

[f] This is for the full length rod with only uranium oxide.

[g] Full-length Rod

[h] Central Zone Pellets

[i] This is the active length of the uranium oxide fuel rods. The gadolinia bearing rods are 144 inches and the part length rods are 84 inches.

[j] Data omitted is considered proprietary to GNF and is available in Reference 52.

TABLE 4.2-5: MATERIAL PROPERTIES*

Zircaloy-2 Cladding

Thermal Conductivity T = (600 to 800°F) k = 9-10 (Btu/hr-ft-°F)

Coefficient of Linear Thermal Expansion

$$\frac{1}{L_o} \frac{\Delta L}{\Delta T} \sim 3 \times 10^{-6} \ (°F)$$

Total Elongation (Irradiated) $\geq$ 1%

UO$_2$ Pellets

Thermal Conductivity = $\frac{3978.1}{692.61 + T} + 6.02366 \times 10^{-12} (T + 460)^3$

(Btu/hr-ft-°F)

Melting Temperature = $5080 - 63.5 \times 10^{-4} E$ (°F)

(where E = Exposure MWd/Mt)

---

* Additional information on material properties is presented in
  Section 4.3 of Reference 4 and Section 4 of Reference 3 for the
  initial fuel load, and Reference 67 for the current GNF2 fuel .

TABLE 4.2-6: POST SHIPMENT FUEL INSPECTION PLAN

Characteristic	Method
Container Damage and Leak	Visual
Bundle Damage	Visual
Cleanliness	Visual
Rod Integrity	Visual
Lock Tab Washers	Visual
Channel Integrity	Visual
Channel Cleanliness	Visual
Fastener Integrity and Installation	Visual and Torque Wrench
Spacer Damage	Visual
Rod to Rod	Feeler Gauge, when required
Seal Guard Removal	Visual
Upper Tie Plate	Visual

TABLE 4.2-7: DELETED

TABLE 4.2-8: DELETED

TABLE 4.2-9: DELETED

TABLE 4.2-10: DELETED

TABLE 4.2-11: DELETED

TABLE 4.2-12: DELETED

TABLE 4.2-13: DELETED

TABLE 4.2-14: [HISTORICAL INFORMATION] GENERAL ELECTRIC ASSESSMENT OF NRC FISSION GAS CORRECTION FACTOR FOR GRAND GULF (INITIAL CYCLE)

Fuel Type	Exposure (GWd/MT)	GE Evaluation of PCT Increase NRC Correction Factor °F	Plant Margin to 2200 F (°F)	Net PCT Decrease Model Improvement (°F)*	Overall Margin (°F)
P8x8R	22	10	115	150	255
	28	30	186	150	306
	33	70	318	150	398
	39	130	436	150	456
	44	200	508	150	458

* Models used for Grand Gulf (Modified Bromley and CCFL) have been approved by the NRC and are estimated to result in a PCT decrease of at least 150°F at all exposures.
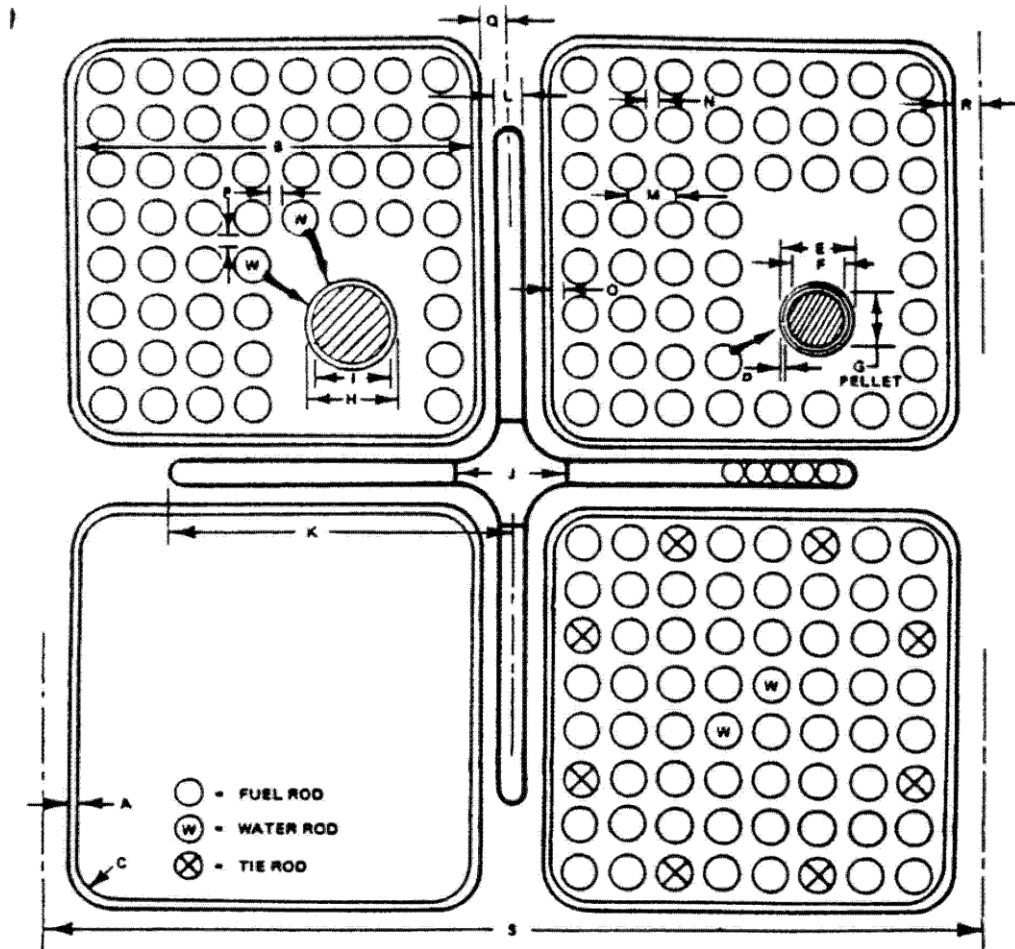
	CHANNEL			FUEL ROD			PELLET	WATER ROD	
DIM I.D.	A	B	C	D	E	F	G	H	I
DIM INCHES	0.120	5.215	0.380	0.032	0.483	0.419	0.410	0.591	0.531

	CONTROL ROD			BUNDLE LATTICE				CELL		
DIM I.D.	J	K	L	M	N	O	P	Q	R	S
DIM INCHES	1.55	4.902	0.328	0.636	0.153	0.140	0.099	0.2725	0.2725	12.00

For subsequent reloads, see references.

GRAND GULF NUCLEAR STATION UNIT 1 UPDATED FINAL SAFETY ANALYSIS REPORT	CORE CELL NOMINAL DIMENSIONS (Initial Core) [HISTORICAL INFORMATION] FIGURE 4.2-1

CONTROL ROD GAP

UPPER TIE PLATE

CENTERING SPRING

TOP GUIDE

CHANNEL
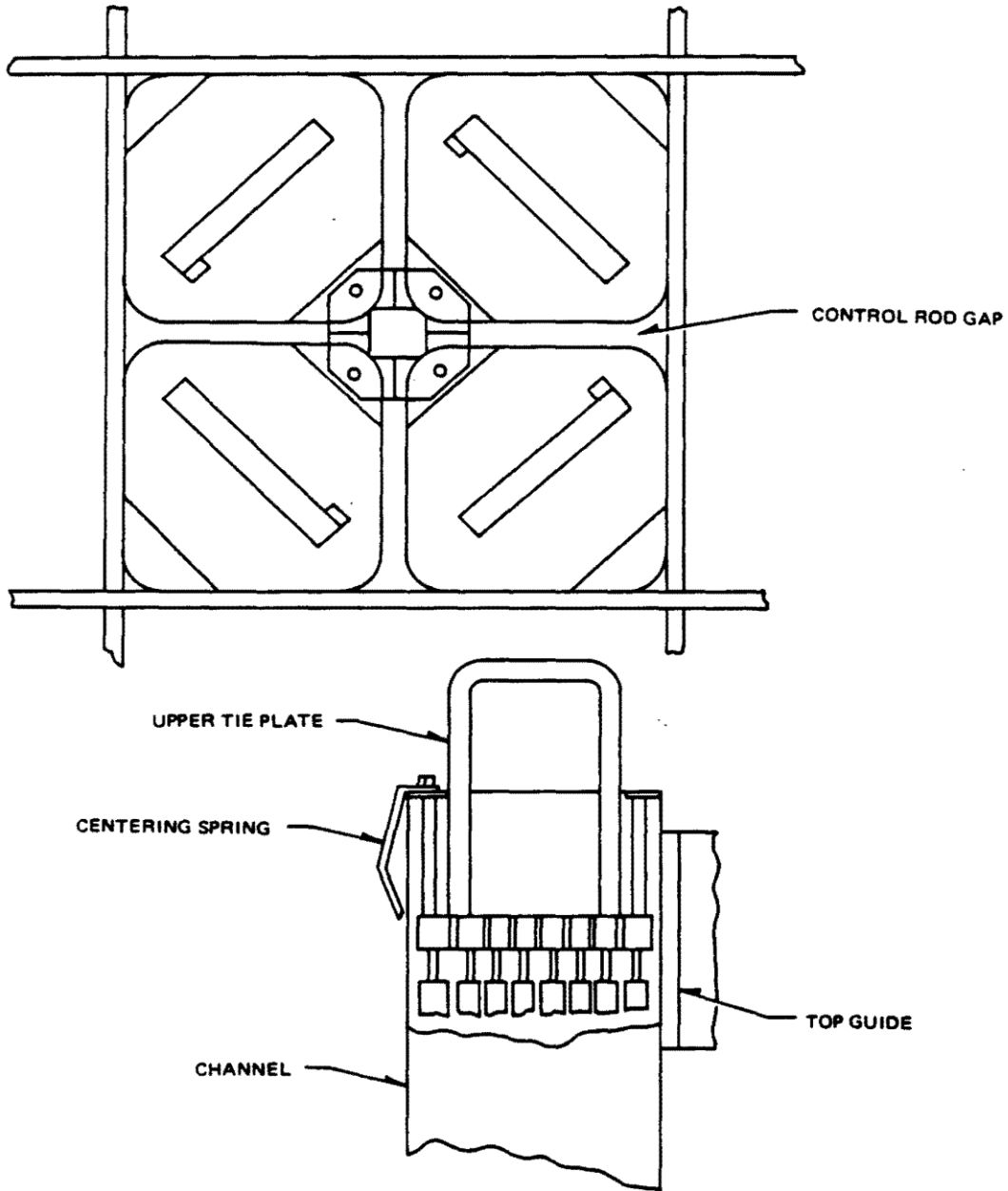
GRAND GULF NUCLEAR STATION UNIT 1 UPDATED FINAL SAFETY ANALYSIS REPORT	SCHEMATIC OF FOUR-BUNDLE CELL ARRANGEMENT FIGURE 4.2-2

BAIL HANDLE

UPPER TIE PLATE

FUEL BUNDLE

FUEL ROD INTERIM SPACER

FINGER SPRING (TYPICAL OF 4)

CHANNEL FASTNER ASSEMBLY

UPPER TIE PLATE

FUEL CLADDING

FUEL CLADDING

FUEL CHANNEL

LOWER TIE PLATE

NOSE PIECE

EXPANSION SPRING

PLENUM SPRING

FUEL PELLET

FUEL ROD
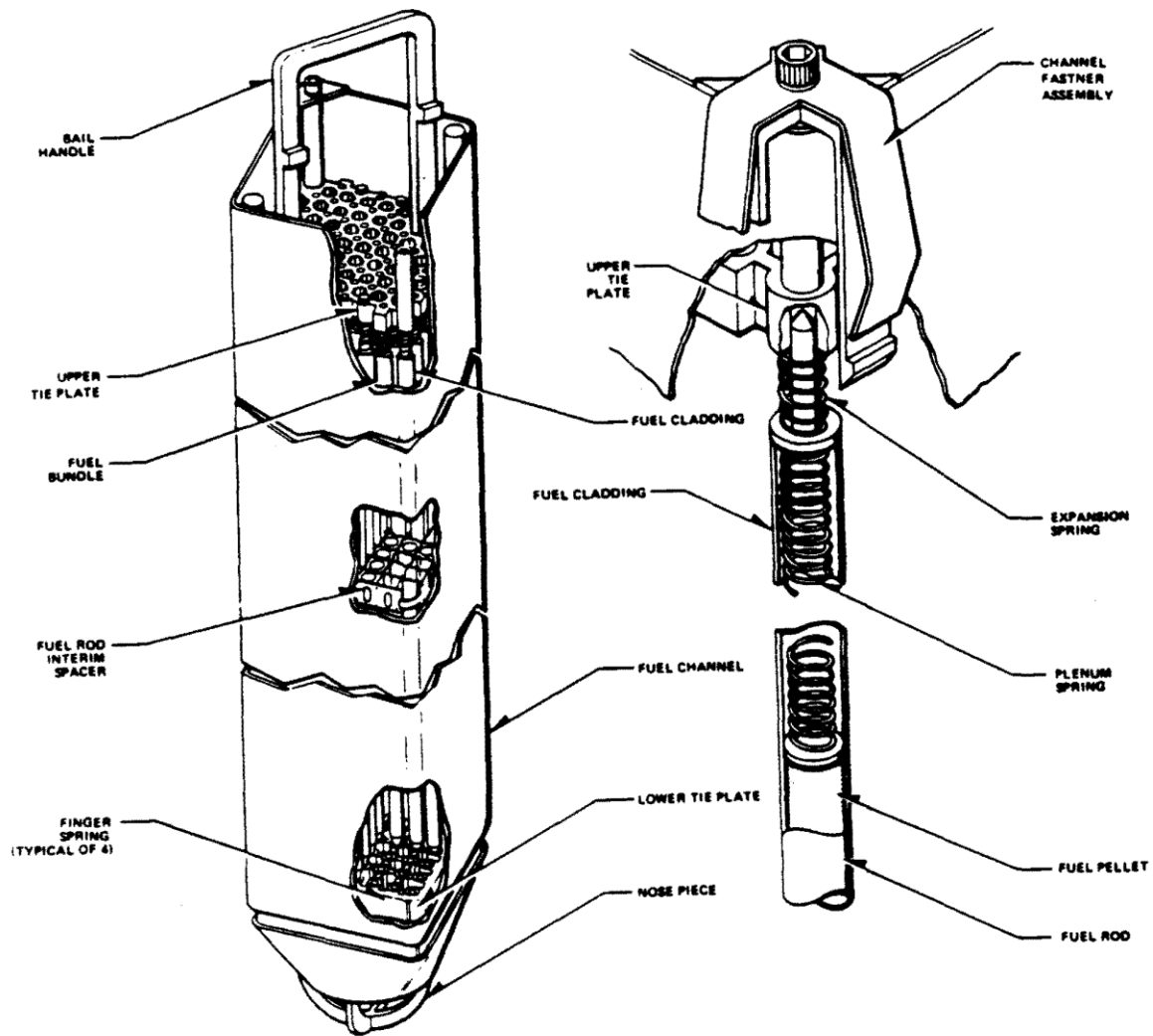
GRAND GULF NUCLEAR STATION UNIT 1 UPDATED FINAL SAFETY ANALYSIS REPORT	FUEL ASSEMBLY (TYPICAL)
	FIGURE 4.2-3

TYPICAL FUEL ROD

ACTIVE FUEL LENGTH

LOWER TIE PLATE CASTING

SPACER TYPICAL OF SEVEN

CHANNEL

UPPER TIE PLATE

SPACER DETAIL

WS   SPACER POSITIONING WATER ROD
W   WATER ROD
T   TIE ROD
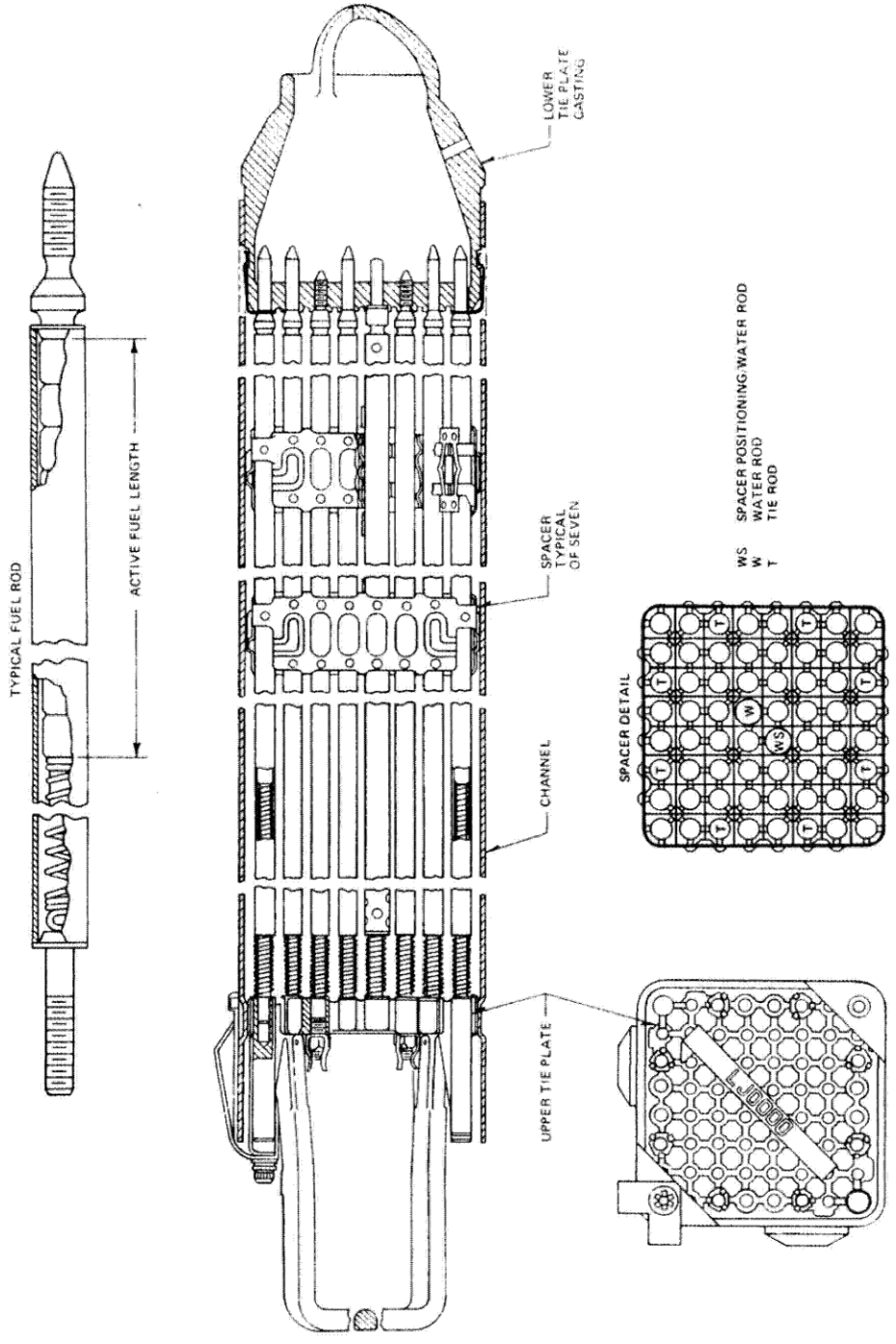
The above is for the Initial Core. For subsequent reloads, see references.

GRAND GULF NUCLEAR STATION
UNIT 1
UPDATED FINAL SAFETY ANALYSIS
REPORT

FUEL ASSEMBLY
CROSS SECTION
[HISTORICAL INFORMATION]
FIGURE 4.2-4
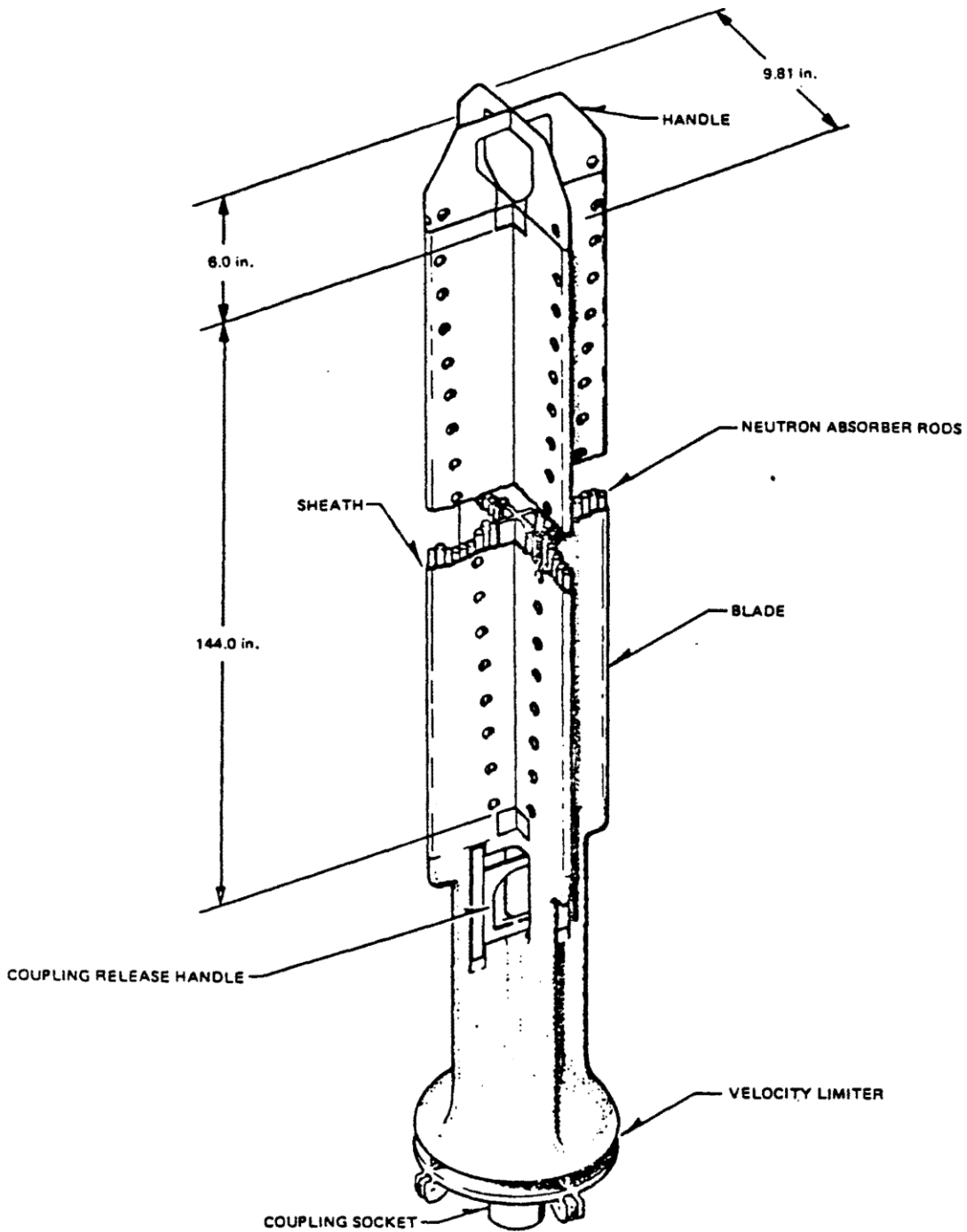
GRAND GULF NUCLEAR STATION UNIT 1 UPDATED FINAL SAFETY ANALYSIS REPORT	CONTROL ROD ASSEMBLY
	FIGURE 4.2-5
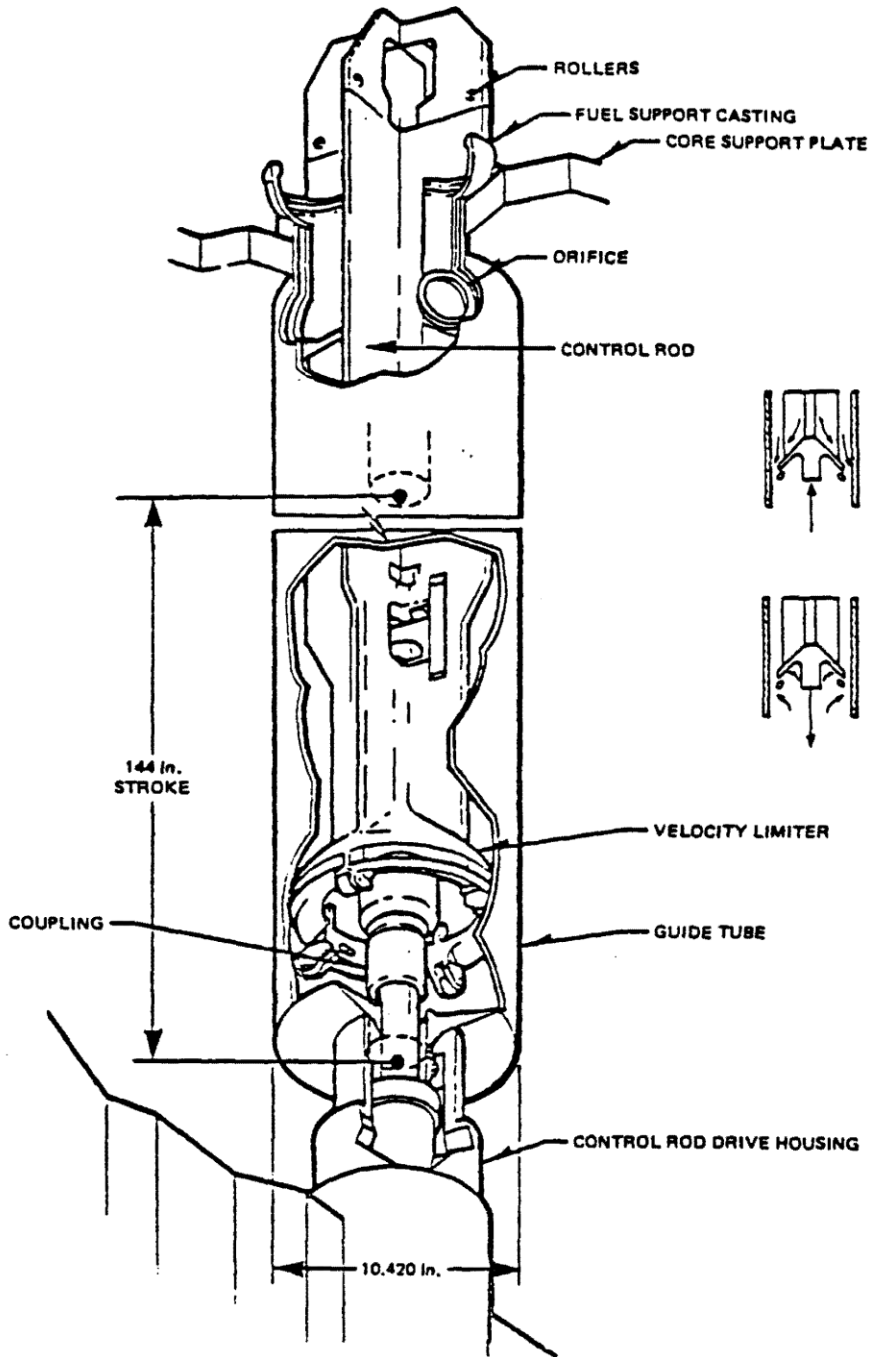
GRAND GULF NUCLEAR STATION UNIT 1 UPDATED FINAL SAFETY ANALYSIS REPORT	CONTROL ROD VELOCITY LIMITER FIGURE 4.2-6a
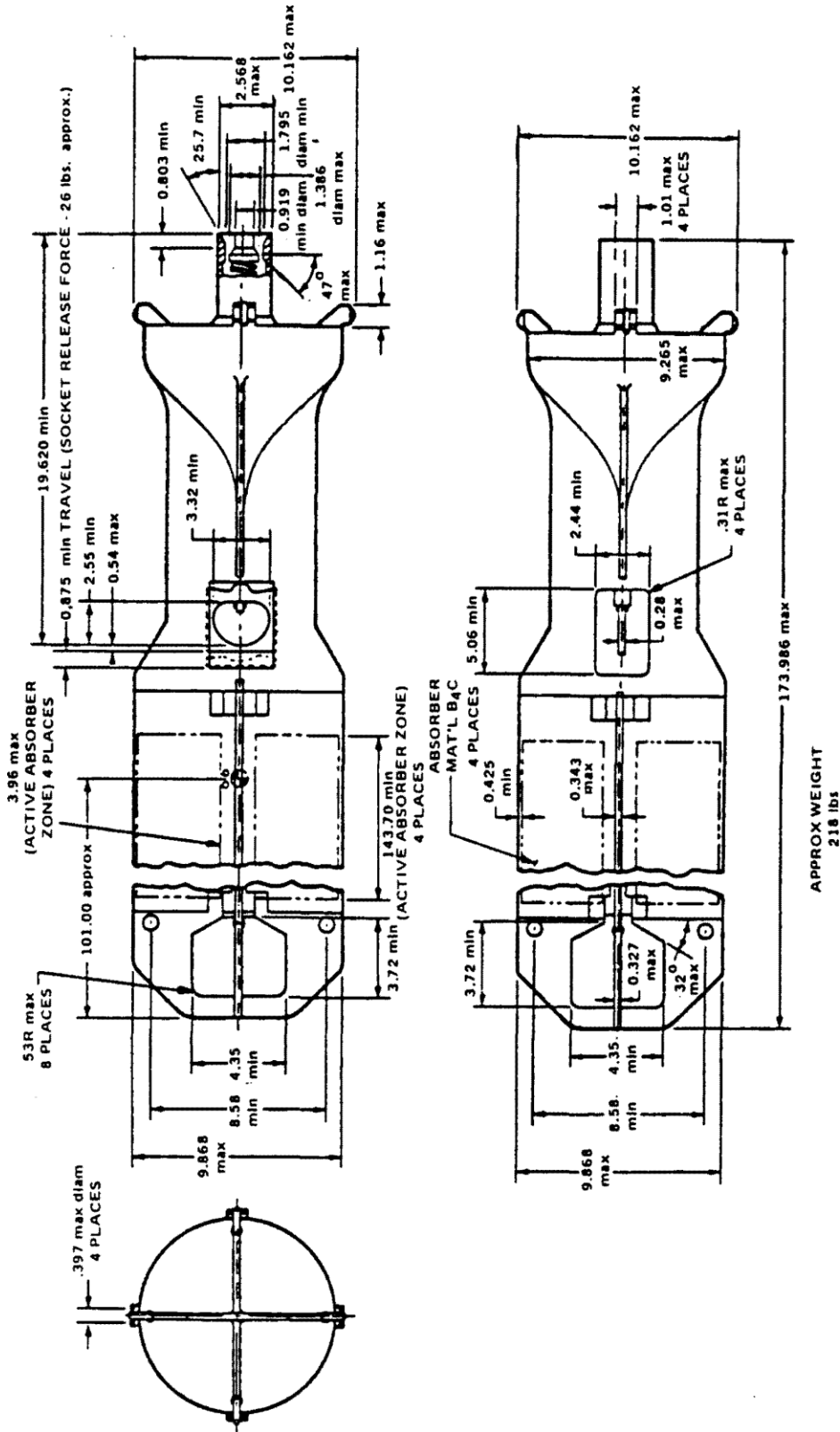
GRAND GULF NUCLEAR STATION
UNIT 1
UPDATED FINAL SAFETY ANALYSIS
REPORT

CONTROL ROD INFORMATION DIAGRAM
FOR C-LATTICE

FIGURE 4.2-6b

UFSAR FIGURE 4.2-6c
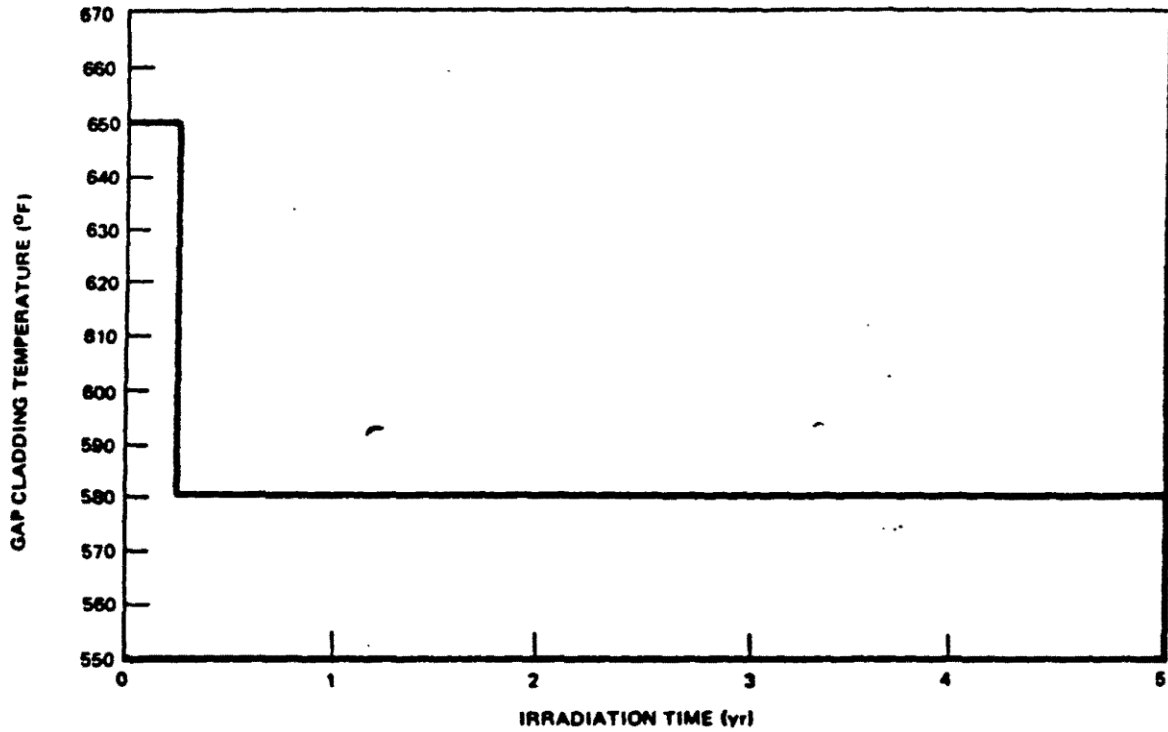
APPLICABLE ONLY TO THE INITIAL CORE LOADING.

[HISTORICAL INFORMATION]

GRAND GULF NUCLEAR STATION UNIT 1 UPDATED FINAL SAFETY ANALYSIS REPORT	FUEL CLADDING AVERAGE TEMPERATURE AT A FUEL COLUMN AXIAL GAP FIGURE 4.2-7
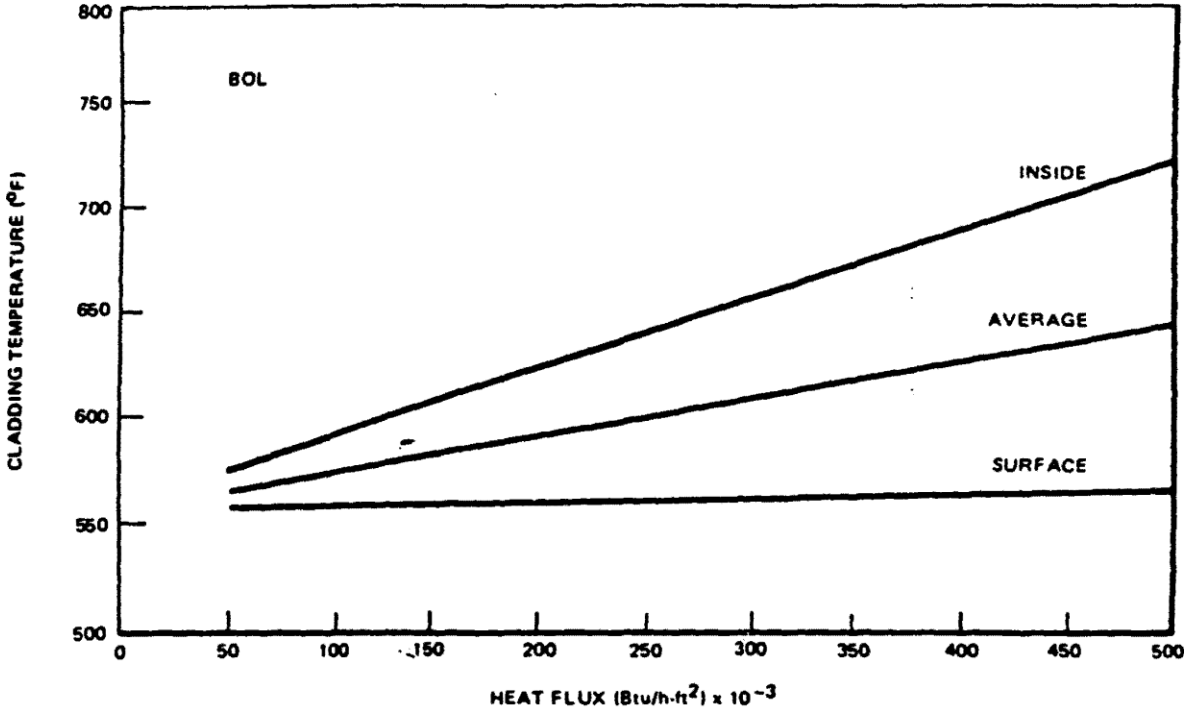
TYPICAL   [HISTORICAL INFORMATION]

GRAND GULF NUCLEAR STATION UNIT 1 UPDATED FINAL SAFETY ANALYSIS REPORT	CLADDING TEMPERATURE VERSUS HEAT FLUX, BEGINNING OF LIFE FIGURE 4.2-8
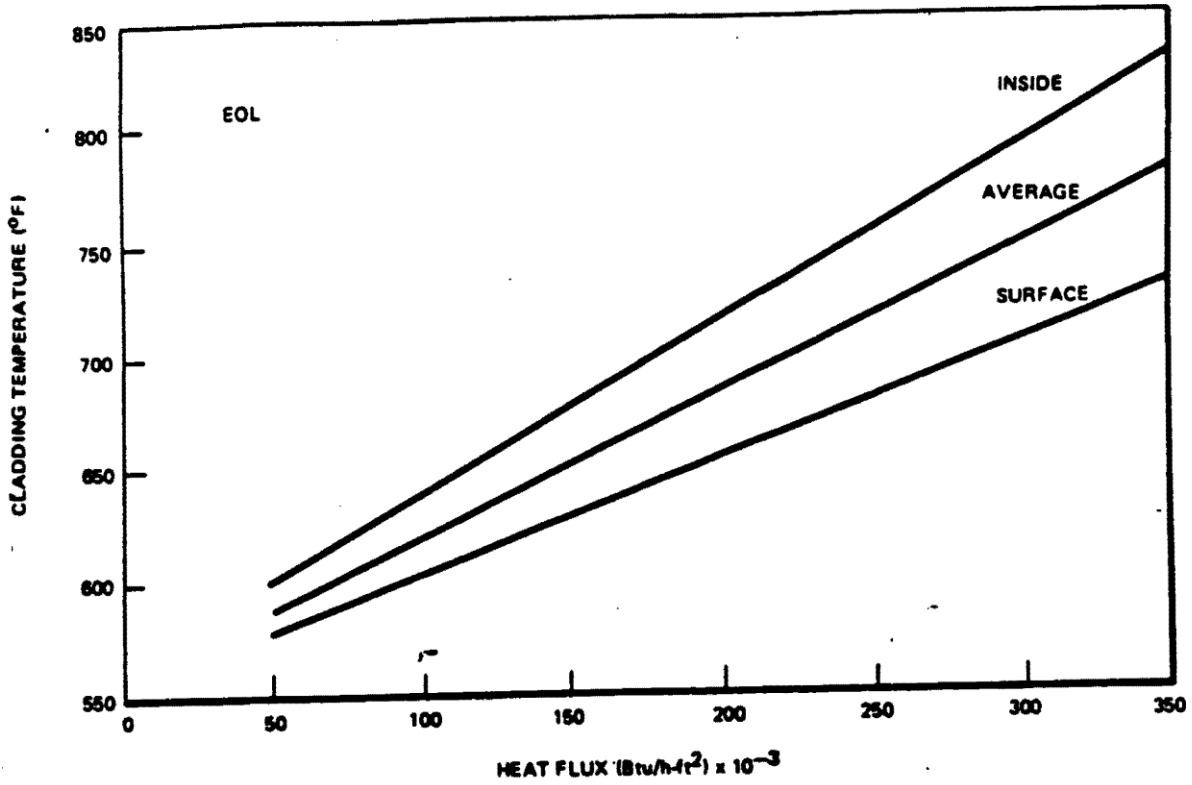
TYPICAL

[HISTORICAL INFORMATION]

GRAND GULF NUCLEAR STATION UNIT 1 UPDATED FINAL SAFETY ANALYSIS REPORT	CLADDING TEMPERATURE VERSUS HEAT FLUX, END OF LIFE FIGURE 4.2-9

ASSUMPTIONS:
(1) ALL RODS IN THE BUNDLE ARE AT THE SAME TEMPERATURE
(2) RODS REACH INDICATED TEMPERATURE INSTANTANEOUSLY

TYPICAL

[HISTORICAL INFORMATION]
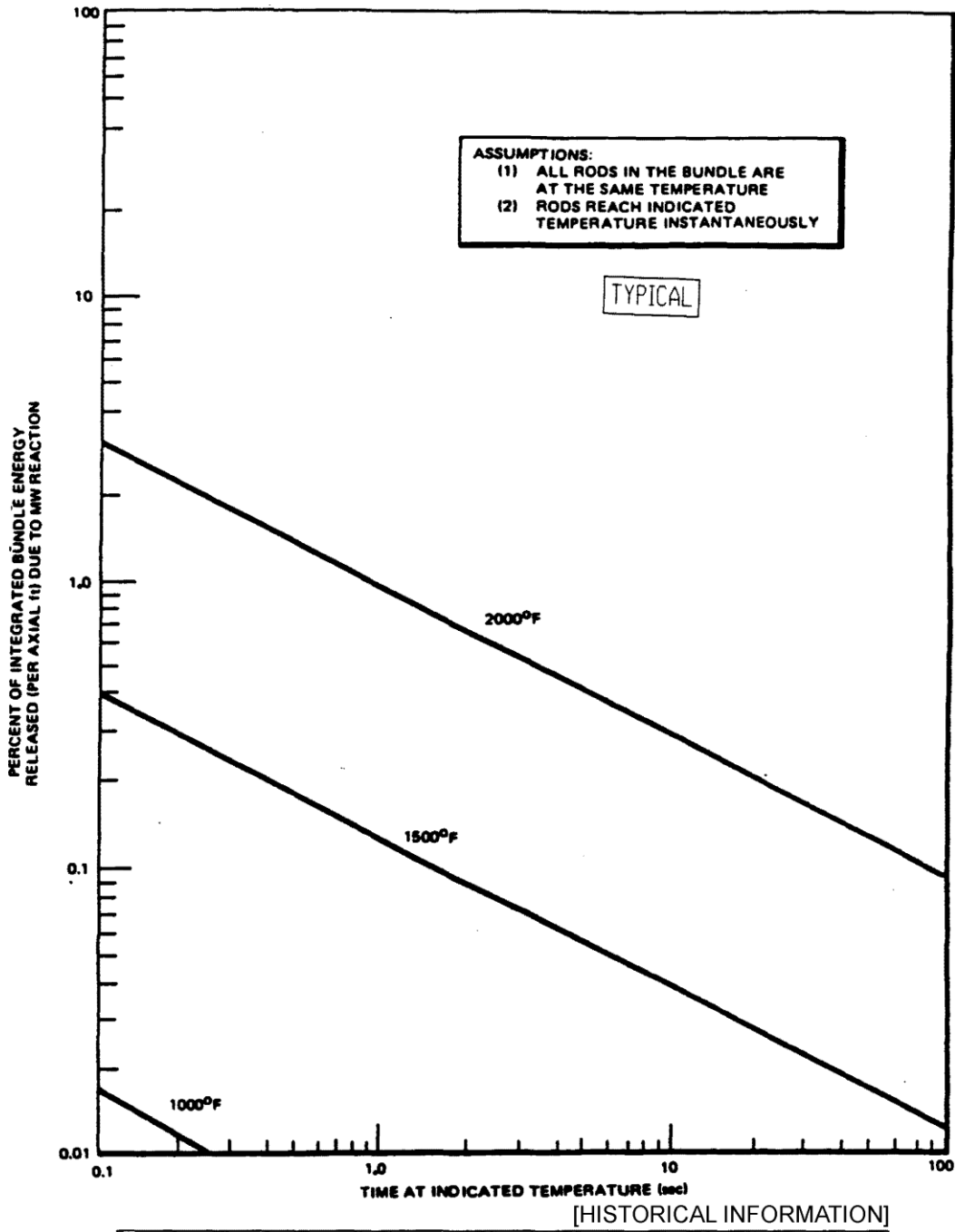
| GRAND GULF NUCLEAR STATION UNIT 1 UPDATED FINAL SAFETY ANALYSIS REPORT | FUEL ENERGY RELEASE AS A FUNCTION OF TIME FIGURE 4.2-10 |

4.3   NUCLEAR DESIGN

4.3.1   Design Bases

The nuclear design bases are conveniently divided into two specific categories. The safety design bases are those which are required for the plant to operate from safety considerations. The second category is the plant performance design bases which are required in order to meet the objective of producing power in an efficient manner.

4.3.1.1   Safety Design Bases

The safety design bases are requirements which protect the nuclear fuel from damage which would result in release of radioactivity which would represent an undue risk to the health and safety of the public. In general, the safety bases fall into two categories, the reactivity basis which prevents an uncontrolled positive reactivity excursion and the overpower bases which prevent the core from operating beyond the fuel integrity limits.

4.3.1.1.1   Reactivity Basis

The nuclear core and fuel design meets the following bases:

The core system is capable of being rendered subcritical at any time or at core conditions with the highest worth control rod fully withdrawn.

4.3.1.1.2   Overpower Bases

The nuclear core and fuel design meets the following basis:

   a.   The void coefficient shall be negative over the entire operating range.

   b.   The limits on Linear Heat Generation Rate (LHGR), Minimum Critical Power Ratio (MCPR), and the Maximum Average Planar Linear Heat Generation Rate (MAPLHGR), shall not be exceeded during steady-state operation.

   c.   The nuclear characteristics of the design shall exhibit no tendency toward divergent operation.

4.3.1.2   Plant Performance Design Bases

The core and fuel design meets the following bases:

   a.   The design shall have adequate excess reactivity to attain
         the desired cycle length.

   b.   The design shall be capable of operating at rated
         conditions without exceeding limits.

   c.   The core and fuel design and the reactivity control system
         shall allow continuous, stable regulation of reactivity.

   d.   The core and fuel design shall have adequate reactivity
         feedback to facilitate normal operation.

4.3.2   Description

The BWR core design utilizes a light-water moderated reactor,
fueled with slightly enriched uranium dioxide. The use of water as
a moderator produces a neutron energy spectrum in which fissions
are caused principally by thermal neutrons. At operating
conditions the moderator boils, producing a spatially variable
density of steam voids in the core. The BWR design provides a
system for which reactivity changes are inversely proportional to
the steam void content in the moderator. This void feedback effect
is one of the inherent safety features of the BWR system. Any
system input which increases reactor power, either in a local or
gross sense, produces additional steam voids which reduce
reactivity and thereby reduce the power.

The fuel for the BWR is uranium dioxide enriched up to
approximately 2 to 5 weight percent in U-235 with the remainder
being U-238. Early in the fuel life, the fissioning of the U-235
produces the majority of the energy. The presence of U-238 in the
uranium dioxide fuel leads to the production of significant
quantities of plutonium during core operation. This plutonium
contributes to both fuel reactivity and reactor power production,
i.e., approximately 50 percent at end-of-life. In addition,
direct fissioning of U-238 by fast neutrons yields approximately
7 to 10 percent of the total power and contributes to an increase
of delayed neutrons in the core. In addition, the U-238 also has a
strong negative Doppler reactivity coefficient that can limit the
peak power during excursions.

Typical reactor core dimensions are shown in Table 4.2-4.

4.3.2.1   Nuclear Design Description

[HISTORICAL INFORMATION] [The initial fuel loading was composed
of three distinct bundle types, each with a unique rod-by-rod
enrichment distribution. The bottom and top of two of these
initial core bundles contained a natural uranium blanket. The
third bundle type contained only natural uranium fuel. The three
unique bundle types were distributed in the initial core based on
the principal of minimizing radial power peaking and maximizing
core reactivity for the end-of-cycle state.

The same basic zonal concept of fuel loading is carried into the
reload cycles. The lowest reactivity fuel is loaded on the
periphery, a high reactivity ring is loaded adjacent to the
periphery, and a medium reactivity zone forms the central part of
the core.

The reload fuel loading is composed of one or more distinct bundle
types, each with a unique rod-by-rod enrichment distribution.
Reload fuel has consisted of several distinct bundle mechanical
designs: 8x8 with two water rods, 9x9 with five water rods, 9x9
with two large water rods, 10x10 with one large water channel, and
10x10 with two large water rods. The reload 8x8 design is similar
to the initial cycle fuel. The 9x9 fuel contains 76 fuel rods and
five water rods, the 9x9 with two water rods has 74 fuel rods, the
10x10 fuel with one large water channel has 91 fuel rods, and the
10x10 with two water rods has 92 fuel rods. The five water rods
are located in the interior region of the fuel assembly in a cross
configuration (Reference 22) or slightly dispersed in the
interior (Reference 22). The 9x9 and 10x10 two water rod designs
have both water rods centrally located in the fuel rod array,
Reference 11. The 10x10 water channel design has a centrally
located water channel, which displaces 9 fuel rod locations
(Reference 32). These water rods serve the same function as those
found in the 8x8 designs. Gadolinia and enriched uranium may be
placed radially and axially in the fuel assembly to control
reactivity, flatten axial power, and optimize shutdown margin. A
loading plan for a typical core reload using 9x9 fuel is shown in
Figure 4.3-1.]

4.3.2.1.1   Fuel Nuclear Properties

The bundle reactivity is a complex function of several important
physical properties. The important properties consist of the
average bundle enrichment, the gadolinia rod location and

gadolinia concentration, the void fraction, and the accumulated exposure. The variation in reactivity (k-infinity as a function of void fraction and exposure) for a typical reload bundle is presented in Figure 4.3-7. At low exposure the reactivity effect due to void formation is readily apparent; however, at higher exposure, due to the effect of void history, the curves cross. The primary reason for this behavior is the greater rate of plutonium formation at the higher void fraction. The isotopic concentrations as a function of exposure are presented in Figure 4.3-8 for the important heavy element isotopes. Gadolinia in the form of Gd_2O_3 is selectively placed in fuel rods in the bundles to provide reactivity control, and is distributed axially to flatten the axial power distribution.

Early in the fuel bundle life, approximately 93 percent of the power is produced by fissions in U-235 with the remainder coming from fast fissions in U-238. At high exposures typical of discharge, the power production due to plutonium exceeds that of the U-235. The fraction of fissions in the important isotopes is shown in Figure 4.3-9.

Other bundle parameters such as neutron generation time and delayed neutron fraction as a function of exposure at core average voids are shown in Figures 4.3-10 and 4.3-11, respectively.

The variation of the core-wide nuclear characteristics is a function of the characteristics of each bundle in the core. With the three unique initial core bundles and the various reload situations, any description of the gross core characteristics can only be expressed in terms of the overall core performance.

4.3.2.2   Power Distribution

The core is designed such that the resultant operating power distributions meet the plant Technical Specifications. The two primary criteria for thermal limits are the maximum linear heat generation rate (MLHGR) and the minimum critical power ratio (MCPR). In addition, a maximum average planar linear heat generation rate (MAPLHGR) limit is applied to each bundle. Each of these is a function of both the gross three-dimensional power distribution and the local rod-to-rod power distribution. In order to allow sufficient design flexibility, separate target peaking factors are used for the local and the gross power distributions. The local peaking factor is defined as the ratio of

the power density in the highest power rod in the lattice, at a cross section through the bundle, to the average power density in the lattice at that location.

Target peaking factors may be used in the design process to determine if a preliminary core design is acceptable. However, variations from these target peaking factors are considered acceptable providing the Technical Specifications are not exceeded anywhere in the core. Appropriate design allowances are included at the design stage to ensure that these Technical Specification limits are met. During operation of the plant the power distributions are measured by the in-core instrumentation system and thermal margins are calculated by the core monitoring computer.

4.3.2.2.1   Local Power Distribution

The local rod-to-rod power distribution and the associated CPR power distribution factor (R-factor or F-effective) are direct functions of the lattice fuel rod enrichment and gadolinia distribution. Near the outside of the lattice where the thermal flux peaks due to interbundle water gaps, some lower enrichment fuel rods are utilized to minimize power peaking. Closer to the center of the bundle, higher enrichment fuel rods are used to increase the power generation and flatten the power distribution. In addition, two or more water rods or a water channel containing unvoided water are in the interior of the lattice in order to increase the thermal flux and produce more power in the center of the lattice. The combination of these factors results in the relatively flat local power distribution. The fuel rods which contain gadolinia produce relatively little power early in bundle life; however, as the gadolinia is depleted, the power in these rods increases.

The local power distributions at beginning of a typical reload cycle at various void conditions are shown in Figure 4.3-12. The variation of the maximum local peaking factor as a function of exposure at various void conditions is shown in Figure 4.3-14. The high power rods deplete at a greater rate and the local power distribution, at end-of-bundle life is shown in Figure 4.3-16. The local power distribution tends to flatten with increasing void fraction. The presence of a control blade adjacent to the bundle significantly perturbs the local power distribution. The controlled local power distribution for a typical reload bundle is shown in Figure 4.3-18. Although the local peaking factor is

quite large in this case, the gross power in a controlled bundle is sufficiently low such that a controlled lattice is seldom limiting.

4.3.2.2.2   Radial Power Distribution

The integrated bundle power, commonly referred to as the radial power, is the primary factor for determining MCPR. At rated conditions the MCPR is directly proportional to the radial power peaking. The radial power distribution is a complex function of the control rod pattern in the core, the fuel bundle type and distribution, and the void condition for that bundle and power. A three-dimensional BWR simulator (Refs. 1, 21, or 24) is used to calculate the three-dimensional power distribution in the core and the power is axially integrated to determine average bundle power. The bundle radial power distributions for typical beginning and end-of-cycle conditions are presented in Figures 4.3-21 and 4.3.21a. Radial peaking factors of -1.25 to -2.0 throughout the cycle are typical.

The radial distribution is controlled by both the radial reactivity zones and the control rods. The control rods are inserted at the center of the core first and then spiral outward as the reactivity control is needed. Near end of cycle the ring of high enrichment bundles adjacent to the periphery provides radial power flattening without recourse to control rods.

4.3.2.2.3   Axial Power Distribution

The axial power distributions obtained in a BWR are a function of the control rod pattern, the axial gadolinia distribution, U-235 enrichment, and the exposure distribution. The effect of voids is to skew the power toward the bottom of the core; the effect of the bottom entry control rods is to reduce the power in the bottom of the core; and the effect of the axial gadolinia and uranium shaping is to flatten the power near the bottom. Since the void distribution is determined primarily from the power shape, the three mechanisms available for optimizing the axial power shape are the control rods, U-235 enrichment and the gadolinia. Detailed three-dimensional calculations are performed to determine the axial gadolinia distribution which provides the desired axial power shape through the cycle.

Typical beginning-of-cycle axial power shape are shown in Figures 4.3-22 and 4.3.22a along with the end-of-cycle Haling (Reference 16) power shape.

For a reload condition, the exposure shape existing in the bundles which remain from previous cycles helps provide the necessary power shaping. Additional power shaping may be provided by axially varying the gadolinia and enriched uranium placed in the reload bundles.

4.3.2.2.4   Deleted

4.3.2.2.5   Power Distribution Measurements

The measurement of the power distribution within the reactor core together with instrumentation correlations and operation limits are discussed in Reference 1.

4.3.2.2.6   Power Distribution Accuracy

The accuracy of the calculated local rod-to-rod power distribution is discussed in Reference 1. The accuracy of the radial, axial and the gross three-dimensional power distribution calculations is discussed in Reference 1.

4.3.2.2.7   Power Distribution Anomalies

Stringent inspection procedures are planned to ensure the correct assembly of the reactor core. Although a misplacement of a bundle in the core would be a very improbable event, calculations have been performed in order to determine the effects of such accidents. These results are presented in Chapter 15.

The inherent design characteristics of the BWR are well suited to limit gross power tilting. The stabilizing nature of the large moderator void coefficient effectively reduces perturbations in the power distribution. In addition, the incore instrumentation system together with the core monitoring computer provide the operator with prompt information on power distribution so that he can readily use control rods or other means to limit the undesirable effects of power tilting. Because of these design characteristics, it is not necessary to allocate a specific margin in the peaking factor to account for power tilt. If, for some reason, the power distribution could not be maintained within normal limits using control rods, then the operating power limits would have to be reduced as prescribed in the Technical Specifications.

4.3.2.3 Reactivity Feedback

Reactivity feedback, the change in reactivity produced by a change in core conditions, can be used to calculate the response of the core to external disturbances. The base initial condition of the system and the postulated initiating event determines which of the several defined feedback mechanisms are significant in evaluating the response of the reactor. [HISTORICAL INFORMATION] [The core response can be determined with a point kinetics model using reactivity coefficients or a one dimensional (1-D) model. The 1-D model relies on nuclear cross sections and other neutronic parameters rather than reactivity coefficients. One dimensional models are typically used in the reload analyses, References 1 and 31.]

There are three primary reactivity feedback mechanisms which characterize the dynamic behavior of boiling water reactors over all operating states. These are the Doppler reactivity effect, the moderator temperature reactivity effect, and the moderator void reactivity effect. Also associated with the BWR is a power reactivity effect; however, this coefficient is merely a combination of the Doppler and void reactivity feedback mechanisms in the power operating range.

Reload transient analysis methods use group-averaged cross sections and neutronic parameters in a 1-D model to predict transient reactivity response to changes in core conditions rather than point model reactivity coefficients. As such, reactivity coefficients are not calculated for the reload fuel to analyze transients, References 1 and 20.

Reload methodology for analyzing the Control Rod Drop Accident (CRDA) is based on a generic parametric analysis (Ref. 1 and 25) that calculates the fuel enthalpy rise during the postulated CRDA over a wide range of reactor operating conditions. The CRDA analysis assumption complies with GE's Banked Position Withdrawal Sequencing (BPWS) constraints (Ref. 9). Based on BWR Owner's Group methodology, the CRDA has been shown to be inherently self limiting for core powers above 10% rated due to the presence of voids in the core (Ref. 26).

4.3.2.3.1 Void Reactivity Effect

The most important of these feedback mechanisms is the void reactivity. The void feedback must be large enough to prevent power oscillation due to spatial xenon changes yet small enough

that pressurization transients do not unduly limit plant operation. In addition, the void effect in a BWR has the ability to flatten the radial power distribution and to provide ease of reactor control due to the void feedback mechanism. The overall void feedback is always negative over the complete operating range since the BWR design is undermoderated. The reactivity change due to the formation of voids results from the reduction in neutrons slowing down due to the decrease in the water-to-fuel ratio.

4.3.2.3.2   Moderator Temperature Effect

The moderator temperature feedback mechanism is the least important of the reactivity since its effect is limited to a very small portion of the reactor operating range. Once the reactor reaches the power producing range, boiling begins and the moderator temperature remains essentially constant. As with the void effect, the moderator temperature effect is associated with a change in the moderating power of the water. The temperature feedback is negative for most of the operating cycle; however, near the end of cycle, the overall moderator temperature effect becomes slightly positive due to the fact that the uncontrolled BWR lattice is slightly overmoderated near the end of cycle. This, combined with the fact that more control rods must be withdrawn from the reactor core near the end of cycle to establish criticality, results in the slightly positive overall moderator temperature feedback.

The range of the moderator temperature feedback encountered in current BWR lattices does not include any that are significant from the safety point of view. Typically, the temperature coefficient may range from $+4 \times 10^{-5}$ $\Delta k/k$-°F to -14×10^{-5} $\Delta k/k$-°F, depending on base temperature and core exposure. The small magnitude of this effect, relative to that associated with steam voids and combined with the long time-constant associated with transfer of heat from the fuel to the coolant, makes the reactivity contribution of moderator temperature change insignificant during rapid transients.

4.3.2.3.3   Doppler Reactivity Effect

The Doppler reactivity effect is the change in reactivity due to a change in the temperature of the fuel. This change is due to the broadening of the resonance absorption cross sections as the temperature increases. At beginning of life, the Doppler

contribution is primarily due to U-238; however, the buildup of Pu-240 with exposure adds to the Doppler feedback. [HISTORICAL INFORMATION] [The application of the Doppler coefficient to the analysis of the rod drop accident is discussed in References 1, 8, 19 and 25. A plot of the Doppler reactivity coefficient as a function of average lattice fuel temperature for a typical initial cycle bundle is shown in Figure 4.3-24.]

4.3.2.3.4   Power Effect

The power feedback effect is determined from the composite of all the significant individual sources of reactivity change associated with a change in reactor thermal power assuming xenon reactivity remains constant. A typical power coefficient at rated conditions is approximately $-0.05 \ \Delta k/k \div \Delta P/P$. This value is well within the range required for adequately damping power and spatial xenon disturbances.

4.3.2.4   Control Requirements

The core and fuel design, in conjunction with the reactivity control system, provides an inherently stable system BWRs.

The control rod system is designed to provide adequate control of the maximum excess reactivity anticipated during the fuel cycle operation. The core loading, however, has an excess reactivity somewhat higher than that of the control rod worth. Thus, the basis for design of the burnable poison loading is that it shall compensate for the reactivity difference between the control rod system capability and the excess reactivity. The safety design basis requires that the core, in its maximum reactivity condition, be subcritical with the control rod of the highest worth fully withdrawn and all others fully inserted. Therefore, the shutdown capability is evaluated at the most reactive moderator temperature in a xenon-free condition. This limit allows control rod testing at any time in core life and assures that the reactor can be made subcritical by control rods alone.

4.3.2.4.1   Shutdown Reactivity

To assure that the safety design basis is satisfied, an additional design margin is adopted: k_{eff} is calculated to be less than or equal to 0.99 with the control rod of highest worth fully

withdrawn. [HISTORICAL INFORMATION] [Typical reload core shutdown |
reactivity as a function of fuel exposure is shown in Figure 4.3-
25.] |

The shutdown reactivity curve shows the calculated values of k_{eff}
for the shutdown condition (20 C, highest worth rod withdrawn).
Cold shutdown margin is typically at a minimum at the beginning of
cycle due to the large excess reactivity of the fresh fuel. Cold
shutdown margin increases as the core is depleted due to the
competing reactivity effects of spent and fresh fuel. Margin may
decrease towards the end of cycle due to the depletion of
gadolinia in the top of the core. The k_{eff} peak and the point of
burnable poison depletion are a function of the fuel nuclear
design (enrichment level, gadolinia concentration, etc.).

The cold (20 C) reactor condition may not be the most limiting
with regard to shutdown criteria. For this reason, shutdown
margin calculations are performed at the most limiting
temperature.

Reduction of control rod effectiveness during one operating cycle
is not a major concern with the BWR. Using normal control rod
sequencing, the control rod worth remains essentially constant
over the BWR operating cycle.

The bias addresses potential for differences between distributed
and local criticals. The accuracy with which shutdown reactivity
is calculated is discussed in Reference 1. Basically, the |
accuracy is characterized as a bias and an uncertainty. The bias
is a reactivity correction applied directly to the calculated
results. For example:

k_{eff} (Expected) = k_{eff} (Calculated) + Δk (Bias)

[HISTORICAL INFORMATION] [This bias has been incorporated into |
the shutdown curves shown in Figure 4.3-25. The 1-percent design
margin is satisfied after the bias correction is applied.] |

4.3.2.4.2   Reactivity Variations

The excess reactivity designed into the initial core is
controlled by a control rod system supplemented by gadolinia-
urania fuel rods. The average fuel enrichment for the initial core
loading is chosen to provide excess reactivity in the fuel
assemblies sufficient to overcome the neutron losses caused by

core neutron leakage, moderator heating and boiling, fuel temperature rise, equilibrium xenon and samarium poisoning, plus an allowance for fuel depletion.

Control rods are used during the fuel burnup, partly to balance the power distribution effect of steam voids as indicated by the in-core flux monitors. In combination, the control rod and void distributions are used to flatten gross power. The design provides considerable flexibility to control the gross distribution. This permits control of fuel burnup and isotopic composition throughout the core to the extent necessary to counteract the effects of voids on axial power distribution at the end of a fuel cycle, when a few control rods remain in the core.

Reactivity balances have not normally been used in describing BWR behavior because of the strong dependence of, for example, rod worth on temperature and void fraction; therefore, the design process does not produce components of a reactivity balance at the conditions of interest. Instead, it gives the k_{eff} representing all effects combined. Further, any listing of components of a reactivity balance is quite ambiguous unless the sequence of the changes is clearly defined.

Consider, for example, the reactivity effect of control rods and burnable poison. The combined worth of these two absorbers would be considerably different than the sum of their individual worths. Even this combined worth would be of questionable significance unless the path and conditions of other parameters (i.e., temperature, void, xenon, etc.) were completely specified. Many other illustrations could be presented showing that the reactivity balance approach, which may be appropriate in some types of reactors, is completely inappropriate in a BWR. This is related to the large potential excess reactivity in a BWR combined with the dependence of interaction (shadowing) factors on reactor state.

In order to understand the various reactivity effects in a BWR design, certain reactivity states can be defined which provide information about BWR behavior. [HISTORICAL INFORMATION] [Typical data are presented in Table 4.3-2 and show the predicted reactivity, k_{eff}, for various cold, xenon-free conditions. For the purposes of this table, middle of cycle is defined as the most reactive point in the cycle. The reactivity and control fraction values for a variety of operating conditions are shown in Table 4.3-3. The worth of various reactivity effects can be estimated by

taking the differences between reactivity states with all but one variable constant. Estimates of the temperature defect, the power defect, the xenon defect and the excess reactivity can be inferred.]

4.3.2.5   Control Rod Patterns and Reactivity Worths

Actual operating reactor rod patterns are based upon the measured distributions in the plant. All rod patterns will be such that the limits are met throughout the cycle.

For BWR plants, control rod patterns are not uniquely specified in advance; rather, during normal operation, the control rod patterns are selected based on the measured core power distributions within the constraints imposed by the systems indicated in the following sections. [HISTORICAL INFORMATION] [Typical control rod patterns are calculated during the design phase to insure that all safety and performances criteria are satisfied. Control rod patterns and the associated power distributions for a typical BWR are presented in Appendix A of Reference 14. These control rod patterns are calculated with the BWR core simulator (Refs. 1, 19 and 21). The ability of this model to predict control rod worth at hot and cold conditions can be inferred from the detailed reactivity data presented in References 1, 19 and 21. Verification of the advanced nodal code used by the reload fuel vendor is presented in References 1, 19, 21, 24, and 27. Comparisons between calculation and measurement are presented for BWR/3, BWR/4, and BWR/6 reactor types. Tables 5.2-1 through 5.2-12 in Reference 19 and Tables 7.2 and 7.3 in Reference 24 present information similar to that of Reference 1 above, and show that rod worths for hot and cold conditions are accurately predicted.]

4.3.2.5.1   Rod Control and Information System

Control rod patterns and associated control rod reactivity worths are regulated by the rod control and information system (RCIS). This system utilizes redundant inputs to provide rod pattern control over the complete range of reactor operations. The control rod worths are limited to such an extent that the rod drop accident (RDA) and the power range rod withdrawal error (RWE) become unimportant. The RCIS provides for stable control of core reactivity in both the single rod or rod gang mode of operation. The Bank Position (BP) mode of RCIS provides protection from a RDA from startup to the low power setpoint (LPSP). The Rod Withdrawal

Limiter (RWL) provides protection from the RWE for all conditions above the LPSP. Each of these modes is described in the following sections.

4.3.2.5.2   Bank Position Mode

The BP mode restricts control rod patterns to prescribed withdrawal sequences from the all-rods-inserted startup condition until about 20 percent of rated power. This mode minimizes control rod worths to the extent that they are not an important concern in the operation of a BWR. The consequences of a RDA or a RWE in this range are significantly less severe than that required to violate fuel integrity limits. This system is described in detail in Reference 9. Above the LPSP, control rod worths are very small due to the formation of voids in the moderator. Improved analysis based on BWR Owner's Group methodology (Reference 26) has shown the CRDA to be inherently self limiting for core powers above 10% rated due to the presence of voids in the core. Therefore, restrictions on control rod patterns are not required to minimize control rod worths.

4.3.2.5.3   RWL Mode

Above the low power set point the RCIS relies on the RWL mode to provide regulation of control rod withdrawals in order to prevent the occurrence of a rod withdrawal error. This mode limits the withdrawal of a single control rod or a gang of control rods to a predetermined increment depending on the power level. The system senses the location of the rod or rods and automatically blocks withdrawal if the preset increment is exceeded. The preset limit is determined by generic analyses such that the ΔMCPR and ΔLHGR are less than the limiting transient. Withdrawal limits are 12 inches between the upper power setpoint and 100 percent power and 24 inches between the lower power setpoint and the upper power setpoint. Withdrawal limits below the lower power setpoint are enforced by the rod pattern controller.

4.3.2.5.4   Control Rod Operation

The control rods can be operated either individually or in a gang composed of up to four rods. The purpose of the ganged rods is to reduce the time required for plant startup or recovery from a scram. The RCIS provides regulation of control rod operation regardless of whether rods are being moved in single or ganged mode. The assignment of control rods to RCIS groups is shown in

Figures 4.3-27 and 28 for A and B patterns, respectively. Also shown in these figures is the division of the groups into gangs of one to four rods which can be moved simultaneously.

4.3.2.5.5   Scram Reactivity

The reactor protection system (RPS) responds to some abnormal operational transients by initiating a scram. The RPS and the control rod drive (CRD) system act quickly enough to prevent the initiating disturbance from driving the fuel beyond transient limits. [HISTORICAL INFORMATION] [The scram reactivity curve at the end-of-cycle 1 is shown in Figure 4.3-26. Also shown is the calculated value multiplied by 0.80, the standard transient safety conservatism factor, and the design limit scram curve. These data show that the design limit curve is not violated. In particular, the design limit curve is not violated for control fractions between 0.0 and 0.6, the range of importance for transient analyses.]

At the hot-operating condition, the control rod, power, delayed neutron, and void distributions must all be properly accounted for as a function of time. Therefore, the scram reactivity is calculated using a one dimensional (axial) finite-differenced space-time model which is coupled with a single channel thermal-hydraulic model. The finite-differenced space-time model uses three prompt and six delayed neutron energy groups, and has been compared to, and verified by, analysis of published results obtained using the industry standard computer code (Ref. 10). Similar information for the reload vendor analysis code is provided in References 1 and 31.

The transient thermal-hydraulic model employed for this calculation is described in detail in Reference 1. The neutronics employs a three-group neutron energy model with thermal-hydraulic coupling, and the principal features of this nuclear model can be identified as those of the WIGL3 nuclear model (Reference 10), except three-energy groups are used. The scram reactivity curve calculated for end-of-cycle 1 is calculated with the pressure held constant. The coupled neutronics and thermal-hydraulics properly accounts for the redistribution of the power, neutron flux, and voids during scram.

The conservative scram reactivity used for transient analysis is lower than the curve (Figure 4.3-26) by at least a factor of 0.8 as described. Part of the conservatism is to account for

pressurization effects on the scram reactivity (i.e., only one conservative scram curve is used for all transient analyses, whether they are pressure increase transients or not).

Reload analyses use a 1-D model (References 1 and 31). Plant variables are considered at conservative values. Variables covered by the Technical Specifications (e.g., scram insertion speed and delay time) are consistent with the Technical Specification values. Code uncertainties are addressed by applying a deterministic integral power multiplier in the analysis process (Reference 31) or adders to the calculated delta CPR (Reference 1). Other calculational uncertainties are addressed in the MCPR safety limit analysis (Ref. 1 and 18). Scram reactivity for the reload core is obtained from three-dimensional neutronics calculations. This procedure is in accordance with the treatment of uncertainties described in References 1, 18 and 31. The nuclear and thermal hydraulic model for the reload analysis codes are described in Reference 1 and 31. The higher core energy requirements of EPU may reduce the hot excess reactivity and reduce operating shutdown margin. These changes are handled through appropriate fuel and core design such that, on a cycle specific basis, the plant shutdown and reactivity margins continue to meet NRC-approved limits established in Reference 1 and these limits are evaluated for each reload core. The reload core analysis will ensure that the minimum shutdown margin requirements are met for each core design and that the current design and TS cold shutdown margin will be met (Ref. 44).

4.3.2.6   Criticality of Reactor During Refueling

The maximum allowable value of k_{eff} is controlled in accordance with the Technical Specifications. For each reload cycle the maximum core reactivity is calculated with the highest worth rod withdrawn to show at least 1.0 percent Δk margin. Control rod system interlock prevent the withdrawal of more than one rod while in the REFUEL mode.

4.3.2.7   Stability

4.3.2.7.1   Xenon Transients

Boiling water reactors do not have instability problems due to xenon. This has been demonstrated by operating BWRs for which xenon instabilities have never been observed, (such instabilities would readily be detected by the LPRMs), by special tests which

have been conducted on operating BWRs in an attempt to force the reactor into xenon instability, and by calculations. All of these indicators have proven that xenon transients are highly damped in a BWR due to the large negative power coefficient.

Analysis and experiments conducted in this area are reported in Reference 12.

4.3.2.7.2   Thermal-hydraulic Stability

This subject is covered in subsection 4.4.4.6.

4.3.2.8   Vessel Irradiations

The neutron fluxes at the vessel have been calculated using the three dimensional (3D) transport code described in subsection 4.1.4.5. The discrete ordinates code was used in a distributed source mode with cylindrical geometry. The coolant water region between the fuel channel and the shroud was described as containing saturated water at 550°F and 1050 psi. The material compositions for the stainless steel in the shroud and the carbon steel in the vessel contain the mixtures by weight as specified in the ASME material specifications for ASME SA 240, 304L, and ASME SA 533 grade B. In the region between the shroud and the vessel, the presence of the jet pumps was included. A simple diagram showing the regions, dimensions and weight fractions are shown in Figure 4.3-29.

Calculations of the best estimate neutron fluence, and its uncertainty, to the GGNS reactor pressure vessel (RPV), core shroud and top guide horizontal and vertical welds, as well as to several beltline vessel nozzels have been performed. The fluence calculations were carried out using a three-dimensional (3D) neutron transport model for each fuel cycle starting from cycle 1 through cycle 21. The 3D neutron transport calculations were benchmarked on a plant-specific basis by comparing calculated results against previously performed core region 2D synthesis data as well as by calculation of the measured-to-calculated (M/C) ratios for GGNS dosimetry. In addition, a comprehensive benchmarking report, Reference 41, of MP Machinery and Testing, LLC (MPM)methods has been submitted.

The neutron transport calculational procedures and dosimetry analysis methods meet standards specified by the NRC and ASTM as appropriate. In particular, the transport analysis meets the requirements of Regulatory Guide 1.190 (RG 1.190). Since RG 1.190

is focused on 2D synthesis methods, it is strictly applicable to analyses in the active fuel region. Nevertheless, the guidance provided in RG 1.190 was followed to the extent practical for modeling work in the region above and below the active fuel region. The 3D neutron transport calculations were used to determine detailed fluence profiles at the end of cycle 21 (28.088 EFPY), and projected to exposures of 35 EFPY and 54 EFPY, Reference 42.

Summary of Shroud and Top Guide Fluence Results

The fluences reported, Reference 42, were calculated at the inner diameter (ID) surface of the welds. With the exception of horizontal welds H4 and H5, all horizontal shroud weld fluences are below 5E+20 n/cm^2 through at least 54 EFPY. At the end of cycle 21, the maximum fluence to shroud welds H4 and H5 are 1.22E+21 n/cm^2 and 4.88E+20 n/cm^2, respectively.

With the exception of the top guide vertical welds V7 and V8, all vertical shroud weld fluences are below 5E+20 n/cm^2 at the end of cycle 21 (28.088 EFPY). When extrapolated to 54 EFPY exposure, the vertical shroud weld fluences are still below 5E+20 n/cm^2 except for the vertical welds V7 and V8, and welds V13 through V16. Welds V7 and V8 are located in the plate at the bottom of the top guide. These welds extend across the entire diameter of the plate and thus lie, in part, directly above the reactor core. Weld V7 is defined from the core centerline to the top guide OD at 90 degrees, and V8 extends from the core centerline to the top guide OD at 270 degrees. As a result of the high void fraction of the water-steam mixture above the core, there is relatively little water shielding for this plate, and the fast neutron flux is therefore very high. The maximum exposure to this weld is calculated to be about 2.32E+21 n/cm^2 at the end of cycle 21. For this weld, the fluence at various radial points from 0 to the outer edge of the top guide is calculated and included in the appendices.

Summary of Vessel, Vessel Internals, and Cycle 1 Dosimetry Results

The transport calculations were also performed to evaluate fluence for the surveillance capsule and for the reactor vessel. Comparisons with dosimetry measurements at the GGNS surveillance capsule location at the end of cycle 1 were made and excellent

agreement was found. The measured-to-calculated (M/C) ratio averaged over all of the dosimeters is 0.98, which is a significant improvement over the past result (0.92) obtained using 2D synthesis. The surveillance capsule fluence lead factor for the vessel inner radius (wetted surface) maximum fluence location was calculated to be 0.41. This is not of concern at present since the BWR Vessel Internals Project (BWRVIP) has put the GGNS capsules on reserve and there are no current plans to pull and analyze these capsules.

Maximum fluence to the reactor vessel wetted surface was calculated to be $1.74E+18$ n/cm^2 (E> 1 Mev) at the end of cycle 21, and $4.03+18$ n/cm^2 (E> 1 MeV) after 54 EFPY. Included is the calculated dpa attenuation through the vessel as well as the dpa attenuation determined using the RG 1.99 (Rev 2) equation. The dpa attenuation for locations above and below the active fuel region was calculated for the shell 1, 2 and 3 plates and welds and also for the N1, N2, N6, and N12 nozzles.

The NRC defines the beltline region in 10CFR50, Appendix G as "the region of the reactor vessel (shell material including welds, heat affected zones, and plates or forgings) that directly surrounds the effective height of the active core and adjacent regions of the reactor vessel that are predicted to experience sufficient neutron radiation damage to be considered in the selection of the most limiting material with regard to radiation damage." Entergy has requested that MPM use a fast fluence of $1.0E+17$ n/cm^2 to define the extent of the beltline region. At EOC 20 (26.220 EFPY), the vessel fluence will exceed $1.0E+17$ n/cm^2 at locations about 9.3 inches below the bottom of active fuel (BAF) in shell 1 region up to about 11.4 inches above the top of active fuel (TAF) in shell 2 region. The peak above TAF, which is due largely to flux from the top of the core, occurs at around 190 inches above BAF. This peak does not exceed $1.0E+17$ n/cm^2 at the projected end of cycle 20. However, it does come close and, as discussed below, exceeds this threshold by the end of cycle 21, thereby extending the beltline region into shell course 3. The extension of the beltline below circumferential weld AB necessitates inclusion of radiation damage effects in the shell 1 plates and welds in the Pressure Temperature (PT) curve analysis at the present time.

The axial fluence profile at EOC 21 (28.088 EFPY) shows that the vessel maximum fast fluence exceeds $1.0E+17$ n/cm^2 outside of the 150 inch active fuel region, and extends above horizontal weld AC and below weld AB. In particular, at EOC 21, the vessel fluence will exceed $1.0E+17$ n/cm^2 at locations about 10.3 inches below BAF, and 41.4 inches above the TAF. This necessitates inclusion of radiation damage effects in the shell 1 and shell 3 plates and welds in the PT curve analysis for future exposures. At 54 EFPY, the vessel fluence will exceed $1.0E+17$ n/cm^2 at locations about 17.1 inches below BAF and about 56.1 inches above TAF.

The vessel has nozzle penetrations at several locations, and neutron exposure at the nozzles is of concern for neutron damage analysis. Four sets of nozzle were evaluated. For nozzles below the core, the maximum fluence point occurs at the top of the nozzle. The reverse is true for nozzles above the core. Results indicate that the N12 (water level instrumentation) nozzles have exceeded a fluence level of $1.0E+17$ n/cm^2 at the end of cycle 21.

In addition to the fluence analysis for the RPV, calculation of fluences at the nineteen component locations was completed in support of the RPV internals mechanical evaluation, Reference 43. The fluences for the nineteen components were evaluated at locations that were selected to ensure conservative data. In the case of the shroud, the peak on the ID surface of the shroud is reported. For plates, such as the core plate, the peak anywhere on the plane defining the plate has been calculated. For components with discrete angular positions, such as the shroud support legs, the peak reported is the peak over the 360 degrees at the elevation of the legs. For the components with specified axial ranges, such as the core plate bolts and the top guide bolts, the peak was determined as well as the average over the axial extent of the bolts at the peak azimuthal location. Review of the results show that portions of the jet pumps will experience fluences above $1.0 E+20$ n/cm^2. If flaws are discovered, this high fluence level will require a more restrictive flaw tolerance analysis. Therefore, a decision was made to calculate fluences along the entire axial extent of the jet pumps for use in possible future fracture mechanics evaluations. To achieve this objective, the radial coordinates of the surface of the jet pumps closest to the core were determined as a function of axial height.

Benchmarking and Uncertainty Analysis

Fluence values for the capsule, vessel, and shroud in the beltline region (except for the very top and bottom of the core) are estimated to have uncertainties of 14.7%, 15.8%, and 13.3%, respectively. These uncertainties are within the value of ±20% specified by RG 1.190. Moreover, the 3D calculations, Reference 41, have been benchmarked against GGNS cycle 1 capsule dosimetry measurements which are in excellent agreement (M/C = 0.98). Additional benchmarking of the MPM calculational methodology is provided by comparisons of previous calculations using the same methodology with Nine Mile Point Unit 1 (NMP-1) capsule and shroud measurements (boat samples were cut from the shroud), NMP-2 capsule measurements, and River Bend capsule measurements. All of these benchmarks yield M/C ratios within the value of ± 20% specified by RG 1.190. The calculations of shroud, vessel, and capsule fluence meet all of the requirements of RG 1.190. Similarly, the results of calculations performed above and below the core meet the requirements of RG 1.190 except for the ± 20% criterion.

Regulatory Guide 1.190 requires that the overall fluence calculation bias and uncertainty must be determined by an appropriate combination of the analytic uncertainty analysis results and the results of the uncertainty analysis based on the comparisons to the operating reactor and simulator benchmark measurements. The regulatory guide states that this combination may be a weighted average that accounts for the reliability of the individual estimates. The regulatory guide goes on to state that if the analytical uncertainty at the 1 sigma level is greater than 30%, the methodology of the regulatory guide is not applicable and the application will be reviewed on an individual basis. For the upper shroud and top guide welds, and for the N6 nozzle, the uncertainties are greater than 30%. Based on guidance provided in Equation 6 of Regulatory Guide 1.190, it would seem reasonable to multiply the calculated fluences by 1 plus the 1 sigma uncertainty for the cases where the uncertainty is over 30%.

The updated vessel fluence results are evaluated in Section 5.3.1.6.2.

4.3.3   Analytical Methods

The analytical methods and nuclear data used to determine the nuclear characteristics are similar to those in use for design and analysis of water-moderated reactors.

The Lattice Physics Model (Refs. 1, 19, 21, and 24) is used to calculate lattice reactivity characteristics, few group flux averaged cross sections and local rod-to-rod power and exposure distributions. These data are generated for various temperature, void, exposure, and control conditions as required to represent the reactor core behavior.

The BWR Core Simulator (Refs. 1, 21, and 24) is a large three-dimensional code which provides for spatially varying voids, control rods, burnable poisons, Xenon, and exposure. This code is used to calculate three-dimensional power and exposure distributions, control rod patterns, and thermal-hydraulic characteristics throughout core life.

These methods have been compared extensively to experiments and plant operating data. The results are presented in References 1, 21 and 24.

4.3.4   Deleted

4.3.4.1   Deleted

4.3.4.1.1   Deleted

4.3.4.1.2   Deleted

4.3.4.1.3   Deleted

4.3.4.1.4   Deleted

4.3.4.1.5   Deleted

4.3.4.1.6   Deleted

4.3.5   Regulatory Requirements

Commitment	Due Date
Entergy will identify the outside of the beltline region dosimetry sample locations	Complete
Entergy will revise the affected sections of Chapter 4 of the GGNS UFSAR upon approval of the Fluence Calculation Methodology LAR	Complete
Entergy will schedule collection of samples from outside the beltline region	Complete

Entergy will confirm that future M/C measured-to-calculated fluence values at the dosimetry sample locations are reasonably close to one	August 19, 2019 (Original Due Date: November 30, 2016)
Entergy will include the definition of "reasonably close to one" regarding M/C fluence values at the dosimetry sample locations	August 19, 2019 (Original Due Date: November 30, 2016)
Entergy will provide plans to address if future M/C fluence values at the dosimetry sample locations are not reasonably close to one	August 19, 2019 (Original Due Date: December 30, 2016)

The NRC staff has determined that the above regulatory requirements provide the basis to qualify the 3D fluence method for fluence calculations outside of the original beltline region and to provide more detail regarding the plans for installing dosimetry capsule installation and/or scrapings. The NRC staff has agreed that if unforeseen situations occur, sample collection may be delayed but no later than the 2018 refueling outage. As such, these regulatory commitments must be incorporated into the UFSAR and any future changes to this action must be incorporated into the UFSAR and any future changes to this action must be evaluated under the criteria of 10 CFR 50.59.

4.3.6   References

1.   General Electric Standard Application for Reactor Fuel (GESTAR II), NEDE-24011-P-A, Latest Approved Version

2.   Deleted

3.   Deleted

4.   Deleted

5.   Deleted

6.   Deleted

7.   Deleted

8.   Stirn, R. C., et al., Rod Drop Accident Analysis For Large Boiling Water Reactors, General Electric Co., Atomic Power Equipment Department, March 1972 (NEDO-10527). (Also Supplement 1, July 1972 and Supplement 2, January 1973.)

9.   Paone, C. J., Banked Position Withdrawal Sequence, September 1976 (NEDO-21231)

10.   Caldwell, W. R., et al., "WIGLE-A Program for the Solution of the Two-Group Space-Time Diffusion Equations in Slab Geometry," WAPDTM-416 (1964)

11.   "GE Fuel Bundle Designs," NEDE-31152P, Latest Approved Version

12.   Crowther, R. L., "Xenon Considerations in Design of Boiling Water Reactors," June 1968 (APED-5640)

13.   Deleted

14.   Grossenbacker, R. J., Holtzclaw, K. W., Rawlings, J. C., and Stien, N. S., "BWR/4 and BWR/5 Fuel Design," October 1976 (NEDO-20944)

15.   Deleted

16.   Haling, R. K., Operating Strategy for Maintaining an Optimum Power Distribution Throughout Life, Paper Presented at ANS Topical Meeting, San Francisco, September 1963 (TID-7672)

17.   Deleted

18.   Deleted

19.   Stout, R. B., et al., Exxon Nuclear Methodology for Boiling Water Reactors: Neutronics Methods for Design and Analysis, March 1983 (XN-NF-80-19(P)(A) Vol, 1, as supplemented)

20. White, J. A., Exxon Nuclear Methodology for Boiling Water Reactors: THERMEX: Thermal Limits Methodology Summary Description, January 1987, (XN-NF-80-19(P)(A) Vol. 3, Rev. 2)

21. Brown, O. C., et al., Advanced Nuclear Fuels Methodology for Boiling Water Reactors: Benchmark Results for the CASMO-3G/ MICROBURN-B Calculation Methodology, February 1989 (XN-NF-80-19(P) Vol. 1, Suppl 3)

22. Dunnivant, W. S., Generic Mechanical Design for Advanced Nuclear Fuels 9x9-5 BWR Reload Fuel, November 1990 (ANF-88-152(P)(A) Amendment 1, as supplemented)

23. Zerressen, K. W., et al., ANFB Critical Power Correlation, April 1990 (ANF-1125(P)(A) as supplemented)

24. EMF-2158(P)(A) Revision 0, "Siemens Power Corporation Methodology for Boiling Water Reactors: Evaluation and Validation of CASMO-4/MICROBURN-B2," Siemens Power Corporation, October 1999.

25. Chandler, J. C., Exxon Nuclear Methodology for Boiling Water Reactors: Application of the ENC Methodology to BWR Reloads, June 1986 (XN-NF-80-19(P)(A) Vol. 4, Rev. 1)

26. Safety Evaluation by the Office of Nuclear Reactor Regulation Relating to Amendment 17 of GE Topical Report NEDE-24011-P, "General Electric Standard Application for Reactor Fuel", dated 12-27-87

27. Copeland, R. A. (ANF) to Lambros, Lois (NRC), "TIP Asymmetry Uncertainty", 07-20-90 (RAC:083:90)

28. Deleted

29. Deleted

30. Deleted

31. ANF-913(P)(A) Volume 1 Revision 1 and Volume 1 Supplements 2, 3, and 4, "COTRANSA2: A Computer Program for Boiling Water Reactor Transient Analyses," Advanced Nuclear Fuels Corporation, August 1990.

32. EMF-2481(P) Revision 0, "Fuel Design Report for Grand Gulf Unit 1 Cycle 12 Atrium-10 Fuel Assemblies," Siemens Power Corporation, November 2000.

33. Deleted

34. Deleted

35. Deleted

36. Deleted

37. TAC No. MB6687, "Nine Mile Point Nuclear Station, Unit No. 1 - Issuance of Amendment RE: Pressure-Temperature Limit Curves and Tables," October 27 2003.

38. "TORT-DORT-PC, Two and Three Dimensional Discrete Ordinates Transport", Version 2.7.3, CCC-543, RCISS Computer Code Collection.

39. "BUGLE-96, Coupled 47 Neutron, 20 Gamma Ray Group Cross Section Library Derived from ENDF/B-VI for LWR Shielding and Pressure Vessel Dosimetry Applications", RSICC Data Library Collection.

40. "Casmo-4/Simulate-3, Studsvik's Advanced Three-Dimensional Two Group Reactor Analysis Code."

41. MPM-614993, Rev. 5, Benchmarking of MPM Methods For Nuclear Plant Neutron Transport Calculations.

42. MPM-814779, Rev. 5, Neutron Transport Analysis For Grand Gulf Nuclear Station, May 2015.

43. GGNS-NE-15-00003, Rev. 0, Grand Gulf Nuclear Station Fluence Effect on RPV Internal Components at EPU Operating Conditions.

44. Letter, A. B. Wang, NRC to Vice President, Operations, Entergy Operations, Inc., Grand Gulf Nuclear Station, "Grand Gulf Nuclear Station Unit 1 - Issuance of Amendment RE: Extended Power Uprate (TAC No. ME4679)," July 18, 2012.

TABLE 4.3-1: DELETED

TABLE 4.3-2: [HISTORICAL INFORMATION] TYPICAL REACTIVITY DATA FOR THE COLD, XENON FREE STATE

BPWS Rod Groups Withdrawn	Condition % Controlled	BOC	MOC	EOC
–	100	0.927	0.917	0.903
1 & 2	75	0.994	0.982	0.968
1,2, 3 & 4	50	1.032	1.019	1.000
All Rods Out	0	1.112	1.097	1.073
	Highest Worth Rod Withdrawn	0.973	0.961	0.953
	H.W.R. Core Co-Ord.	(18.51)	(18.51)	(22.55)

BOC = Beginning of Cycle

MOC = Middle of Cycle

EOC = End of Cycle

BPWS = Bank Position Withdrawal Sequence Rod

TABLE 4.3-3: [HISTORICAL INFORMATION] TYPICAL REACTIVITY AND CONTROL FRACTION FOR VARIOUS REACTOR STATES

Condition	Beginning of Cycle		Middle of Cycle		End of Cycle	
	k_{eff}	CF	k_{eff}	CF	k_{eff}	CF
Cold, No Xenon, Critical* Zero Power	0.994	0.75	1.004	0.61	1.000	0.50
Hot, No Xenon, Critical* Zero Power	1.006	0.50	1.000	0.50	1.010	0.44
Hot, No Xenon, Critical* Rated Power	1.000	0.24	0.996	0.25	0.995	0.11
Hot, With Xenon, Critical* Rated Power	0.998	0.16	0.999	0.13	0.999	0.0
Cold, No Xenon Zero Power	1.032	0.50	1.019	0.50	1.031	0.44
Hot, No Xenon Zero Power	1.079	0.24	1.078	0.25	1.062	0.11
Hot, No Xenon Rated Power	1.027	0.16	1.027	0.13	1.026	0.0
Hot, With Xenon	1.036	0.0	1.032	0.0	0.999	0.0

* Control rod patterns adjusted approximately to critical. The deviations from k_{eff} = 1.000 were allowed to minimize analysis effort. The Δk between conditions with the same control fraction remain valid.

TABLE 4.3-4: DELETED

TABLE 4.3-5: DELETED

TABLE 4.3-6: DELETED

TABLE 4.3-7: DELETED
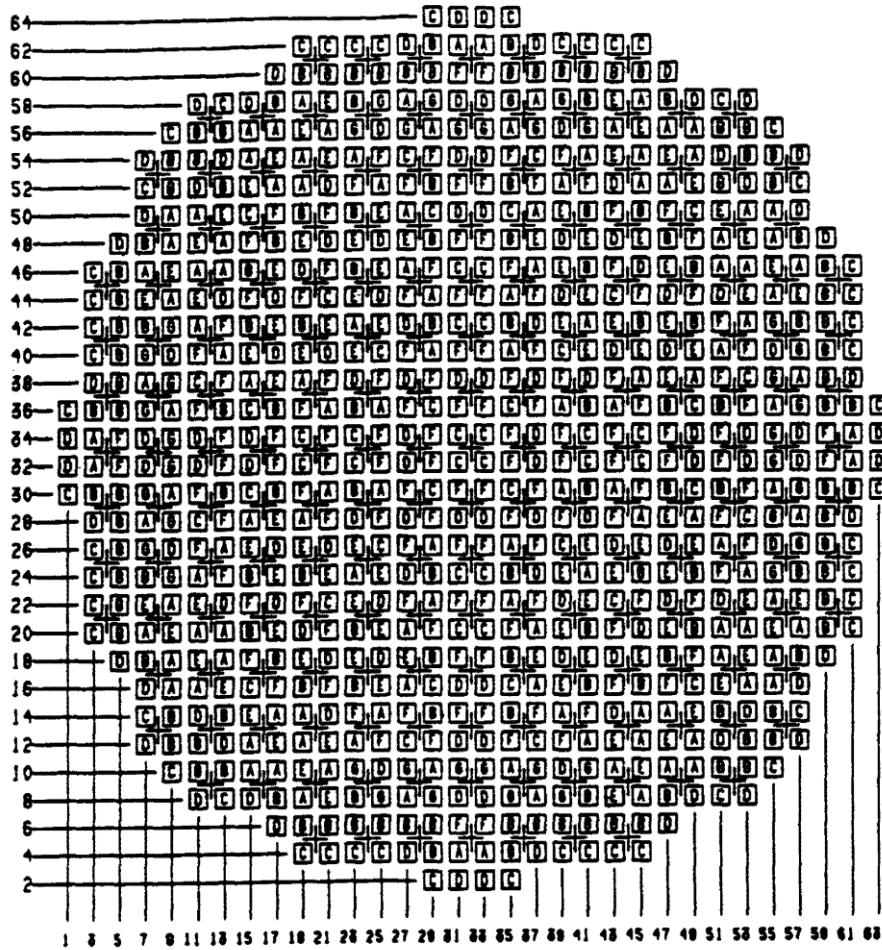
Fuel Type			
A=SIE9–5–P9SZBB306–9GZ–120U–150–T	(Cycle 8)	E=GE11–P9SUB355–15GZ–120T–146–T	(Cycle 9)
B=SIE9–5–P9SZBB355–9GZ–120U–150–T	(Cycle 8)	F=GE11–P9SUB371–12GZ1–120T–146–T	(Cycle 9)
C=SIE9–5–P9SZBB343–9GZ–120U–150–T	(Cycle 7)	G=GE11–P9SUB391–13GZ–120T–146–T	(Cycle 9)
D=SIE9–5–P9SZBB320–9GZ–120U–150–T	(Cycle 7)		

GRAND GULF NUCLEAR STATION	TYPICAL RELOAD CORE LOADING MAP
UNIT 1	[HISTORICAL INFORMATION]
UPDATED FINAL SAFETY ANALYSIS REPORT	FIGURE 4.3-1

Figure 4.3-2 through 4.3-6

Deleted
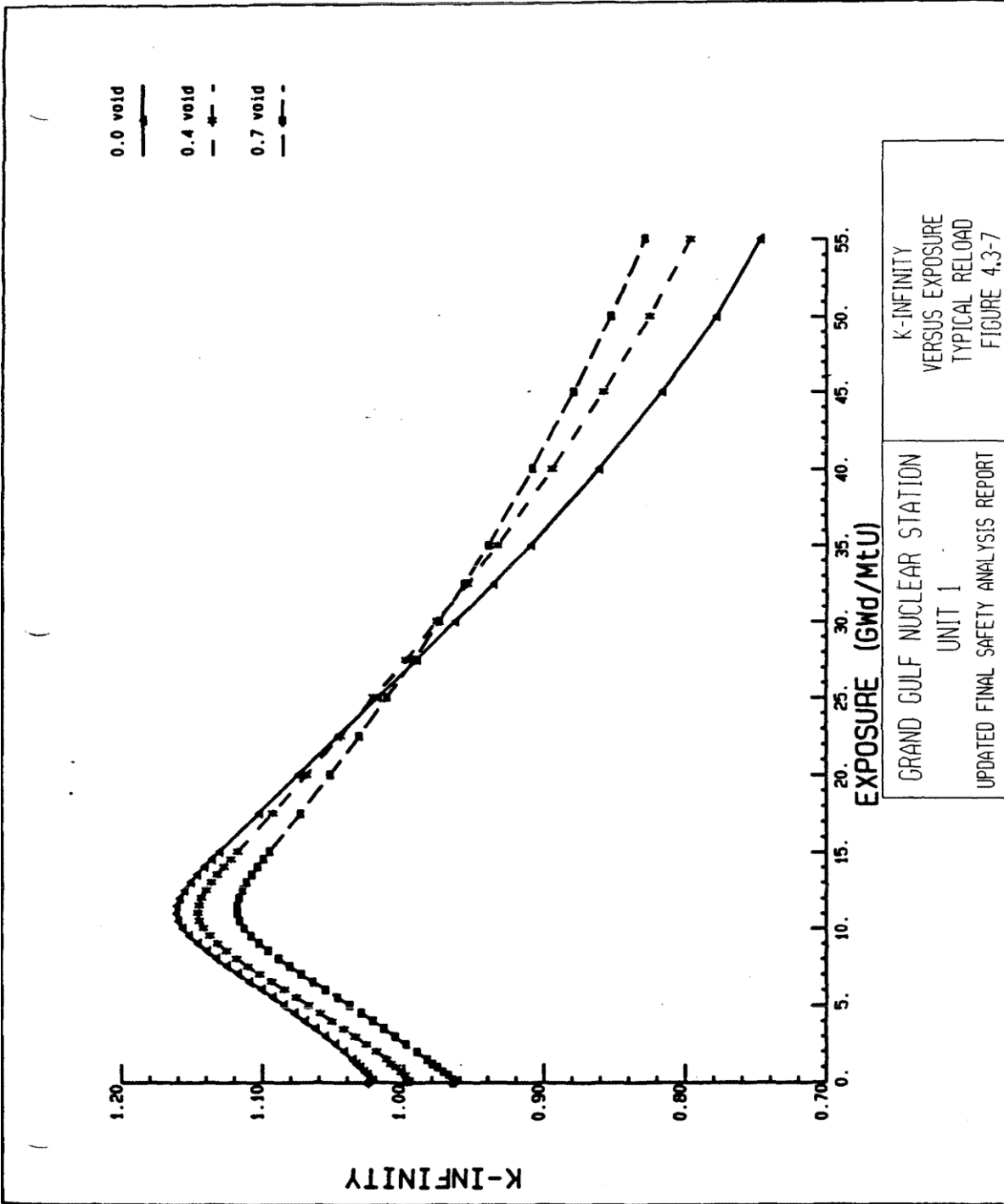
K-INFINITY
VERSUS EXPOSURE
TYPICAL RELOAD
FIGURE 4.3-7

GRAND GULF NUCLEAR STATION
UNIT 1
UPDATED FINAL SAFETY ANALYSIS REPORT
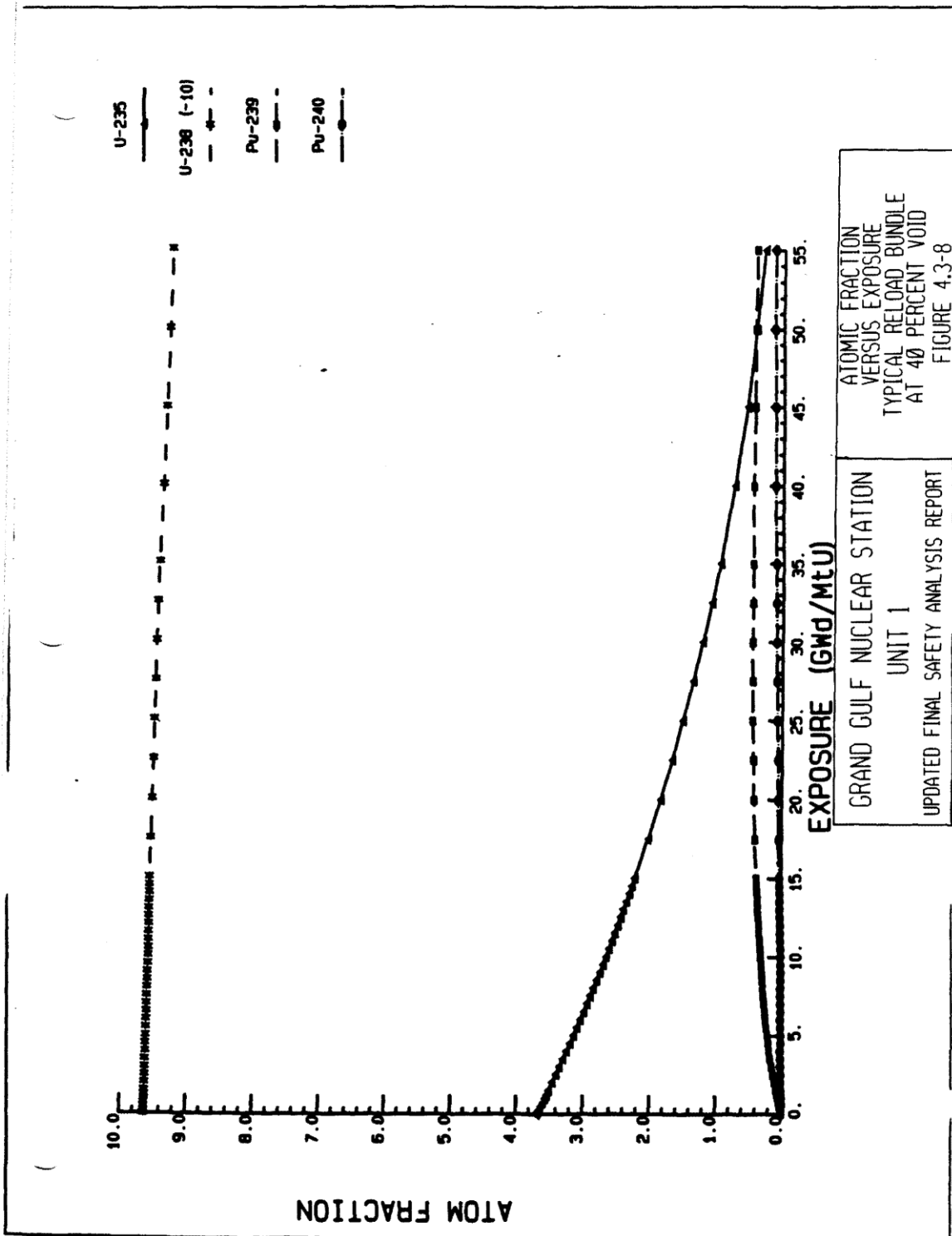
GRAND GULF NUCLEAR STATION
UNIT 1
UPDATED FINAL SAFETY ANALYSIS REPORT

ATOMIC FRACTION
VERSUS EXPOSURE
TYPICAL RELOAD BUNDLE
AT 40 PERCENT VOID
FIGURE 4.3-8

FISSION FRACTION
VERSUS EXPOSURE
TYPICAL RELOAD
AT 40 PERCENT VOID
FIGURE 4.3-9

GRAND GULF NUCLEAR STATION
UNIT 1
UPDATED FINAL SAFETY ANALYSIS REPORT

NEUTRON GENERATION TIME
VERSUS EXPOSURE
TYPICAL RELOAD
FIGURE 4.3-10

GRAND GULF NUCLEAR STATION
UNIT 1
UPDATED FINAL SAFETY ANALYSIS REPORT

DELAYED NEUTRON FRACTION
VERSUS EXPOSURE
TYPICAL RELOAD BUNDLE
FIGURE 4.3-11
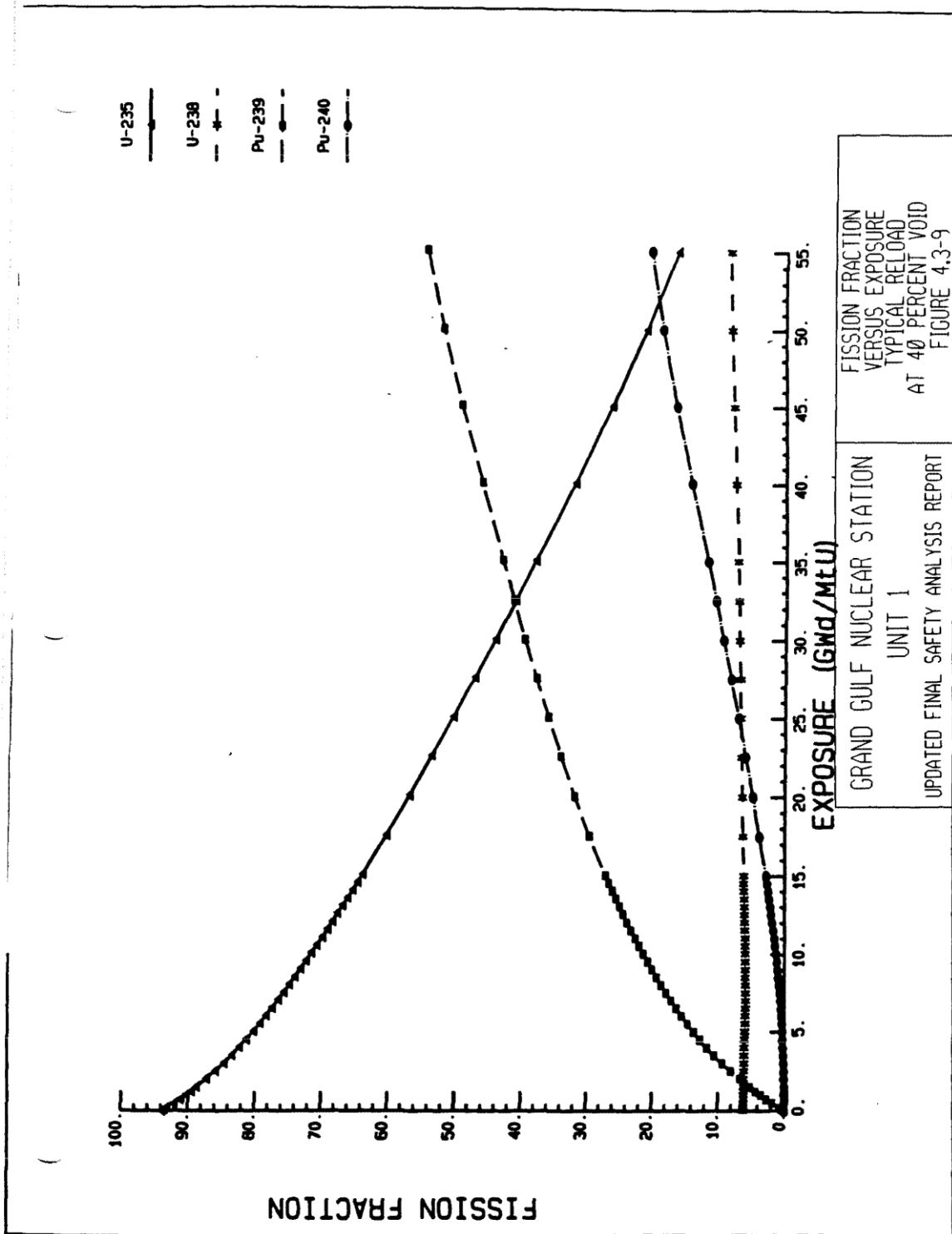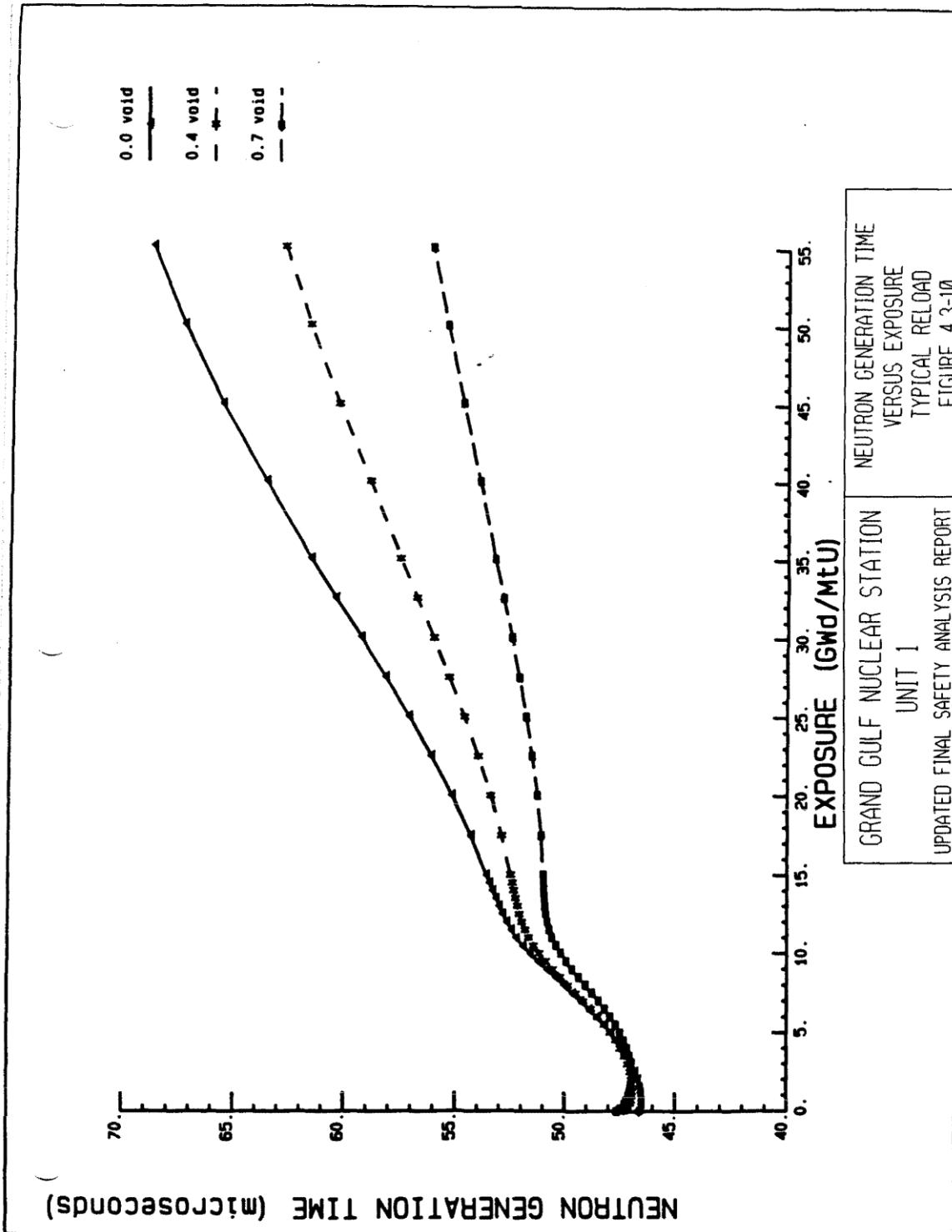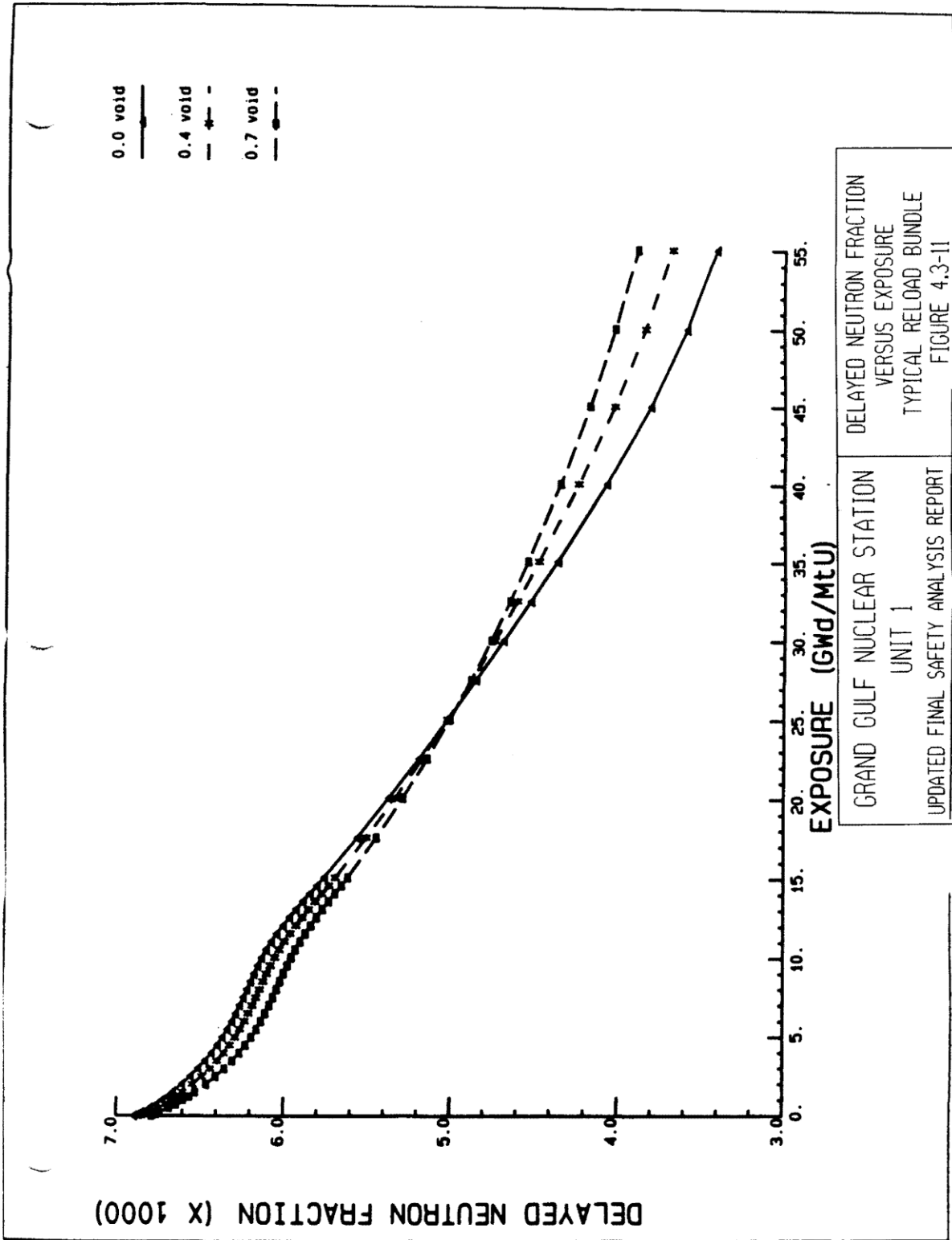
GRAND GULF NUCLEAR STATION
UNIT 1

UPDATED FINAL SAFETY ANALYSIS REPORT

```
CONTROL ROD
X  +--------+
   |  .910  |       0.00 void
 ^ |  .925  |       0.40 void
 X |  .932  |       0.70 void
   +--------+--------+
   | 1.090  |  .326  |
   | 1.112  |  .365  |
   | 1.126  |  .406  |
   +--------+--------+--------+
   | 1.139  |  .997  | 1.043  |
   | 1.142  | 1.010  | 1.035  |
   | 1.141  | 1.022  | 1.033  |
   +--------+--------+--------+--------+
   | 1.102  | 1.059  | 1.100  | 1.060  |
   | 1.095  | 1.059  | 1.072  | 1.015  |
   | 1.084  | 1.059  | 1.052  |  .983  |
   +--------+--------+--------+--------+--------+
   | 1.157  |  .317  | 1.104  |        |        |
   | 1.155  |  .351  | 1.071  |   W    |   W    |
   | 1.146  |  .386  | 1.047  |        |        |
   +--------+--------+--------+--------+--------+--------+
   | 1.102  | 1.058  | 1.095  | 1.300  |        | 1.060  |
   | 1.094  | 1.057  | 1.068  | 1.243  |   W    | 1.014  |
   | 1.083  | 1.058  | 1.048  | 1.201  |        |  .982  |
   +--------+--------+--------+--------+--------+--------+--------+
   | 1.139  |  .996  | 1.040  | 1.095  | 1.103  | 1.100  | 1.042  |
   | 1.141  | 1.008  | 1.032  | 1.067  | 1.071  | 1.071  | 1.034  |
   | 1.139  | 1.021  | 1.030  | 1.047  | 1.046  | 1.051  | 1.031  |
   +--------+--------+--------+--------+--------+--------+--------+--------+
   | 1.089  |  .326  |  .996  | 1.058  |  .317  | 1.058  |  .996  |  .326  |
   | 1.110  |  .365  | 1.008  | 1.057  |  .350  | 1.058  | 1.009  |  .365  |
   | 1.124  |  .406  | 1.020  | 1.057  |  .386  | 1.058  | 1.021  |  .406  |
   +--------+--------+--------+--------+--------+--------+--------+--------+--------+
   |  .909  | 1.089  | 1.138  | 1.101  | 1.156  | 1.101  | 1.138  | 1.088  |  .908  |
   |  .924  | 1.110  | 1.141  | 1.094  | 1.154  | 1.094  | 1.141  | 1.110  |  .923  |
   |  .931  | 1.123  | 1.139  | 1.083  | 1.145  | 1.083  | 1.139  | 1.123  |  .930  |
   +--------+--------+--------+--------+--------+--------+--------+--------+--------+
```

GRAND GULF NUCLEAR STATION UNIT 1 UPDATED FINAL SAFETY ANALYSIS REPORT	UNCONTROLLED LOCAL POWER DISTRIBUTION TYPICAL RELOAD FUEL, BOL FIGURE 4.3-12

Figure 4.3-13

Deleted
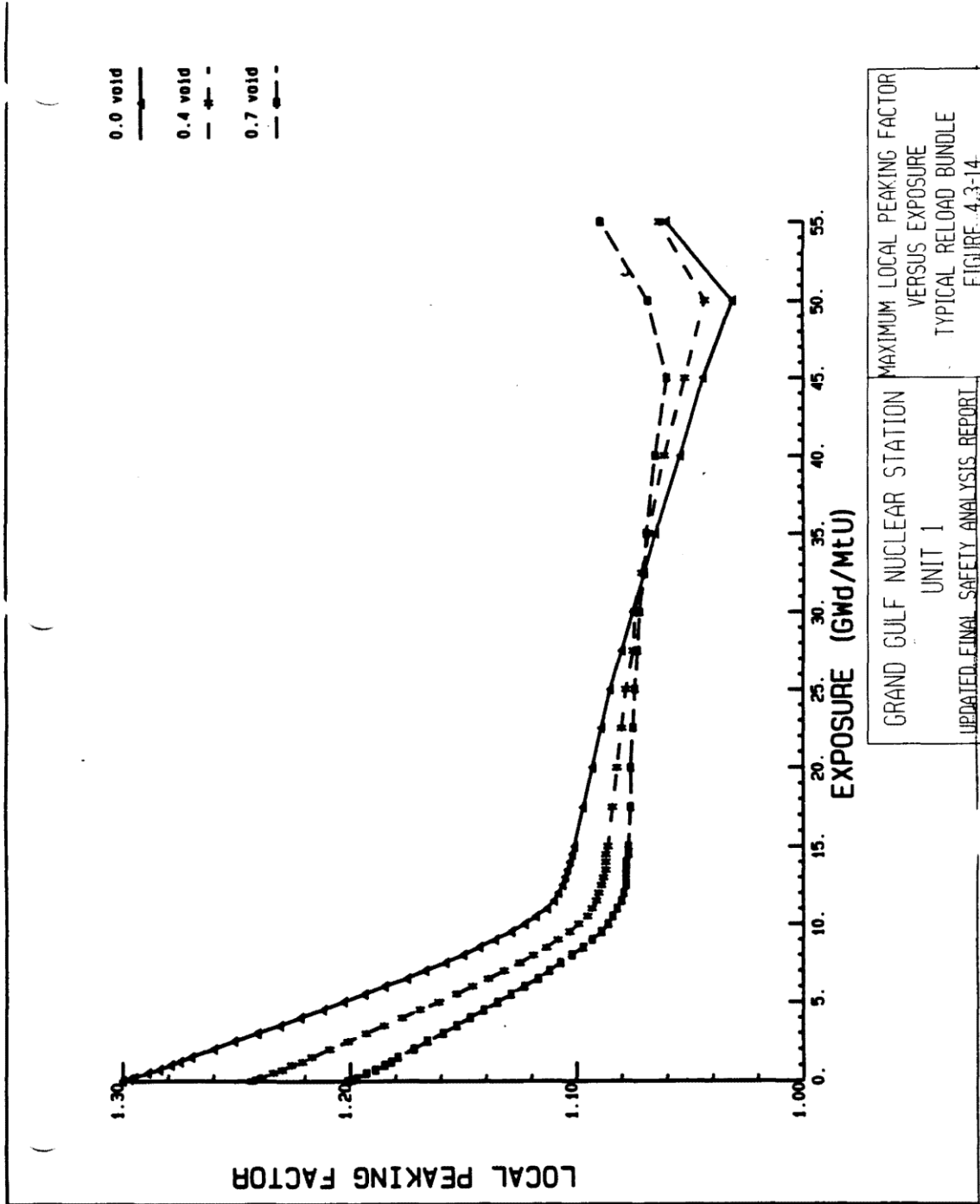
MAXIMUM LOCAL PEAKING FACTOR
VERSUS EXPOSURE
TYPICAL RELOAD BUNDLE
FIGURE 4.3-14

GRAND GULF NUCLEAR STATION
UNIT 1
UPDATED FINAL SAFETY ANALYSIS REPORT

Figure 4.3-15

Deleted

```
CONTROL ROD
X  +-------+
   | 1.060 |          0.00 void
^  | 1.063 |          0.40 void
X  | 1.089 |          0.70 void
   +-------+-------+
   | 1.017 | .920  |
   | 1.017 | .911  |
   | 1.033 | .897  |
   +-------+-------+-------+
   | 1.011 | .995  | 1.012 |
   | 1.015 | .989  | 1.006 |
   | 1.030 | .975  | .987  |
   +-------+-------+-------+-------+
   | 1.013 | .987  | .999  | 1.024 |
   | 1.016 | .985  | 1.001 | 1.027 |
   | 1.029 | .969  | .990  | 1.034 |
   +-------+-------+-------+-------+-------+
   | 1.024 | .906  | 1.003 |       |       |
   | 1.030 | .896  | 1.008 |   W   |   W   |
   | 1.044 | .874  | 1.002 |       |       |
   +-------+-------+-------+-------+-------+-------+
   | 1.013 | .987  | 1.000 | 1.021 |       | 1.024 |
   | 1.016 | .985  | 1.003 | 1.035 |   W   | 1.027 |
   | 1.029 | .970  | .991  | 1.049 |       | 1.034 |
   +-------+-------+-------+-------+-------+-------+-------+
   | 1.012 | .996  | 1.013 | 1.000 | 1.003 | .999  | 1.012 |
   | 1.015 | .989  | 1.007 | 1.003 | 1.008 | 1.001 | 1.006 |
   | 1.030 | .975  | .988  | .991  | 1.002 | .990  | .987  |
   +-------+-------+-------+-------+-------+-------+-------+-------+
   | 1.017 | .920  | .996  | .987  | .906  | .987  | .995  | .920  |
   | 1.018 | .911  | .989  | .985  | .896  | .985  | .989  | .911  |
   | 1.033 | .898  | .975  | .970  | .874  | .969  | .975  | .898  |
   +-------+-------+-------+-------+-------+-------+-------+-------+-------+
   | 1.060 | 1.017 | 1.012 | 1.013 | 1.024 | 1.013 | 1.011 | 1.017 | 1.060 |
   | 1.063 | 1.018 | 1.015 | 1.016 | 1.030 | 1.016 | 1.015 | 1.017 | 1.063 |
   | 1.089 | 1.033 | 1.030 | 1.029 | 1.044 | 1.029 | 1.029 | 1.033 | 1.089 |
   +-------+-------+-------+-------+-------+-------+-------+-------+-------+
```

GRAND GULF NUCLEAR STATION UNIT 1 UPDATED FINAL SAFETY ANALYSIS REPORT	UNCONTROLLED LOCAL POWER DISTRIBUTION TYPICAL RELOAD FUEL, EOL FIGURE 4.3-16

Figure 4.3-17

Deleted

CONTROL ROD

```
v  +-------+
   | .376  |        0.00 void
X  | .403  |        0.40 void
X  | .427  |        0.70 void
   +-------+-------+
   | .491  | .280  |
   | .518  | .323  |
   | .540  | .368  |
   +-------+-------+-------+
   | .572  | .722  | .909  |
   | .588  | .713  | .871  |
   | .600  | .702  | .831  |
   +-------+-------+-------+-------+
   | .595  | .824  | 1.059 | 1.125 |
   | .608  | .804  | 1.000 | 1.053 |
   | .616  | .781  | .938  | .984  |
   +-------+-------+-------+-------+-------+
   | .648  | .310  | 1.140 |       |       |
   | .671  | .351  | 1.079 |   W   |   W   |
   | .688  | .392  | 1.018 |       |       |
   +-------+-------+-------+-------+-------+-------+
   | .667  | .916  | 1.152 | 1.494 |       | 1.307 |
   | .689  | .906  | 1.103 | 1.416 |   W   | 1.253 |
   | .708  | .897  | 1.057 | 1.346 |       | 1.213 |
   +-------+-------+-------+-------+-------+-------+-------+
   | .747  | .895  | 1.123 | 1.283 | 1.352 | 1.390 | 1.346 |
   | .781  | .903  | 1.102 | 1.240 | 1.308 | 1.351 | 1.333 |
   | .814  | .914  | 1.084 | 1.202 | 1.271 | 1.322 | 1.329 |
   +-------+-------+-------+-------+-------+-------+-------+-------+
   | .831  | .347  | 1.131 | 1.270 | .380  | 1.373 | 1.316 | .412  |
   | .882  | .397  | 1.140 | 1.263 | .425  | 1.371 | 1.331 | .466  |
   | .930  | .451  | 1.149 | 1.256 | .475  | 1.372 | 1.351 | .526  |
   +-------+-------+-------+-------+-------+-------+-------+-------+-------+
   | .839  | 1.142 | 1.308 | 1.340 | 1.471 | 1.440 | 1.518 | 1.477 | 1.235 |
   | .880  | 1.174 | 1.312 | 1.330 | 1.466 | 1.430 | 1.521 | 1.505 | 1.256 |
   | .913  | 1.199 | 1.309 | 1.315 | 1.456 | 1.419 | 1.525 | 1.535 | 1.276 |
   +-------+-------+-------+-------+-------+-------+-------+-------+-------+
```

GRAND GULF NUCLEAR STATION UNIT 1 UPDATED FINAL SAFETY ANALYSIS REPORT	CONTROLLED POWER DISTRIBUTION TYPICAL RELOAD FUEL, BOL FIGURE 4.3-18

Figure 4.3-19

Deleted

Figure 4.3-20

Deleted

Figure 4.3-21

Deleted

Figure 4.3-22

Deleted

Figure 4.3-22A Deleted

Figure 4.3-23

Deleted

Figure 4.3-23A

Deleted
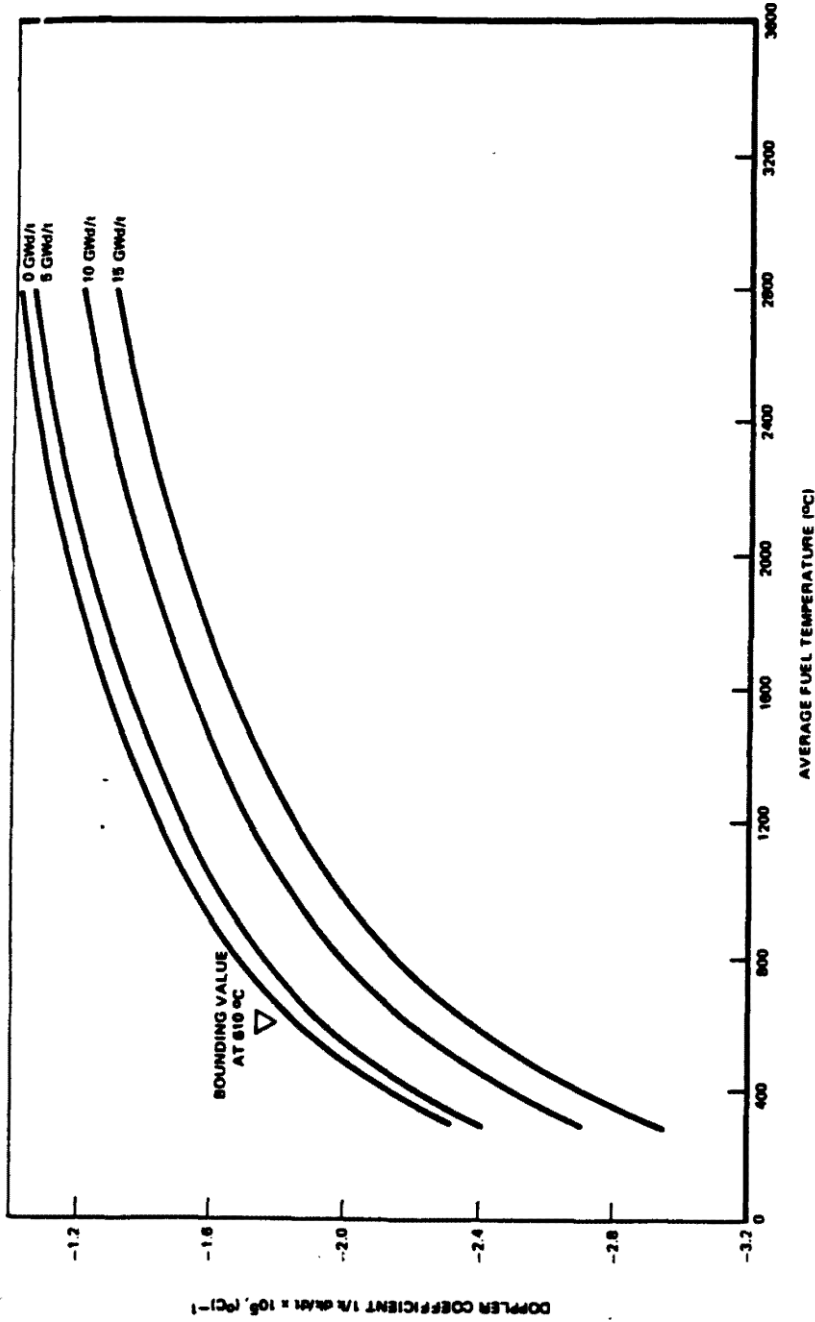
[HISTORICAL INFORMATION]

DOPPLER REACTIVITY COEFFICIENT AS A FUNCTION OF
FUEL EXPOSURE AND AVERAGE FUEL TEMPERATURE AT AN
AVERAGE VOID CONTENT OF 40 PERCENT INITIAL CYCLE
HIGH ENRICHMENT DOMINANT FUEL TYPE
FIGURE 4.3-24

GRAND GULF NUCLEAR STATION
UNIT 1
UPDATED FINAL SAFETY ANALYSIS REPORT
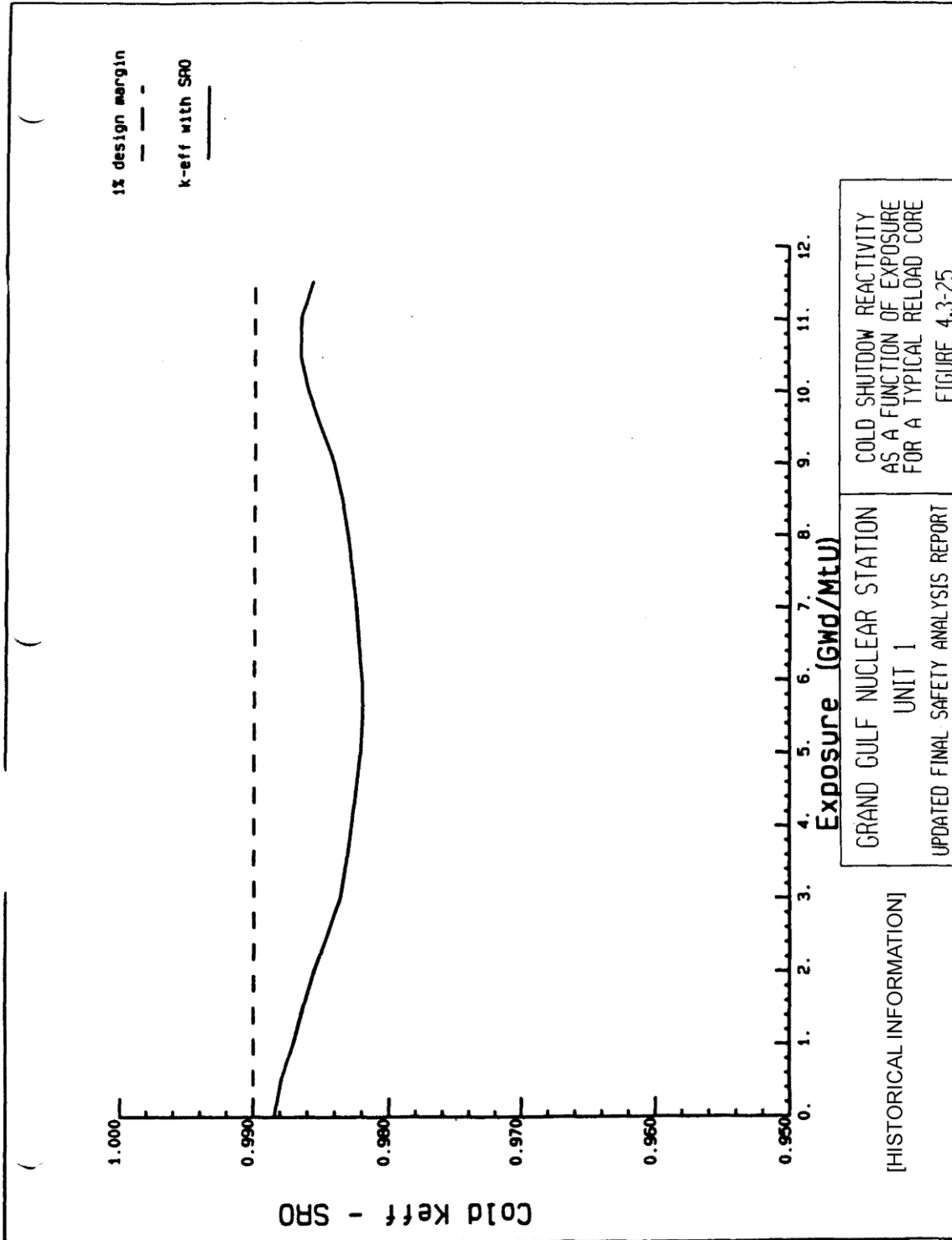
COLD SHUTDOWN REACTIVITY
AS A FUNCTION OF EXPOSURE
FOR A TYPICAL RELOAD CORE

FIGURE 4.3-25

GRAND GULF NUCLEAR STATION
UNIT 1

UPDATED FINAL SAFETY ANALYSIS REPORT

[HISTORICAL INFORMATION]
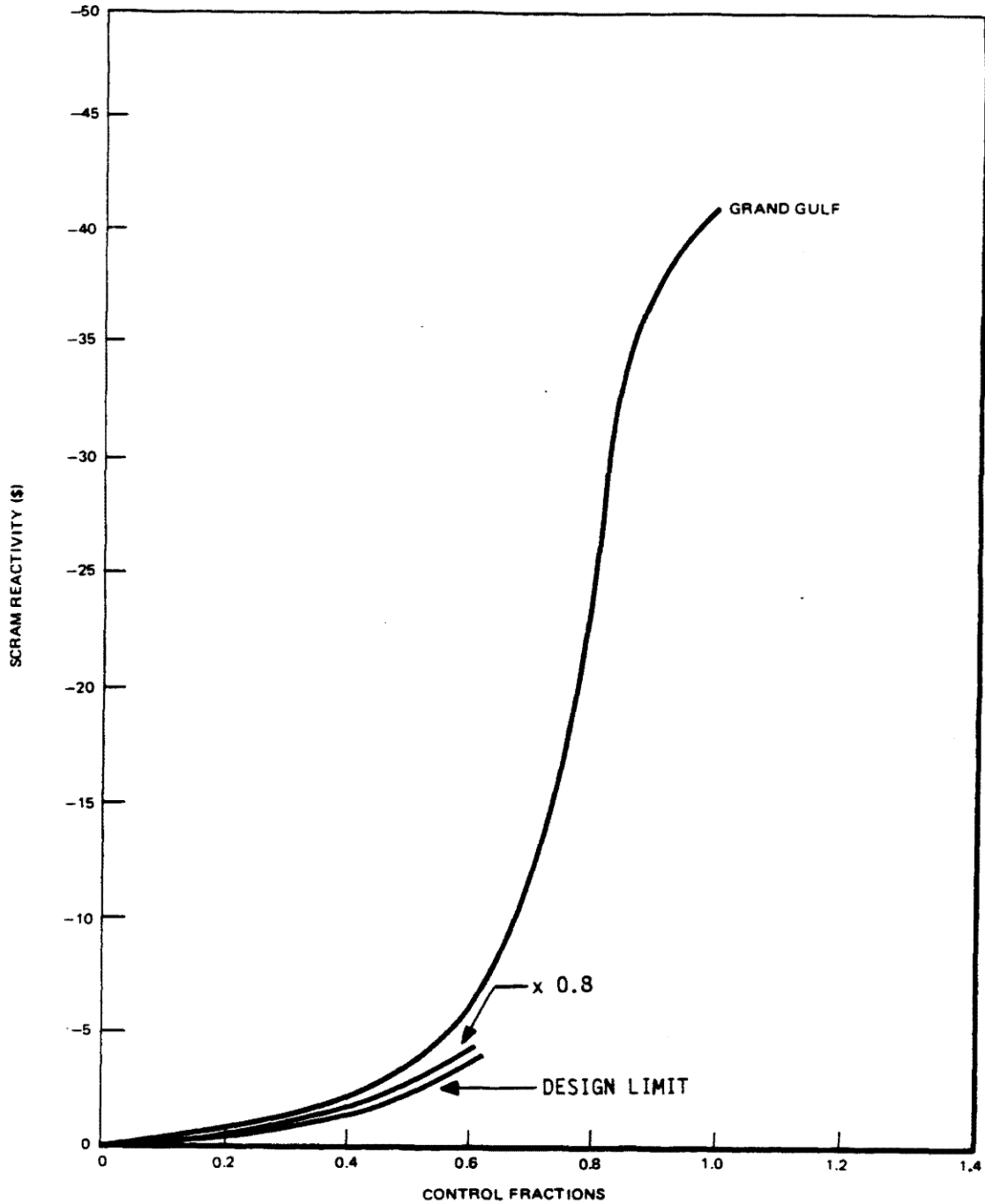
GRAND GULF NUCLEAR STATION UNIT 1 UPDATED FINAL SAFETY ANALYSIS REPORT	HOT OPERATING, END-OF-CYCLE 1 SCRAM REACTIVITY ($) FIGURE 4.3-26

[HISTORICAL INFORMATION]

Figure 4.3-27

Deleted

Figure 4.3-27a

Deleted

Figure 4.3-28

Deleted

Figure 4.3-28a

Deleted
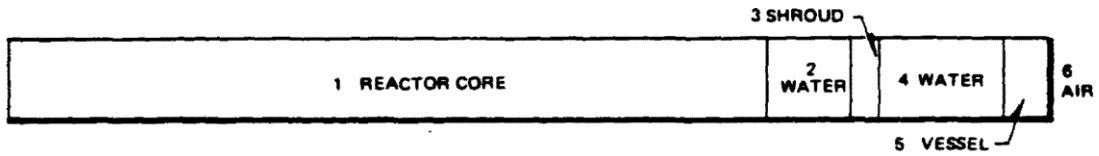
MATERIAL		RADIUS (in.)	MATERIAL	MATERIAL DENSITY
NO.	NAME		WATER	0.318 g/cm^3
1	REACTOR CORE	95.75	UO_2	2.334 g/cm^3
			ZIRCONIUM	0.978 g/cm^3
			304L STAINLESS STEEL	From ASME SA240
2	WATER	105.94	WATER	0.74 g/cm^3
3	SHROUD	107.94	304L STAINLESS STEEL	FROM ASME SA 240
4	WATER	125.5	WATER	0.74 g/cm^3
5	VESSEL	131.68	CARBON STEEL	FROM ASME SA 240
6	AIR		AIR	$1.3 \times 10^{-3} \text{ g/cc}$

GRAND GULF NUCLEAR STATION UNIT 1 UPDATED FINAL SAFETY ANALYSIS REPORT	MODEL FOR ONE-DIMENSIONAL TRANSPORT ANALYSIS OF VESSEL FLUENCE
	FIGURE 4.3-29

Figure 4.3-30

Deleted

4.4   THERMAL AND HYDRAULIC DESIGN

4.4.1   Design Basis

4.4.1.1   Safety Design Bases

Thermal-hydraulic design of the core establishes:

a.   Actuation limits for the devices of the nuclear safety systems such that no fuel damage occurs as a result of moderate frequency transient events. Specifically the Minimum Critical Power Ratio (MCPR) operating limit is specified such that at least 99.9 percent of the fuel rods in the core are not expected to experience boiling transition during the most severe moderate* frequency transient events.

b.   The thermal-hydraulic safety limits for use in evaluating the safety margin relating the consequences of fuel barrier failure to public safety.

c.   That the nuclear system exhibits no inherent tendency toward divergent or limit cycle oscillations which would compromise the integrity of the fuel or nuclear system process barrier.

4.4.1.2   Power Generation Design Bases

The thermal-hydraulic design of the core provides the following operational characteristics:

a.   The ability to achieve rated core power output throughout the design life of the fuel without sustaining premature fuel failure

b.   Flexibility to adjust core output over the range of plant load and load maneuvering requirements in a stable, predictable manner without sustaining fuel damage

_____

* Per Regulatory Guide 1.70, Revision 2.

4.4.1.3   Requirements for Steady State Conditions

Steady State Limits

For purposes of maintaining adequate thermal margin during normal steady state operation, the minimum critical power ratio must not be less than the required MCPR operating limit, the average planar linear heat generation rate (APLHGR) must be maintained below the required maximum APLHGR (MAPLHGR), and the maximum linear heat generation rate must be maintained below the design LHGR for the plant. This does not specify the operating power nor does it specify peaking factors. These parameters are determined subject to a number of constraints including the thermal limits given previously. The core and fuel design basis for steady state operation, i.e., MCPR, MAPLHGR and LHGR limits, have been defined to provide margin between the steady state operating conditions and any fuel damage condition to accommodate uncertainties and to assure that no fuel damage results even during the worst anticipated transient condition at any time in life.

4.4.1.4   Requirements for Transient Conditions

Transient Limits

The transient thermal limits are established such that no fuel damage is expected to occur during the most severe moderate frequency transient event. Fuel damage is defined as perforation of the cladding that permits release of fission products. Mechanisms that cause fuel damage in reactor transients are:

  a.   Severe overheating of fuel cladding caused by inadequate cooling

  b.   Fracture of the fuel cladding caused by relative expansion of the uranium dioxide pellet inside the fuel cladding

For design purposes, the transient limit requirement is met if at least 99.9 percent of the fuel rods in the core do not experience boiling transition during any moderate frequency transient event. No fuel damage would be expected to occur even if a fuel rod actually experienced a boiling transition.

A value of 1 percent plastic strain of Zircaloy cladding is conservatively defined as the limit below which fuel damage from overstraining the fuel cladding is not expected to occur. Available data indicate that the threshold for damage is in excess

of this value. The linear heat generation rates that would cause this amount of cladding strain are discussed in Section 4.2.3 for the current core reload.

4.4.1.5   Summary of Design Bases

In summary, the steady state operating limits have been established to assure that the design basis is satisfied for the most severe moderate frequency transient event. An overpower which occurs during an incident of a moderate frequency transient event must meet the plant transient MCPR limit and must limit the peak linear heat generation rate below that which will cause damage due to overstraining of the cladding. Demonstration that the transient limits are not exceeded is sufficient to conclude that the design basis is satisfied.

The MCPR, MAPLHGR and LHGR limits are sufficiently general so that no other limits need to be stated. For example, cladding surface temperatures will always be maintained within 10 to 15°F of the coolant temperature as long as the boiling process is in the nucleate regime. The cladding and fuel bundle integrity criterion is assured as long as MCPR, MAPLHGR and LHGR limits are met. There are no additional design criteria on coolant void fraction, core coolant flow-velocities, or flow distribution, nor are they needed. The flow distribution is controlled by the MCPR requirement. The coolant flow velocities and void fraction become constraints upon the mechanical and physics design of reactor components and are partially constrained by stability and control requirements.

4.4.2   Description of Thermal-hydraulic Design of the Reactor Core

4.4.2.1   Summary Comparison

An evaluation of plant performance from a thermal and hydraulic standpoint is provided in subsection 4.4.3.

[HISTORICAL INFORMATION] [A tabulation of thermal and hydraulic parameters of typical cores is given in Table 4.4-1.]

4.4.2.2   Critical Power Ratio

There are three different types of boiling heat transfer to water in a forced convection system: nucleate boiling, transition boiling, and film boiling. Nucleate boiling, at lower heat

transfer rates, is an extremely efficient mode of heat transfer, allowing large quantities of heat to be transferred with a very small temperature rise at the heated wall. As heat transfer rate is increased, the boiling heat transfer surface alternates between film and nucleate boiling, leading to fluctuations in heated wall temperatures. The point of departure from the nucleate boiling region into the transition boiling region is called the boiling transition. Transition boiling begins at the critical power and is characterized by fluctuations in cladding surface temperature. Film boiling occurs at the highest heat transfer rates; it begins as transition boiling comes to an end. Film boiling heat transfer is characterized by stable wall temperatures which are higher than those experienced during nucleate boiling.

4.4.2.2.1   Boiling Correlations

The occurrence of boiling transition is a function of the local steam quality, inlet subcooling, assembly power distribution, mass flow rate, pressure, flow geometry, and local peaking pattern. Extensive experimental investigations have been performed over the entire design range of these variables. The applicable critical power correlations are the GEXL correlation (References 1, 31, and 35) for the initial core and Reference 65 for the current GEH core reload. The correlations are based on accurate test data of prototypic simulations of reactor fuel assemblies operating under conditions duplicating those in actual reactor designs. The correlations are a "best fit" to the data and are used together with a statistical analysis to assure adequate reactor thermal margins.

The figure of merit used for reactor design and operation is the Critical Power Ratio (CPR). This is defined as the ratio of the bundle power at which transition boiling occurs to the bundle power at the reactor condition of interest (i.e., the ratio of critical bundle power to operating bundle power). In this definition, the critical power is determined at the same mass flux, inlet temperature, and pressure which exist at the specified reactor condition.

In general, the CPR is not affected as crud accumulates on fuel rods (References 36 and 37). Therefore, no modifications to the critical power correlations are made to account for crud deposition.

The initial core was sized with sufficient coolant flow to assure that the MCPR was maintained at or above the operating limit at rated conditions.

The MCPR operating limits are provided in the Core Operating Limits Report for reload cores and are determined based on the fuel and core design to assure that the applicable MCPR safety limits are not exceeded during anticipated transients.

4.4.2.3   Thermal Operating Limits

The limiting constraints in the design of the reactor core are stated in terms of the MAPLHGR limit, the LHGR limit and the MCPR operating limit for the plant. The design philosophy used to assure that these limits are met involves the selection of one or more power distributions which are more limiting than expected operating conditions and subsequent verification that, under these more stringent conditions, the design limits are met. Therefore, the "design power distribution" is an extreme condition of power. It is a fair and stringent test of the operability of the reactor as designed to comply with the foregoing limits. Expected operating conditions are less severe than those represented by a design power distribution which gives the maximum allowable MAPLHGR, the maximum allowable LHGR and the MCPR operating limits for the plant. However, it must be established that operation with a less severe power distribution is not a necessary condition for the safety of the reactor Because there are an infinite number of operating reactor states which can exist (with variations in rod patterns, time in cycle, power level, power distribution, flow, etc.) which are within the design constraints, it is not possible to determine them all. However, constant monitoring of operating conditions using the available plant measurements can ensure compliance with design objectives.

4.4.2.3.1   Design Power Distribution

Thermal design of the reactor – including the selection of the core size and effective heat transfer area, the design steam quality, the total recirculation flow, the inlet subcooling, and the specification of internal flow distribution – was performed by the NSSS vendor and is based on the concept and application of a design power distribution. The design power distribution is an appropriately conservative representation of the most limiting thermal operating state at rated conditions and includes design

allowances for the combined effects (on the fuel rod, and the fuel assembly heat flux and temperature) of the gross and local steady state power density distributions and adjustments of the control rods.

4.4.2.3.2   Design LHGR and MAPLHGR

[HISTORICAL INFORMATION] [The maximum and core average linear heat generation rates used in the initial core design which is a typical BWR design, are shown in Table 4.4-1.] The core average value multiplied by the overall peaking factor yields the maximum LHGR.

Fuel type specific LHGR limits and MAPLHGR limits are provided in the Core Operating Limits Report for the current cycle.

4.4.2.4   Void Fraction Distribution

[HISTORICAL INFORMATION] [Typical core average and maximum exit void fractions in the core at rated condition are given in Table 4.4-1 for different BWR core sizes. The axial distribution of core void fractions for the average radial channel and the maximum radial channel (end of node value) of a typical core are given in Table 4.4-2. The core average and maximum exit value is also provided. Similar distributions for steam quality are provided in Table 4.4-3. The core average axial power distribution used to produce these tables is given in Table 4.4-2a.]

4.4.2.5   Core Coolant Flow Distribution and Orificing Pattern

Correct distribution of core coolant flow among the fuel assemblies is accomplished by the use of an accurately calibrated fixed orifice at the inlet of each fuel assembly. The orifices are located in the fuel support piece. They serve to control the flow distribution and, hence, the coolant conditions within prescribed bounds throughout the design range of core operation. The sizing and design of the orifices ensure stable flow in each fuel assembly during all phases of operation at normal operating conditions.

The core is divided into two orificed flow zones. The outer zone is a narrow, reduced-power region around the periphery of the core. The inner zone consists of the core center region. No other control of flow and stream distribution other than that

incidentally supplied by adjusting the power distribution with the control rods, is used or needed. The orifices can be changed during refueling, if necessary.

[HISTORICAL INFORMATION] [Core flow distribution calculations were performed for the initial core using the design power distribution which consists of a hot and average powered assembly in each of the two orifice zones. The design bundle power and resulting relative flow distribution for a typical BWR/6 are given in Table 4.4-4.]

The flow distribution to the fuel assemblies is calculated on the assumption that the pressure drop across all fuel assemblies is the same. This assumption has been confirmed by measuring the flow distribution in a modern boiling water reactor as reported in Reference 2.

There is reasonable assurance, therefore, that the calculated flow distribution throughout the core is in close agreement with the actual flow distribution of an operating reactor.

The use of the design power distribution for the initial core discussed in References 1 and 31 ensures the orificing chosen covers the range of normal operation. The expected shifts in power production during core life are less severe and are bounded by the design power distribution.

The coolant flow distribution for reload cores is calculated in the same manner as for the initial core except that predicted core power distributions are modeled for each fuel type in the central and peripheral orifice zones for design and licensing calculations.

4.4.2.6   Core Pressure Drop and Hydraulic Loads

[HISTORICAL INFORMATION] [The pressure drops and hydraulic loads for the various core components under the steady state design conditions are included in Table 4.4-1 for the initial core, which is a typical BWR/6 core.] Analyses for the most limiting conditions, the recirculation line break and the steam line break, are reported in Chapter 15, "Accident Analyses."

The components of bundle pressure drop considered are friction, local elevation, and acceleration. [HISTORICAL INFORMATION] [The theory and constitutive relationships for calculating pressure drops are provided in References 3 and 4 for the initial core.

Pressure drop measurements made in operating reactors confirm that the total measured core pressure drop and calculated core pressure drop are in good agreement.] Models for pressure drop across the core for the current reload are given in Reference 43.

4.4.2.6.1   Deleted

4.4.2.6.2   Deleted

4.4.2.6.3   Deleted

4.4.2.6.4   Deleted

4.4.2.7   Correlation and Physical Data

4.4.2.7.1   Pressure Drop Correlations

Correlations have been developed to fit measured data to the formulations discussed in References 43, 55, 56, and 57. Friction pressure drops for multirod geometries representative of BWR fuel bundles were measured to calibrate the orifices and lower tie plates in single-phase flow, and the spacers and upper tie plates in both single- and two-phase flow The range of test variables is specified to include the range of interest to BWRs. Applicability of the correlations is confirmed by full scale prototype flow tests.

4.4.2.7.2   Void Fraction Correlation

The void fraction correlation used for the initial core and the GE reload cores is a version of the Zuber-Findlay model (Ref. 11) where the concentration parameter and void drift coefficient are based on comparison with a large quantity of world-wide data (Refs. 13 through 24).

4.4.2.7.3   Heat Transfer Correlation

The Jens-Lottes (Ref. 5) wall superheat equation was used in fuel design for the initial core and the GE reload cores to determine the cladding-to-coolant heat transfer coefficients for nucleate boiling.

4.4.2.8   Thermal Effects of Operational Transients

The evaluation of the core's capability to withstand the thermal effects resulting from anticipated operational transients is covered in Chapter 15, Accident Analyses.

4.4.2.9   Uncertainties in Estimates

Uncertainties in thermal-hydraulic parameters are considered in the statistical analysis which is the basis for setting the transient MCPR limit such that at least 99.9 percent of the fuel rods in the core are expected not to experience boiling transition during any moderate frequency transient event. The statistical model and analytical procedure are described in detail in Reference 1 for the initial core and in References 1 and 43 for the current GEH reload core. The current cycle uncertainties considered and their input values used in the analysis are provided in References 63 and 64.

4.4.2.10   Flux Tilt Considerations

For flux tilt considerations, refer to subsection 4.3.2.2.7.

4.4.3   Description of the Thermal and Hydraulic Design of the Reactor Coolant System

The thermal and hydraulic design of the reactor coolant system is described in this section.

4.4.3.1   Plant Configuration Data

4.4.3.1.1   Reactor Coolant System Configuration

The reactor coolant system is described in Section 5.4 and shown in isometric perspective in Figure 5.4-1. The piping sizes, fittings, and valves are listed in Table 5.4-1.

4.4.3.1.2   Reactor Coolant System Thermal Hydraulic Data

The steady state distribution of temperature, pressure, and flow rate for each flowpath in the reactor coolant system is shown in Figure 5.1-1.

4.4.3.1.3   Reactor Coolant System Geometric Data

Volumes of regions and components within the reactor vessel are shown in Figure 5.1-2.

Table 4.4-8 provides the flow path length, height, liquid level, minimum elevations, and minimum flow areas for each major flow path volume within the reactor vessel and recirculation loops of the reactor coolant systems.

Table 4.4-9 provides the lengths and sizes of all safety injection lines to the reactor coolant system.

4.4.3.2   Operating Restrictions on Pumps

Expected recirculation pump performance curves are shown in Figure 5.4-4. These curves are valid for all conditions with a normal operating range varying from approximately 20 percent to 115 percent of rated pump flow.

The pump characteristics including considerations of NPSH requirements are the same for the conditions of two pump and one pump operation as described in subsection 5.4.1. Subsection **4.4.3.3** gives the operating limits imposed on the recirculation pumps by cavitation, pump loads, bearing design flow starvation, and pump speed.

4.4.3.3   Power-Flow Operating Map

4.4.3.3.1   Limits for Normal Operation

A boiling water reactor must operate with certain restrictions because of pump net positive suction head (NPSH), overall plant control characteristics, core thermal power limits, etc. The power-flow map for the power range of operation is shown in Figure 4.4-5. The power-flow map is comprised of lines delineating core thermal power and total core flow limits (e.g., MEOD Upper Boundary Flow Control Line) and lines representative of typical reactor operating states for various plant conditions (e.g. Natural Circulation Line). The nuclear system equipment, nuclear instrumentation, and the reactor protection system, in conjunction with operating procedures, maintain operations within the core thermal power and total core flow limits established by this map for normal operating conditions. A description of this map is as follows:

Natural Circulation Line: This line (Line A) represents typical operating states of the reactor for the normal control rod withdrawal sequence in the absence of recirculation pump operation.

It is based on operating data collected during startup testing and may not reflect current conditions which affect observed reactor state. Analyses performed for low-flow or natural circulation

conditions typically use a bounding minimum core flow value. Therefore this line does not represent an operational or design bases limit on reactor operation.

Maximum Extended Load Line Limit Analysis Plus (MELLLA+) Boundary Area: This area expands the Region IV operating domain and is designed to be used in two recirculation loop operation. The results are a minimum core flow at 100% current licensed thermal power (4408 MWt). Neither single loop operation (SLO) nor operation with feedwater heaters out-of-service (FWHOOS) is allowed in this operating area (Reference 66).

MEOD Upper Boundary Flow Control Line: This line passes through 100 percent power at approximately 93 percent flow. The operating state for the reactor follows this line (or similar ones) during recirculation flow changes with a fixed control rod pattern. The line is based on a constant xenon concentration at rated power and 92.8 percent flow.

Constant Position Lines for Flow Control Valve: These lines (e.g. Lines B and C) represent the typical change in flow associated with power changes while maintaining flow-control valves at a constant position.

Cavitation Protection Line: This line results from the recirculation pump, flow control valve, and jet pump NPSH requirements and defines the minimum core thermal power allowed as a function of total core flow during normal reactor operation.

Maximum Core Flow Line: This line represents the maximum core flow allowed (105 percent) during normal reactor operation.

4.4.3.3.2   Regions of the Power Flow Map

Region I This region defines the system operational capability with the recirculation pumps and motors being driven by the low frequency motor-generator set at 25 percent speed. Flow is controlled by the flow control valve and power changes during normal startup and shutdown will be in this region. The normal operating procedure is to start up along curve B - FCV wide open at 25 percent speed. This region is bounded by Lines A and B.

Region II This region shows the area of changeover from the 25 percent pump speed regime to the 100 percent pump speed operating regime. This region is bounded by Lines B and C.

Region III This is the low power area of the operating map where

cavitation can be expected in the recirculation pumps, jet pumps, or flow control valves. Operation within this region is precluded by system interlocks which trip the main motor from the 100 percent speed power source to the 25 percent speed power source. This region is bounded by Line B and the Cavitation Protection Line.

Region IV This represents the normal operating zone of the map where power changes can be made by either control rod movement or by core flow changes through use of the flow control valve. This region also comprises the MELLLA+ boundary area. This region is bounded below by Line C and the Cavitation Protection Line.

4.4.3.3.3   Design Features for Power-Flow Control

The following limits and design features are employed to maintain power-flow conditions to the required values shown in Figure 4.4-5.

a.   Minimum power limits flows. To prevent cavitation in the recirculation pump, jet pumps and flow control valves, the recirculation system is provided with an interlock to trip off the 60 Hz power source and close the 15 Hz power source if the difference between steam line temperature and recirculation pump inlet temperature is less than a preset value (typically 8°F). This differential temperature is measured using high accuracy RTDs with a sensing error of less than 0.2°F at the two standard deviation (2) confidence level. This action is initiated electronically through a 15 second time delay.

Minimum power limit. During low power the temperature differential interlock may not provide sufficient cavitation protection to the flow control valves. Therefore, the system is provided with an interlock to trip off the 60 Hz power source and close the 15 Hz power source if the feedwater flow falls below a preset level. The feedwater flow rate is measured by existing process control instruments. The speed change action is initiated electronically through a 15 second time delay.

b.   Pump Bearing Limit. For pumps as large as the recirculation pumps, practical limits of pump bearing design require that minimum pump flow be limited to 20 percent of rated. To assure this minimum flow, the system is designed so that the minimum flow control valve position will allow this rate of flow.

c.   <u>Valve Position</u>. To prevent structural or cavitation damage to the recirculation pump due to pump suction flow starvation, the system is provided with an interlock to prevent starting the pumps, or to trip the pumps if the suction or discharge block valves are at less than 90 percent open position. This circuit is activated by a position limit switch and is active before the pump is started.

4.4.3.3.3.1   Flow Control

The principal modes of normal operation with valve flow control low frequency motor generator set are summarized as follows. The recirculation pumps are started on the 100 percent speed power source in order to unseat the pump bearings. Suction and discharge block valves are full open and the flow control valve is in the minimum position. When the pump is at full speed, the main power source is tripped and the pump allowed to coast down to 25 percent speed where the low frequency motor generator set will power the pump and motor. The flow control valve is then opened to the maximum position at which point reactor heatup and pressurization can commence. When operating pressure has been established, reactor power can be increased. This power-flow increase will follow a flow control valve constant position line within Region I of the flow control map shown in Figure 4.4-5.

When reactor power is greater than approximately 30 percent of rated, the low feedwater flow interlock is cleared and the main recirculation pumps can be switched to the 60 Hz power source. The flow control valve is closed to the minimum position before the speed change to prevent large increases in core power and a potential flux scram. An FCV position permissive switch is located on the valve to prevent speed change without closure first. Following speed change, the system is brought to the desired power-flow level within the normal operating area of the map (Region IV) by opening the flow control valves and by withdrawing control rods.

Control rod withdrawal with constant flow control valve position will result in power-flow changes along lines of constant C_V (constant position). Flow control valve movement with constant control rod position will result in power-flow changes along, or nearly parallel to, the rated flow control line.

4.4.3.4   Temperature-Power Operating Map (PWR)

Not applicable.

4.4.3.5   Deleted

4.4.3.6   Natural Circulation of Reactor Coolant

[HISTORICAL INFORMATION] [A Grand Gulf analysis indicates that
the absolute minimum water level for natural circulation between
the downcomer and the core region is the elevation of the jet pump
suction inlet, which is 8.34 feet above the elevation of the
bottom of the active fuel (BAF) for the GGNS vessel and about 21
feet below normal water level. An analysis of small-break
accidents (SBA) with all systems operable was provided to the NRC
in NEDO 24708A, Revision 1, December 1980. As can be seen from
that analysis, the water level both inside and outside the core
shroud did not fall below the top of the active fuel (TAF). It is
assumed, therefore, that for an SBA, sufficient inventory is
conservatively maintained such that the water level is maintained
$\geq$8.34 feet above BAF or at the level of the jet pump suction. For
water levels higher than the jet pump suction inlet, naturally
induced flow will be maintained by the density difference between
the downcomer region and the core, provided such density
difference head is sufficient to balance the irreversible losses
in the loop. The minimum required water level can thus be higher
than the jet pump inlet and will depend on the pressure in the RPV
and decay heat. The latter is a function of time after scram. This
level is determined for chosen RPV conditions by balancing the
hydrostatic driving head between the downcomer and the core
against the pressure drop for vanishing flow; thus, different RPV
levels were considered with decay heat generation spanning a time
period up to several days after shutdown. The minimum required
downcomer water levels in order to provide natural circulation
through the core are summarized below:

Minimum Downcomer Water Level (Feet above BAF) for RPV Internal
Natural Circulation

Time from Scram	Decay Heat[*] (% rated core power)	RPV Pressure (PSIA)		
		1035	300	15
20 seconds	4.3	13	9	8.34[**]
4 hours	0.86	23	16	8.34**
7 days	0.086	33	24	12.0

Minimum Downcomer Water Level (Feet above BAF) for RPV Internal
Natural Circulation (Continued)

	Decay Heat[*]	RPV Pressure (PSIA)		
Time from Scram	(% rated core power)	1035	300	15

_____

   [*] ANS Standard 5.1, September 1978 revision
   [**]Elevation on jet pump suction inlet

It should be noted that for a decay heat level less than 0.1 percent at a system pressure of 1035 psia, the required level (33 feet)[1] is well above the normal operating water level (29.5 feet)[1]. However, it is unlikely that such a high system pressure will exist 7 days from scramming the control rods, and the calculation is intended as a reference only.

The conservative levels cited in the preceding table were used to calculate the core flow due to natural circulation. Since the above levels are minimums, it should be noted that the flow rates would be the lowest flow achieved.

It should also be noted that the core will remain covered when the downcomer water level is at its minimum allowed for the RPV internal natural circulation; i.e., the two-phase swollen water level will be above the TAF. In general, the BWR natural circulation will have two-phase flow in the core region when downcomer water level is below normal operating level, as indicated in the above table. Due to the high void fraction at core exit, especially when RPV pressure is low (void fraction approximately 70 percent), the required downcomer level can be much lower than the level inside the shroud.

If plant conditions warranted the use of RHR system operation in the shutdown cooling mode, the downcomer water would be subcooled. The effects of shutdown cooling flow on flow created by natural circulation were considered in the Grand Gulf analysis. This analysis indicates that natural circulation will continue to function as the reactor core is cooled.

An additional Grand Gulf specific analysis was performed to further demonstrate the natural circulation flow rates. As presented in the letter dated October 23, 1981 (AECM-81/410),

_____

   [1] Reference level is bottom of active fuel.

core flow calculations were performed at a reactor pressure of 15 psia and 1 percent decay heat rate (2.3 hours after scram). The results are as follows:

Reactor Coolant Downcomer Temperature (F)	Natural Circulation Flow % of Nominal Core Flow
200	1.9
190	1.3
180	1.1
160	0.8
140	0.6
120	0.5

The above flow rates are conservatively based on the minimum water level necessary to afford natural circulation in the GGNS reactor vessel.]

4.4.3.7   Thermal and Hydraulic Characteristics Summary Table

[HISTORICAL INFORMATION] [The thermal-hydraulic characteristics are provided in Table 4.4-1 for the initial core and in figures and tables of Sections 5.1 and 5.4 for other portions of the reactor coolant system. The Grand Gulf core is a 251-800 design. Data from other reactor designs are provided for comparison.]

4.4.4   Evaluation

The design basis employed for the thermal and hydraulic characteristics incorporated in the core design, in conjunction with the plant equipment characteristics, nuclear instrumentation, and the reactor protection system, is to require that no fuel damage occur during normal operation or during abnormal operational transients. Demonstration that the applicable thermal-hydraulic limits are not exceeded is given by analyses.

4.4.4.1   Critical Power

Approved critical power correlations are utilized in thermal-hydraulic evaluations for the initial and current reload core. These correlations are discussed in subsection 4.4.2.2.1.

4.4.4.2   Core Hydraulics

Core hydraulic models and correlations are discussed in subsections 4.4.2.6, 4.4.2.7, and 4.4.4.5.

4.4.4.3   Influence of Power Distributions

The influence of power distributions on the thermal-hydraulic design is discussed in Reference 1, Appendix V for the initial core.

4.4.4.4   Core Thermal Response

The thermal response of the core for accidents and expected transient conditions is discussed in Chapter 15, Accident Analyses.

4.4.4.5   Analytical Methods

The analytical methods, thermodynamic data, and hydrodynamic data used in determining the thermal and hydraulic characteristics of the core are similar to those used throughout the nuclear power industry.

Core thermal-hydraulic analyses are performed with the aid of a digital computer program. This program models the reactor core through a hydraulic description of orifices, lower tie plates, fuel rods, fuel rod spacers, upper tie plates, fuel channel, and the core bypass flow paths.

4.4.4.5.1   Reactor Model

The reactor model includes a hydraulic representation of the orifice, lower tie plate, fuel rod spacers, upper tie plate, fuel channel, fuel rods, water rods, and fuel rod spacers.

The code can handle a number of fuel channel types and bypass flow paths. Usually, there is one fuel assembly representing each of the "hot" channel types. The average channel types make up the balance of the core.

The computer program iterates on flow through each flow path (fuel assemblies and bypass paths) until the total differential pressure (plenum to plenum) across each path is equal, and the sum of the flows through each path equals the total core flow.

[HISTORICAL INFORMATION] [For the initial core, orificing is selected to optimize the core flow distribution between orifice regions as discussed in subsection 4.4.2.5. The core design pressure is determined from the required turbine throttle pressure, the steam line pressure drop, steam dryer pressure drop, and the steam separator pressure drop. The core inlet enthalpy is determined from the reactor and turbine heat balances. The required core flow is then determined by applying the procedures of this section and specifications such that the thermal limits of Reference 1 are satisfied. The results of applying these methods and specifications are:

  a.   Flow for each bundle type

  b.   Flow for each bypass path

  c.   Core pressure drop

  d.   Fluid property axial distribution for each bundle type

  e.   CPR calculations for each bundle type]

For reload cores, the appropriate orificing, core flow, and system pressure drops are used as model input The same type of calculations that were used for the initial core are done to calculate the parameters stated in a-e above.

4.4.4.5.2   System Flow Balances

The basic assumption used by the code in performing the hydraulic analysis is that the flow entering the core will divide itself between the fuel bundles and the bypass flow paths such that each assembly and bypass flow path experience the same pressure drop. The bypass flow paths considered are described in Table 4.4-7 and shown in Figure 4.4-1. Due to the large flow area, the pressure drop in the bypass region above the core plate is essentially all elevation head. Thus, the sum of the core plate differential pressure and the bypass region elevation head is equal to the core differential pressure in subsection 4.4.2.6.

The total core flow less the control rod cooling flow enters the lower plenum through the jet pumps A fraction of this passes through the various bypass paths. The remainder passes through the orifice in the fuel support (experiencing a pressure loss) where more flow is lost through the fit-up between the fuel support and the lower tie plate and also through the lower tie

plate holes into the bypass region. The majority of the flow continues through the lower tie plate (experiencing a pressure loss) where some flow is lost through the flow path defined by the fuel channel and lower tie plate, and restricted by the finger springs, into the bypass region.

Full-scale tests have been performed to establish the flow coefficients for the major flow paths (Ref. 12). The results of these tests were used in support of the flow coefficients used in the initial core design. These tests simulate actual plant configurations which have several parallel flow paths and, therefore, the flow coefficients for the individual paths could not be separated. However, analytical models of the individual flow paths were developed as an independent check of the tests. he models were derived for actual BWR design dimensions and considered the effects of dimensional variations. These models predicted the test results when the "as-built" dimensions were applied. When using these models for hydraulic design calculations, nominal drawing dimensions are used. This is done to yield the most accurate prediction of the expected bypass flow. With the large number of components in a typical BWR core, deviations from the nominal dimensions will tend to statistically cancel resulting in a total bypass flow best represented by that calculated using nominal dimensions.

The balance of the flow enters the fuel bundle from the lower tie plate and passes through the fuel rod channel spaces. A small portion of the in-channel flow enters the non-fueled rods through orifice holes in each rod just above the lower tie plate. This flow, normally referred to as the water rod flow, remixes with the active coolant channel flow below the upper tie plate. The water rod flow is typically, a few percent of the fuel bundle flow.

4.4.4.5.3   System Heat Balances

Within the fuel assembly, heat balances on the active coolant are performed nodally. Fluid properties are expressed as the bundle average at the particular node of interest. In evaluating fluid properties, a constant pressure model is used.

The core power is divided into two parts: an active coolant power and a bypass flow power. The bypass flow is heated by neutron-slowing down and gamma heating in the water and by heat transfer through the channel walls. Heat is also transferred to the bypass flow from structures and control elements which are themselves

heated by gamma absorption and by (n, a) reaction in the control material. The fraction of total reactor power deposited in the bypass region is approximately 2 percent. A similar phenomena occurs with the fuel bundle to the active coolant and the water rod flows. The net effect is that approximately 96 percent of the core power is conducted through the fuel cladding and appears as heat flux.

In design analyses, the power is allocated to the individual fuel bundles using a relative power factor. The power distribution along the length of the fuel bundle is specified with axial power factors which distribute the bundle's power among the axial nodes. A nodal local peaking factor is used to establish the peak heat flux at each nodal location.

The relative (radial) and axial power distributions when used with the bundle flow determine the axial coolant property distribution resulting in sufficient information to calculate the pressure drop components within each fuel assembly type. Once the equal pressure drop criterion has been satisfied, the critical bundle power is determined by an iterative process for each fuel type.

4.4.4.6   Thermal-hydraulic Stability Analysis

4.4.4.6.1   Original Analysis

This section describes the evaluation of BWR thermal-hydraulic stability for the initial plant design and subsequent reload core and fuel designs. This evaluation is supplanted by implementation of the long-term core stability solution Option III described in Section 4.4.4.6.2.

4.4.4.6.1.1 Introduction

[HISTORICAL INFORMATION] [There are many definitions of stability, but for feedback processes and control systems it can be defined as follows: A system is stable if, following a disturbance, the transient settles to a steady, noncyclic state.

A system may also be acceptably safe even if oscillatory, provided that any limit cycle of the oscillations is less than a prescribed magnitude. Instability then, is either a continual departure from a final steady-state value or a greater-than-prescribed limit cycle about the final steady-state value.

The mechanism for instability can be explained in terms of frequency response. Consider a sinusoidal input to a feedback control system which for the moment has the feedback disconnected. If there were no time lags or delays between input and output, the output would be in phase with the input. Connecting the output so as to subtract from the input (negative, feedback or 180 degrees out-of-phase connection) would result in stable closed loop operation. However, natural laws can cause phase shift between output and input and should the phase shift reach 180 degrees, the feedback signal would be reinforcing the input signal rather than subtracting from it. If the feedback signal were equal to or larger than the input signal (loop gain equal to one or greater), the input signal could be disconnected and the system would continue to oscillate. If the feedback signal were less than the input signal (loop gains less than one), the oscillations would die out.

It is possible for an unstable process to be stabilized by adding a control system. In general, however, it is preferable that a process with inherent feedback be designed to be stable by itself before it is combined with other processes and control systems. The design of the BWR is based on this premise, that individual system components are stable.]

4.4.4.6.1.2   Description

[HISTORICAL INFORMATION] [Three types of stability considered in the design of boiling water reactors are: (1) reactor core (reactivity) stability, (2) channel hydrodynamic stability, and (3) total system stability. Reactivity feedback instability of the reactor core could drive the reactor into power oscillations. Hydrodynamic channel instability could impede heat transfer to the moderator and drive the reactor into power oscillations. The total system stability considers control system dynamics combined with basic process dynamics. A stable system is analytically demonstrated if no inherent limit cycle or divergent oscillation develops within the system as a result of calculated step disturbances of any critical variable, such as steam flow, pressure, neutron flux, and recirculation flow.

The criteria to be considered are stated in terms of two compatible parameters. First is the decay ratio x_2/x designed as the ratio of the magnitude of the second overshoot to the first overshoot resulting from a step perturbation. A plot of the decay ratio is a graphic representation of the physical responsiveness

of the system, which is readily evaluated in a time-domain analysis. Second is the damping coefficient, δ_n, the definition of which corresponds to the pole pair closest to the δ_n axis in the s-plane for the system closed loop transfer function. This parameter also applies to the frequency-domain interpretation. The damping coefficient is related to the decay ratio as shown in Figure 4.4-2.]

4.4.4.6.1.3   Stability Criteria

[HISTORICAL INFORMATION] [The assurance that the total plant is stable and, therefore, has significant safety margin shall be demonstrated analytically when the decay ratio, x_2/x is less than 1.0 or, equivalently, when the damping coefficient, δ_n, is greater than zero for each type of stability discussed. Special attention is given to differentiate between inherent system limit cycles and small, acceptable limit cycles that are always present, even in the most stable reactors. The latter are caused by physical nonlinearities (deadband, stiction, etc.) in real control systems and are not representative of inherent hydrodynamic or reactivity instabilities in the reactor. The ultimate performance limit criteria for the three types of dynamic performance are summarized below in terms of decay ratio and damping coefficient:

Channel hydrodynamic stability	$x_2/x < 1$, $\delta_n > 0$
Reactor core (reactivity) stability	$x_2/x < 1$, $\delta_n > 0$
Total system stability	$x_2/x < 1$, $\delta_n > 0$

These criteria shall be satisfied for all attainable conditions of the reactor that may be encountered in the course of plant operation. For stability purposes the most severe power/flow conditions to which these criteria can be applied correspond to natural circulation flow at a power corresponding to the rod block power limit condition.

Although the ultimate performance limit criteria assure absolute reactor stability, an operational design guide based on acceptable performance standards of the control industry for most process systems (Ref. 8) is observed. The operational design guide analysis for dynamic transient performance was conducted for the total system, the reactor core, and the channel hydrodynamics in support of the initial core design.

The assurance that the plant has the desirable operational dynamic characteristics within the limits specified for the decay ratio, x_2/x, or the damping coefficient, δ_n, was demonstrated analytically for the initial core as follows:

Channel hydrodynamic performance $\qquad$ $x_2/x \leq 0.5$, $\delta_n \geq 0.11$

Reactor core (reactivity) performance $\qquad$ $x_2/x \leq 0.25$, $\delta_n \geq 0.22$

Total system performance $\qquad$ $x_2/x \leq 0.25$, $\delta_n \geq 0.22$

These limits were satisfied for at least all expected power and flow conditions expected to be encountered during normal operation for the initial core. The most limiting condition expected corresponds to that attained starting from rated power and flow and reducing flow, potentially to natural circulation, with a corresponding power reduction. The power and flow condition at which the above limits are analytically attained was recognized as the operational boundary for normal control for the initial core.

The reload fuel is designed to be thermal-hydraulically and neutronically compatible with the fuel resident in the core. The reload fuel and core design ensures that the core is stable by demonstrating analytically that the stability margin is not changing significantly from cycle to cycle.]

4.4.4.6.1.4   Analysis Approach

[HISTORICAL INFORMATION] [The total system stability analysis evaluates the relative stability of the total system, from time responses generated by applying step changes to the input variables to the total system stability model. The observed time response of an output variable of a high order dynamic system represents a superposition of the system's several response modes. The relative intensity of each particular mode in the time response is determined by the zeros (the roots of the numerator) of the transfer function relating to a given output variable to a particular input. Therefore, in judging the relative stability of the system, the observer should separate the distinct modes in the time response and apply the relative stability criterion (0.25 decay ratio) to each modal response.

The approach used here, of disturbing one input variable and applying the relative stability criterion to the resulting system response is a good approximation to the modal separation. It is particularly applicable in calculating ultimate stability since, as a system tends toward instability a single oscillatory mode tends to dominate the observed time response (Ref. 9).

For the initial core, the channel hydrodynamic operation design guide limit given above ($x_2/x \leq 0.5$, $\delta_n \geq 0.11$) allows locally more responsive operation than is allowed for the complete core or the total system. This is justified for a stable channel by the fact that the response of an individual component can be less damped than the total system as long as total performance is uncompromised and local transients are not harmful. These can both be satisfied in the presence of a highly responsive, but stable, channel. Because of the short period of natural resonance relative to the slow response of heat transfer, the local channel transients will not be manifest as significant local heat flux transients.

For reload cores, technical specification restrictions associated with the operating domain are established to ensure core thermal-hydraulic stability. In addition, thermal-hydraulic analyses are done to demonstrate that the stability performance of the reload core is equivalent to the stability performance for previous cycle.]

4.4.4.6.1.5   Mathematical Model

[HISTORICAL INFORMATION] [For the initial core, the mathematical model representing the core examines the linearized reactivity response of a reactor system with density-dependent reactivity feedback caused by boiling. The core model, (Refs. 25-30), shown in block diagram form in Figure 4.4-3 solves the dynamic equations that represent the reactor core in the frequency domain.

The plant model considers the entire reactor system, neutronics, heat transfer, hydraulics, and the basic processes, as well as associated control systems such as the flow controller, pressure regulator, feedwater controller, etc. Although, the control systems may be stable when analyzed individually, final control system settings must be made in conjunction with the operating reactor so that the entire system is stable. The plant model yields results that are essentially equivalent to those achieved

with the core model and allows the addition of the controllers, which have adjustable features permitting the attainment of the desired performance.

The plant model solves the dynamic equations that present the BWR system in the time domain. The variables, such as steam flow and pressure, are represented as a function of time. The extensiveness of this model (Ref. 10) is shown in block diagram form in Figure 4.4-3. Many of the blocks are extensive systems in themselves.

For reload cores, the continued applicability of the technical specification restrictions associated with the operating domain that has been established to assure thermal-hydraulic stability is demonstrated.]

4.4.4.6.1.6   Benchmarks

[HISTORICAL INFORMATION] [A comparison of the analysis results with measurements shows the analytical methods to be an effective and useful design tool in its application to boiling water reactor core evaluation.]

4.4.4.6.1.7   Analytical Results

[HISTORICAL INFORMATION] [Using actual initial core design parameters, calculated responses of important nuclear system variables to step disturbances from control rod reactivity, pressure regulator set point, level controller set point, and turbine load set point were tested for rated power-flow conditions and at the nominal power corresponding to the lower end of the automatic power-flow control path. The analysis responses met the relative stability criterion for all test cases.

Based on the initial core analysis, it was concluded that for all normal operating points over the flow control range the decay ratio of the total system responses is less than 0.25, good dynamic performance is expected, and the ratio conforms with the operational design guide.

For reload cores, a confirmatory analysis is performed to demonstrate the continued applicability of the core stability Technical Specification. The analysis is based on comparison of core stability performance to previously analyzed cycles. A stability code is used to calculate the variations in decay ratio from cycle to cycle for expected operating conditions at representative state points near the stability exclusion region.

The stability exclusion region as defined in the Technical Specifications, has been demonstrated to be applicable to SPC 8x8, and 9x9-5, GE11, AREVA ATRIUM-10, and GE14 fueled cores.]

4.4.4.6.1.8   Deleted

4.4.4.6.2.   Option III Stability Solution

4.4.4.6.2.1   Introduction

The stability licensing basis for U.S. nuclear power plants is set forth in GDC-12. GDC-12 requires assurance that power oscillations which can result in conditions exceeding specified acceptable fuel design limits are either not possible or can be reliably and readily detected and suppressed. The occurrence of neutronic/thermal-hydraulic oscillations at a BWR was discussed in NRC Bulletin 88-07, Supplement 1. The bulletin also discussed the BWR Owners' Group efforts to address this issue through the development of generic long-term stability solutions which could be implemented at all plants. Subsequently, in response to NRC Generic Letter 94-02, GGNS implemented the BWR Owners' Group Enhanced Option I-A (E1A) stability solution as described in References 45 - 48. With the installation of the digital Power Range Neutron Monitoring System, GGNS replaced the E1A stability solution with Option III, which is described in detail References 45, 49, 50, and 56. The Option III is replaced by DSS-CD in the licensing basis and reload analysis. Option III remains functional and serves as defense-in-depth.

Approval of the Operating License Amendment 205 (Reference 65) allowed GGNS plant operation in the expanded Maximum Extended Load Line Limit Analysis Plus (MELLLA+) operating domain with the Detect and Suppress Solution - Confirmation Density (DSS-CD) long term reactor core thermal-hydraulic stability solution. DSS-CD evaluations are core reload dependent and are confirmed using a plant specific availability checklist for each reload cycle. In the event that the OPRM system is declared inoperable, Grand Gulf will operate under Backup Stability Protection (BSP) as required by the plant Technical Specifications and defined in the Core Operating Limits Report (COLR). Cycle specific setpoints are determined and documented in the Supplemental Reload Licensing Report (SRLR), Section 15 (Reference 67). This solution integrates licensing and defense-in-depth features into a progressive, multi-regional protection scheme which provides assurance of substantial protection against all contemplated core instability scenarios.

4.4.4.6.2.2   Option III solution Description

Grand Gulf has implemented the DSS-CD solution consistent with the MELLLA+ safety evaluations used to support operation at the current licensed thermal power of 4408 MWt with core flow as low as 80% of rated flow (Reference 66). Susceptibility to channel hydraulic instability may increase for the higher power/flow ratio associated with MELLLA+ operations following a recirculation pump trip event from rated power.

The Detect and Suppress Solution — Confirmation Density (DSS-CD) stability solution has been shown to provide an early trip signal upon instability inception prior to any significant oscillation amplitude growth and Minimum Critical Power Ratio (MCPR) degradation for both core wide and regional mode oscillations.

The DSS-CD stability solution is based on the evaluations contained in NEDC-33075P-A, Revision 6, Licensing Topical Report General Electric Boiling Water Reactor Detect and Suppress Solution - Confirmation Density. This report provides the licensing basis and methodology used to demonstrate the adequacy of the DSS-CD solution to reliably detect and suppress anticipated stability related power oscillations. The MELLLA+ Thermal Hydraulic Stability task report (Reference 68) includes the generic and plant specific evaluations of the thermal hydraulic stability for Grand Gulf.

The DSS-CD hardware design is unchanged from the Option III solution. The firmware/software is modified relative to Option III to reflect the specific DSS-CD stability detection methods. The DSS-CD design provides automatic detection and suppression of reactor instability events to minimize reliance on the operator to suppress instability events. However, alarms are provided to alert the operator of an increase in the number of confirmed period counts so actions can be taken to avoid a reactor scram.

The basic input unit of the DSS-CD system is the oscillation power range monitor (OPRM) cell. The OPRM cell consists of inputs from closely spaced local power range monitor (LPRM) detectors. A minimum of 2 operable LPRMs are required for an OPRM cell to be considered operable. The signals from the individual LPRM detectors in a cell are averaged to produce the OPRM cell signal. For the DSS-CD solution the maximum number of LPRM detectors per OPRM cell is limited to four. Each of the four independent OPRM channels consists of many OPRM cells distributed throughout the core so that each channel provides monitoring of the entire core.

The DSS-CD solution includes four separate algorithms for

detecting stability related oscillations: Confirmation Density Algorithm (CDA), Period Based Detection Algorithm (PBDA), Amplitude Based Algorithm (ABA), and Growth Rate Algorithm (GRA). The PBDA, ABA, and GRA detection algorithms provide the protection basis for Option III. They are retained in DSS-CD as defense-in-depth algorithms and are not part of the licensing basis for the DSS-CD solution, which is accomplished solely by the CDA. The CDA is designed to recognize an instability and initiate control rod insertion before the power oscillations increase much above the noise level. DSS-CD provides protection against violation of the Safety Limit Minimum Critical Power Ratio for anticipated oscillations.

The CDA capability of early detection and suppression of instability events is achieved by relying on the successive confirmation period element of PBDA. The CDA employs a low amplitude OPRM signal discriminator to minimize unnecessary spurious reactor scrams from neutron flux oscillations at or close to the OPRM signal noise level. The CDA identifies a confirmation density (CD), which is the fraction of operable OPRM cells in an OPRM channel that reach a target successive oscillation period confirmation count. When the CD exceeds a preset number of OPRM cells and any of the confirming OPRM cell signals reaches or exceeds the amplitude discriminator setpoint (SAD), an OPRM channel trip signal is generated by the CDA.

A reactor trip is generated when multiple channel trips are generated, consistent with the reactor protection system (RPS) logic design. The bi-stable characteristic of the CD, where the value remains at zero except at the instability threshold, when it rapidly transitions to unity, provides excellent discrimination between stable and unstable operation. The instability suppression by the DSS-CD for high growth instability events occurs within a few full oscillation periods from the time the instability is sensed by the PBDA. Because the solution does not rely on oscillation growth to a specified high amplitude setpoint, suppression occurs within a short time from oscillation inception or close to the low amplitude OPRM signal discriminator and significant margin to the SLMCPR is provided.

The NRC staff has reviewed the design concept and found it acceptable, because the DSS-CD solution complies with Criteria 10 and 12 of 10 CFR Part 50, Appendix A, and the DSS-CD solution enhances overall plant safety by providing reliable, automatic oscillation detection and suppression function while avoiding unnecessary scrams.

Backup Stability Protection (BSP) may be used when the OPRM is

temporarily inoperable. The SRLR describes two BSP options that are based on selected elements from three distinct constituents. The three constituents are: BSP Manual Regions, BSP Boundary, and Automated BSP (ABSP) setpoints. These regions are calculated on a cycle specific basis and are included in the SRLR (Reference 67).

4.4.5 Testing and Verification

[HISTORICAL INFORMATION] [The testing and verification techniques to be used to assure that the planned thermal and hydraulic design characteristics of the core have been provided and will remain within required limits throughout core lifetime are discussed in Chapter 14, Initial Test Program. A summary is as follows:

a. Pre-operational Testing

   Tests are performed during the pre-operational test program to confirm that construction is complete and that all process and safety equipment is operational. Baseline data are taken to assist in the evaluation of subsequent tests. Heat balance instrumentation, measuring jet pump flow and core temperatures, is calibrated and set points verified.

b. Initial Startup

   Hot functional tests are conducted with the reactor between 5 and 10 percent power. Core performance is monitored continuously to assure that the reactor is operating within allowable limits (e.g., peaking factors, linear heat generation rate, etc.) and is evaluated periodically to verify the core expected and actual performance margins.]

4.4.6 Instrumentation Requirements

The reactor vessel instrumentation monitors the key reactor vessel operating parameters during planned operations. This ensures sufficient control of the parameters. The following reactor vessel sensors are discussed in subsections 7.7.1.1 and 7.6.1.5.

a. Reactor Vessel Temperature

b. Reactor Vessel Water Level

c. Reactor Vessel Coolant Flow Rates and Differential

Pressures

d.   Reactor Vessel Internal Pressure

e.   Nuclear In-core Monitoring System

4.4.6.1   Loose Parts Monitoring

The Loose Parts Monitoring System (LPMS) was designed to provide a mechanism for early detection and warning of loose metallic parts within the primary NSSS system, specifically within the reactor pressure vessel and the external recirculation system loops. The system was engineered and supplied by Babcock and Wilcox (B&W).

4.4.6.1.1   Power Generation Design Bases

The LPMS was designed to provide early detection and warning of loose parts in the primary system to avoid or mitigate safety-related damage to or malfunctions of primary system components.

Additional primary design considerations provide for the inclusion of electronic features to enhance the analysis function when action is required to investigate potential loose parts.

4.4.6.1.2   System Description

Sensors are classified as "active" channels and are setup for on-line monitoring, while other sensors are classified as "passive" channels and are used as spares in the case of failures or as additional diagnostic tools to assist in the confirmation of the presence and/or location of a loose metallic part. The sensors are each rated for high temperature, high radiation environmental conditions and are well suited for the operating BWR drywell environment. Each sensor is attached to a 10/32-inch, ½-inch-long stud which is inserted, to its full length into a mounting yoke that is mechanically attached to the sensor mounting location structure. Sensor and impact locations are shown in Figure 4.4-10.

The output of the accelerometers is transmitted via coaxial hard-line cables to remote charge preamplifiers (line drivers) located within several feet of the sensors. The preamplifiers are used as impedance converters to change the high output impedance of the accelerometers to a low impedance output needed for reliable signal transmission and for reduction of cable signal-to-noise ratios. The output of the preamp, are routed, via twisted shielded pair cable through the containment electrical penetration to the Loose Parts Monitoring Cabinet located in the Control Building. The active channel field cables are terminated within the cabinets in the individual loose parts detector module. The loose part detector modules provide the signal conditioning, amplification, and filtering functions for the required sensor channels. The modules contain two adjustable active filters, a high pass and a low pass filter which allow band limiting of the signal in order to maximize the frequencies typical of loose part impacts. One of the most important features of the loose part detector modules is the Automatic Gain Control circuitry. This circuitry normalizes the steady state background level while

allowing sudden transient signals indicative of a loose part impact to pass through to a comparator-latch circuit which initiates the channel alarm signal.

The loose part detector modules also contain metering for direct visual observation of the channel output in terms of g's RMS, and high and low level alarm indicator lamps.

The output of the loose part detector modules is available to be monitored by the Dual Channel Audio Monitor, which is a two channel speaker system with a variable volume control. The audio monitor has been included with the system because the accelerometer acts as a very sensitive microphone in the acoustic range.

4.4.6.1.3   System Operation

The LPMS may be set to alarm locally for detected noises having the characteristics of metal-to-metal impacts.

A loose part is considered to be a metallic object that can be physically moved by fluid flow. In general, loose parts are classified into two generic categories, captive and free. Captive loose parts are the result of an unanticipated mechanical failure which causes a metallic object to impact its surrounding structures without being physically severed from its original structure. Free loose parts, on the other hand, are free to migrate from one physical location to another. This movement of the metallic object is caused by its suspension in the surrounding primary fluid. The primary concern of loose parts entrapped in a high-velocity fluid system is the potential severe mechanical damage that may result if the metallic object is allowed to impact structures.

Metal-to-metal impacts resulting from loose parts excite the preferential ringing modes of the NSSS components. The modes are typically between 1 and 10 kHz and are easily detected by externally mounted accelerometers.

After installation of a strategically located accelerometer array, as identified above, the overall and individual channel characteristics of the accelerometer system will be determined before operation monitoring.

The LPMS includes provisions to allow external analysis and diagnostic data acquisition capabilities, such as:

a. Deleted

b. Data gathering - transient or unusual plant conditions

c. Limitations and location of the problem, captive or loose part

d. Diagnostic phase which includes location, energy content, and damage assessment

Once operations of the NSSS have commenced, each accelerometer channel will exhibit its own particular and unique frequency spectrum. This frequency signature, or normal background, results from such internal sources as primary flow turbulence, recirculation pump vibrations, feedwater and steam flow turbulence, structural responses of NSSS components and secondary plant equipment, and a host of other localized noise sources. In addition, external sources, such as airborne noises from fans and other equipment, contribute to the overall background.

To achieve more reliable detection of unusual noises indicative of metal-to-metal impact, a spectral comparison of the measured local metal-to-metal acoustical resonances and the normal background will be performed. Based on the spectral comparison, the broad-band signal is band-limited to the portion of the spectra that maximizes the signal-to-noise ratio. This band-limited signal, which in most cases eliminates or minimizes the contributions of normal acoustical background, is then monitored for sudden transients indicative of metal-to-metal impacts. A transient must exceed a threshold which is a function of the plant background noise level before it can activate the alarm circuitry. The background level is derived in an RMS converter circuit having a time constant long enough to be largely unaffected by rapid transients and therefore always proportional to the background level. Normal plant transients cause a shift in the background level and will not activate the alarm circuitry, thereby affecting a reduction in spurious alarms.

Once an unusual noise characteristic of a metal-to-metal impact is detected by the loose parts monitor, it is essential to determine the source or cause of the alarm. The first and simplest form of diagnosis is audio interpretation, but this method is very

subjective and can result in a number of erroneous conclusions to the uneducated listener. Background noises, such as throttled steam and flow turbulence, can be easily distinguished. Metal-to-metal impacts can also be readily recognized because of their characteristic spectral content. In addition, the metal-to-metal impacts caused by a bona fide loose part will occur with a random repetitious rate. Further insight can be gained by using a real-time spectrum analyzer, observing the transient spectra of the impact, and comparing the transient spectrum to known metallic impact and background spectra.

Storage of Data for Comparison - Significant departure from the baseline tape may indicate the presence of an unusual noise. This shall ascertain whether the departure is due to electrical noises which are found to be periodic in nature and have individual wave forms or mechanical noises which are a result of the normal plant operation.

Equipment environmental design is provided in Table 4.4-10.

4.4.6.1.4   Safety Evaluation

The LPMS is to be used for information purposes only by the operator. The operator does not rely on the information provided by the LPMS for the performance of any safety-related action. In addition, the system will withstand, without loss of function, the normal operating radiation, vibration, temperature, and humidity environment.

4.4.6.1.5   Deleted

4.4.6.1.6   Deleted

4.4.7   Deleted

4.4.8   References

1.   General Electric Thermal Analysis Basis (GETAB): Data, Correlation, and Design Application, General Electric Company, January 1977 (NEDO-10958A)

2.   Core Flow Distribution in a Modern Boiling Water Reactor as Measured in Monticello, January 1971 (NEDO-10299)

3.   Martinelli, R. C., and Nelson, D. E., "Prediction of Pressure Drops During Forced Convection Boiling of Water," ASME Trans., 70, PP 695-702, 1948

4.   Baroczy, C. J., "A Systematic Correlation for Two-Phase Pressure Drop," Heat Transfer Conference (Los Angeles), AICLE, Preprint No. 37, 1966

5.   Jens, W. H., and Lottes, P. A., Analysis of Heat Transfer, Burnout, Pressure Drop, and Density Data for High Pressure Water, USAEC Report 4627, 1972

6.   XN-NF-80-19, Volume 3, Revision 2, "Exxon Nuclear Methodology for Boiling Water Reactors, Thermex: Thermal Limits Methodology Summary Description."

7.   Lahey, R. T., and Moody, F. J., "The Thermal-Hydraulics of a Boiling Water Nuclear Reactor," ANS Monograph, 1977.

8.   Process Instruments and Controls Handbook, Considine, McGraw-Hill Book Co., 1957

9.   Zadeh and Desoer, Linear System Theory, McGraw-Hill Book Co., 1963

10. Analytical Methods of Plant Transient Evaluations for General Electric Boiling Water Reactor, General Electric Company, BWR Systems Department, February 1973, (NEDO-10802)

11. Zuber, N., and Findlay, J. A., "Average Volumetric Concentration in Two-Phase Flow Systems," Trans. ASME,

Journal of Heat Transfer, November 1965

12.   "Supplemental Information for Plant Modification to Eliminate Significant In-Core Vibration," NEDE-21156, Class III, January 1976

13.   Isbin, H. S., Rodriguez, H. A., Larson, H. C., and Pattie, B. D., "Void Fractions in Two-Phase Flow," A.I. Ch.E. Journal, Volume 5, No. 4, 427-432, December 1959

14.   Isbin, H. S., Sher, N. C., Eddy, K. C., "Void Fractions in Two-Phase Steam-Water Flow," A.I. Ch.E Journal, Volume 3, No. 1, 136-142, March 1957

15.   Marchaterre, J. F., "The Effect of Pressure on Boiling Density in Multiple Rectangular Channels," ANL-5522, February 1956

16.   Janssen, E., and Kervinen, J. A., "Two-Phase Pressure Drop in Straight Pipes and Channels; Water-Steam Mixtures at 600 to 1400 psia," GEAP-4616, May 1964

17.   Cook, W. H., "Boiling Density in Vertical Rectangular Multichannel Section with Natural Circulation,"ANL-5621, November 1956

18.   Mauer, G. W., "A Method of Predicting Steady State Boiling Vapor Fractions in Reactor Coolant Channels,"WAPD-BT-19, June 1960

19.   Rouhani, S. Z., "Void Measurements in the Region of Subcooled and Low Quality Boiling," Symposium on Two-Phase Flow, University of Exeter, Devon, England, June 1965

20.   Firstenberg, A., and Neal, L. G., "Kinetic Studies of Heterogeneous Water Reactors," STL 372-38, April 15, 1966

21.   Ferrel, J. K., "A Study of Convection Boiling Inside Channels," North Carolina State University, Raleigh, N.C., September 30, 1964

22.   Rouhani, S. Z., "Void Measurements in the Region of Subcooled and Low Quality Boiling," Part II, AE-RTL-788, Akticbolaget, Atomenergi, Studsvik, Sweden, April 1966

23.   Christensen, H., "Power-to-Void Transfer Functions," ANL-

6385, July 1961

24. Egen, R. A., Dingee, D. A., Chastain, J. W., "Vapor Formation and Behavior in Boiling Heat Transfer," BMI-1163, February 1957

25. Jones, A. B., "Hydrodynamic Stability of a Boiling Channel," KAPL-2170, October 2, 1961

26. Jones, A. B., "Hydrodynamic Stability of a Boiling Channel," Part 2, KAPL-2208, April 20, 1962

27. Jones, A. B., and Dight, D. G., "Hydrodynamic Stability of a Boiling Channel," Part 3, KAPL-2290, June 28, 1963

28. Jones, A. B., "Hydrodynamic Stability of a Boiling Channel," Part 4, KAPL-3070, August 18, 1964.

29. Jones, A. B., and Yarbrough, W. M., "Reactivity Stability of a Boiling Reactor," Part 1, KAPL-3072, September 14, 1964

30. Jones, A. B., "Reactivity Stability of a Boiling Reactor," Part 2, KAPL-3093, March 1, 1965

31. Elkins, R. B., "Fuel Rod Prepressurization Amendment 1," May 1978 (NEDO-23786-1)

32. Deleted

33. Deleted

34. Deleted

35. Basis for BWR/6 8 x 8 Fuel Thermal Analysis Application, June 1979 (NEDE-24196)

36. McBeth, R. V., Trenberth, R., and Wood, R. W., "An Investigation into the Effects of Crud Deposits on Surface Temperature, Dry-Out, and Pressure Drop, with Forced Convection Boiling of Water at 69 Bar in an Annular Test Section," AEEW-R-705, 1971

37. Green, S. J., LeTourneau, B. W., and Peterson, A. C., "Thermal and Hydraulic Effects of Crud Deposited on Electrically Heated Rod Bundles," WAPD-TM-918, September 1970

38. ANF-524(P)(A) Revision 2 and Supplements 1 and 2, "ANF Critical Power Methodology for Boiling Water Reactors," Advanced Nuclear Fuels Corporation, November 1990.

39. Ohkawa, K., and Lahey, R. T., "The Analysis of Proposed BWR Inlet Flow Blockage Experiments in PBF," NES-486, December 1978.

40. Deleted

41. Deleted

42. Deleted

43. General Electric Standard Application for Reactor Fuel, GESTAR II, NEDE-24011-P-A, Latest Approved Revision

44. GE Fuel Bundle Designs, July 1996, NEDE-31152 P

45. NEDO-32339-A, Revision 1, "Reactor Stability Long-Term Solution: Enhanced Option I-A," April 1998.

46. Deleted

47. Deleted

48. Deleted

49. NEDO-31960-A, "BWR Owners' Group Long-Term Stability Solutions Licensing Methodology," November 1995.

50. NEDO-31960-A, Supplement 1, "BWR Owners' Group Long-Term Stability Solutions Licensing Methodology," November 1995.

51. Deleted

52. Deleted

53. Deleted

54. Deleted

55. XN-NF-79-59(P)(A), "Methodology for Calculation of Pressure Drop in BWR Fuel Assemblies," Exxon Nuclear Company, November 1983.

56. NEDC-32410P-A, "Nuclear Measurement Analysis and Control

Power Range Neutron Monitor (NUMAC PRNM) Retrofit Plus Option III Stability Trip Function," Volumes 1 and 2, and Supplement 1, October 1995 and November 1997.

57. NEDO-32465-A, "Reactor Stability Detect and Suppress Solutions Licensing Basis Methodology for Reload Applications", Reactor August 1996.

58. GE Nuclear Energy Report OG-02-0119-260, "Backup Stability Protection (BSP) for Inoperable Option III Solution", July 17, 2002.

59. Deleted

60. BWR Owners' Group Topical Report NEDC 32975P-A, Revision 0, "Regulatory Relaxation for BWR Loose Parts Monitoring Systems", February 2001.

61. Deleted

62. Deleted

63. GE Nuclear Energy, "Methodology and Uncertainties for Safety Limit MCPR Evaluations," NEDC-32601P-A, August 1999.

64. GE Nuclear Energy, "Power Distribution Uncertainties for Safety Limit MCPR Evaluations," NEDC-32694P-A, August 1999.

65. Global Nuclear Fuel, "GEXL17 Correlation for GNF2 Fuel," NEDC-3329P-A, Revision 3, June 2009.

66. NRC letter to GGNS, "Grand Gulf Nuclear Station, Unit 1 – Issuance of Amendment Regarding Maximum Extended Load Line Limit Analysis Plus," August 31, 2015, GNRI-2015/00109.

67. EHC-NE-18-0022, Rev. 1, "Supplemental Reload Licensing Report for Grand Gulf Nuclear Station Reload 21 Cycle 22," May 2018.

68. GNS-NE-12-00026, Rev. 0, "GGNS MELLA+ Thermal Hydraulic Stability," August 2012.

**TABLE 4.4-1: [HISTORICAL INFORMATION] THERMAL AND HYDRAULIC
DESIGN CHARACTERISTICS OF THE REACTOR CORE (TYPICAL)**

General Operating Conditions	BWR/6 218-624	BWR/6 238-748	BWR/6 251-800
Reference design thermal output, Mwt	2894	3579	3833
Power level for engineered safety features, Mwt	3039	3758	3993
Steam flow rate, at 420°F final feedwater temperature millions lb/hr	12.451	15.396	16.492
Core coolant flow rate, millions lb/hr	84.5	104.0	112.5
Feedwater flow rate, millions lb/hr	12.420	15.358	16.637
System pressure, nominal in steam dome, psia	1040	1040	1040
System pressure, nominal core design, psia	1055	1055	1055
Coolant saturation temperature at core design pressure, °F	551.12	551.12	551.12
Average power density, kW/liter	52.41	54.07	54.145
Maximum Linear Heat Generation Rate kW/ft	13.4	13.4	13.4
Average Linear Heat Generation Rate kW/ft	5.80	5.80	5.935
Core total heat transfer area, ft²	61,151	73,303	78,398
Maximum heat flux, Btu/hr-sq ft	361,600	361,600	361,600

TABLE 4.4-1: [HISTORICAL INFORMATION] THERMAL AND HYDRAULIC DESIGN CHARACTERISTICS OF THE REACTOR CORE (TYPICAL)(Continued)

General Operating Conditions	BWR/6 218-624	BWR/6 238-748	BWR/6 251-800
Average heat flux, Btu/hr-sq ft	154,600	159,500	160,151
Core inlet enthalpy at 420°F FFWT, Btu/lb	527.8	527.7	527.9
Core inlet temperature, at 420°F FFWT, °F	533.0	532.6	533.10
Core maximum exit voids within assemblies,%	76.2	78.9	76.3
Core average void fraction, active coolant	0.411	0.440	0.412
Maximum fuel temperature, °F	3435	3435	3435
Active coolant flow area per assembly, in.^{2}	15.164	15.164	15.164
Core average inlet velocity, ft/sec	6.82	6.98	7.07
Maximum inlet velocity, ft/sec	7.9	8.54	8.57
Total core pressure drop, psi	24.46	26.04	25.87
Core support plate pressure drop, psi	20.04	21.62	21.45
Average orifice pressure drop Central region, psi	5.43	5.71	5.81
Peripheral region, psi	17.45	18.44	18.59
Maximum channel pressure loading, psi	13.66	14.99	14.65

TABLE 4.4-1A: DELETED

TABLE 4.4-2: [HISTORICAL INFORMATION] TYPICAL BWR 6 VOID DISTRIBUTION

Core Average Value = 0.438

Maximum Exit Value = 0.763

Active Fuel Length = 150 inches

	NODE	CORE AVERAGE (AVERAGE NODE VALUE)	MAXIMUM CHANNEL (END OF NODE VALUE)
Bottom	1	0.0	0.0
	2	0.002	0.027
	3	0.032	0.151
	4	0.103	0.281
	5	0.189	0.378
	6	0.267	0.449
	7	0.332	0.503
	8	0.383	0.545
	9	0.425	0.579
	10	0.460	0.607
	11	0.490	0.630
	12	0.515	0.651
	13	0.537	0.669
	14	0.556	0.684
	15	0.573	0.698
	16	0.588	0.711
	17	0.601	0.721
	18	0.614	0.731
	19	0.624	0.740
	20	0.632	0.747
	21	0.640	0.753
	22	0.647	0.758
	23	0.652	0.761
Top	24	0.654	0.763

TABLE 4.4-2A: [HISTORICAL INFORMATION] AXIAL POWER DISTRIBUTION |
USED TO GENERATE VOID AND QUALITY DISTRIBUTIONS - BWR/6

	NODE	AXIAL POWER FACTOR
Bottom of Core	1	0.35
	2	1.10
	3	1.12
	4	1.50
	5	1.48
	6	1.46
	7	1.41
	8	1.35
	9	1.29
	10	1.24
	11	1.19
	12	1.14
	13	1.10
	14	1.05
	15	1.01
	16	0.96
	17	0.91
	18	0.86
	19	0.78
	20	0.72
	21	0.63
	22	0.52
	23	0.37
Top of Core	24	0.16

TABLE 4.4-3: [HISTORICAL INFORMATION] TYPICAL BWR 6 FLOW QUALITY DISTRIBUTION

Core Average Value = 0.083

Maximum Exit Value = 0.273

Active Fuel Length = 150 inches

	NODE	CORE AVERAGE (AVERAGE NODE VALUE)	MAXIMUM CHANNEL (END OF NODE VALUE)
Bottom	1	0.0	0.0
	2	0.0	0.001
	3	0.001	0.007
	4	0.003	0.022
	5	0.012	0.040
	6	0.021	0.058
	7	0.032	0.076
	8	0.043	0.094
	9	0.054	0.110
	10	0.064	0.126
	11	0.074	0.142
	12	0.084	0.156
	13	0.094	0.171
	14	0.102	0.184
	15	0.111	0.197
	16	0.119	0.209
	17	0.126	0.221
	18	0.134	0.232
	19	0.141	0.242
	20	0.147	0.252
	21	0.153	0.260
	22	0.157	0.266
	23	0.161	0.271
Top	24	0.163	0.273

TABLE 4.4-4: [HISTORICAL INFORMATION] TYPICAL BWR 6 CORE FLOW DISTRIBUTION

Orifice Zone Description	Central Hot	Central Average	Peripheral Hot	Peripheral Average
Relative Assembly Power	1.4	1.084	0.50	0.35
Relative Assembly Flow	0.923	1.05	0.62	0.64

TABLE 4.4-5: DELETED

TABLE 4.4-6: DELETED

TABLE 4.4-7: BYPASS FLOW PATHS

Flow Path Description	Driving Pressures	Number of Paths
1a. Between Fuel Support and the Control Rod Guide Tube (Upper Path)	Core Plate Differential	One/Control Rod
1b. Between Fuel Support and the Control Rod Guide Tube (Lower Path)	Core Plate Differential	One/Control Rod
2. Between Core Plate and Control Rod Guide Tube	Core Plate Differential	One/Control Rod
3. Between Core Support and the In-Core Support Instrument Guide Tube	Core Plate Differential	One/Instrument
4. Between Core Plate and shroud	Core Plate Differential	One
5. Between Control Rod Guide Tube and Control Rod Drive Housing	Core Plate Differential	One/Control Rod
6. Between Fuel Support and Lower Tie Plate	Channel Wall Differential Plus Lower Tie Plate Differential	One/Channel
7. Control Rod Drive Coolant	Independent of Core	One/Control Rod
8. Between Fuel Channel and Lower Tie Plate	Channel Wall Differential	One/Channel
9. Holes in Lower Tie Plate	Lower Tie Plate/Bypass Region Differential	Two/Assembly

TABLE 4.4-8: REACTOR COOLANT SYSTEM GEOMETRIC DATA

	Flow Path Length (in.)	Height and Liquid Level (in.)	Elevation of Bottom of Each Volume* (in.)	Minimum Flow Areas (sq ft)
A. Lower Plenum	216.5	216.5 216.5	-172.0	106.0
B. Core**	164.5	164.5 164.5	44.0	168.5 includes bypass
C. Upper Plenum and Separators	179.5	179.5 179.5	208.5	66.5
D. Dome (Above Normal Water Level)	310.0	310.0 0	387.5	343.5
E. Downcomer Area	316.0	316.0 316.0	-31.5	69.5
F. Recirculation Loops and Jet Pumps (one loop)	117.0	412.0 412.0	-405.0	145.0/in.²

* Reference point is recirculation nozzle outlet centerline

** Initial core loading

TABLE 4.4-9: LENGTHS OF SAFETY INJECTION LINES

LPCS System

                              16" φ pipe - 136' - 1-1/2"
                              14" φ pipe - 179' - 8-1/4"
                      Total pipe footage - 315' - 9-3/4"

HPCS System

                              16" φ pipe - 102' - 7"
                              14" φ pipe - 147' - 11"
                              12" φ pipe - 12' - 3-9/16"
                      Total pipe footage - 262' - 9-9/16"

RHR - "A"

                              18" φ pipe - 161' - 7-7/8"
                              14" φ pipe - 68' - 4-3/8"
                              12" φ pipe - 19' - 0-7/8"
                      Total pipe footage - 249' - 1-1/8"

RHR - "B"

                              18" φ pipe - 145' - 2-9/16"
                              14" φ pipe - 159' - 6-3/16"
                              12" φ pipe - 11' - 0-1/2"
                      Total pipe footage - 315' - 9-1/4"

RHR - "C"

                              18" φ pipe - 127' - 7-5/8"
                              12" φ pipe - 143' - 2-3/4"
                      Total pipe footage - 270' - 10'3/8"

 Lengths are from pump discharge to RPV nozzle.

TABLE 4.4-10: EQUIPMENT ENVIRONMENTAL DESIGN

Equipment		Environmental Design
1.	Accelerometers	Vibration:	500g peak
		Shock:	3,000g peak
		Temperature:	-65 to 700°F
		Humidity:	100% noncondensing
		Radiation:	6.2 x 10^{10} rad integrated
2.	Hardline cable	Temperature:	-300 to 900°F
		Humidity:	100% noncondensing
		Materials:	Stainless steel and magnesium oxide hardened against radiation
3.	Preamplifier	Temperature:	0 to 160°F
		Humidity:	100% noncondensing
4.	Control room equipment	Temperature:	40 to 100°F operating, 75°F normal
		Humidity:	20 to 80%; can accommodate brief periods of higher humidity, but not continuous higher humidity
		Pressure:	Atmospheric
		Relative Humidity:	50% normal, free of salt or industrial pollutants

TABLE 4.4-11: (SHEETS 1 THRU 14) DELETED

TABLE 4.4-12: LPMS SENSOR ACTIVE/PASSIVE STATUS

ACCELEROMETER NUMBER	LOCATION	STATUS
1C87-YE-N001	RPV Bottom (CRD Housing) – 0° (119')	Active
1C87-YE-N002	RPV Bottom (CRD Housing) – 0° (119')	Passive
1C87-YE-N003	RPV Bottom (CRD Housing) – 180° (119')	Active
1C87-YE-N004	RPV Bottom (CRD Housing) – 180° (119')	Passive
1C87-YE-N005	Recirc Pump A Suction – 180° (134')	Active
1C87-YE-N006	Recirc Pump B Suction – 0° (134')	Active
1C87-YE-N007	Feedwater Header A – 32° (143')	Passive
1C87-YE-N008	Feedwater Header B – 328° (143')	Passive
1C87-YE-N009	Main Steam Line A – 72° (176')	Active
1C87-YE-N010	Main Steam Line B – 252° (176')	Active
1C87-YE-N011	Main Steam Line C – 108° (176')	Passive
1C87-YE-N012	Main Steam Line D – 288° (176')	Passive
1C87-YE-N013	Recirc Pump A Discharge – 90° (110')	Passive
1C87-YE-N014	Recirc Pump B Discharge – 270° (110')	Passive
1C87-YE-N015	HPCS Injection Header – 240° (163')	Active
1C87-YE-N016	LPCS Injection Header – 240° (163')	Active

NOTE: PERIPHERAL FUEL SUPPORTS ARE WELDED INTO THE CORE SUPPORT PLATE. FOR THESE BUNDLES, PATH NUMBERS 1, 2, 5 AND 7 DO NOT EXIST

1. CONTROL ROD GUIDE TUBE FUEL SUPPORT
2. CONTROL ROD GUIDE TUBE CORE SUPPORT PLATE
3. CORE SUPPORT PLATE IN-CORE GUIDE TUBE
4. CORE SUPPORT PLATE SHROUD
5. CONTROL ROD GUIDE TUBE DRIVE HOUSING
6. FUEL SUPPORT LOWER TIE PLATE
7. CONTROL ROD DRIVE COOLING WATER
8. CHANNEL LOWER TIE PLATE
9. ALTERNATE FLOW PATH HOLES

GRAND GULF NUCLEAR STATION UNIT 1 UPDATED FINAL SAFETY ANALYSIS REPORT	SCHEMATIC OF REACTOR ASSEMBLY SHOWING THE BYPASS FLOW PATHS FIGURE 4.4-1
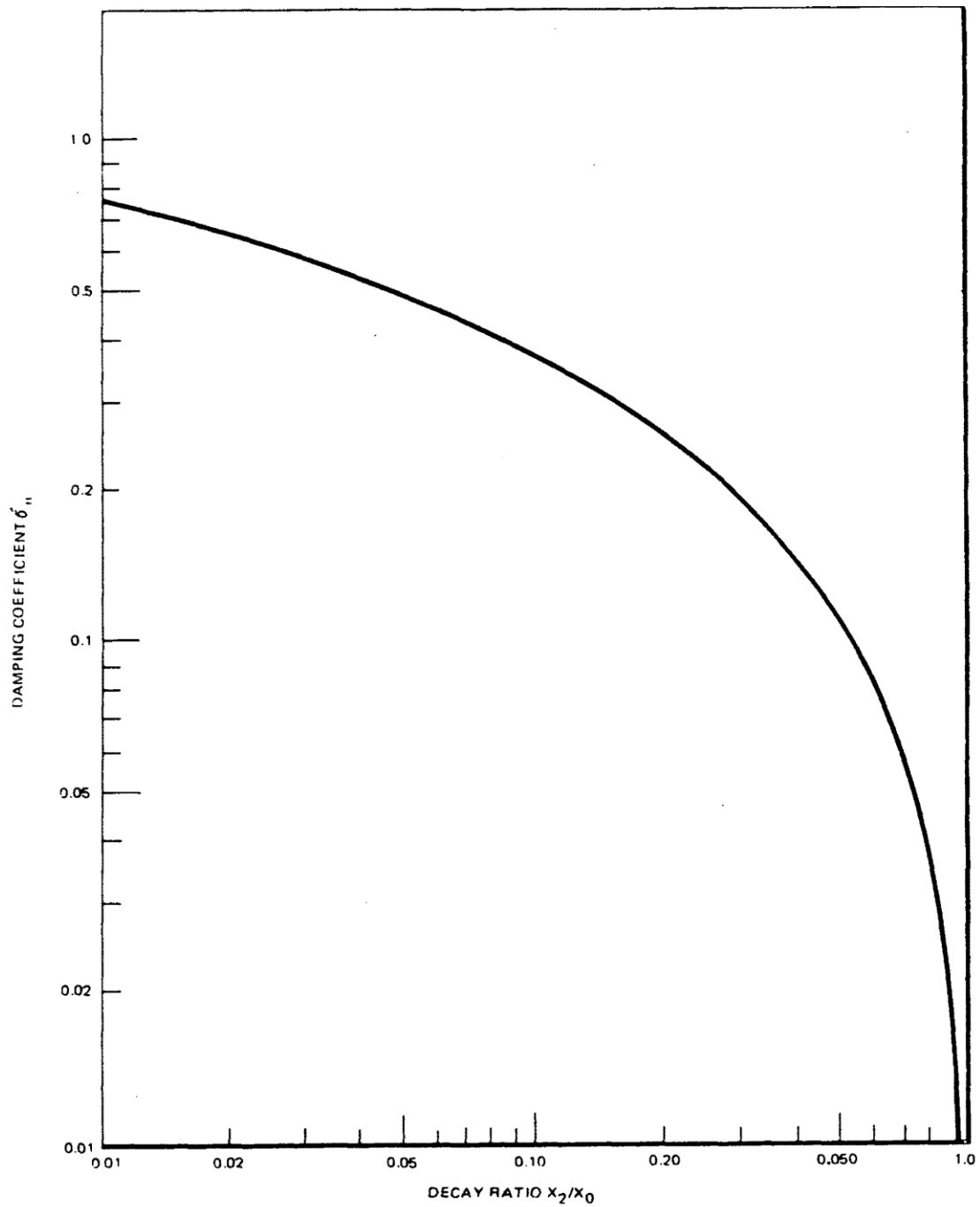
GRAND GULF NUCLEAR STATION UNIT 1 UPDATED FINAL SAFETY ANALYSIS REPORT	DAMPING COEFFICIENT VERSUS DECAY RATIO (SECOND ORDER SYSTEMS) FIGURE 4.4-2 [HISTORICAL INFORMATION]
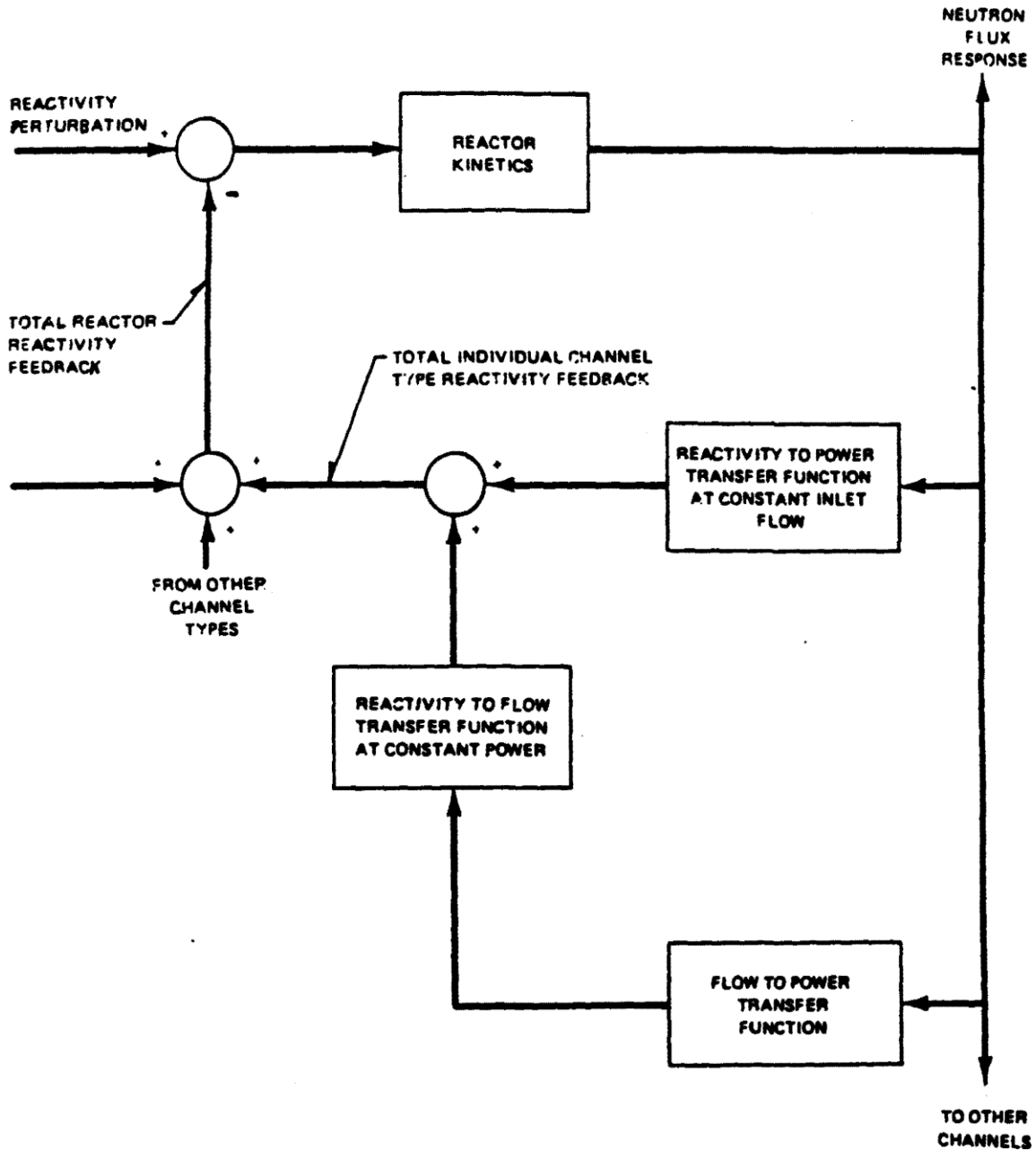
[HISTORICAL INFORMATION]

GRAND GULF NUCLEAR STATION UNIT 1 UPDATED FINAL SAFETY ANALYSIS REPORT	HYDRODYNAMIC AND CORE STABILITY MODEL FOR INITIAL CORE FIGURE 4.4-3

Figure 4.4-4

Deleted

GRAND GULF NUCLEAR STATION
UNIT 1
UPDATED FINAL SAFETY ANALYSIS REPORT
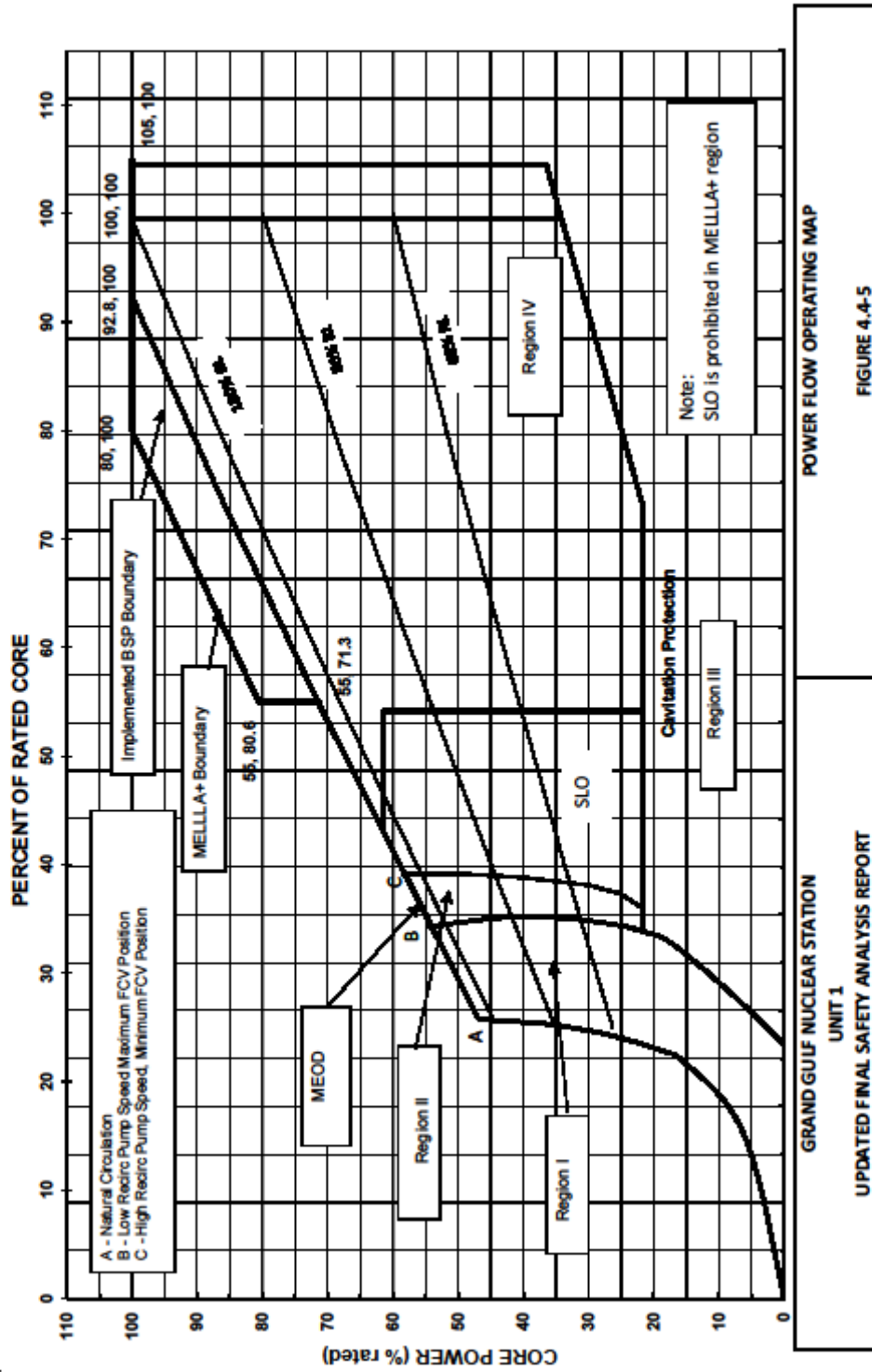
POWER FLOW OPERATING MAP

FIGURE 4.4-5

Figure 4.4-6

Deleted

Figure 4.4-7A through Figure 4.4-7C

Deleted

Figure 4.4-8A through Figure 4.4-8D

Deleted

Figure 4.4-9A through Figure 4.4-9D

Deleted

SENSOR AND IMPACT LOCATIONS
(ELEVATION)

MAIN STEAM LINES
ELEVATION APPROX. 176'

LOCATION	SENSOR	AZMUTH
MAIN STM A	N009	72
MAIN STM B	N010	252
MAIN STM C	N011	108
MAIN STM D	N012	288

FEEDWATER LINES
ELEVATION APPROX. 143'

LOCATION	SENSOR	AZMUTH
FEEDWATER A	N007	32
FEEDWATER B	N008	328

HPCS & LPCS
ELEVATION APPROX. 163'

LOCATION	SENSOR	AZMUTH
HPCS	N015	240
LPCS	N016	120

RECIRC SUCTION
ELEVATION APPROX. 134'

LOCATION	SENSOR	AZMUTH
REC A SUC	N005	180
REC B SUC	N006	

RECIRC DISCHARGE
ELEVATION APPROX. 110'

LOCATION	SENSOR	AZMUTH
REC A DIS	N013	90
REC B DIS	N014	270

CRD
ELEVATION APPROX. 119'

LOCATION	SENSOR	AZMUTH
CRD 3261	N001	0
CRD 3661	N002	0
CRD 3605	N003	180
CRD 3205	N004	180

GRAND GULF NUCLEAR STATION UNIT 1 UPDATED FINAL SAFETY ANALYSIS REPORT	LPMS SENSOR AND IMPACT LOCATIONS FIGURE 4.4-10
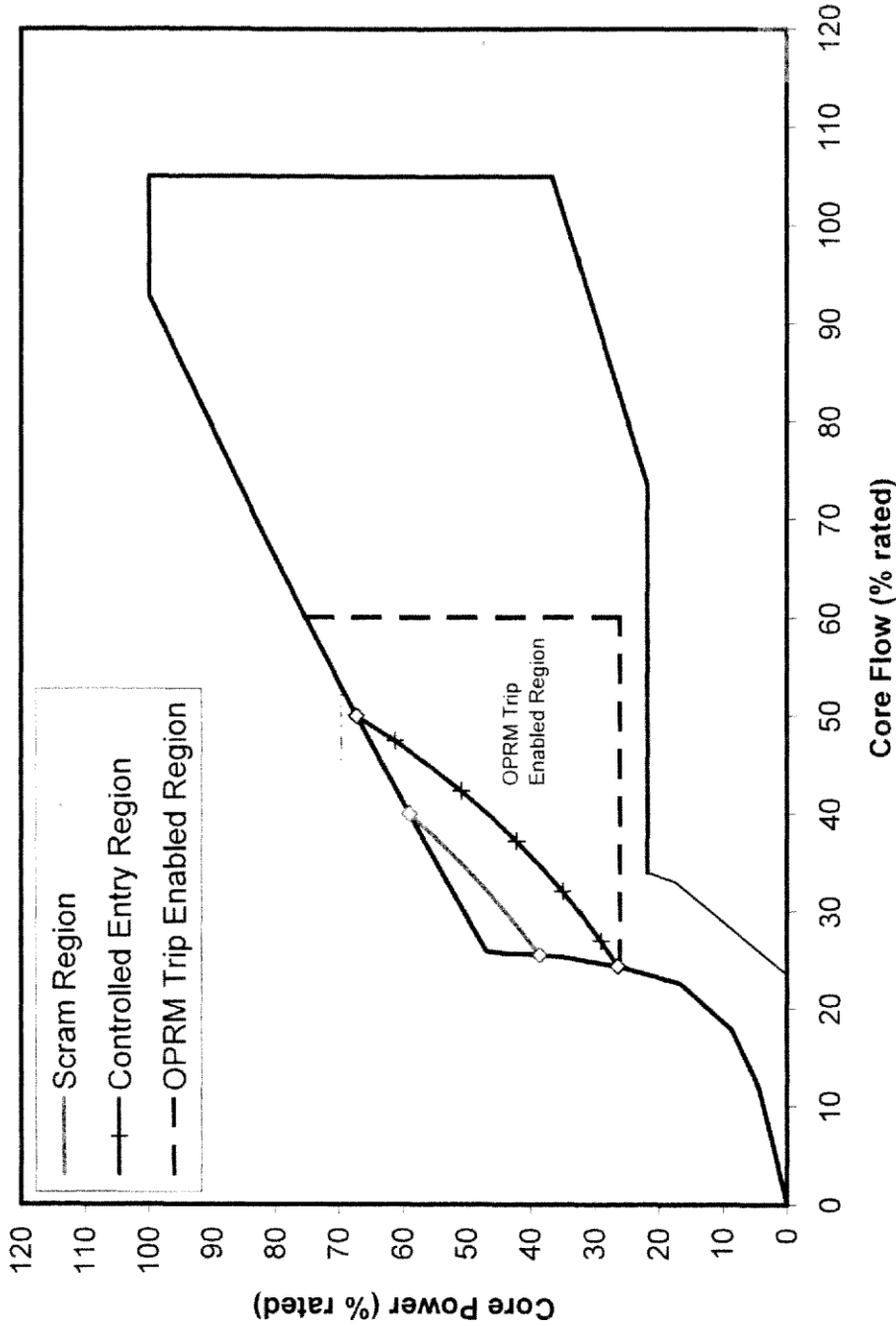
GRAND GULF NUCLEAR STATION
UNIT 1
UPDATED FINAL SAFETY ANALYSIS REPORT

POWER FLOW MAP
(TYPICAL)

FIGURE 4.4-11

4.5   REACTOR MATERIALS

4.5.1   Control Rod System Structural Materials

4.5.1.1   Material Specifications

The following material listing applies to the control rod drive mechanism supplied for this application. The position indicator and minor nonstructural items are omitted.

a.   Cylinder, Tube, and Flange Assembly

Flange	ASME SA 182 Grade F304
Plugs	ASME SA 182 Grade F304
Cylinder	ASTM A269 Grade TP 304
Outer Tube	ASTM A269 Grade TP 304
Collet Retainer Tube:	
Tube	ASME SA 351 Grade CF-3
Spacer	ASME SA 351 Grade CF-3

b.   Piston Tube Assembly

Piston Tube	ASME SA 479 Grade XM-19
Nose	ASME SA 479 Grade XM-19
Base	ASME SA 479 Grade XM-19
Ind. Tube	ASME SA 312 Type 316
Cap	ASME SA 182 Grade F316

c.   Drive Assembly

Coupling Spud	Inconel X-750
Index Tube	ASME SA 479 Grade XM-19
Piston Head	Armco 17-4 PH
Coupling	ASME SA 312 Grade TP 304 or ASTM A511 Grade MT 304
Magnet Housing	ASME SA 312 Grade TP 304 or ASTM A511 Grade MT 304

d.   Collet Assembly

Collet Piston	ASTM A269 Grade TP 304 or ASME SA 312 Grade TP 304
Finger	Inconel X-750
Retainer	ASTM A269 Grade TP 304 or ASTM A511 Grade MT 304

Guide Cap	ASTM A269 Grade TP 304

e. Miscellaneous Parts

Stop Piston	ARMO 17-4 PH
Connector	ASTM A276 Type 304
O-Ring Spacer	ASME SA 240 Type 304
Nut	ASME SA 479 Grade XM-19
Barrel	ASTM A269 Grade TP 304 or ASME SA 312 Grade TP 304 or ASME SA 240 Type 304
Collet Spring	Inconel X-750
Ring Flange	ASME SA 182 Grade F304
Buffer Shaft	ARMCO 17-4 PH
Buffer Piston	ARMCO 17-4 PH
Buffer Spring	Inconel X-750
Nut (hex)	Inconel X-750

The materials listed under ASTM specification number are all in the annealed condition (with the exception of the outer tube in the cylinder, tube, and flange assembly), and their properties are readily available. The outer tube is approximately 1/8 hard, and has a tensile of 90,000/125,000 psi, yield of 50,000/ 85,000 psi, and minimum elongation of 25 percent.

The coupling spud, collet fingers, buffer spring, nut (hex), and collet spring are fabricated from Inconel X-750 in the annealed or equalized condition, and heat treated to produce a tensile of 165,000 psi minimum, yield of 105,000 psi minimum and elongation of 20 percent minimum. The piston head, stop piston, buffer shaft, and buffer piston are Armco 17-4 PH in condition H 1100, with a tensile of 140,000 psi minimum, yield of 115,000 psi minimum and elongation of 15 percent minimum.

These are widely used materials, whose properties are well known. The parts are readily accessible for inspection and replaceable if necessary.

[HISTORICAL INFORMATION] [All materials, except SA 479 Grade XM-19, have been successfully used for the past 10 to 15 years in similar drive mechanisms. Extensive laboratory tests have demonstrated that ASME SA 479 Grade XM-19 is a suitable material and that it is resistant to stress corrosion in a BWR environment.]

4.5.1.2   Special Materials

No cold worked austenitic stainless steels with a yield strength greater than 90,000 psi are employed in the Control Rod Drive system. Hardenable martensitic stainless steels are not used. Armco 17-4 PH (precipitation hardened stainless steel) is used for the piston head. This material is aged to the H-1100 condition to produce resistance to stress corrosion cracking in the BWR environments. Armco 17-4 PH (H-100) has been successfully used for the past 10 to 15 years in BWR drive mechanisms.

4.5.1.3   Processes, Inspections and Tests

All austenitic stainless steel used in the control rod drive system is solution annealed material with one exception, the outer tube in the cylinder, tube, and flange assembly. See subsection 4.5.1.1. Proper solution annealing is verified by testing per ASTM-A262 Recommended Practices for Detecting Susceptibility to Intergranular Attack in Stainless Steels.

Two special processes are employed which subject selected 300 series stainless steel components to temperatures in the sensitization range.

   a.   The cylinder and spacer (cylinder, tube, and flange assembly) and the retainer (collet assembly) are hard surfaced with Colmonoy 6.

   b.   The collet piston and guide cap are nitrided to provide a wear resistant surface. Colmonoy hard surfacing is applied by the flame process. Nitriding is accomplished using a proprietary process called "New Malcomizing." Components are exposed to a temperature of about 1080 F for approximately 20 hours during the nitriding cycle.

[HISTORICAL INFORMATION] [Colmonoy hard surfaced components in drive mechanisms have performed successfully since 1960. Nitrided components have been used in control rod drives since 1967. It is normal practice to remove some control rod drives at each refueling outage. At this time, both the Colmonoy hard surfaced parts and nitrided surfaces are accessible for visual examination.

In addition, dye penetrant examinations have been performed on nitrided surfaces of the longest service drives. This inspection program is adequate to detect any incipient defects before they could become serious enough to cause operating problems.]

Welding is performed in accordance with Section IX of the ASME Boiler and Pressure Vessel Code. Heat input for stainless steel welds is restricted to a maximum of 50,000 Joules per inch and interpass temperature to 350 F. Heating above 800 F (except for welding) is prohibited unless the welds are subsequently solution annealed. These controls are employed to avoid severe sensitization and comply with the intent of Regulatory Guide 1.44.

4.5.1.4   Control of Delta Ferrite Content

All type 308 weld metal is purchased to a specification which requires a minimum of 5 percent delta ferrite. This amount of ferrite is adequate to prevent any micro-fissuring (hot cracking) in austenitic stainless steel welds.

[HISTORICAL INFORMATION] [An extensive test program performed by General Electric Company, with the concurrence of the Regulatory Staff, has demonstrated that controlling weld filler metal ferrite at 5 percent minimum produces production welds which meet the requirements of Regulatory Guide 1.31, Control of Stainless Steel Welding. A total of approximately 400 production welds in five BWR plants were measured and all welds met the requirements of the Interim Regulatory Position to Regulatory Guide 1.31.]

4.5.1.5   Protection of Materials During Fabrication, Shipping, and Storage

All the control rod drive parts listed above (subsection 4.5.1.1) are fabricated under a process specification which limits contaminants in cutting, grinding, and tapping coolants and lubricants. It also restricts all other processing materials (marking inks, tape etc.) to those which are completely removable by the applied cleaning process. All contaminants are then required to be removed by the appropriate cleaning process prior to any of the following:

a.   Any processing which increases part temperature above 200 F

b.   Assembly which results in decrease of accessibility for cleaning

c.   Release of parts for shipment

The specification for packaging and shipping the control rod drive provides the following:

> The drive is rinsed in hot deionized water and dried in preparation for shipment. The ends of the drive are then covered with a vapor tight barrier with desiccant. Packaging is designed to protect the drive and prevent damage to the vapor barrier. The planned storage period considered in the design of the container and packaging is two years. This packaging has been qualified and in use for a number of years. Periodic audits have indicated satisfactory protection.

The degree of surface cleanliness obtained by these procedures meets the requirements of Regulatory Guide 1.37.

Site or warehouse storage specifications require inside heated storage comparable to level B of ANSI 45.2.2. After the second year, a yearly inspection of 10 percent of the humidity indicators (packaged with the drives) is required to verify that the units are dry.

4.5.2   Reactor Internal Materials

4.5.2.1   Material Specifications

Materials used for the Core Support Structure:

> Shroud Support - Nickel Chrome Iron Alloy, ASME SB166 or SB168
>
> Shroud, core plate, grid, and internal structures welded to these components - ASME SA240, SA182, SA479, SA312, SA249, or SA213 (all Type 304L)
>
> Peripheral fuel supports - SA312 Type 304
>
> Core plate and top guide studs and nuts, and core plate wedges - ASME SA479, SA193 Grade B8, SA194 Grade 8 (all Type 304)
>
> Top guide pins - ASME SA479 (Type 316 or XM-19)

Control rod drive housing - ASME SA312 Type 304, SA182 Grade F304

Control rod drive guide tube - ASME SA351 Type CF8, SA358, SA312, SA249 Type 304

Orificed fuel support - ASME SA351 Type CF8

Materials Employed in Other Reactor Internal Structures

a. Steam Separator and Steam Dryer (Original Equipment, dryer replaced per EC23898)

    All materials are Type 304 stainless steel.

    Plate, Sheet, and Strip   ASTM A240, Type 304

    Forgings   ASTM A182, Grade F304

    Bars   ASTM A276 Type 304

    Pipe   ASTM A312 Grade TP 304

    Tube   ASTM A269 Grade TP 304

    Castings   ASTM A351 Grade CF8

b. Jet Pump Assemblies

    The components in the Jet Pump Assemblies are a Riser, Inlet, Mixer, Diffuser, and Riser Brace. Materials used for these components are to the following specifications.

    Castings   ASTM A351 Grade CF8 and ASME SA351 Grade CF3

    Bars   ASTM A276 Type 304 and ASTM A370 Grade E38 and E55

    Bolts   ASTM A193 Grade B8 or B8M

    Sheet and Plate   ASTM A240 Type 304, ASTM A276 Type 304, ASTM A358, and ASME SA240 Type 304L

    Tubing   ASTM A269 Grade TP 304

    Pipe   ASTM A358 Type 304 and ASME SA312 Grade TP 304

    Welded Fittings   ASTM A403 Grade WP304

    Forgings   ASME SA152 Grade F304, ASTM B166, and ASTM A637 Grade 688

Materials in the Jet Pump Assemblies which are not Type 304 stainless steel are listed below:

a.   The Inlet Mixer Adaptor casting, the wedge casting, bracket casting adjusting screw casting, and the Diffuser collar casting are Type 304 hard surfaced with Stellite 6 for slip fit joints.

b.   The Diffuser is a bi-metallic component made by welding a Type 304 forged ring to a forged Inconel 600 ring, made to Specification ASTM B166.

c.   The Inlet-Mixer contains a pin, insert, and beam made of Inconel X-750 to General Electric Specifications 25A5830 and B50YP154, and ASTM A370 Grade E38 and E55 (Pin and Insert).

d.   The Jet Pump Beam Bolt is SS316L.

All core support structures are fabricated from ASME specified materials, and designed in accordance with the requirements of ASME Code, Section III, Appendix I. The other reactor internals are non-coded, and they are fabricated from ASTM specification materials. Material requirements in the ASTM specifications are identical to requirements in corresponding ASME material specifications. The allowable stress levels specified in ASME Code, Section III, Appendix I, are used as a guide in the design of all non-coded internal structures in the BWR.

4.5.2.2   Controls on Welding

Core support structures are fabricated in accordance with requirements of ASME Code, Section III, Subsection NG. Other internals are not required to meet ASME Code requirements; however, they are fabricated to the requirements of ASME Section IX.

4.5.2.3   Nondestructive Examination of Wrought Seamless Tubular Products

For core support structures, wrought seamless tubular products were supplied in accordance with applicable ASME material specifications. These specifications require examination of the tubular product by radiographic and/or ultrasonic methods according to Paragraph NG-2550 of ASME Code, Section III. In addition, the specification for tubular products employed for CRD housings external to the RPV meet requirements of Paragraph NB-2550 which meets the intent of Regulatory Guide 1.66.

Other internals are non-coded, and wrought seamless tubular products were supplied in accordance with the applicable ASTM material specifications. These specifications require a hydrostatic test on each length of tubing.

4.5.2.4   Fabrication and Processing of Austenitic Stainless Steel - Regulatory Guide Conformance

Regulatory Guide 1.31, Control of Stainless Steel Welding

All austenitic stainless steel weld filler materials were supplied with a minimum of 5 percent delta ferrite. This amount of ferrite is considered adequate to prevent micro-fissuring in austenitic stainless steel welds.

[HISTORICAL INFORMATION] [An extensive test program performed by General Electric Company, with the concurrence of the Regulatory Staff, has demonstrated that controlling weld filler metal ferrite at 5 percent minimum produces production welds which meet the requirements of Regulatory Guide 1.31, Control of Stainless Steel Welding. A total of approximately 400 production welds in five BWR plants were measured and all welds met the requirements of the Interim Regulatory Position to Regulatory Guide 1.31.]

Regulatory Guide 1.34, Control of Electroslag Weld Properties

Electroslag welding is not employed for any reactor internals.

Regulatory Guide 1.36, Non-metallic Thermal Insulation for Austenitic Stainless Steel

Non-metallic thermal insulation is not employed for any components in the reactor vessel. For external applications, all non-metallic insulation meets the requirements of Regulatory Guide 1.36

Regulatory Guide 1.44, Control of the Use of Sensitized Stainless Steel

All wrought austenitic stainless steel was purchased in the solution heat treated condition. Heating above 800 F was prohibited (except for welding) unless the stainless steel was subsequently solution annealed. Purchase specifications restricted the maximum weld heat input to 110,000 Joules per inch, and the weld interpass temperature to 350 F maximum. Welding was performed in accordance with Section IX of the ASME Boiler and

Pressure Vessel Code. These controls were employed to avoid severe sensitization and comply with the intent of Regulatory Guide 1.44.

Regulatory Guide 1.71, Welder Qualification for Areas of Limited Accessibility

There are very few restrictive welds involved in the fabrication of items described in this section, and a limited number of field welds were required since this application utilized the shop installed internals approach. For the shop installed internals, mock-up welding was performed on the welds with most difficult access. Mock-ups were examined with radiography or by sectioning.

4.5.2.5   Contamination, Protection, and Cleaning of Austenitic Stainless Steel

Exposure to contaminant was avoided by carefully controlling all cleaning and processing materials which contact stainless steel during manufacture and construction. Any inadvertent surface contamination was removed to avoid potential detrimental effects.

Special care was exercised to insure removal of surface contaminants prior to any heating operation. Water quality for rinsing, flushing, and testing was controlled and monitored.

The degree of cleanliness obtained by these procedures meets the requirements of Regulatory Guide 1.37.

4.5.3   Control Rod Drive Housing Supports

The American Institute of Steel Construction (AISC) Manual of Steel Construction, "Specification for the Design, Fabrication and Erection of Structural Steel for Buildings," was used in designing the CRD housing support system. However, to provide a structure that absorbs as much energy as practical without yielding, the allowable tension and bending stresses used were 90 percent of yield and the shear stress used was 60 percent of yield. These design stresses are 1.5 times the AISC allowable stresses (60 percent and 40 percent of yield, respectively).

For purposes of mechanical design, the postulated failure resulting in the highest forces is an instantaneous circumferential separation of the CRD housing from the reactor vessel, with the reactor at an operating pressure of 1086 psig (at the bottom of the vessel) acting on the area of the separated

housing. The weight of the separated housing, control rod drive, and blade, plus the pressure of 1086 psig acting on the area of the separated housing, gives a force of approximately 32,000 lbs. This force is used to calculate the impact force, conservatively assuming that the housing travels through a 1-in. gap before it contacts the supports. The impact force (109,000 lbs) is then treated as a static load in design. The CRD housing supports are designed as seismic Category I equipment in accordance with Section 3.2.

All CRD housing support subassemblies are fabricated of ASTM-A-36 structural steel, except for the following items:

	Material
Grid	ASTM-A-441
Disc Springs	Schnerr, Type BS-125-71-8
Hex bolts and nuts	ASTM-A-307
6 x 4 x 3/8 tubes	ASTM-A-500 Grade B

4.6 FUNCTIONAL DESIGN OF REACTIVITY CONTROL SYSTEMS

Functional design of the control rod drive system (CRDS) is discussed below. Functional designs of the recirculation flow control system and the standby liquid control system are given in subsections 5.4.1 and 9.3.5, respectively. Conformance of these systems to the General Design Criteria is given in Section 3.1.

4.6.1   Information for CRDS

4.6.1.1   Control Rod Drive System Design

4.6.1.1.1   Design Bases

4.6.1.1.1.1   General Design Bases

4.6.1.1.1.1.1   Safety Design Bases

The control rod drive mechanical system meets the following safety design bases:

   a.   Design shall provide for a sufficiently rapid control rod insertion that no fuel damage results from any abnormal operating transient.

   b.   Design shall include positioning devices, each of which individually supports and positions a control rod.

   c.   Each positioning device shall:

      1.   Prevent its control rod from initiating withdrawal as a result of a single malfunction

      2.   Be individually operated so that a failure in one positioning device does not affect the operation of any other positioning device

      3.   Be individually energized when rapid control rod insertion (scram) is signaled so that failure of power sources external to the positioning device does not prevent other positioning devices' control rods from being inserted.

   d.   An alternate rod insertion (ARI) system is available which is in compliance with the criteria of 10CFR50.62 imposed for the postulated failure of normal scram during

anticipated transients (ATWS). This criteria contains the requirement that the ARI system must have redundant scram air header exhaust valve paths.

4.6.1.1.1.1.2   Power Generation Design Basis

The control rod system drive design provides for positioning the control rods to control power generation in the core.

4.6.1.1.2   Description

The control rod drive system (CRDS) controls gross changes in-core reactivity by incrementally positioning neutron absorbing control rods within the reactor core in response to manual control signals. It is also required to quickly shut down the reactor (scram) in emergency situations by rapidly inserting withdrawn control rods into the core in response to a manual or automatic signal. The control rod drive system consists of locking piston control rod drive mechanisms, and the CRD hydraulic system (including power supply and regulation, hydraulic control units, interconnecting piping, instrumentation, and electrical controls).

4.6.1.1.2.1   Control Rod Drive Mechanisms

The CRD mechanism (drive) used for positioning the control rod in the reactor core is a double-acting, mechanically latched, hydraulic cylinder using water as its operating fluid. (See Figures 4.6-1, 4.6-2, 4.6-3, and 4.6-4.) The individual drives are mounted on the bottom head of the reactor pressure vessel. The drives do not interfere with refueling and are operative even when the head is removed from the reactor vessel.

The drives are also readily accessible for inspection and servicing. The bottom location makes maximum utilization of the water in the reactor as a neutron shield and gives the least possible neutron exposure to the drive components. Using water from the condensate treatment system and/or condensate storage tanks as the operating fluid eliminates the need for special hydraulic fluid. Drives are able to utilize simple piston seals whose leakage does not contaminate the reactor water but provides cooling for the drive mechanisms and their seals.

The drives are capable of inserting or withdrawing a control rod at a slow, controlled rate, as well as providing rapid insertion when required. A mechanism on the drive locks the control rod at 6-inch increments of stroke over the length of the core.

A coupling spud at the top end of the drive index tube (piston rod) engages and locks into a mating socket at the base of the control rod. The weight of the control rod is sufficient to engage and lock this coupling. Once locked, the drive and rod form an integral unit that must be manually unlocked by specific procedures before the components can be separated.

The drive holds its control rod in distinct latch positions until the hydraulic system actuates movement to a new position. Withdrawal of each rod is limited by the seating of the rod in its guide tube. Withdrawal beyond this position to the over-travel limit can be accomplished only if the rod and drive are uncoupled. Withdrawal to the over-travel limit is annunciated by an alarm.

The individual rod indicators, grouped in one control panel display, correspond to relative rod locations in the core. A separate, smaller display is located just below the large display on the vertical part of the benchboard. This display presents the positions of the control rod selected for movement and the other rods in the affected rod group.

For display purposes the control rods are considered in groups of four adjacent rods centered around a common core volume. Each group is monitored by four LPRM strings (see subsection 7.6.1.5, Neutron Monitoring System). Rod groups at the periphery of the core may have less than four rods. The small rod display shows the positions, in digital form, of the rods in the group to which the selected rod belongs. A white light indicates which of the four rods is the one selected for movement.

4.6.1.1.2.2   Drive Components

Figure 4.6-2 illustrates the operating principle of a drive. Figures 4.6-3 and 4.6-4 illustrate the drive in more detail. The main components of the drive and their functions are described below.

4.6.1.1.2.2.1   Drive Piston

The drive piston is mounted at the lower end of the index tube.
This tube functions as a piston rod. The drive piston and index
tube make up the main moving assembly in the drive. The drive
piston operates between positive end stops, with a hydraulic
cushion provided at the upper end only. The piston has both inside
and outside seal rings and operates in an annular space between an
inner cylinder (fixed piston tube) and an outer cylinder (drive
cylinder). Because the type of inner seal used is effective in
only one direction, the lower sets of seal rings are mounted with
one set sealing in each direction.

A pair of nonmetallic bushings prevents metal-to-metal contact
between the piston assembly and the inner cylinder surface. The
outer piston rings are segmented step-cut seals with expander
springs holding the segments against the cylinder wall. A pair of
split bushings on the outside of the piston prevents piston
contact with the cylinder wall. The effective piston area for
downtravel, or withdrawal, is approximately 1.2 sq in. versus 4.1
sq in. for uptravel, or insertion. This difference in driving area
tends to balance the control rod weight and assures a higher force
for insertion than for withdrawal.

4.6.1.1.2.2.2   Index Tube

The index tube is a long hollow shaft made of nitrided stainless
steel. Circumferential locking grooves, spaced every 6 inches
along the outer surface, transmit the weight of the control rod to
the collet assembly.

4.6.1.1.2.2.3   Collet Assembly

The collet assembly serves as the index tube locking mechanism. It
is located in the upper part of the drive unit. This assembly
prevents the index tube from accidentally moving downward. The
assembly consists of the collet fingers, a return spring, a guide
cap, a collet housing (part of the cylinder, tube, and flange),
and the collet piston.

Locking is accomplished by fingers mounted on the collet piston at
the top of the drive cylinder. In the locked or latched position
the fingers engage a locking groove in the index tube.

The collet piston is normally held in the latched position by a force of approximately 150 lbs supplied by a spring. Metal piston rings are used to seal the collet piston from reactor vessel pressure. The collet assembly will not unlatch until the collet fingers are unloaded by a short, automatically sequenced, drive-in signal. A pressure, approximately 180 psi above reactor vessel pressure, must then be applied to the collet piston to overcome spring force, slide the collet up against the conical surface in the guide cap, and spread the fingers out so they do not engage a locking groove.

A guide cap is fixed in the upper end of the drive assembly. This member provides the unlocking cam surface for the collet fingers and serves as the upper bushing for the index tube.

If reactor water is used during a scram to supplement accumulator pressure, it is drawn through a filter on the guide cap.

4.6.1.1.2.2.4 Piston Tube

The piston tube is an inner cylinder, or column, extending upward inside the drive piston and index tube. The piston tube is fixed to the bottom flange of the drive and remains stationary. Water is brought to the upper side of the drive piston through this tube. A buffer shaft, at the upper end of the piston tube, supports the stop piston and buffer components.

4.6.1.1.2.2.5 Stop Piston

A stationary piston, called the stop piston, is mounted on the upper end of the piston tube. This piston provides the seal between reactor vessel pressure and the space above the drive piston. It also functions as a positive end stop at the upper limit of control rod travel. Piston rings and bushings, similar to those used on the drive piston, are mounted on the upper portion of the stop piston. The lower portion of the stop piston forms a thin-walled cylinder containing the buffer piston, its metal seal ring, and the buffer piston return spring. As the drive piston reaches the upper end of the scram stroke it strikes the buffer piston. A series of orifices in the buffer shaft provides a progressive water shutoff to cushion the buffer piston as it is driven to its limit of travel. The high pressures generated in the buffer are confined to the cylinder portion of the stop piston, and are not applied to the stop piston and drive piston seals.

The center tube of the drive mechanism forms a well to contain the position indicator probe. The probe is an aluminum extrusion attached to a cast aluminum housing. Mounted on the extrusion are hermetically sealed, magnetically operated, position indicator switches. The entire probe assembly is protected by a thin-walled stainless steel tube. The switches are actuated by a ring magnet located at the bottom of the drive piston.

The drive piston, piston tube, and indicator tube are all of nonmagnetic stainless steel, allowing the individual switches to be operated by the magnet as the piston passes. Two switches are located at each position corresponding to an index tube groove, thus allowing redundant indication at each latching point. Two additional switches are located at each midpoint between latching points to indicate the intermediate positions during drive motion. Thus, indication is provided for each 3 inches of travel. Duplicate switches are provided for the full-in and full-out positions. Redundant overtravel switches are located at a position below the normal full-out position. Because the limit of downtravel is normally provided by the control rod itself as it reaches the backseat position, the drive can pass this position and actuate the overtravel switches only if it is uncoupled from its control rod. A convenient means is thus provided to verify that the drive and control rod are coupled after installation of a drive or at any time during plant operation.

4.6.1.1.2.2.6 Flange and Cylinder Assembly

A flange and cylinder assembly is made up of a heavy flange welded to the drive cylinder. A sealing surface on the upper face of this flange forms the seal to the drive housing flange. The seals contain reactor pressure and the two hydraulic control pressures. Teflon coated, stainless steel rings are used for these seals. The drive flange contains the integral ball, or two-way, check (ball-shuttle) valve. This valve directs either the reactor vessel pressure or the driving pressure, whichever is higher, to the underside of the drive piston. Reactor vessel pressure is admitted to this valve from the annular space between the drive and drive housing through passages in the flange.

Water used to operate the collet piston passes between the outer tube and the cylinder tube. The inside of the cylinder tube is honed to provide the surface required for the drive piston seals.

Both the cylinder tube and outer tube are welded to the drive
flange. The upper ends of these tubes have a sliding fit to allow
for differential expansion.

The upper end of the index tube is threaded to receive a coupling
spud. The coupling (see Figure 4.6-1) accommodates a small amount
of angular misalignment between the drive and the control rod. Six
spring fingers allow the coupling spud to enter the mating socket
on the control rod. A plug then enters the spud and prevents
uncoupling.

Two means of uncoupling are provided. With the reactor vessel head
removed, the lock plug can be raised against the spring force of
approximately 50 pounds by a rod extending up through the center
of the control rod to an unlocking handle located above the
control rod velocity limiter. The control rod, with the lock plug
raised, can then be lifted from the drive.

4.6.1.1.2.2.7   Lock Plug

The lock plug can also be pushed up from below, if it is desired
to uncouple a drive without removing the reactor pressure vessel
head for access. In this case, the central portion of the drive
mechanism is pushed up against the uncoupling rod assembly, which
raises the lock plug and allows the coupling spud to disengage the
socket as the drive piston and index tube are driven down.

The control rod is heavy enough to force the spud fingers to enter
the socket and push the lock plug up, allowing the spud to enter
the socket completely and the plug to snap back into place.
Therefore, the drive can be coupled to the control rod using only
the weight of the control rod. However, with the lock plug in
place, a force in excess of 50,000 lbs is required to pull the
coupling apart.

4.6.1.1.2.3 Materials of Construction

Factors that determine the choice of construction materials are
discussed in the following subsections.

4.6.1.1.2.3.1   Index Tube

The index tube must withstand the locking and unlocking action of
the collet fingers. A compatible bearing combination must be
provided that is able to withstand moderate misalignment forces.
The reactor environment limits the choice of materials suitable

for corrosion resistance. The column and tensile loads can be satisfied by an annealed, single phase, nitrogen strengthened, austenitic stainless steel. The wear and bearing requirements are provided by Malcomizing the complete tube. To obtain suitable corrosion resistance, a carefully controlled process of surface preparation is employed.

4.6.1.1.2.3.2   Coupling Spud

The coupling spud is made of Inconel 750 that is aged for maximum physical strength and the required corrosion resistance. Because misalignment tends to cause chafing in the semispherical contact area, the part is protected by a thin chromium plating (Electrolyzed). This plating also prevents galling of the threads attaching the coupling spud to the index tube.

4.6.1.1.2.3.3   Collet Fingers

Inconel 750 is used for the collet fingers, which must function as leaf springs when cammed open to the unlocked position. Colmonoy 6 hard facing provides a long wearing surface, adequate for design life, to the area contacting the index tube and unlocking cam surface of the guide cap.

4.6.1.1.2.3.4   Seals and Bushings

Graphitar 14 is selected for seals and bushings on the drive piston and stop piston. The material is inert and has a low friction coefficient when water-lubricated. Because some loss of Graphitar strength is experienced at higher temperatures, the drive is supplied with cooling water to hold temperatures below 250 F. The Graphitar is relatively soft, which is advantageous when an occasional particle of foreign matter reaches a seal. The resulting scratches in the seal reduce sealing efficiency until worn smooth, but the drive design can tolerate considerable water leakage past the seals into the reactor vessel.

4.6.1.1.2.3.5   Summary

All drive components exposed to reactor vessel water are made of austenitic stainless steel except the following:

   a.   Seals and bushings on the drive piston and stop piston are
         Graphitar 14.

b.   All springs and members requiring spring action (collet fingers, coupling spud, and spring washers) are made of Inconel-750.

c.   The ball check valve is a Haynes Stellite cobalt-base alloy.

d.   Elastomeric O-ring seals are ethylene propylene.

e.   Metal piston rings are Haynes 25 alloy.

f.   Certain wear surfaces are hard-faced with Colmonoy 6.

g.   Nitriding by a proprietary new Malcomizing process and chromium plating are used in certain areas where resistance to abrasion is necessary.

h.   The drive piston head, stop piston, buffer shaft, and buffer piston are made of Armco 17-4PH.

i.   Certain fasteners and locking devices are made of Inconel-750 or 600.

Pressure-containing portions of the drives are designed and fabricated in accordance with requirements of Section III of the ASME Boiler and Pressure Vessel Code.

4.6.1.1.2.4   Control Rod Drive Hydraulic System

The control rod drive hydraulic system (Figures 4.6-7 through 4.6-10) supplies and controls the pressure and flow to and from the drives through hydraulic control units (HCU). The water discharged from the drives during a scram flows through the HCUs to the scram discharge volume. The water discharged from a drive during a normal control rod positioning operation flows through the HCU, the exhaust header, and is returned to the reactor vessel via the HCUs of the nonmoving drives. There are as many HCUs as the number of control rod drives.

4.6.1.1.2.4.1   Hydraulic Requirements

The CRD hydraulic system design is shown in Figures 4.6-7 through 4.6-10. The hydraulic requirements, identified by the function they perform, are as follows:

a.   An accumulator hydraulic charging pressure of approximately 1750 to 2000 psig is required. Flow to the accumulators is required only during scram reset or system startup.

b.   Drive water header pressure of approximately 260 psi above reactor vessel pressure is required. A flow rate of approximately 4 gpm to insert each control rod and 2 gpm to withdraw each control rod is required.

c.   Cooling water to the drives is required at approximately 0.34 gpm per drive unit.

d.   The scram discharge volume is sized to receive and contain all the water discharged by the drives during a scram; a minimum volume of 3.34 gal. per drive is required (excluding the instrument volume).

4.6.1.1.2.4.2   System Description

The CRD hydraulic systems provide the required functions with the pumps, filter, valves, instrumentation, and piping shown in Figures 4.6-7 and 4.6-8 and described in the following paragraphs.

Duplicate components are included, where necessary, to assure continuous system operation if an inservice component requires maintenance.

4.6.1.1.2.4.2.1   Supply Pump

One supply pump pressurizes the system with water from the condensate treatment system and/or condensate storage tanks. The water from the condensate system is of a controlled high quality and is not laden with particulate matter. One spare pump is provided for standby. A discharge check valve prevents backflow through the nonoperating pump. A portion of the pump discharge flow is diverted through a minimum flow bypass line to the condensate storage tank. This flow is controlled by an orifice and is sufficient to prevent immediate pump damage if the pump discharge is inadvertently closed. When CRD flow is maximized during an emergency condition, the minimum flow bypass line isolation valves are manually closed to allow adequate flow as required by NUREG-0619. In addition, the standby pump suction and drive water filters are valved in, to prevent pump trip on low suction pressure.

Condensate water is processed by three filters in the system. The pump backwash suction filter is an automatic backwash type with a 50-micron rating. The redundant pump suction filters are disposable element types with a 25-micron absolute rating. A 250-micron strainer in the filter bypass line protects the pump when the filters are being serviced. The drive water filter downstream of the pump is a cleanable element type with a 50-micron absolute rating. A differential pressure indicator and control room alarm monitor the filter element as it collects foreign materials.

The filters used in the CRD system are of a rugged design, and failure of the filters is not considered likely. Alarms are provided to give an early warning to the operator that maintenance is required.

The pump backwash suction filter is designed to remove any large particles from the system flow. The filter is capable of being automatically backwashed. If in automatic, backwashing occurs either by an interval timer or upon a high differential pressure (4.75 psid). If the automatic backwash cycle should fail (i.e., failure of motor drive to rotate the filter element), an alarm sounds in the main control room on high differential pressure (7.0 psid). Upon receipt of the alarm, sufficient time is provided to manually backwash the suction filter since the filter can withstand a maximum differential pressure of 15 psid. Normally during CRD pump operation, this filter is manually backwashed when the control room alarm indicating high differential pressure is received. A filter bypass is provided to allow for repairs/ maintenance of the filter.

The only known mode of failure of the suction and discharge filter elements is for them to collapse due to high differential pressure. The CRD pump suction filter can withstand a maximum differential pressure of 75 psid, and an alarm in the control room indicates high suction filter differential pressure at 5.0 psid. The suction filter element is additionally protected and strengthened by a stainless steel, perforated center tube. The CRD pump discharge filter can withstand a maximum differential pressure of 300 psid, and an alarm in the control room indicates high differential pressure at 20 psid. The discharge filter element is constructed entirely of stainless steel.

If the CRD system backwash suction, pump suction, and pump discharge filters were bypassed completely, the possible presence of corrosion particles would not affect the reliability of the

scram function of the CRD system. The minimum performance and operability requirements of the drives during reactor operation are specified in the Technical Specifications.

4.6.1.1.2.4.2.2 Accumulator Charging Pressure

Accumulator charging pressure is established by the discharge pressure of the system supply pump. During scram the scram inlet (and outlet) valves open and permit the stored energy in the accumulators to discharge into the drives. The resulting pressure decrease in the charging water header allows the CRD supply pump to run out (i.e., flow rate to increase substantially) into the control rod drives via the charging water header. The flow sensing system upstream of the accumulator charging header detects high flow and closes the flow control valve. This action maintains increased flow through the charging water header.

Pressure in the charging header is monitored in the control room with a pressure indicator and low pressure alarm.

During normal operation the flow control valve maintains a constant system flow rate. This flow is used for drive flow, drive cooling, and system stability.

4.6.1.1.2.4.2.3 Drive Water Pressure

Drive water pressure required in the drive header is maintained by the drive pressure control valve, which is manually adjusted from the control room. A flow rate approximately equal to the sum of the flow rate required to insert four control rods normally passes from the drive water pressure stage through eight solenoid operated stabilizing valves (arranged in parallel) and then goes into the return line downstream from the drive pressure control valve. The flow through two stabilizing valves equals the drive insert flow for one drive; that of one stabilizing valve equals the drive withdrawal flow for one drive. When operating a drive(s), the required flow is diverted to the drives by closing the appropriate stabilizing valves. Thus, flow through the drive pressure control valve is always constant.

Flow indicators in the drive water header and in the line downstream from the stabilizing valves allow the flow rate through the stabilizing valves to be adjusted when necessary. Differential pressure between the reactor vessel and the drive pressure stage is indicated in the control room.

4.6.1.1.2.4.2.4   Cooling Water Header

The cooling water header is located downstream of the pressure
control valve. Water not required for moving a drive is used for
cooling the drives. A flow indicator in the control room monitors
cooling water flow. A differential pressure indicator in the
control room indicates the difference between reactor vessel
pressure and drive cooling water pressure. Although the drives
can function without cooling water, seal life is shortened by long
term exposure to reactor temperatures. The temperature of each
control rod drive is recorded on a multipoint temperature
recorder located locally in the auxiliary building, and the high
temperatures are annunciated in the control room.

4.6.1.1.2.4.2.5   Alternate Rod Insertion (ARI)

The ARI system at GGNS consists of three parallel vent paths from
the scram pilot air header. Each vent path consists of two
solenoid valves in series for a total of six vent valves
(Reference Figure 4.6-7). These solenoid valves are normally de-
energized. They are energized from redundant ARI scram initiation
trip systems to open and depressurize the scram pilot air header
which causes the pressure-to-close CRD scram valves to open. Each
ARI scram initiation trip system is tripped on conditions
indicative of an ATWS event (RPV high pressure or low level). The
trip logic is two-out-of-two for pressure or two-out-of-two for
level. The trip function may also be initiated manually.

The ARI system uses the same trip channels (transmitters and trip
units) as the RPT system. Therefore, the ARI trip function and the
RPT trip function will be initiated simultaneously. The
instrumentation setpoints for the RPV pressure and water level
trip channels are established such that the normal scram paths for
these variables would already be initiated.

Test switches in the scram pilot air header vent path solenoid
valve circuits and an additional instrument air supply valve
allow testing of these valves by opening one channel of the series
installed valves (either inboard or outboard) at a time while the
other channel maintains the vent path solenoid valves closed so as
to not disturb the reactor protection system. When the 3-way
instrument air supply block/vent path valve is energized, a
bypass solenoid valve opens providing an alternate path for
instrument air around the supply block valve during testing.

The ARI system initiates the scram function of the control rod drive system independently of the reactor protection system.

4.6.1.1.2.4.2.6   Scram Discharge Volume

The scram discharge system described below meets the criteria enumerated in the Generic Safety Evaluation Report - BWR Scram Discharge System. The scram discharge volume consists of header piping which connects to each HCU and drains into an instrument volume. The header piping is sized to receive and contain all the water discharged by the drives during a scram, independent of the instrument volume.

During normal plant operation the scram discharge volume is empty, and vented to atmosphere through its open vent and drain valves. When a scram occurs, upon a signal from the safety circuit or the ARI system, redundant vent and drain valves are closed to conserve reactor water. Lights in the control room indicate the position of these valves.

During a scram, the scram discharge volume partly fills with water discharged from above the drive pistons. After scram is completed, the control rod drive seal leakage from the reactor continues to flow into the scram discharge volume until the discharge volume pressure equals the reactor vessel pressure. A check valve in each HCU prevents reverse flow from the scram discharge header volume to the drive. When the initial scram signal is cleared from the reactor protection system (and the ARI system when applicable), the scram discharge volume signal is overridden with keylock bypass switches, and the scram discharge volume is drained and returned to atmospheric pressure.

Remote manual switches in the pilot valve solenoid circuits allow the discharge volume vent and drain valves to be tested without disturbing the reactor protection system. Closing the scram discharge volume valves allows the outlet scram valve seats to be leak-tested by timing the accumulation of leakage inside the scram discharge volume.

Eight electronic liquid-level switches activated by six transmitters connected to the instrument volume, monitor the volume for abnormal water level. They are set at three different levels. At the lowest level, two redundant switches actuate to indicate that the volume is not completely empty during post-scram draining or to indicate that the volume starts to fill through leakage accumulation at other times during reactor

operation. At the second level, two redundant switches produce a rod withdrawal block to prevent further withdrawal of any control rod, when leakage accumulates to half the capacity of the instrument volume. The remaining four switches are interconnected with the trip channels of the reactor trip system and will initiate a reactor scram should water accumulation fill the instrument volume. Additionally, four float type level switches are connected to the instrument volume to monitor the volume for abnormal water level. These four level switches are also interconnected with the trip channels of the reactor trip system and are redundant to the level indicating switches activated by the transmitters.

A minimum scram discharge volume of 3.34 gallons per drive is specified through the system design specifications. This minimum scram discharge volume is based on conservative assumptions as to the performance of the scram system and ensures the scram discharge volume can receive and contain water exhausted by a full reactor scram without adversely affecting control-rod-drive scram performance.

No single failure in the scram system design will prevent a reactor scram. The system requirements state that there shall be no reduction in the pipe size of the header piping going from the Scram Discharge Volume (SDV) to and including the Scram Discharge Instrument Volume (SDIV). This hydraulic coupling permits operability of the scram level instrumentation prior to loss of system function. The scram level instrumentation will ensure no single active failure prevents a reactor scram.

Redundant vent and drain valves are provided as part of the SDV modifications. The redundant SDV valve configuration ensures that no single failure can result in an uncontrolled loss of reactor coolant. An additional solenoid-operated pilot valve controls the redundant vent and drain valve. The vent and drain system is therefore sufficiently redundant to avoid a failure to isolate the SDV due to solenoid failure. The redundant vent and drain valves' opening and closing sequences are controlled to minimize excessive hydrodynamic forces.

The redundant float type level switch design is diverse from the already redundant level transmitter configuration. Instrument taps have been relocated from the vent and drain piping to the scram discharge instrument volume to protect the level sensing instrumentation from the flow dynamics in the scram discharge

system. This instrumentation arrangement will ensure the automatic scram function on high SDIV water level in the event of a single active or passive failure.

The SDV and associated vent and drain piping is classified as safety-related and required to meet the ASME Section III Class II and Seismic Category I requirements. Design parameters such as temperature, pressure, and frequency for limiting modes of operation provide a design basis for supply of equipment as well as the interfacing piping design and analysis.

All SDV piping is continuously sloped from its high point to its low point.

Plant surveillance procedures provide for the verification that level instrumentation has been properly returned to service following testing.

The consequences of a postulated slow or partial loss of air is considered in the SDV sizing design basis. The effect on scram performance of CRD seal leakage passing through the scram discharge valves and, collectively, through the SDV has been evaluated. Based on maximum expected seal leakage flow, adequate SDV is available to perform the scram function. The SDIV connects integrally with the SDV as shown on Figure 4.6-7. Therefore, any accumulation of CRD seal leakage in the SDV/SDIV will be detected by the level instrumentation. SDIV level instrumentation logic provides for water accumulation alarms, rod block signals, and scram signals.

During the slow or partial loss of air pressure event, the operator will receive several control room indications that will lead the operator to initiate a reactor scram if the scram has not already occurred automatically due to high SDIV water level. For this postulated event, low air supply pressure will be alarmed and annunciated, and random rod drift will occur. The drifting rods would be annunciated and the condition alarmed. In most cases, due to either a limiting condition of operation or an undesirable rod pattern, as determined by Reactor Engineering, the operator will initiate a reactor scram.

If CRD leakage to the SDV is less than the amount that will accumulate in the SDIV, the leakage will flow through the drain line to the suppression pool. The maximum SDV discharge flow rate which would not cause accumulation in the SDIV is expected to be approximately 50 gpm. The suppression pool is a monitored volume

which normally receives the drainage from the SDV following a
scram. It is equipped with a cleanup system which is designed to
reduce the activity of the water in the suppression pool at a rate
sufficient to allow normal access to the containment by plant
operators within 36 hours after a scram has occurred. Vacuum
breakers on the SDV vent line preclude water from siphoning back
into the SDIV from the suppression pool.

The air lines which control the opening and closing of the scram
valves are connected directly to the air lines controlling the
opening and closing of the SDV vent and drain valves, with no
check valves or other obstructing devices. A slow or partial loss
of air pressure which causes the scram valves to open will also
cause the SDV vent and drain valves to close. Even if the scram
valves open before the SDV vent and drain valves close, leakage
will either continue to drain into the suppression pool or will
accumulate in the SDV, causing the alarms and signals described
above. The SDV will isolate automatically upon initiation of a
reactor scram.

In conclusion, ample control room information, system safeguards,
and scram system capability ensure that no adverse effects can
result from the postulated slow or partial loss of air supply
pressure event.

4.6.1.1.2.4.3   Hydraulic Control Units

Each hydraulic control unit (HCU) furnishes pressurized water, on
signal, to a drive unit. The drive then positions its control rod
as required. Operation of the electrical system that supplies
scram and normal control rod positioning signals to the HCU is
described in subsection 7.7.1.2, Rod Control and Information
System.

The basic components in each HCU are manual, pneumatic, and
electrical valves; an accumulator; related piping; electrical
connections; filters; and instrumentation (see Figure 4.6-5). The
components and their functions are described in the following
paragraphs.

4.6.1.1.2.4.3.1   Insert Drive Valve

The insert drive valve is solenoid-operated and opens on an insert
signal. The valve supplies drive water to the bottom side of the
main drive piston.

4.6.1.1.2.4.3.2   Insert Exhaust Valve

The insert exhaust solenoid valve also opens on an insert signal. The valve discharges water from above the drive piston to the exhaust water header.

4.6.1.1.2.4.3.3   Withdraw Drive Valve

The withdraw drive valve is solenoid-operated and opens on a withdraw signal. The valve supplies drive water to the top of the drive piston.

4.6.1.1.2.4.3.4   Withdraw Exhaust Valve

The solenoid-operated withdraw exhaust valve opens on a withdraw signal and discharges water from below the main drive piston to the exhaust header. It also serves as the settle valve, which opens following any normal drive movement (insert or withdraw) to allow the control rod and its drive to settle back into the nearest latch position.

4.6.1.1.2.4.3.5   Speed Control Valves

The speed control valves regulate the control rod insertion and withdrawal rates during normal operation. They are manually adjustable flow control valves used to regulate the water flow to and from the volume beneath the main drive piston. A correctly adjusted valve does not require readjustment except to compensate for changes in drive seal leakage.

4.6.1.1.2.4.3.6   Scram Pilot Valves

The scram pilot valves are operated from the reactor protection system trip system. A scram pilot valve with two solenoids controls both the scram inlet valve and the scram exhaust valve. The scram pilot valves are three-way, solenoid-operated, normally energized valves. On loss of electrical signal to the solenoids, such as the loss of external ac power, the inlet port closes and the exhaust port opens. The pilot valves (Figures 4.6-7 through 4.6-9) are designed so that the trip system signal must be removed from both solenoids before air pressure can be discharged from the scram valve operators. This prevents the inadvertent scram of a single drive in the event of a failure of one of the pilot valve solenoids.

4.6.1.1.2.4.3.7   Scram Inlet Valve

The scram inlet valve opens to supply pressurized water to the bottom of the drive piston. This quick opening globe valve is operated by an internal spring and system pressure. It is closed by air pressure applied to the top of its diaphragm operator. A position indicator switch on this valve energizes a light in the control room as soon as the valve starts to open.

4.6.1.1.2.4.3.8 Scram Exhaust Valve

The scram exhaust valve opens slightly before the scram inlet valve, exhausting water from above the drive piston. The exhaust valve opens faster than the inlet valve because of a larger spring in the valve operator. Otherwise the valves are similar.

4.6.1.1.2.4.3.9 Scram Accumulator

The scram accumulator stores sufficient energy to fully insert a control rod at any vessel pressure. The accumulator is a hydraulic cylinder with a free-floating piston. The piston separates the water on top from the nitrogen below. A check valve in the accumulator charging line prevents loss of water pressure in the event supply pressure is lost.

During normal plant operation, the accumulator piston is seated at the bottom of its cylinder. Accumulator pressure is continuously monitored. Loss of nitrogen decreases the nitrogen pressure, which actuates a pressure switch and sounds an alarm in the control room.

To ensure that the accumulator is always able to produce a scram, it is continuously monitored for water leakage. A float type level switch actuates an alarm if water leaks past the piston barrier and collects in the accumulator instrumentation block.

Loss of pressure and/or leakage from any of the accumulators is detected by PSL-130 and LS-129, respectively, for each accumulator, as shown in Figure 4.6-8.

4.6.1.1.2.5 Control Rod Drive System Operation

The control rod drive system performs rod insertion, rod withdrawal, and scram. These operational functions are described below.

4.6.1.1.2.5.1   Rod Insertion

Rod insertion is initiated by a signal from the operator to the insert valve solenoids. This signal causes both insert valves to open. The insert drive valve applies reactor pressure plus approximately 90 psi to the bottom of the drive piston. The insert exhaust valve allows water from above the drive piston to discharge to the exhaust header.

As is illustrated in Figure 4.6-3, the locking mechanism is a ratchet-type device and does not interfere with rod insertion. The speed at which the drive moves is determined by the flow through the insert speed control valve, which is set for approximately 4 gpm for a shim speed (nonscram operation) of 3 in./sec. During normal insertion, the pressure on the downstream side of the speed control valve is 90 to 100 psi above reactor vessel pressure. However, if the drive slows for any reason, the flow through, and pressure drop across, the insert speed control valve will decrease; the full differential pressure (260 psi) will then be available to cause continued insertion. With 260-psi differential pressure acting on the drive piston, the piston exerts an upward force of 1040 lbs.

4.6.1.1.2.5.2   Rod Withdrawal

Rod withdrawal is, by design, more involved than insertion. The collet finger (latch) must be raised to reach the unlocked position (see Figure 4.6-3). The notches in the index tube and the collet fingers are shaped so that the downward force on the index tube holds the collet fingers in place. The index tube must be lifted before the collet fingers can be released. This is done by opening the drive insert valves (in the manner described in the preceding paragraph) for approximately 1 sec. The withdraw valves are then opened, applying driving pressure above the drive piston and opening the area below the piston to the exhaust header. Pressure is simultaneously applied to the collet piston. As the piston raises, the collet fingers are cammed outward, away from the index tube, by the guide cap.

The pressure required to release the latch is set and maintained at a level high enough to overcome the force of the latch return spring plus the force of reactor pressure opposing movement of the collet piston. When this occurs, the index tube is unlatched and free to move in the withdraw direction. Water displaced by the drive piston flows out through the withdraw speed control valve,

which is set to give the control rod a shim speed of 3 in./sec. The entire valving sequence is automatically controlled and is initiated by a single operation of the rod withdraw switch.

4.6.1.1.2.5.3   Scram

During a scram the scram pilot valve and scram valves are operated as previously described. With the scram valves open, accumulator pressure is admitted under the drive piston, and the area over the drive piston is vented to the scram discharge volume.

The large differential pressure (initially approximately 1750 psi and always several hundred psi, depending on reactor vessel pressure) produces a large upward force on the index tube and control rod. This force gives the rod a high initial acceleration and provides a large margin of force to overcome friction. After the initial acceleration is achieved, the drive continues at a diminishing velocity. This characteristic provides a high initial rod insertion rate. As the drive piston nears the top of its stroke, the piston reaches the buffer and the driveline is brought to a stop at the full-in position.

Prior to a scram signal the accumulator in the hydraulic control unit has approximately 1750-2000 psig on the water side and 1175-1225 psig on the nitrogen side. As the inlet scram valve opens, the full water side pressure is available at the control rod drive acting on a 4.1 sq in. area. As CRD motion begins, this pressure drops to the gas side pressure less line losses between the accumulator and the CRD. When the drive reaches the full in position, the accumulator completely discharges with a resulting gas side pressure of approximately 1200 psig.

The control rod drive accumulators are necessary to scram the control rods within the required time. Each drive, however, has an internal ballcheck valve which allows reactor pressure to be admitted under the drive piston. If the reactor is above 600 psi this valve ensures rod insertion in the event the accumulator is not charged or the inlet scram valve fails to open. The insertion time, however, will be much slower than the scram time with a properly functioning scram system.

The control rod drive system, with accumulators, provides the following scram performances at full power operation, in terms of average elapsed time after the opening of the reactor protection system trip actuator (scram signal) for the drives to attain the scram strokes listed:

Percent of full stroke	1	10	40	75
Stroke in inches	1.4	14.4	57.6	108
Time in sec	0.138	0.317	0.874	1.620

4.6.1.1.2.6   Instrumentation

The instrumentation for both the control rods and control rod drives is defined by that given for the rod control and information system. The objective of the rod control and information system is to provide the operator with the means to make changes in nuclear reactivity so that reactor power level and power distribution can be controlled. The system allows the operator to manipulate control rods.

The design bases and further discussion are covered in Chapter 7, Instrumentation.

4.6.1.2   Control Rod Drive Housing Supports

4.6.1.2.1   Safety Objective

The control rod drive (CRD) housing supports prevent any significant nuclear transient in the event a drive housing breaks or separates from the bottom of the reactor vessel.

4.6.1.2.2   Safety Design Bases

The CRD housing supports meet the following safety design bases:

a.   Following a postulated CRD housing failure, control rod downward motion shall be limited so that any resulting nuclear transient could not be sufficient to cause fuel damage.

b.   The clearance between the CRD housings and the supports shall be sufficient to prevent vertical contact stresses caused by thermal expansion during plant operation.

4.6.1.2.3   Description

The CRD housing supports are shown in Figure 4.6-6. Horizontal beams are installed immediately below the bottom head of the reactor vessel, between the rows of CRD housings. The beams are supported by brackets welded to the steel form liner of the drive room in the reactor support pedestal.

Hanger rods, approximately 10 ft. long and 1-3/4 in. in diameter, are supported from the beams on stacks of disc springs. These springs compress approximately 2 inches under the design load.

The support bars are bolted between the bottom ends of the hanger rods. The spring pivots at the top, and the beveled, loose fitting ends on the support bars prevent substantial bending moment in the hanger rods if the support bars are overloaded.

Individual grids rest on the support bars between adjacent beams. Because a single piece grid would be difficult to handle in the limited work space and because it is necessary that control rod drives, position indicators, and in-core instrumentation components be accessible for inspection and maintenance, each grid is designed for in-place assembly or disassembly. Each grid assembly is made from two grid plates, a clamp, and a bolt. The top part of the clamp guides the grid to its correct position directly below the respective CRD housing that it would support in the postulated accident.

When the support bars and grids are installed, a gap of approximately 1 in. at room temperature (approximately 70 F) is provided between the grid and the bottom contact surface of the control rod drive flange. During system heatup, this gap is reduced by a net downward expansion of the housings with respect to the supports. In the hot operating condition, the gap is approximately 1/4 in.

In the postulated CRD housing failure, the CRD housing supports are loaded when the lower contact surface of the CRD flange contacts the grid. The resulting load is then carried by two grid plates, two support bars, four hanger rods, their disc springs, and two adjacent beams.

The American Institute of Steel Construction (AISC) Manual of Steel Construction, "Specification for the Design, Fabrication and Erection of Structural Steel for Buildings," was used in designing the CRD housing support system. However, to provide a

structure that absorbs as much energy as practical without yielding, the allowable tension and bending stresses used were 90 percent of yield and the shear stress used was 60 percent of yield. These design stresses are 1.5 times the AISC allowable stresses (60 percent and 40 percent of yield, respectively).

For purposes of mechanical design, the postulated failure resulting in the highest forces is an instantaneous circumferential separation of the CRD housing from the reactor vessel, with an internal pressure of 1250 psig (reactor vessel design pressure) acting on the area of the separated housing. The weight of the separated housing, control rod drive, and blade, plus the pressure of 1250 psig acting on the area of the separated housing, gives a force of approximately 35,000 lbs. This force is multiplied by a factor of 3 for impact, conservatively assuming that the housing travels through a 1-in. gap before it contacts the supports. The total force (105,000 lb) is then treated as a static load in design.

All CRD housing support subassemblies are fabricated of commonly available structural steel, except for the disc springs, which are Schnorr, Type BS-125-71-8.

4.6.2 Evaluations of the CRDS

4.6.2.1 Failure Mode and Effects Analysis

The evaluation of failure of the control rod drive system (CRDS) is covered under Nuclear Safety Operational Analysis (NSOA) in Appendix 15A, in subsection 15A.6.6.3 and in Figure 15A.6-45.

4.6.2.2 Protection from Common Mode Failures

The control rod drive system is a diverse reactivity system designed in conformance with IEEE Std. 384 and Regulatory Guide 1.75 for electrical separation criteria. There is no common mode failure which would preclude the insertion of at least 50 percent of the control rods and injection of boron into the vessel by the SLCS.

A fault tree analysis was completed for both of these systems, and the calculated unreliability is $<10^{-7}$/reactor year. This unreliability is an estimate of the failure to fully insert at least 50 percent of the control rods into the core (assuming all rods were initially out) combined with a failure to inject boron into the vessel by the SLCS.

The evaluation of failure of the control rod drive system (CRDS) is covered under Nuclear Safety Operational Analysis (NSOA) in Appendix 15A, in subsection 15A.6.6.3 and in Figure 15A.6-45.

4.6.2.3   Safety Evaluation

Safety evaluation of the control rods, CRDS, and control rod drive housing supports is described below. Further description of control rods is contained in Section 4.2.

4.6.2.3.1   Control Rods

4.6.2.3.1.1   Materials Adequacy Throughout Design Lifetime

The adequacy of the materials throughout the design life was evaluated in the mechanical design of the control rods. The primary materials, B_4C powder, hafnium, RAD RESIST 304S, and 304 austenitic stainless steel, have been found suitable in meeting the demands of the BWR environment.

4.6.2.3.1.2   Dimensional and Tolerance Analysis

Layout studies are done to assure that, given the worst combination of extreme detail part tolerance ranges at assembly, no interference exists which will restrict the passage of control rods. In addition, preoperational verification is made on each control blade system to show that the acceptable levels of operational performance are met.

4.6.2.3.1.3   Thermal Analysis of the Tendency to Warp

The various parts of the control rod assembly remain at approximately the same temperature during reactor operation, negating the problem of distortion or warpage. What little differential thermal growth could exist is allowed for in the mechanical design. A minimum axial gap is maintained between absorber rod tubes and the control rod frame assembly for the purpose. In addition, dissimilar metals are avoided to further this end.

4.6.2.3.1.4   Forces for Expulsion

An analysis has been performed which evaluates the maximum pressure forces which could tend to eject a control rod from the core. The results of this analysis are given in subsection 4.6.2.3.2.2.2 under Rupture of Hydraulic Line(s) to Drive Housing

Flange. In summary, if the collet were to remain open, which is unlikely, calculations indicate that the steady-state control rod withdrawal velocity would be 2 ft./sec. for a pressure-under line break, the limiting case for rod withdrawal.

4.6.2.3.1.5   Functional Failure of Critical Components

The consequences of a functional failure of critical components have been evaluated and the results are covered in subsection 4.6.2.3.2.2, Analysis of Malfunction Relating to Rod Withdrawal.

4.6.2.3.1.6   Precluding Excessive Rates of Reactivity Addition

In order to preclude excessive rates of reactivity addition, analysis has been performed both on the velocity limiter device and the effect of probable control rod failures (see subsection 4.6.2.3.2.2, Analysis of Malfunction Relating to Rod Withdrawal.)

4.6.2.3.1.7   Effect of Fuel Rod Failure on Control Rod Channel Clearances

The control rod drive mechanical design ensures a sufficiently rapid insertion of control rods to preclude the occurrence of fuel rod failures which could hinder reactor shutdown by causing significant distortions in channel clearances.

4.6.2.3.1.8   Mechanical Damage

Analysis has been performed for all areas of the control system showing that system mechanical damage does not affect the capability to continuously provide reactivity control.

In addition to the analysis performed on the control rod drive (subsection 4.6.2.3.2.2, Analysis of Malfunction Relating to Rod Withdrawal and subsection 4.6.2.3.2.3, Scram Reliability) and the control rod blade, the following discussion summarizes the analysis performed on the control rod guide tube.

The guide tube can be subjected to any or all of the following loads:

   a.   Inward load due to pressure differential

   b.   Lateral loads due to flow across the guide tube

   c.   Dead Weight

d.   Seismic (Vertical and Horizontal)

e.   Vibration

In all cases analysis was performed considering both a
recirculation line break and a steam line break. These events
result in the largest hydraulic loadings on a control rod guide
tube.

Two primary modes of failure were considered in the guide tube
analysis: exceeding allowable stress and excessive elastic
deformation. It was found that the allowable stress limit will not
be exceeded and that the elastic deformations of the guide tube
never are great enough to cause the free movement of the control
rod to be jeopardized.

4.6.2.3.1.9   Evaluation of Control Rod Velocity Limiter

The control rod velocity limiter limits the free fall velocity of
the control rod to a value that minimizes damage to the nuclear
system process barrier. This velocity is evaluated by the rod drop
accident analysis in Chapter 15, Accident Analyses.

4.6.2.3.2   Control Rod Drives

4.6.2.3.2.1   Evaluation of Scram Time

The rod scram function of the control rod drive system provides
the negative reactivity insertion required by safety design basis
4.6.1.1.1.1.a. The scram time shown in the description is
adequate as shown by the transient analyses of Chapter 15,
Accident Analyses.

Generic analyses performed for EPU identified that an increase in
transient response time due to EPU increases the scram time. The
scram response time was evaluated for GGNS for normal operating
conditions and it was determined that since the normal reactor
dome pressure did not change the scram time performance is
essentially the same. For the ASME overpressure protection
analyses, the GGNS response times are not bounded by the generic
envelope and scram times for GGNS have been revised. The mean
scram based operating limit (Option B) is now used for the plant
specific reload analysis core design which is based on actual
testing as required in the plant Technical Specifications. (Ref.
2) The use of Opinion B allows credit for actual faster scram
speeds to provide for a lower minimum critical power ratio (MCPR)

operating limit. This lower limit ensures that the MCPR safety limit is not exceeded while providing for additional operating margin. The Option B scram times come form the MCPR margin improvement options described in Reference 3.

4.6.2.3.2.2   Analysis of Malfunction Relating to Rod Withdrawal

There are no known single malfunctions that cause the unplanned withdrawal of even a single control rod. However, if multiple malfunctions are postulated, studies show that an unplanned rod withdrawal can occur at withdrawal speeds that vary with the combination of malfunctions postulated. In all cases the subsequent withdrawal speeds are less than that assumed in the rod drop accident analysis as discussed in Chapter 15, Accident Analyses. Therefore, the physical and radiological consequences of such rod withdrawals are less than those analyzed in the rod drop accident.

4.6.2.3.2.2.1   Drive Housing Fails at Attachment Weld

The bottom head of the reactor vessel has a penetration for each control rod drive location. A drive housing is raised into position inside each penetration and fastened by welding. The drive is raised into the drive housing and bolted to a flange at the bottom of the housing. The CRD housing material at the vessel penetration is seamless, type Inconel 600, tubing with a minimum tensile strength of 80,000 psi, and type 304 stainless steel pipe below the vessel with a minimum strength of 75,000 psi. The basic failure considered here is a complete circumferential crack through the housing wall at an elevation just below the J-weld.

Static loads on the housing wall include the weight of the drive and the control rod, the weight of the housing below the J-weld, and the reactor pressure acting on the 6-in. diameter cross-sectional area of the housing and the drive. Dynamic loading results from the reaction force during drive operation.

If the housing were to fail as described, the following sequence of events is foreseen. The housing would separate from the vessel. The control rod drive and housing would be blown downward against the support structure by reactor pressure acting on the cross-sectional area of the housing and the drive. The downward motion of the drive and associated parts would be determined by the gap between the bottom of the drive and the support structure and by the deflection of the support structure under load. In the current design, maximum deflection is approximately 3 in. If the collet

were to remain latched, no further control rod ejection would occur (Ref. 1); the housing would not drop far enough to clear the vessel penetration. Reactor water would leak at a rate no greater than approximately 220 gpm through the diametral clearance of 0.015-inch between the housing and the vessel penetration.

If the basic housing failure were to occur while the control rod is being withdrawn (this is a small fraction of the total drive operating time) and if the collet were to stay unlatched, the following sequence of events is foreseen. The housing would separate from the vessel. The drive and housing would be blown downward against the control rod drive housing support. Calculations indicate that the steady-state rod withdrawal velocity would be 0.3 ft./sec. During withdrawal, pressure under the collet piston would be approximately 250 psi greater than the pressure over it. Therefore, the collet would be held in the unlatched position until driving pressure was removed from the pressure-over port.

4.6.2.3.2.2.2   Rupture of Hydraulic Line(s) to Drive Housing Flange

There are three types of possible rupture of hydraulic lines to the drive housing flange: (1) pressure-under line break; (2) pressure-over line break; and (3) coincident breakage of both of these lines.

4.6.2.3.2.2.2.1   Pressure-Under Line Break

For the case of a pressure-under line break, a partial or complete circumferential opening is postulated at or near the point where the line enters the housing flange. Failure is more likely to occur after another basic failure wherein the drive housing or housing flange separates from the reactor vessel. Failure of the housing, however, does not necessarily lead directly to failure of the hydraulic lines.

If the pressure-under line were to fail and if the collet were latched, no control rod withdrawal would occur. There would be no pressure differential across the collet piston and, therefore, no tendency to unlatch the collet. Consequently, the associated control rod could not be withdrawn, but if reactor pressure is greater than 600 psig, it will insert on a scram signal.

The ball check valve is designed to seal off a broken pressure-under line by using reactor pressure to shift the check ball to its upper seat. If the ball check valve were prevented from seating, reactor water would leak to the atmosphere. Because of the broken line, cooling water could not be supplied to the drive involved. Loss of cooling water would cause no immediate damage to the drive. However, prolonged exposure of the drive to temperatures at or near reactor temperature could lead to deterioration of material in the seals. High temperature would be indicated to the operator by the thermocouple in the position indicator probe. A second indication would be high cooling water flow.

If the basic line failure were to occur while the control rod is being withdrawn the hydraulic force would not be sufficient to hold the collet open, and spring force normally would cause the collet to latch and stop rod withdrawal. However, if the collet were to remain open, calculations indicate that the steady-state control rod withdrawal velocity would be 2 ft./sec.

4.6.2.3.2.2.2.2   Pressure-over Line Break

The case of the pressure-over line breakage considers the complete breakage of the line at or near the point where it enters the housing flange. If the line were to break, pressure over the drive piston would drop from reactor pressure to atmospheric pressure. Any significant reactor pressure (approximately 600 psig or greater) would act on the bottom of the drive piston and fully insert the drive. Insertion would occur regardless of the operational mode at the time of the failure. After full insertion, reactor water would leak past the stop piston seals. This leakage would exhaust to the atmosphere through the broken pressure-over line. The leakage rate at 1000 psi reactor pressure is estimated to be 4 gpm nominal but not more than 10 gpm, based on experimental measurements. If the reactor were hot, drive temperature would increase. This situation would be indicated to the reactor operator by the drift alarm, by the fully inserted drive, by a high drive temperature (indicated on a recorder in the control room), and by operation of the drywell sump pump.

4.6.2.3.2.2.2.3   Simultaneous Breakage of the Pressure-over Pressure-under Lines

For the simultaneous breakage of the pressure-over and pressure-under lines, pressures above and below the drive piston would drop to zero, and the ball check valve would close the broken pressure-under line. Reactor water would flow from the annulus outside the drive, through the vessel ports, and to the space below the drive piston. As in the case of pressure-over line breakage, the drive would then insert (if the reactor were above 600 psi) at a speed dependent on reactor pressure. Full insertion would occur regardless of the operational mode at the time of failure. Reactor water would leak past the drive seals and out the broken pressure-over line to the atmosphere, as described above. Drive temperature would increase. Indication in the control room would include the drift alarm, the fully inserted drive, the high drive temperature indicated on a recorder in the control room, and operation of the drywell sump pump.

4.6.2.3.2.2.3   All Drive Flange Bolts Fail in Tension

Each control rod drive is bolted to a flange at the bottom of a drive housing. The flange is welded to the drive housing. Bolts are made of AISI-4140 steel, with a minimum tensile strength of 125,000 psi. Each bolt has an allowable load capacity of 15,200 pounds. Capacity of the eight bolts is 121,600 pounds. As a result of the reactor design pressure of 1250 psig, the major load on all eight bolts is 30,400 pounds.

If a progressive or simultaneous failure of all bolts were to occur, the drive would separate from the housing. The control rod and the drive would be blown downward against the support structure. Impact velocity and support structure loading would be slightly less than that for drive housing failure, because reactor pressure would act on the drive cross-sectional area only and the housing would remain attached to the reactor vessel. The drive would be isolated from the cooling water supply. Reactor water would flow downward past the velocity limiter piston, through the large drive filter, and into the annular space between the thermal sleeve and the drive. For worst-case leakage calculations, the large filter is assumed to be deformed or swept out of the way so it would offer no significant flow restriction. At a point near the top of the annulus, where pressure would have dropped to 350 psi, the water would flash to steam and cause choke-flow conditions. Steam would flow down the annulus and out the space between the housing and the drive flanges to the drywell. Steam formation would limit the leakage rate to approximately 681 gpm.

If the collet were latched, control rod ejection would be limited to the distance the drive can drop before coming to rest on the support structure. There would be no tendency for the collet to unlatch, because pressure below the collet piston would drop to zero. Pressure forces, in fact, exert 1435 pounds to hold the collet in the latched position.

If the bolts failed during control rod withdrawal, pressure below the collet piston would drop to zero. The collet, with 1650 pounds return force, would latch and stop rod withdrawal.

4.6.2.3.2.2.4   Weld Joining Flange to Housing Fails in Tension

The failure considered is a crack in or near the weld that joins the flange to the housing. This crack extends through the wall and completely around the housing. The flange material is forged, Type 304 stainless steel, with a minimum tensile strength of 75,000 psi. The housing material is seamless, Type 304 stainless steel pipe, with a minimum tensile strength of 75,000 psi. The conventional, full penetration weld of Type 308 stainless steel has a minimum tensile strength approximately the same as that for the parent metal. The design pressure and temperature are 1250 psig and 575 F. Reactor pressure acting on the cross-sectional area of the drive; the weight of the control rod, drive, and flange; and the dynamic reaction force during drive operation result in a maximum tensile stress at the weld of approximately 5100 psi.

If the basic flange-to-housing joint failure occurred, the flange and the attached drive would be blown downward against the support structure. The support structure loading would be slightly less than that for drive housing failure, because reactor pressure would act only on the drive cross-sectional area. Lack of differential pressure across the collet piston would cause the collet to remain latched and limit control rod motion to approximately 3 in. Downward drive movement would be small, therefore, most of the drive would remain inside the housing. The pressure-under and pressure-over lines are flexible enough to withstand the small displacement and remain attached to the flange. Reactor water would follow the same leakage path described above for the flangebolt failure, except that exit to the drywell would be through the gap between the lower end of the housing and the top of the flange. Water would flash to steam in the annulus surrounding the drive. The leakage rate would be no greater than approximately 681 gpm.

If the basic failure were to occur during control rod withdrawal (a small fraction of the total operating time) and if the collet were held unlatched, the flange would separate from the housing. The drive and flange would be blown downward against the support structure. The calculated steady-state rod withdrawal velocity would be 0.13 ft./sec. Because pressure-under and pressure-over lines remain intact, driving water pressure would continue to the drive, and the normal exhaust line restriction would exist. The pressure below the velocity limiter piston would drop below normal as a result of leakage from the gap between the housing and the flange. This differential pressure across the velocity limiter piston would result in a net downward force of approximately 70 lbs. Leakage out of the housing would greatly reduce the pressure in the annulus surrounding the drive. Thus, the net downward force on the drive piston would be less than normal. The overall effect of these events would be to reduce rod withdrawal to approximately one-half of normal speed. With a 560 psi differential across the collet piston, the collet would remain unlatched; however, it should relatch as soon as the drive signal is removed.

4.6.2.3.2.2.5   Housing Wall Ruptures

This failure is a vertical split in the drive housing wall just below the bottom head of the reactor vessel. The flow area of the hole is considered equivalent to the annular area between the drive and the thermal sleeve. Thus, flow through this annular area, rather than flow through the hole in the housing, would govern leakage flow. The CRD housing is made of Inconel 600 seamless tubing (at the penetration to the vessel), with a minimum tensile strength of 80,000 psi, and of Type 304 stainless steel seamless pipe below the vessel with a minimum tensile strength of 75,000 psi. The maximum hoop stress of 9,000 psi results primarily from the reactor design pressure (1250 psig) acting on the inside of the housing.

If such a rupture were to occur, reactor water would flash to steam and leak through the hole in the housing to the drywell at approximately 1030 gpm. Choke-flow conditions would exist, as described previously for the flange-bolt failure. However, leakage flow would be greater because flow resistance would be less, that is, the leaking water and steam would not have to flow down the length of the housing to reach the drywell. A critical pressure of 350 psi causes the water to flash to steam.

No pressure differential across the collet piston would tend to unlatch the collet; but the drive would insert as a result of loss of pressure in the drive housing causing a pressure drop in the space above the drive piston.

If this failure occurred during control rod withdrawal, drive withdrawal would stop, but the collet would remain unlatched. The drive would be stopped by a reduction of the net downward force action on the drive line. The net force reduction would occur when the leakage flow of 1030 gpm reduces the pressure in the annulus outside the drive to approximately 540 psig, thereby reducing the pressure acting on top of the drive piston to the same value. A pressure differential of approximately 710 psi would exist across the collet piston and hold the collet unlatched as long as the operator held the withdraw signal.

4.6.2.3.2.2.6   Flange Plug Blows Out

To connect the vessel ports with the bottom of the ball check valve, a hole of 3/4-inch diameter is drilled in the drive flange. The outer end of this hole is sealed with a plug of 0.812 in. diameter and 0.25 in. thickness. A full-penetration, Type 308 stainless steel weld holds the plug in place. The postulated failure is a full circumferential crack in this weld and subsequent blowout of the plug.

If the weld were to fail, the plug were to blow out, and the collet remained latched, there would be no control rod motion. There would be no pressure differential across the collet piston acting to unlatch the collet. Reactor water would leak past the velocity limiter piston, down the annulus between the drive and the thermal sleeve, through the vessel ports and drilled passage, and out the open plug hole to the drywell at approximately 320 gpm. Leakage calculations assume only liquid flows from the flange. Actually, hot reactor water would flash to steam, and choke-flow conditions would exist. Thus, the expected leakage rate would be lower than the calculated value. Drive temperature would increase and initiate an alarm in the control room.

If this failure were to occur during control rod withdrawal and if the collet were to stay unlatched, calculations indicate that control rod withdrawal speed would be approximately 0.24 ft./sec. Leakage from the open plug hole in the flange would cause reactor water to flow downward past the velocity limiter piston. A small

differential pressure across the piston would result in an
insignificant driving force of approximately 10 lb, tending to
increase withdraw velocity.

A pressure differential of 295 psi across the collet piston would
hold the collet unlatched as long as the driving signal was
maintained.

Flow resistance of the exhaust path from the drive would be normal
because the ball check valve would be seated at the lower end of
its travel by pressure under the drive piston.

4.6.2.3.2.2.7   Ball Check Valve Plug Blows Out

As a means of access for machining the ball check valve cavity, a
1.25 in. diameter hole has been drilled in the flange forging.
This hole is sealed with a plug of 1.31 in. diameter and 0.38 in.
thickness. A full-penetration weld, utilizing Type 308 stainless
steel filler, holds the plug in place. The failure postulated is a
circumferential crack in this weld leading to a blowout of the
plug.

If the plug were to blow out while the drive was latched, there
would be no control rod motion. No pressure differential would
exist across the collet piston to unlatch the collet. As in the
previous failure, reactor water would flow past the velocity
limiter, down the annulus between the drive and thermal sleeve,
through the vessel ports and drilled passage, through the ball
check valve cage and out the open plug hole to the drywell. The
leakage calculations indicate the flow rate would be 350 gpm.
This calculation assumes liquid flow, but flashing of the hot
reactor water to steam would reduce this rate to a lower value.
Drive temperature would rapidly increase and initiate an alarm in
the control room.

If the plug failure were to occur during control rod withdrawal,
(it would not be possible to unlatch the drive after such a
failure) the collet would relatch at the first locking groove. If
the collet were to stick, calculations indicate the control rod
withdrawal speed would be 11.8 ft./sec. There would be a large
retarding force exerted by the velocity limiter due to a 35 psi
pressure differential across the velocity limiter piston.

4.6.2.3.2.2.8   Drive Pressure Control Valve Closure (Reactor Pressure, 0 psig)

The pressure to move a drive is generated by the pressure drop of practically the full system flow through the drive pressure control valve. This valve is either a motor operated valve or a standby manual valve; either one is adjusted to a fixed opening. The normal pressure drop across this valve develops a pressure 260 psi in excess of reactor pressure.

If the flow through the drive pressure control valve were to be stopped, as by a valve closure or flow blockage, the drive pressure would increase to the shutoff pressure of the supply pump. The occurrence of this condition during withdrawal of a drive at zero vessel pressure will result in a drive pressure increase from 260 psig to no more than 2000 psig. Calculations indicate that the drive would accelerate from 3 in./sec. to approximately 7 in./sec. A pressure differential of 1970 psi across the collet piston would hold the collet unlatched. Flow would be upward, past the velocity limiter piston, but retarding force would be negligible. Rod movement would stop as soon as the driving signal was removed.

4.6.2.3.2.2.9   Ball Check Valve Fails to Close Passage to Vessel Ports

Should the ball check valve sealing the passage to the vessel ports be dislodged and prevented from reseating following the insert portion of a drive withdrawal sequence, water below the drive piston would return to the reactor through the vessel ports and the annulus between the drive and the housing rather than through the speed control valve. Because the flow resistance of this return path would be lower than normal, the calculated withdrawal speed would be 2 ft./sec. During withdrawal, differential pressure across the collet piston would be approximately 40 psi. Therefore, the collet would tend to latch and would have to stick open before continuous withdrawal at 2 ft./sec. could occur. Water would flow upward past the velocity limiter piston, generating a small retarding force of approximately 120 lbs.

4.6.2.3.2.2.10   Hydraulic Control Unit Valve Failures

Various failures of the valves in the HCU can be postulated, but none could produce differential pressures approaching those described in the preceding paragraphs and none alone could

produce a high velocity withdrawal. Leakage through either one or both of the scram valves produces a pressure that tends to insert the control rod rather than to withdraw it. If the pressure in the scram discharge volume should exceed reactor pressure following a scram, a check valve in the line to the scram discharge header prevents this pressure from operating the drive mechanisms.

4.6.2.3.2.2.11   Collet Fingers Fail to Latch

The failure is presumed to occur when the drive withdraw signal is removed. If the collet fails to latch, the drive continues to withdraw at a fraction of the normal speed. This assumption is made because there is no known means for the collet fingers to become unlocked without some initiating signal. Because the collet fingers will not cam open under a load, accidental application of a down signal does not unlock them. (The drive must be given a short insert signal to unload the fingers and cam them open before the collet can be driven to the unlock position.) If the drive withdrawal valve fails to close following a rod withdrawal, the collet would remain open and the drive continue to move at a reduced speed.

4.6.2.3.2.2.12   Withdrawal Speed Control Valve Failure

Normal withdrawal speed is determined by differential pressures in the drive and is set for a nominal value of 3 in./sec. Withdrawal speed is maintained by the pressure regulating system and is independent of reactor vessel pressure. Tests have shown that accidental opening of the speed control valve to the full-open position produces a velocity of approximately 6 in./sec.

The control rod drive system prevents unplanned rod withdrawal and it has been shown above that only multiple failures in a drive unit and in its control unit could cause an unplanned rod withdrawal.

4.6.2.3.2.3   Scram Reliability

High scram reliability is the result of a number of features of the CRD system. For example:

a.   An individual accumulator is provided for each control rod drive with sufficient stored energy to scram at any reactor pressure. The reactor vessel itself, at pressures above 600 psi, will supply the necessary force to insert a drive if its accumulator is unavailable.

b.   Each drive mechanism has its own scram and a dual solenoid scram pilot valve so only one drive can be affected if a scram valve fails to open. Both valve solenoids must be deenergized to initiate a scram.

c.   The reactor protection system and the HCUs are designed so that the scram signal and mode of operation override all others.

d.   The collet assembly and index tube are designed so they will not restrain or prevent control rod insertion during scram.

e.   The scram discharge volume is monitored for accumulated water and the reactor will scram before the volume is reduced to a point that could interfere with a scram.

4.6.2.3.2.4   Control Rod Support and Operation

As described above, each control rod is independently supported and controlled as required by safety design bases.

4.6.2.3.3   Control Rod Drive Housing Supports

Downward travel of the CRD housing and its control rod following the postulated housing failure equals the sum of these distances: (1) the compression of the disc springs under dynamic loading, and (2) the initial gap between the grid and the bottom contact surface of the CRD flange. If the reactor were cold and pressurized, the downward motion of the control rod would be limited to the spring compression (approximately 2 in.) plus a gap of approximately 1 in. If the reactor were hot and pressurized, the gap would be approximately 1/4 in. and the spring compression would be slightly less than in the cold condition. In either case, the control rod movement following a housing failure is substantially limited below one drive notch movement (6 in.). Sudden withdrawal of any control rod through a distance of one drive notch at any position in the core does not produce a transient sufficient to damage any radioactive material barrier.

The CRD housing supports are in place during power operation and when the nuclear system is pressurized. If a control rod is ejected during shutdown, the reactor remains subcritical because it is designed to remain subcritical with any one control rod fully withdrawn at any time.

At plant operating temperature, a gap of approximately 1/4 in. exists between the CRD housing and the supports. At lower temperatures the gap is greater. Because the supports do not contact any of the CRD housing except during the postulated accident condition, vertical contact stresses are prevented.

4.6.3   Testing and Verification of the CRDs

4.6.3.1   Control Rod Drives

4.6.3.1.1   Testing and Inspection

[HISTORICAL INFORMATION] [

4.6.3.1.1.1   Development Tests

The development drive (prototype) testing included more than 5000 scrams and approximately 100,000 latching cycles. One prototype was exposed to simulated operating conditions for 5000 hours. These tests demonstrated the following:

a.   The drive easily withstands the forces, pressures, and temperatures imposed.

b.   Wear, abrasion, and corrosion of the nitrided stainless parts are negligible. Mechanical performance of the nitrided surface is superior to that of materials used in earlier operating reactors.

c.   The basic scram speed of the drive has a satisfactory margin above minimum plant requirements at any reactor vessel pressure.

d.   Usable seal lifetimes in excess of 1000 scram cycles can be expected.]

[HISTORICAL INFORMATION] [

4.6.3.1.1.2   Factory Quality Control Tests

Quality control of welding, heat treatment, dimensional tolerances, material verification, and similar factors is maintained throughout the manufacturing process to assure reliable performance of the mechanical reactivity control components. Some of the quality control tests performed on the control rods, control rod drive mechanisms, and hydraulic control units are listed below:

a.   Control rod drive mechanism tests:

1.   Pressure welds on the drives are hydrostatically tested in accordance with ASME codes.

2.   Electrical components are checked for electrical continuity and resistance to ground.

3.   Drive parts that cannot be visually inspected for dirt are flushed with filtered water at high velocity. No significant foreign material is permitted in effluent water.

4.   Seals are tested for leakage to demonstrate correct seal operation.

5.   Each drive is tested for shim motion, latching, and control rod position indication.

6.   Each drive is subjected to cold scram tests at various reactor pressures to verify correct scram performance.

b.   Hydraulic control unit tests:

1.   Hydraulic systems are hydrostatically tested in accordance with the applicable code.

2.   Electrical components and systems are tested for electrical continuity and resistance to ground.

3.   Correct operation of the accumulator pressure and level switches is verified.

4.   The unit's ability to perform its part of a scram is demonstrated.

5.   Correct operation and adjustment of the insert and withdrawal valves is demonstrated.]

4.6.3.1.1.3   Operational Tests

After installation, all rods and drive mechanisms can be tested through their full stroke for operability.

During normal operation, each time a control rod is withdrawn a notch, the operator can observe the in-core monitor indications to verify that the control rod is following the drive mechanism. All control rods that are partially withdrawn from the core can be tested for rod-following by inserting or withdrawing the rod one notch and returning it to its original position, while the operator observes the in-core monitor indications.

To make a positive test of control rod to control rod drive coupling integrity, the operator can withdraw a control rod to the end of its travel and then attempt to withdraw the drive to the overtravel position. Failure of the drive to overtravel demonstrates rod-to-drive coupling integrity.

Hydraulic supply subsystem pressures can be observed from instrumentation in the control room. Scram accumulator pressures can be observed on the nitrogen pressure gages.

[HISTORICAL INFORMATION] [

4.6.3.1.1.4   Acceptance Tests

Criteria for acceptance of the individual control rod drive mechanisms and the associated control and protection systems have been incorporated in specifications and test procedures covering three distinct phases: (1) pre-installation, (2) after installation prior to startup, and (3) during startup testing.

The pre-installation specification defines criteria and acceptable ranges of such characteristics as seal leakage, friction, and scram performance under fixed test conditions which must be met before the component can be shipped.

The after installation, pre-startup tests (Chapter 14) include normal and scram motion and are primarily intended to verify that piping, valves, electrical components, and instrumentation are properly installed. The test specifications include criteria and acceptable ranges for drive speed, time settings, scram valve response times, and control pressures. These tests are intended more to document system condition than as tests of performance. Modifications which included removal of the CRD return line and capping the CRD return line nozzle are discussed in Subsection 5.3.3.1.4.5.1. The preoperational testing program for the CRD system is described in subsection 14.2.12.1.11 and will include testing to verify the modified flow capability as well as the individual performance of modified CRD components and other

aspects of the CRD system potentially affected by the cut and capped CRD return line (equalizing valves, filters, scram times, setting function, etc.).

As fuel is placed in the reactor, the startup test procedure (Chapter 14) will be followed. The tests in this procedure are intended to demonstrate that the initial operational characteristics meet the limits of the specifications over the range of primary coolant temperatures and pressures from ambient to operating. The detailed specifications and procedures have not as yet been prepared but will follow the general pattern established for such specifications and procedures in BWRs presently under construction and in operation.]

4.6.3.1.1.5   Surveillance Tests

The surveillance requirements (SR) for the control rod drive system are described in the Technical Specifications/Technical Requirements Manual (TRM).

4.6.3.1.1.6   Functional Tests

The functional testing program of the control rod drives consists of the 5 year maintenance life and the 1.5X design life test programs as described in subsection 3.9.4.4.

There are a number of failures that can be postulated on the CRD but it would be very difficult to test all possible failures. A partial test program with postulated accident conditions and imposed single failures is available.

[HISTORICAL INFORMATION] [The following tests with imposed single failures have been performed to evaluate the performance of the CRDs under these conditions.

Simulated Ruptured Scram Line Test

Stuck Ball Check Valve in CRD Flange

HCU Drive Down Inlet Flow Control Valve (V122) Failure

HCU Drive Down Outlet Flow Control Valve (V120) Failure

CRD Scram Performance with V120 Malfunction

HCU Drive Up Outlet Control Valve (V121) Failure

HCU Drive Up Inlet Control Valve (V123) Failure

Cooling Water Check Valve (V138) Leakage

CRD Flange Check Valve Leakage

CRD Stabilization Circuit Failure

HCU Filter Restriction

Air Trapped in CRD Hydraulic System

CRD Collet Drop Test

CR Qualification Velocity Limiter Drop Test]

Additional postulated CRD failures are discussed in subsections 4.6.2.3.2.2.1 through 4.6.2.3.2.2.11.

4.6.3.2   Control Rod Drive Housing Supports

4.6.3.2.1   Testing and Inspection

CRD housing supports are removed for inspection and maintenance of the control rod drives. The supports for one control rod can be removed during reactor shutdown, even when the reactor is pressurized, because all control rods are then inserted. When the support structure is reinstalled, it is inspected for correct assembly with particular attention to maintaining the correct gap between the CRD flange lower contact surface and the grid.

4.6.4   Information for Combined Performance of Reactivity Systems

4.6.4.1   Vulnerability to Common Mode Failures

The system is located such that it is protected from common mode failures due to missiles and failures of moderate and high energy piping and fire. Sections 3.5 and 3.6, and subsection 9.5.1 discuss protection of essential systems against missiles, pipe breaks and fire.

4.6.4.2 Accidents Taking Credit for Multiple Reactivity Systems

There are no postulated accidents evaluated in Chapter 15 that take credit for two or more reactivity control systems preventing or mitigating each accident.

4.6.5 Evaluation of Combined Performance

As indicated in subsection 4.6.4.2, credit is not taken for multiple reactivity control systems for any postulated accidents in Chapter 15.

4.6.6 Reference

1. Benecki, J.E., "Impact Testing on Collet Assembly for Control Rod Drive Mechanism 7RD B144A," General Electric Company, Atomic Power Equipment Department, APED-5555, November 1967

2. Letter, A.B. Want, NRC to Vice President, Operations, Entergy Operations, Inc., Grand Gulf Nuclear Station Unit 1 – Issuance of Amendment RE: Extended Power Uprate (TAC No. ME4679)," July 18, 2012.

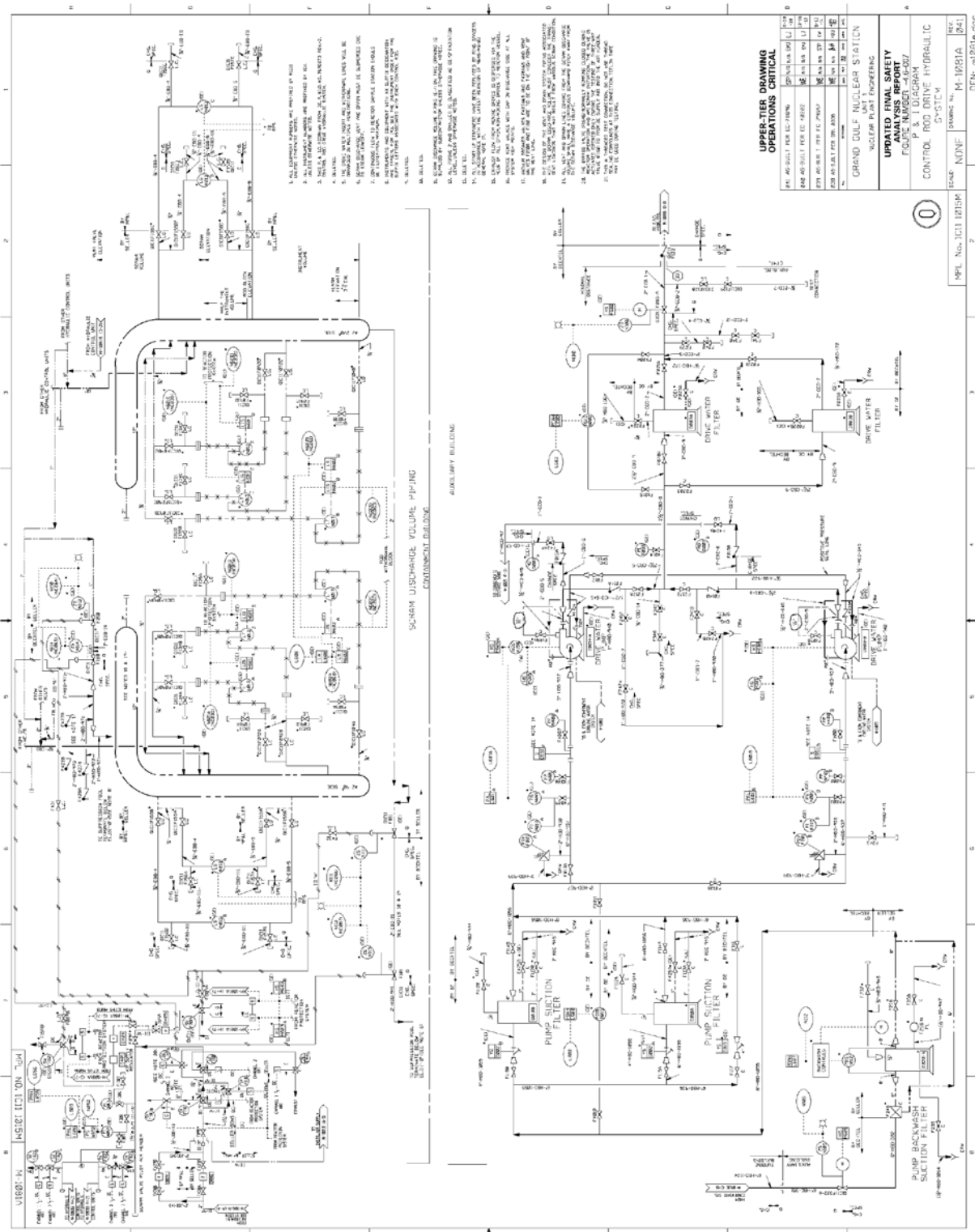General Electric Standard Application for Reactor Fuel (GESTAR II), NEDE-24011-P-A, latest approved revision.
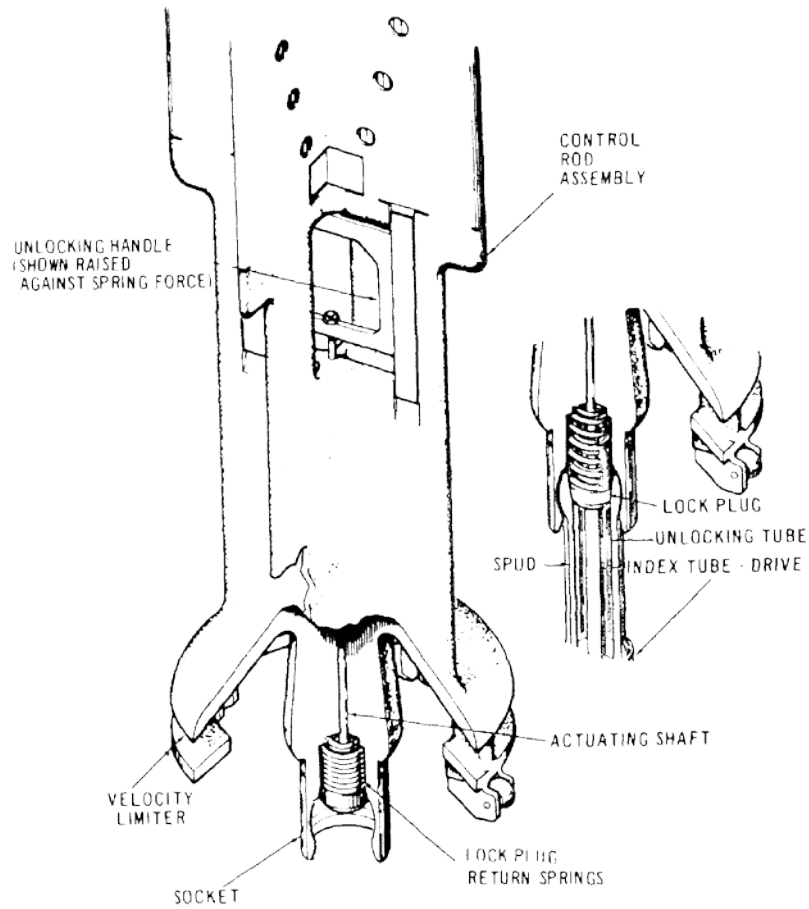
MISSISSIPPI POWER & LIGHT COMPANY GRAND GULF NUCLEAR STATION UNITS 1 & 2 UPDATED FINAL SAFETY ANALYSIS REPORT	CONTROL ROD TO CONTROL ROD DRIVE COUPLING FIGURE 4.6-1

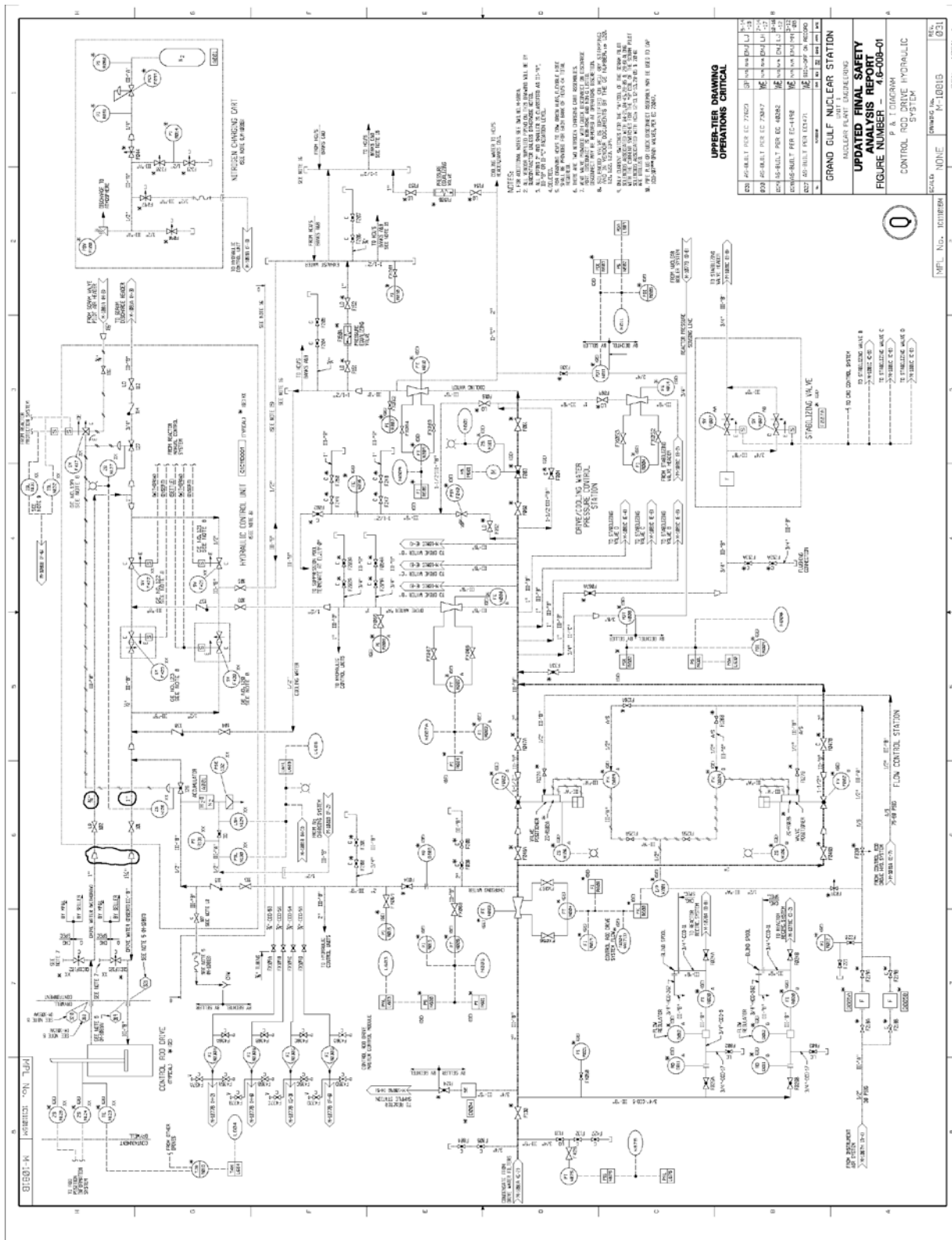| MISSISSIPPI POWER & LIGHT COMPANY GRAND GULF NUCLEAR STATION UNITS 1 & 2 UPDATED FINAL SAFETY ANALYSIS REPORT	CONTROL ROD DRIVE UNIT FIGURE 4.6-2

MISSISSIPPI POWER & LIGHT COMPANY GRAND GULF NUCLEAR STATION UNITS 1 & 2 UPDATED FINAL SAFETY ANALYSIS REPORT	CONTROL ROD DRIVE SCHEMATIC FIGURE 4.6-3

MISSISSIPPI POWER & LIGHT COMPANY GRAND GULF NUCLEAR STATION UNITS 1 & 2 UPDATED FINAL SAFETY ANALYSIS REPORT	CONTROL ROD DRIVE HYDRAULIC CONTROL UNIT FIGURE 4.6 - 5

CONTROL ROD DRIVE HOUSING SUPPORT

MISSISSIPPI POWER & LIGHT COMPANY
GRAND GULF NUCLEAR STATION
UNITS 1 & 2
UPDATED FINAL SAFETY ANALYSIS REPORT

FIGURE 4.6-6

SYSTEM ENERGY RESOURCES, INC.
GRAND GULF NUCLEAR STATION
UNITS 1 & 2
UPDATED FINAL SAFETY ANALYSIS REPORT

CONTROL ROD DRIVE
HYDRAULIC SYSTEM

FIGURE 4.6-8   SHEET 2 OF 2

M-1081C-8

FIGURE 4.6-9
DELETED

System Flow Diagram, Control Rod Drive Hydraulic System, Unit 1. Figure Number — 4.6-010.

APPENDIX 4A   DELETED